PRACA DOKTORSKA

Instytut Chemii Organicznej

Polskiej Akademii Nauk

Justyna Czaban

Praca doktorska

Applications of olefin metathesis in industrial context. Immobilization, multibatch processes, recycling

Praca przedstawiona Radzie Naukowej
Instytutu Chemii Organicznej Polskiej Akademii Nauk
w celu uzyskania stopnia doktora nauk chemicznych

Promotor:

Prof. dr hab. inż. Karol Grela

Warszawa 2015

Niniejsza praca powstała pod kierunkiem
***prof. dr hab. Karola Greli**, któremu pragnę podziękować*
za wszechstronną pomoc oraz możliwość pracy w tematyce metatezy.

Pragnę dedykować swoją dysertację ***rodzicom, rodzeństwu*** *a przede wszystkim* ***mężowi*** *dziękując za cierpliwość, wyrozumiałość oraz wsparcie w chwilach zwątpienia.*

Zespołowi III *IChO PAN,* ***Laboratorium Syntezy Metaloorganicznej*** *UW oraz wszystkim współpracownikom*

Dziękuję za wspólną pracę, pokonywanie codziennych laboratoryjnych trudności. Dziękuję za niezapomniane lata jakie spędziłam w laboratorium IChO PAN, za niesamowitą atmosferę jaką razem tworzyliśmy. Chciałabym podziękować Wam wszystkim i każdemu z osobna (jeżeli o kimś zapomnę wybaczcie):

Osman Ablialimov, Michał Barbasiewicz, Michał Bieniek, Marta Bugaj-Wołukaniec, Daniel Burtscher, Magdalena Dziedzic (Łysiak), Patrycja Czarnecka (Kurtycz), Stefan Czarnocki, Rafał Gawin, Ewa Gronowska (Jabłonka), Łukasz Gułajski, Paweł Horeglat, Magdalena Jawiczuk, Anna Kajetanowicz (Wojtasiewicz), Urszula Karcz, Mariusz Kędziorek, Jan Klajn, Marek Kluciar, Dariusz Kołoda, Wioletta Kośnik, Anna Kozłowska, Sylwester Kurcoń, Kinga Leszczyńska, Rafał Loska, Maura Malińska, Michał Michalak, Kasjan Misztal, Agnieszka Nowak-Król, Keith Ó Proinsias, Rajesh Krishnan Gopalakrishna Panicker, Joanna Paradowska (Lipner), Joanna Piechowska, Michał Pieczykolan, Volodymyr Sashuk, Cezary Samojłowicz, Michał Sienkiewicz, Beata Słomińska, Michał Smoleń, Jakub Socha, Sebastian Stecko, Shafi Syed, Adrian Sytniczuk, Anna Szadkowska, Grzegorz Szczepaniak, Paweł Szczepanik, Marcin Śnieżek, Paweł Świder, Christian Torborg, Łukasz Weseliński, Michał Wierzbicki, Beata Wileńska, Tomasz Wdowik, Łukasz Woźniak, Andrzej Zarecki, Adam Zieliński, Grzegorz Zieliński, Karolina Żukowska

Informacje ogólne

Część doświadczalna niniejszej pracy powstała w Instytucie Chemii Organicznej Polskiej Akademii Nauk, Faculty of Engineering, Department of Chemical Engineering Imperial College London oraz Laboratory of Homogeneous Catalysis, Institute of Catalysis, University of Technology Eindhoven w latach 2008-2013. Od października 2011 roku badania były finansowane ze środków projektu „Modyfikacje kompleksów rutenowych w celu oczyszczania mieszaniny reakcyjnej przy pomocy nanofiltracji." realizowanego w ramach programu „VENTURES" Fundacji na rzecz Nauki Polskiej (Ventures/2011-7/3)

Część wyników badań przedstawiona w niniejszej dysertacji została opublikowana w następujących artykułach oraz patentach:

1. Kajetanowicz, A.; Czaban, J.; Krishnan, G. J.; Malińska, M.; Woźniak, K.; Siddique, H.; Peeva, L. G.; Livingston, A. G.; Grela, K. "Batchwise and Continuous Nanofiltration of POSS®-tagged Grubbs-Hoveyda Type Olefin Metathesis Catalysts" *ChemSusChem* **2013**, *1*, 182-192
2. Azap, C., Wolf, D., Abbenhuis, H. C. L., Gerritsen, G., Wilting, J., Leszczyńska, K., Grela, K., Czaban, J., and Wojtasiewicz, A *Polysilsesquioxane (POSS)-linked Imidazole-based Carbene and Phosphine Ligands for Transition Metal Catalysts Application* US201113582010 20110228 WO2011107417 (A1)
3. Azap, C., Wolf, D., Abbenhuis, H. C. L., Gerritsen, G., Wilting, J., Leszczyńska, K., Grela, K., Czaban, J., and Wojtasiewicz, A. *Polyhedral Oligomeric Silesquioxane (POSS)-linked Ligands*. Patent No. EP20100155081 20100301
4. Ahmadi, A.; McBride, C.; Freire, J. J.; Kajetanowicz, A.; Czaban, J.; Grela K. „Force Field Parametrization and Molecular Dynamics Simulation of Flexible

POSS-Linked (NHC; Phosphine) Ru Catalytic Complexes" *J. Phys. Chem. A* **2011**, *115*, 12017.

Wyniki niniejszej pracy doktorskiej zostały zaprezentowane na konferencjach:

1. 20th International Symposium on Olefin Metathesis (ISOM XX) Nara, Japonia, 14 – 19.07.2013 (poster)
2. 244th American Chemical Society National Meeting & Exposition, Philadelphia, USA, 19 – 23.08.2012 (oral and poster)
3. 9th YoungChem, Kraków, Poland, 12–16.10.2011, (oral)
4. 19th International Symposium on Olefin Metathesis (ISOM XIX) Rennes, Francja, 10 – 15.07.2011 (oral)
5. XIX EuCheMS Conference on Organometallic Chemistry (XIX EuCOMC), Toulouse, Francja, 03 – 07.07.2011 (poster)
6. 241st ACS National Meeting & Exposition, Anaheim, California, USA, 27 – 31.03.2011 (oral)
7. 18th International Conference on Organic Synthesis, Bergen, Norwegia 31.07 – 07.08.2010 (poster)
8. 17th International Symposium on Homogeneous Catalysis (ISHC-17), Poznań, 4 – 09.07.2010 (poster)
9. 18th International Symposium on Olefin Metathesis and Related Chemistry, Leipzig, Germany 02 – 07.08.2009 (poster)
10. 11th JCF-Fruhjahrssymposium, Essen, Niemcy 11 – 15.03.2009 (poster)
11. 6th International Congress of Young Chemists, Kraków 15 – 19.11.2008 (poster)

ABBREVIATIONS

Ac	acetyl group
ADD	1,1'-(azodicarbonyl)dipiperidine
ADMET	acyclic diene metathesis polymerization
aq.	aqueous
Ar	aryl group
ASAP-MS	atmospheric solids analysis probe mass spectrometry
bdmim	1-butyl-2,3-dimethylimidazolium
bmim	1-butyl-3-methylimidazolium
Bn	benzyl group
Boc	*tert*-butoxycarbonyl group
BR	batch reactor
brs	brosyl, *p*-bromobenzenesulfonyl group
Bu	butyl group
°C	temperature in degree Celcius
ca.	about, approximately, around
Calcd	calculated
CM	Cross Metathesis
CMR	catalytic membrane reactor
CSTR	continuous stirred tank reactor
Cy	cyclohexyl group
Da	Dalton
DATA	*N*,*N*-diallyltosylamine
DCE	1,2-dichloroethane
DCM	dichloromethane
dd	doublet of doublets
DEAMM	diethyl allylmalonate
DEDAM	diethyl diallylmalonate
DEDMM	diethyl dimethylallylmalonate
DMC	dimethyl carbonate
DMF	*N*,*N*-dimethylformamide
DMSO	dimethyl sulfoxide
EA	elemental analysis
EI	electron impact
emim	1-ethyl-3-methylimidazolium
Equiv.	equivalents
ESI-MS	electrospray ionization mass spectrometry
Et	etyl group
EtOAc	ethyl acetate
F	feed
FD	field desorption
GC	gas chromatography
hmim	1-hexyl-3-methylimidazolium
HPLC	high performance liquid chromatography
HRMS	high resolution mass spectrometry

Hz	Hertz
i-Bu	isobutyl group
ICP-MS	inductively-coupled plasma mass spectrometry
ICP-OES	inductively-coupled plasma optical emission spectrometry
IL	ionic liquids
IMes	1,3-bis-mesityl-imidazole-2-ylidine
i-Pr	isopropyl group
IR	infrared spectroscopy
J	coupling constant
J	flux
KHMDS	potassium hexamethyldisilazane
KO^tBu	potasium tertbutoxide
L	liter
LAH	lithium aluminium hydride
LHMDS	lithium hexaethyldisilazane
M	molar (mol/L)
m	multiplet
MCM-41	mesoporous molecular sieves
Me	methyl group
MEK	methylethylketone
Mes	2,4,6-trimethylphenyl, mesityl
MF	microfiltration
MNA	2-mercaptonic acid
MNP	magnetic nanoparticle
mol%	mole percent
mp	melting point
MS	mass spectrometry
MSF	siliseous mesostructures cellular foam
MTBE	methyl tert buthyl ether
MW	molecular weight
MWCO	molecular weight cut off
MWE	molecular weight enlargement
NF	nanofiltration
NHC	*N*-heterocyclic carbene
NMR	nuclear magnetic resonance
omim	1-octyl-3-methylimidazolium
ORTEP	oak ridge thermal ellipsoid plot
OSN	organic solvent nanofiltration
P	permeate
PAN	polyacrylonitryle
PASSflow	polymer assisted solution phase synthesis flow-through mode
PCy_3	tricyclohexylphosphine
PDMS	polydimethyl siloxane
PE	polyethylene
PEG	poly(ethyl glycol)
PFR	plug flow reactor
Ph	phenyl group
PI	polyimide

PIB	polyisobutylene
PNB	*para*-nitrobenzoate group
POSS	polyhedral oligomeric silesquioxane
ppb	parts per billion
ppm	parts per million
q	quartet
R	rejection
RCM	Ring Closing Metathesis
RO	reverse osmosis
ROM	Ring Opening Metathesis
ROMP	Ring Opening Metathesis Polymerization
rt	room temperature
s	singlet
SLIP	ionic polymer
SRNF	solvent resistant nanofiltration
t	triplet
TBS	tert-butyldimetylsilyl
TFA	trifluoroacetic acid
TFC	thin film composite
THF	tetrahydrofurane
THP	tris(hydroxymethyl)phosphine
TLC	thin layer chromatography
TMP	transmembrane pressure
TMS	trimethylsilyl
TON	turnover number
TPPO	triphenylphosphine oxide
UF	ultrafiltration
V_p	volume of permeate

INTRODUCTION

Olefin metathesis a very powerful transformation in organic chemistry which allows for creation of C-C double bonds. This importance was underlined by awarding the Noble Prize to Chauvin, Grubbs and Schrock in 2005.

Despite many great achievements, effective removal of the metal impurities is still a major problem in metathesis reaction. Purification of the metathesis reaction on an industrial scale is still under investigation. Main challenges are the scale of the process E-factor and total cost of the process. Liveliness of the catalyst and side reactions caused by products of decomposition of the catalyst are another aspect that has to be considered when developing the purification method. Selected method of purification of the metathesis reaction together with implementation in industrial processes have been described in chapter 1.2.

Nanofiltration is one of the membrane processes, separation processes, which have found numerous industrial applications. Lately it has become more and more popular in purification of organic solvent mixtures. Recent implementations in homogenous catalysis and especially in metathesis reaction have been described in chapter 1.3.

The main goal of the research described herein was to developed ruthenium complexes which will be easily removable from the reaction mixture by nanofiltration. An equally important issue to study was the optimization of the nanofiltration procedure, which means choosing the appropriate solvent, membrane and pressure.

Molecular weight enlargement (MWE) is an attractive method of heterogeneous catalyst recycling which has been adopted in homogeneous catalysis. Of many MWE units known in the literature, POSS gained my attention because of its universality. Herein I present the synthesis of the ruthenium complexes decorated with POSS unit. Such a modification not only increased retention of the catalyst during nanofiltration but, which was the most surprising, increased activity of the examined catalysts.

“We’re all in the same boat,

and we have only one boat”

Paul Anastas

PART 1 – LITERATURE REVIEW

1.1. METATHESIS REACTION

Olefin metathesis is a unique process of carbon-carbon double bond rearrangement mediated by transition metal catalysts. The word metathesis comes from Greek *μεταθεση* which means transposition.

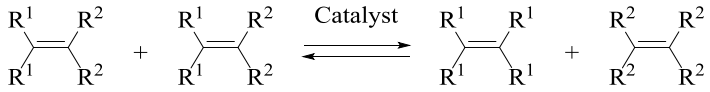

Scheme 1. Olefin metathesis.

The term "olefin metathesis" has been introduced by Calderon and co-workers in 1967 to describe an exchange of two carbenes of an olefin with those of another olefin molecule.[1] Nowadays this methodology[2] is used in a wide range of research fields such as natural products,[3] pharmaceuticals,[4] heterocycles, macrocycles[5] and polymers,[6] and many other. The spectacular success of this reaction culminated in the award of the 2005 Nobel Prize in Chemistry to three outstanding contributors to this research field – Yves Chauvin, Robert H. Grubbs and Richard R. Schrock.

1.1.1. MECHANISM OF OLEFIN METATHESIS

Several mechanistic hypotheses were proposed during the early period of olefin metathesis exploration.[1,7] Finally, after many attempts presented by Bradshaw,[8] Calderon,[9] Pettit[10] and Grubbs[11] the generally accepted mechanism have been introduced by Chauvin and Hérisson in 1971.[12]

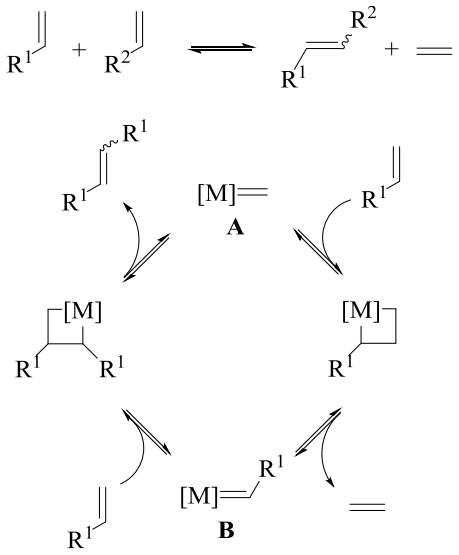

Scheme 2. Mechanism of olefin metathesis.

During the first step, coordination of the substrate onto the metal atom of the catalyst **A** results in formation of the metallacyclobutane intermediate. Next, this intermediate breaks up either with formation volatile olefin (ethylene, when the substrate is terminal), along with a new metal alkylidene **B**, or reverting back to the initiating species. **B** can subsequently react with another olefin, forming an intermediate which finally leads to the product and the starting metal carbene **A**. The product contains a carbene from the alkylidene **B** and the other carbene from the substrate. The newly established metal alkylidene species contains one of the two carbenes of the starting olefin that can restart the cycle. The driving force in the catalytic cycle is release of the volatile olefin. The mechanism has been proved by the studies involving an isolated alkylidene or metalacyclobutane.[13]

1.1.2. METATHETIC TRANSFORMATIONS

The main advantage of the metathesis reaction is universality due to the fact of a set of several different types of transformations: ring-closing metathesis (RCM), ring-opening metathesis (ROM), acyclic diene metathesis polymerization (ADMET), ring-opening metathesis polymerization (ROMP) and cross metathesis (CM) (Scheme 3). All of those transformations can be performed with the same alkylidene catalyst depending on the reaction conditions and the structural features of the substrate.

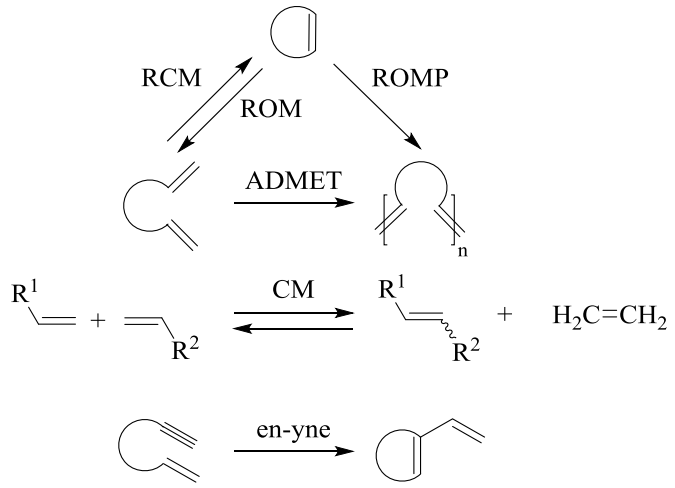

Scheme 3. Types of olefin metathesis.

Careful choice of substrates and reaction conditions can lead to high conversions within those reactions, even though olefin metathesis itself is under thermodynamic control.

Cross metathesis, the one of the most powerful metathetic transformations,[14] is an intermolecular reaction between two olefin partners. There are two issues that must be addressed. The first requirements is to obtain high yields of the product from CM while reducing formation of the undesired self-metathesis. The second is to control *E*/*Z* olefin geometry in the newly formed double bond. When substrates have similar reactivity, CM leads to statistical distribution of products. Desired product will be obtained in maximum yield of 50%. At the same time two undesired by-products will be observed in 25% yield each.

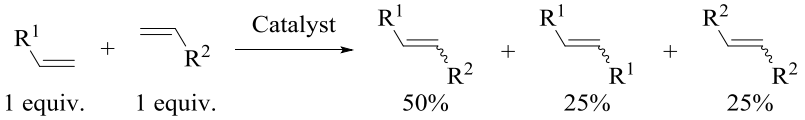

Scheme 4. Statistical distribution of CM products.

There is a variety of different procedures to avoid such situation and increase selectivity, such as applying an excess of one of the partners. Another approach is to choose appropriate CM partners based on categories and rules presented by Grubbs.[15]

Another aspect, that has to be considered during designing a CM reaction, is reactivity of olefins, which is a combination of steric and electronic factors. When

considering steric factors and the rate of initiation of catalyst by various olefins, trend in olefin reactivity according to the structure could be inferred.

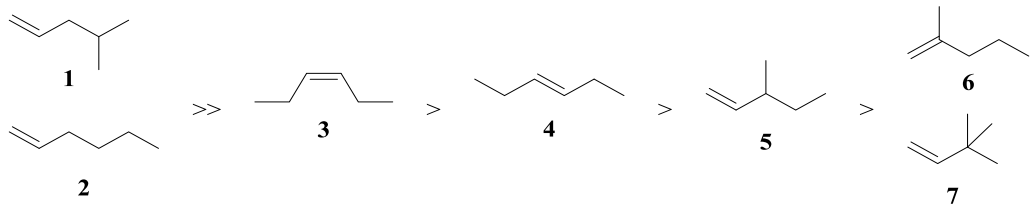

Figure 1. Relative reaction rate of variously substituted alkenes.

Simple terminal alkenes (**1**, **2**) react much faster than others presented on Figure 1. They are the easiest substrate for CM reaction. In case of other CM substrates, if the source of the steric hindrance is located far from the reaction centre, reaction is relatively fast. In the case of *Z* and *E* isomers, *Z* isomers (**3**) react faster than *E* (**4**), which could be explained by differences in steric hindrance between them. Olefin with the steric hindrance source located near the reaction centre (**6**, **7**) are the most difficult substrates and CM of such molecules is very slow.

The most popular metathetic transformation is RCM. Not only because it is one of the major model reactions in screening of the activity of different catalysts (Figure 2), but it is also one of the key steps in many synthetic sequences.[16] When RCM is utilized as a model reaction usually composition of 5 – 7 membered ring is considered because of low strain energy and kinetic control of the process.

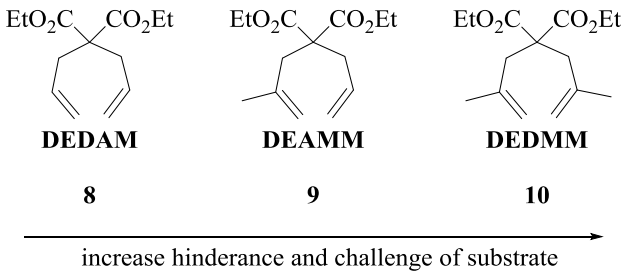

Figure 2. Standard model substrates for RCM reaction: diethyl diallylmalonate (DEDAM, **8**), diethyl allylmethallylmalonate (DEAMM, **9**) and diethyl dimethyallylmalonate (DEDMM, **10**).

1.1.3. CATALYSTS

Almost 60 years of intensive research on the theme bring a variety of different complexes that have ability to catalyse metathesis reaction. From ill-defined multicomponent systems which required harsh conditions and prolonged initiation period,[2f,17] metathesis catalyst evolved to well-defined 14 or 16 electron active species based on molybdenum, tungsten and ruthenium.

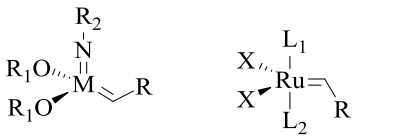

catalyst 14 e⁻ M=Mo, W — precatalyst 16 e⁻

Figure 3. Molybdenum or tungsten catalyst and ruthenium precatalyst.

Molybdenum and tungsten alkylidene complexes are 14 electron active species ready to initiate the catalytic cycle. Whereas ruthenium complexes are 16 or 18 electron and required initiation step, during which they becomes an active 14 electron species. All well-defined ruthenium complexes should have been called metathesis precatalysts, but for better clarity term catalyst is used generally in the literature. Within this dissertation I will also use term "catalyst" for 16 electron ruthenium species.

1.1.3.1. WELL-DEFINED MOLYBDENUM AND TUNGSTEN COMPLEXES

The first single component metathesis catalysts reported in the early 1980s[18] (for example **11**, **12**) required addition of Lewis acid ($AlCl_3$, $AlBr_3$ or $GaBr_3$) as an initiator.

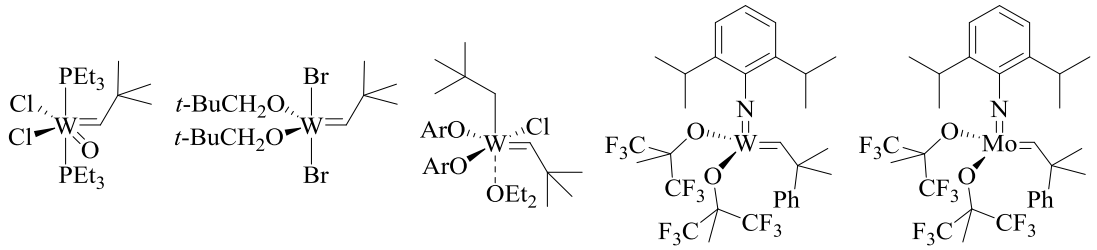

11 Schrock 1980 — **12** Osborn 1982 — **13** Basset 1985 — **14** Schrock 1986 — **15** Schrock 1987

Figure 4. First well-defined olefin metathesis catalysts based on tungsten and molybdenum.

In 1985 Basset *et al.* developed the first example of Lewis-acid-free tungsten based catalyst **13**.[19] This was the key step in designing the new family of active catalysts for metathesis reaction. In 1986 Schrock presented very active tungsten-based catalyst **14**, the first from the "Schrock's family of high oxidation-state catalysts".[20] Subsequently molybdenum catalyst **15** was synthesized.[21]

Molybdenum complexes are the most reactive metathesis catalysts known to date.[22] Although the activity of these kinds of initiators is very high, their sensitivity to air and moisture implies the use of a glove box or Schlenk techniques that hampered its more widespread use by organic chemists or in industrial applications.

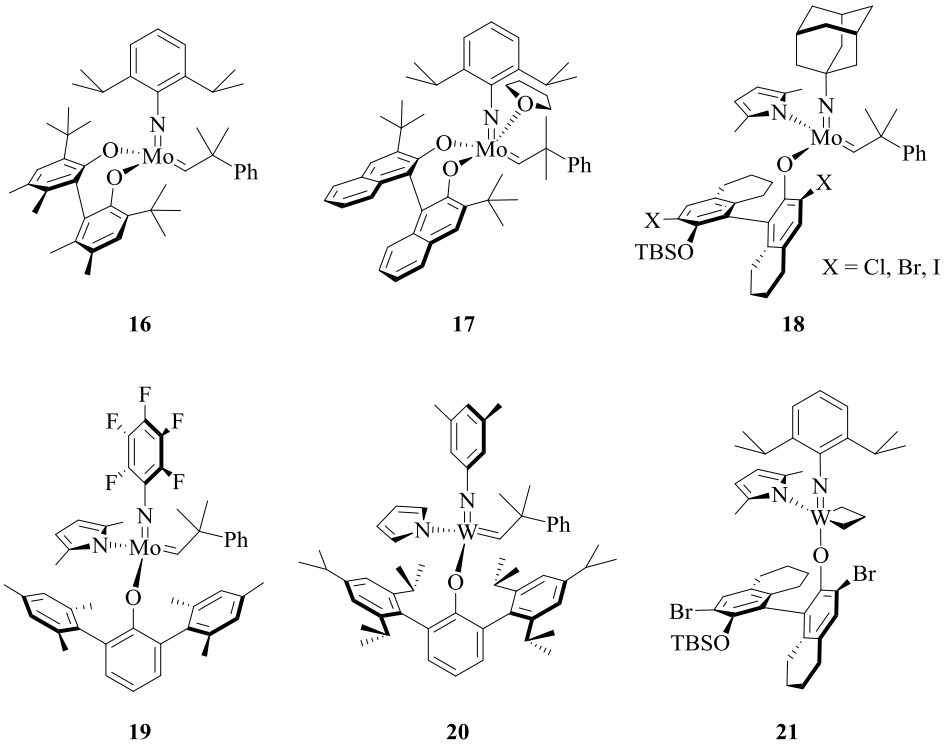

16 **17** **18**

19 **20** **21**

Figure 5. Representative Mo and W based complexes utilized in asymmetric metathesis.

Nonetheless, molybdenum and tungsten complexes containing optically pure aryloxide ligand (usually biphenyl or BINOL derivatives with different substitution pattern), pyrrolide moiety are chiral at metal. Such species are called mono-alkoxide-pyrrolide (MAP) complexes.[23] MAP catalysts are widely used in a variety of asymmetric metathesis reactions[3b,24] and also have the ability to impose high *Z*-selectivity in metathesis reactions.[3a,25]

1.1.3.2. RUTHENIUM CATALYSTS

Ruthenium-based catalysts were discovered about 40 years ago, when ruthenium (III) chloride hydrate was found to be a suitable precatalyst for the ROMP,[26] but until late 1980s ruthenium was underestimated. The first well defined ruthenium alkylidene complex **24** was synthesized by Grubbs in 1992.[27] The complex was active towards ROMP and RCM, and moreover, was stable in the presence of protic solvents. The substitution of triphenylphosphine with the more sterically demanding and stronger σ-donating ligand tricyclohexylphosphine increases the activity of **25** towards acyclic olefins as well as affords good functional group tolerance.[28]

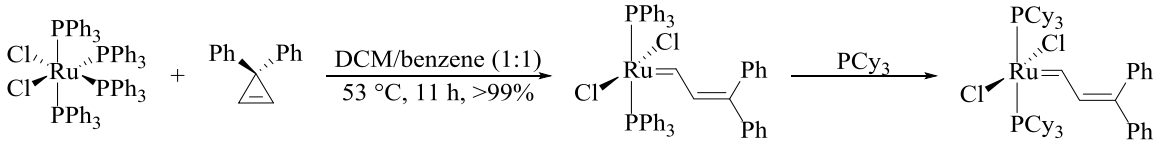

22 **23** **24** **25**

Scheme 5. Synthesis of **24** and **25** reported by Grubbs *et al.*

It was the starting point for the development of well-defined alkylidene ruthenium catalysts, a research area that continues to date. Shortly after, further refinement led to the development of air and moisture stable ruthenium complex **26** also known as the first generation Grubbs catalyst.[13f,g,29]

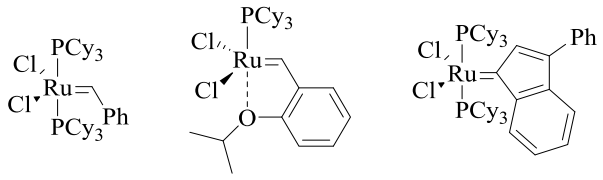

26 **27** **28**

Figure 6. First generation of Grubbs **26**, Hoveyda Grubbs **27** and Indenylidene **28** complexes.

Up to now **26** is the most used metathesis catalyst by organic chemists. It is because of its stability and compatibility with a large variety of functional groups and the fact that it still represents an alternative to more active but also much more expensive catalysts.[2b,3c,30]

Another crucial discovery in the field was presented by Hoveyda in 1997, when benzylidene ligand was replaced with a styrenyl ether moiety.[31] This modification, known

as Hoveyda-Grubbs first generation catalyst (**27**), brings remarkable stability to air and moisture. Additionally, **27** can be easily recovered from the reaction mixture by column chromatography.[32]

An alternative structure of ruthenium catalysts have been reported independently by Hill,[33] Fürstner[34] and Nolan.[35] Reaction **22** with 3,3-diphenylpropyn-3-ol and further replacement of triphenylphosphine with tricyclohexylphosphine led to indenylidene complex **28.** The described indenylidene complex was shown to be more resistant to harsh reaction conditions and have higher tolerance for polar functional group than its benzylidene counterparts and at the same time showed a good activity, selectivity and longevity.[36]

Later, one of the phosphine ligand was replaced by N-heterocyclic carbene (NHC), leading to further spectacular progress in Ru-based catalyst design.[37] The electron-donating ability of the NHC ligand enhanced the efficiency of the catalyst and, hence, the affinity of the Ru centre towards the coordination of olefinic substrate. Soon after, second generation of Grubbs **29**,[38] Grubbs-Hoveyda **30**,[39] and indenylidene **31** complexes have been synthesized.

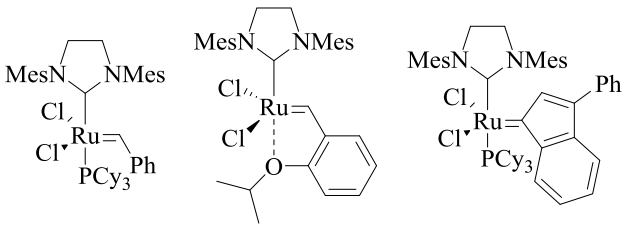

29 **30** **31**

Figure 7. Second generation of Grubbs **29**, Hoveyda Grubbs **30** and indenylidene **31** complexes.

More recent studies led to the development of ruthenium complexes with different catalytic behaviour, such as high activity,[40] initiation of asymmetric olefin metathesis reactions,[41] ability to work in aqueous or protic solvents[42] or carrying out the formation of tetrasubstituted carbon-carbon double bonds.[43]

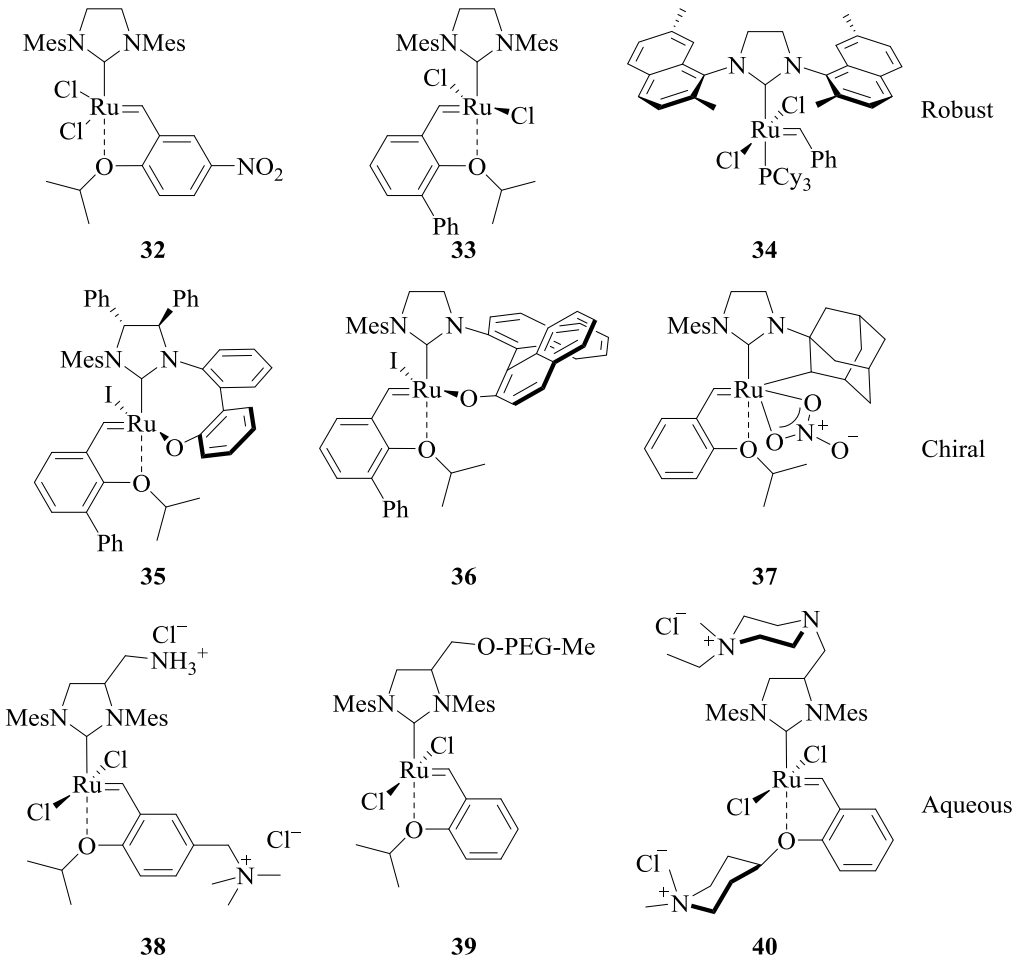

Figure 8. Different paths of modifications of ruthenium complexes.

1.1.3.3. MECHANISMS OF RUTHENIUM COMPLEXES INITIATION

Ruthenium alkylidene complexes require ligand dissociation in order to access the 14 electron intermediate which is mandatory for ruthenacyclobutane formation. Based on kinetic studies three mechanisms of catalyst initiation have been proposed: associative, dissociative and intercharge.[44] In the first step of the dissociative mechanism five coordinate ruthenium complex **I** undergoes phosphine dissociation to form the reactive monophosphine 14 electron intermediate **II**. Highly active **II** reacts with the olefin to afford the 16 electron complex **III**, which undergoes carbon-carbon bond formation to generate a ruthenacyclobutane.

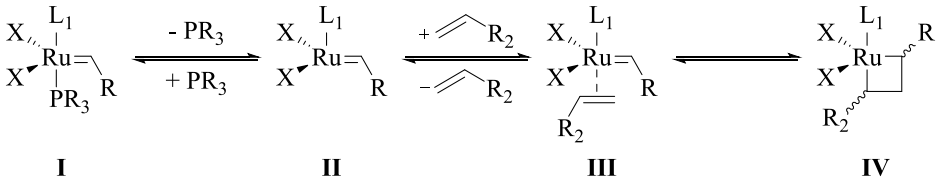

Scheme 6. Dissociative mechanism of catalyst initiation.

Associative mechanism pathway involves metallacyclobutane formation from 18 electron olefin intermediate **V**, generated in the first step. Dissociation of phosphine ligand from **V** leads to formation complex **III** which reacts to afford ruthenacyclobutane.

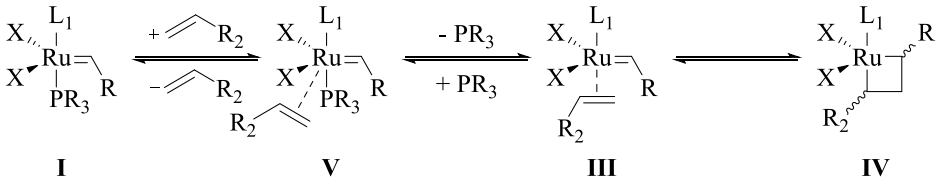

Scheme 7. Associative mechanism of catalyst initiation.

In the intercharge mechanism the binding of alkene and loss of a ligand occur simultaneously.

Kinetic studies confirmed dissociative mechanism of catalyst initiation in the case of complexes alike **I**, whereas for catalysts with chelating alkylidene ligands all three mechanism are plausible, the nature of the catalyst and the reacting olefin determining the path of initiation.[37e,45]

1.2. RECOVERY AND REUSE OF RUTHENIUM BASED METATHESIS CATALYSTS

Despite the widespread use of metathesis transformations and multitude of metathesis catalysts available on the market, effective removal of metal impurities is still a major problem, especially for further proliferation of the metathesis methodology in industry.[46] It is rather challenging because the European Medicines Agency established the permitted ruthenium concentration in the final product at 10 ppm for oral drugs and 1 ppm for parenteral drugs.[2a,47] Such regulations are mandatory especially during the synthesis of biologically active compounds or polymers used in technologically advanced applications. Furthermore, impurities containing ruthenium can cause undesired side-

reactions, as well as they are rather strong dyes can being cause undesired colorization. Such low contamination should be achieved by a cost-efficient method of purification. Implementation of the most common purification methods such as column chromatography or filtration through silica on the industrial scale is rather expensive and difficult. Therefore, the development of an efficient, economical and practical method of purification of the desired product is crucial. Over the decades various industrial chemists and academic research groups worked on this issue and had presented several solutions for the purification of products and the recovery of the catalysts.[48]

Two main aspects in metathesis reaction should be taken under consideration to implement this reaction in industry. First, leaching of ruthenium from the active catalyst in the reaction mixture and, second, recovery and recycling of the ruthenium catalyst.

To approach the leaching problem two strategies can be utilized: treatment of the product by some sequestering agents (so-called scavengers) to eliminate the trace amounts of ruthenium, or design of catalyst that does not leach during the reaction. To easily remove and reuse the catalyst, modification of the catalyst is required.

In the next part of my dissertation I will present different methods of purification applied by academic groups of researchers and then describe how many of those methods have been successfully applied into industry. I divided purification methods into two main groups: applicable to standard catalysts and those that do require modification of the catalyst.

For better understanding of the next part of my dissertation I will briefly describe reactor setups that have been so far applied in metathesis reaction.[49]

Batch reactors are the traditional production equipment, they has not changed much over past century. They suffer from very poor E-factors[a,50] and low overall process efficiencies. Moreover, energy and material intensive operation are required during production. Most of these operations cannot be automated. Up to 80% of overall process costs is estimated to stream from batch-wise downstream purification. As a result of high costs of batch processes, multi-purpose batch or semi-batch reactors were adopted. They suffer not only from poor space-time yield but also difficulties in process control, particularly on scale up.

[a] E-factor = total waste (in kg)/product (kg)

An alternative to batch processes are continuous flow conditions where reactants continuously feed the reactor and emerge continuous stream of product. The benefits of utilization of such type of reactors are: improved heat and mass transfer, greater reaction control (improving reaction yields and selectivity, while reducing reaction and cycle times, and catalyst loading), the ease of heating solvents above their boiling point and up to supercritical conditions, higher safety when dealing with reactive and hazardous intermediates, simplicity of automation and telescoping od multistep reaction. The positive impact of continuous flow chemistry on organometallic catalysis has been covered by many review articles.[51] Flow reactors, compared to stirred tank reactors,[52] have significant processing advantages which cover almost all from the twelve principles of green chemistry.[53]

There are different types of flow reactors, their utilization depends on the method of immobilization of the catalyst and solid support that have been applied. Additionally, continuous flow processes can be improved by new chemical techniques. These techniques include microwave assistance, new solvent systems such as fluorous biphasic system, ionic liquids or supercritical fluids. Membrane reactors or nanofiltration devices are required when the catalyst operates as a size enlarged species in solution.

One of the first continuous flow reactors utilized in metathesis reaction catalyzed by well-defined ruthenium complexes was the packed-bed reactor.[54] Polymer beads grafted with different ligands and coordinated with metal are filled into a glass/metal column which is attached to the pump. Such reactors suffer from uncontrolled fluid dynamics which result in stagnation zones and finally low selectivity and low process efficiency.

PASSflow (Polymer Assisted Solution-Phase Synthesis flow-through mode)[55] reactors are based on monolithic structures which present high void volume and large geometric surface area. Raschig rings could be considered as a flexible concept of a PASSflow reactor. This area was extensively explored by the group of Kirshning.[56]

Fogg and Roberge demonstrated how the reactor parameters affect the efficiency of the metathesis reaction.[57] Three types of reactors have been chosen: plug flow reactor (PFR) continuous stirred tank reactor (CSTR) and batch reactor (BR). As a model reaction the authors chose macrocyclization of 16 membered lactone ring. Reaction

performed in the PFC mode, consisted of two syringe pumps connected to the microstructured mixer and stainless steel coil immersed in oil batch, was found to be less selective and efficient compared to the bath mode. Such results are associated with increasing amount of ethylene that evolved during the reaction and entrapped in the coil. The CSTR setup provide space over the reaction mixture, which was continuously flushed with argon. Such approach allowed to overcome negative effect of ethylene and extensively increased efficiency of the reaction.

Lately Skowerski *et al.* presented a PFC reactor that overcome the ethylene issue.[58] The tube-in-tube reactor consists of a Teflon AF-2400 (an amorphous fluoropolymer, highly permeable to gas and non-permeable to liquid) inner tubing and non-permeable outer tubing.[59] The reaction mixture was passing though the chamber between the inner and outer tubes whereas inner tube was connected to the pump to remove ethylene constantly. Obtained conversions of model RCM reactions were significantly higher compared to those obtained by Fogg in a PFC reactor.

1.2.1. PURIFICATION METHODS APPLICABLE TO CLASSICAL RUTHENIUM CATALYSTS

The strength of purification methods applicable to the classical, commercially available catalysts lies in the easy access to ruthenium complexes, silica gel, activated carbon and multiple scavengers. On the other hand these methods are often time consuming and require use of a large excess of sequestering agent that could initiate side reactions.

Utilization of 5 mol% of ruthenium complex in metathesis reaction caused contamination of the crude product with 14316 ppm of the ruthenium content.[60] Single column chromatography on silica gel decreases Ru contamination to 1912 ppm,[46a] which is still much too high compared to acceptable levels. Cho and Kim were the first to publish the simple purification method. It consists of three consecutive steps: first, stirring of the crude reaction mixture with 10 equivalents of silica (relative to catalyst), then stirring of the filtrate with 50 equivalents of activated charcoal (relative to the crude product). Finally, column chromatography on silica is necessary. Such method allows to decrease ruthenium contamination level down to 12-60 ppm. When first step was omitted ruthenium contamination increased to 304 ppm.[61] This efficient and simple three step

protocol have been used in a few model RCM reactions. Even in the case of high catalyst loading, the presented method was very efficient, which have been proved in the case of macrocycle **42**, with only 12 ppm of ruthenium contamination in the product.

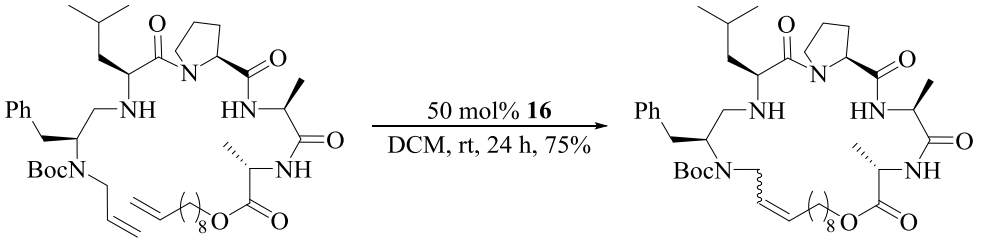

41 **42**

Scheme 8. Example of effective purification of metathesis reaction product.

Although the presented purification protocol is expensive and time consuming, it has been used in the purification of compounds of pharmaceutical interest. Details will be presented in the next part of this dissertation.

1.2.1.1. HOMOGENEOUS SCAVENGERS

Another separation strategy that has been thus far employed is utilization of ruthenium scavengers, such as tris(hydroxymethyl)phosphine (THP),[60] dimethyl sulfoxide,[62] triphenylphosphine oxide, or lead tetraacetate,[63] followed by numerous filtrations through silica gel or alternatively aqueous extraction. Such approach requires a large excess of scavenger compared to the catalyst, and sometimes, because of the high oxidizing power or toxicity of this reagent, the usage of this method is limited.[64]

Grubbs and Meynard reported the utilization of a water-soluble tris(hydroxymethyl)phosphine (THP). Such approach involves formation of the water soluble ruthenium phosphine complex from the ruthenium byproducts.[65] Further aqueous extraction, or stirring with SiO_2 and subsequent filtration led to removal of the ruthenium species.[60] Both protocols work well and reduced the level of ruthenium to 670 ppm and 206 ppm, respectively. However, this process required 89 equivalents of the phosphine scavenger and 2 equivalents of triethylamine, and in case of large scale applications the mixture has to be stirred at least for 12 h.[66] Georg improved Grubbs' protocol and applied much milder sequestering agents: triphenylphosphine oxide (TPPO) and DMSO.[62]

Reaction mixtures were treated with 50 equivalents of TPPO or DMSO over 12 h, then purified by column chromatography. Ruthenium contamination decreased to 240 and 362 ppm respectively. This approach have been examined with different substrates in RCM reaction, the best results have been achieved in case of **44**, with only 220 ppm of ruthenium contamination in the product. Even better results were achieved with DMSO as a sequestering agent. Utilization of large excess SiO_2 (4 g per each 0.001 mmol of catalyst) and DMSO (50 equiv. relative to catalyst) led to the reduction of Ru levels to 8 ppm.[67]

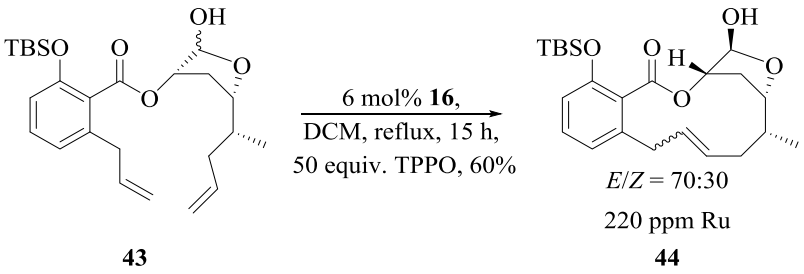

43 **44**

Scheme 9. RCM of **43** with subsequent purification using TPPO.

Another purification protocol has been published by Paquette.[63] It was based on oxidation of ruthenium species with lead tetraacetate, which was added to the crude reaction mixture in slight excess (1.5 equiv.). Ruthenium byproducts and other highly colored impurities have been converted into insoluble solid and filtered out through pad of silica. With this protocol Ru and Pb contamination could be decreased to 60 ppm and 5 ppm, respectively. Recently Knight *et al.* published a similar method.[68] The authors oxidized ruthenium species by the large excess of hydrogen peroxide. Ruthenium level was reduced only to 3020 ppm in case of **26** and 506 ppm in case of **29**, which is still too high compared to acceptable levels. The presented oxidation agents are either toxic to humans or too reactive, which therefore limits their utilization in the most crucial sector – pharmaceutical production.

Buchmeiser presented an alternative method of purification by extensive washing of the reaction mixture with a mixture of DMSO, ethyl vinyl ether and THF (1:1:1), or alternatively THF and ethyl vinyl ether (1:1), followed by methanol washing.[69] Ethyl vinyl ether is known as a quenching agent. It reacts with the ruthenium carbene to form a stable Fisher carbene complex.[70] Such procedure allowed almost quantitative removal of the transition metal residues. Ruthenium contamination in the obtained product was

below 0.1 ppm (below the detection limit of ICP-OES technique). Similar approach have been also presented by Liu and coworkers.[71] They utilized commercially available di(ethylene glycol) vinyl ether **45** and its derivatives **46** and **47** as sequestering agents. Addition of 4 equiv. of vinyl ether derivative followed by filtration through SiO_2 afforded metathesis products with ruthenium levels as low as 2 – 43 ppm.

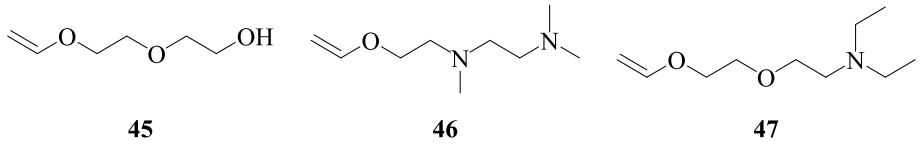

45 **46** **47**

Figure 9. Di(ethylene glycol) vinyl ester and its derivatives used as scavengers.

Recently, Diver proposed a simple method based on the degradation of all kinds of ruthenium catalysts. Isocyanide coordinates to the metal center and produces a very polar complex which can be easily removed using standard column chromatography leading to the decrease of the ruthenium contamination level to 120 ppm.[72] This protocol has been used in purification of ripostatin B after RCM reaction promoted by **32**.[73]

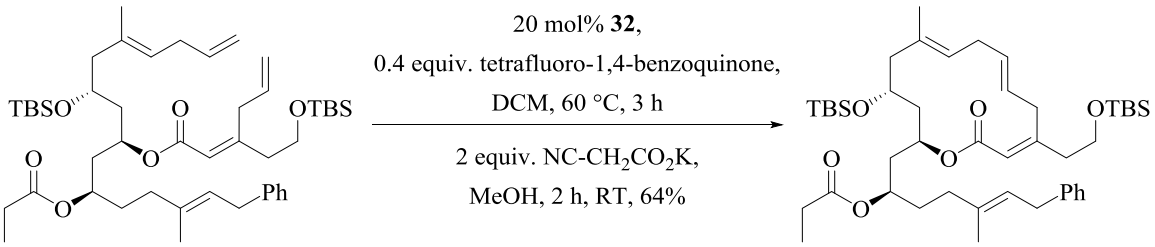

48 **49**

Scheme 10. RCM of ripostatin B precursor.

Apeiron Synthesis presented a family of isocyanide scavengers based on Divers work. Presented compounds are much more effective compared to the parent potassium isocyanoacetate. The highest effectiveness was obtained in toluene, as the addition of 4.4 mol% of **51** or 0.7 mol% of **52** followed by filtration through SiO_2 led to the decrease of ruthenium contamination to <0.0015 ppm.[74]

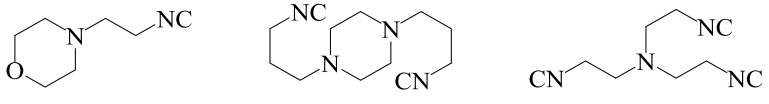

50 **51** **52**

Figure 10. Isocyanide scavengers presented by Apeiron.

The strategy that explored quenching of the metathesis reaction by modification of the solubility of the catalyst has been recently presented by researchers from Boehringer Ingelheim Pharmaceuticals. 2-Mercaptonicotinic acid has been used as a "solubilizing agent" which allowed the purification of RCM product only by extraction with aqueous bicarbonate.[75] Ruthenium contamination in the product was as low as 100 ppm. Details will be described in paragraph 1.2.1.3.

1.2.1.2. IMMOBILIZED, HETEROGENEOUS SCAVENGERS

Solid-supported scavengers have been used in organic synthesis since 1946.[48a,76] These reactive species not only selectively sequester by-products or catalyst of the reaction, but are also able to quench the reaction itself and can be easily removed by filtration. The advantage of heterogeneous scavengers attracted scientists that work on metathesis reaction. Utilization of this methodology in metathesis have been first described in 2004.[77] Breinbauer presented application of resin-bound phosphine **53** as an effective sequestering agent. Treatment of the reaction mixture with 20 equiv. of **53** followed by addition of charcoal and filtration led the decrease of ruthenium content to 1120 ppm.

Georg modified his earlier approach[62] and presented the TPPO anchored to a resin **54**.[67] The best results were observed when the crude product was refluxed with 100 equiv. of **54** and 50 equiv. DMSO and then purified by column chromatography. Ruthenium levels have been reduced to 8 ppm.

In 2006 Crudden presented utilization of mesoporous silicates functionalized with aminopropyltrietoxysilane **55** as sequestering agents.[78] The presented procedure affords 776 ppm of ruthenium content after two consecutive treatments with **55** without any chromatographic purification.

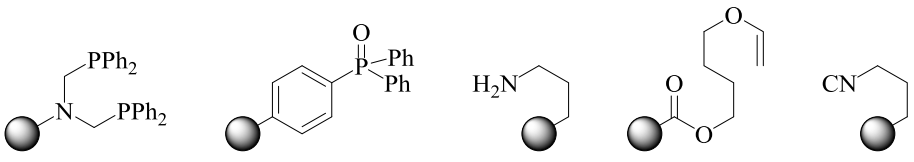

53 **54** **55** **56** **57**

Figure 11. Solid supported scavengers.

Based on the Liu concept[71] Slugovc presented polymer supported 1,4-butenediolvinyl ether derivative **56**.[79] The material was efficient in the removal of **28** from its solution, unfortunately its scavenging properties were not evaluated. This approach have been also used by Bergbreiter *et al.* who presented PIB immobilized vinyl ether.[80]

Davies presented supported isocyanide **57** as sequestering agent.[81] This modification improves the efficiency of purification compared to the previous work.[72] Treatment of the reaction mixture with 60 equiv. of **57** followed by column chromatography lead to 1-6 ppm ruthenium contamination. The effectiveness of this procedure has been evaluated in different metathesis reactions conducted with a variety of ruthenium complexes with almost quantitative sequestration.

Iron oxide nanoparticles Fe@Fe_xO_y are known as good sequestering agents for a variety of metals for aqueous[82] and organic media.[83] This method led to the decrease in ruthenium contamination to 65% (9035 ppm), while in combination with cysteamine further to 556 ppm and with 3-mercaptopropionic acid to 278 ppm.[84]

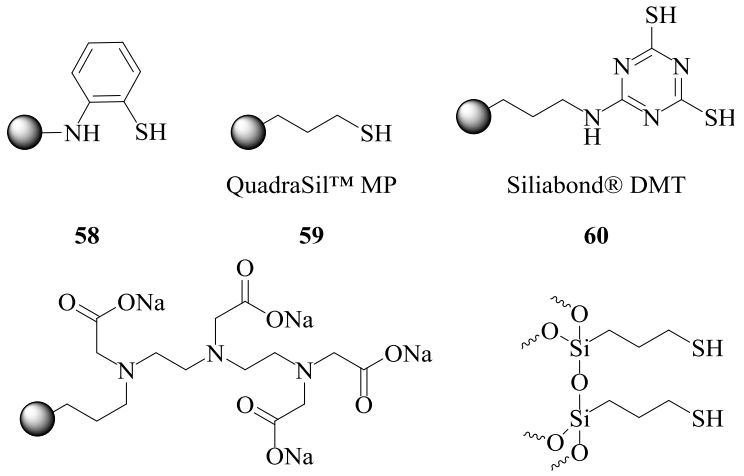

Figure 12. Commercially available solid supported scavengers.

Variety of heterogeneous functionalized polymers and sequestering agents for the removal of traces of heavy metals are commercially available.[85] Treatment of the metathesis product with 100 equiv. of tiol-modified silica as **59** or tetrasodium triaminetetraacetate-modyfied silica **61** lowered ruthenium contamination to 10 ppm.[86]

1.2.1.3. EXAMPLES FROM THE PHARMACEUTICAL INDUSTRY

Despite the great number of metathesis catalysts, there is yet an ongoing quest for the improvement of their activity, justified by the variety and different nature of substrates to which they are applied, and as each reaction needs its own perfect catalyst, it also needs its effective purification method. Meanwhile, it is often hard to predict what kind of catalyst a reaction may require. Consequently, in the pharmaceutical industry[87] extensive screenings of catalysts along with purification procedures are necessary, to identify the catalyst that could deliver optimal productivity, activity, and selectivity, while also being easily removed from the post-reaction mixture.

Researchers at Boehringer Ingelheim have published a series of articles concerning preparation of antiviral drug **64**, a hepatitis C virus NS3 protease inhibitor, which nicely illustrates the issues synthetic chemists are facing in the pharmaceutical industry, as well as the strategies to solve these problems.[88]

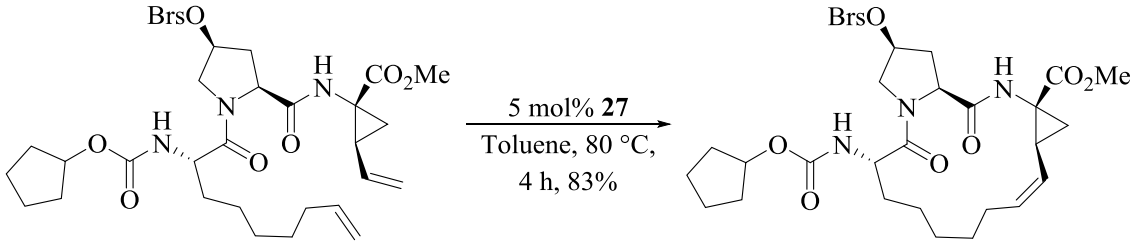

63 **64**

Catalyst (loading)	workup procedure	Ru level (ppm)
26 (5 mol%)	THP (25 equiv.)	623
27 (1.5 mol%)	**59** (10 equiv.)	109
27 (1.5 mol%)	**58** (10 equiv.)	293
27 (1.5 mol%)	**59** (100 equiv.)	262
29 (3.5 mol%)	THP (60 equiv.)	260
29 (3.5 mol%)	THP (60 equiv.), charcoal	32
29 (3.5 mol%)	THP (40 equiv.), charcoal	64

Scheme 11. Screening of the catalysts and workup procedures.

The key step for the preparation of the molecule was a RCM of 15-membered ring. In the beginning of the optimization 5 mol% of **27** have been used to close the ring.[89] The initial work up consisted of several aqueous extractions followed by charcoal treatment. Precipitation of the product afforded the desired macrocycle contaminated with

500-1000 ppm of residual ruthenium. Such amount of ruthenium in the product required optimization of the purification method. Several techniques known in the literature were explored (Scheme 11).[90] Use of THP for aqueous extractions lowered the ruthenium levels to 32-623 ppm. Silica based scavengers (**58**, **59**) were also tested, although with lower level of success.

To make the overall synthesis more convergent, minor changes to the initial synthetic pathway were undertaken for an expedient assembly. For the successful conversion of *para*-nitrobenzoate (PNB) protected substrate **65a** have been used. The RCM of **65a** was accomplished in 90% yield at 60 °C in toluene with the catalyst loading of 3.5 mol%, in 20 hours. Extensive screening of the sequestering agents showed that the best results were obtained when mercaptonicotinic acid as a sequestering agent was used followed by treatment with charcoal in EtOAc and recrystallization from heptane/EtOAc. Such procedure reduce the ruthenium contamination to 4 ppm.[91]

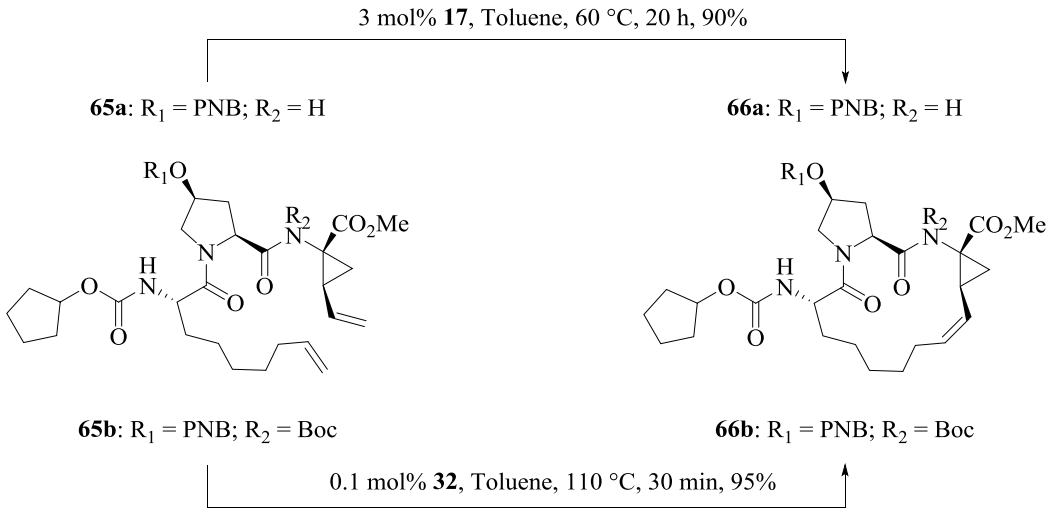

Scheme 12. Influence of protecting group on RCM reaction.

Further modification of the process led to the utilization of substrate **65b** in the presence of catalyst **32**. Using only 0.1 mol% of **32**, the RCM reaction was complete within 30 min in toluene at 110 °C.[92] Using a lower amount of catalyst was not only more economical, but also made the purification step easier especially on industrial scale. In the previous process (**65a** to **66a**) quenching the catalyst and extraction required excess of 2-mercaptonitronic acid (2 kg MNA for 1 kg product), large volumes of bicarbonate and silica filtration with charcoal treatment to reduce the ruthenium contamination to 100–200

ppm. Utilization of much lower catalyst loading led to a 50-fold lower amount of MNA used in purifications process. No filtration through silica or charcoal treatment were necessary. Ruthenium contamination after RCM was below 50 ppm.[75b,93]

Wang and co-workers at GlaxoSmithKline published several RCM approaches for the preparation of potent cathepsin K inhibitor, a candidate for the treatment of osteoporosis and osteoarthritis.[94]

First attempts were based on substrates **67** and **68**. A variety of different ruthenium complexes has been investigated, and the full conversion has been achieved with 10 mol% of **30**. Lower loading of ruthenium complexes led to incomplete reaction. Addition of Ti(O*i*-Pr)$_4$ as additive[95] with **26** and **29** led to decomposition of the starting material. Notably, the residual ruthenium was found to be difficult to remove, as treatment with THP caused decomposition of the product.

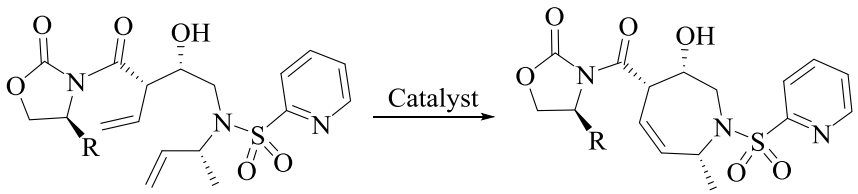

67 R = Bn
68 R = Ph

69 R = Bn
70 R = Ph

Diene	Catalyst (loading)	Conditions	Conversion
67	**30** (10 mol%)	Toluene, reflux	100%
68	**30** (10 mol%)	Toluene, reflux	100%
67	**30** (5 mol%)	Toluene, reflux	60-79%
68	**26** (10 mol%)	DCM, 40 °C	6%
67	**28** (10 mol%)	DCE, RT to 80 °C	7%
68	**29** (10 mol%)	DCE, 80 °C	24%

Scheme 13. RCM of cathepsin K inhibitor precursor.

For the second approach substrate **71** was prepared. The RCM reaction was accomplished with only 1 mol% of **30**. Extensive screening of the sequestering agents showed that silica gel or alumina scavenged only around 50% of Ru contamination. Combination of P(CH$_2$OH)$_4$Cl/NaOH or cysteine/NaOH removed 80% of impurities. Unfortunately, phosphine/base protocol generated formaldehyde as a byproduct, leading to decomposition of the main product. For further investigation and scale-up, basic

aqueous cysteine procedure have been chosen, which decreased ruthenium contamination to 148 ppm.[94b]

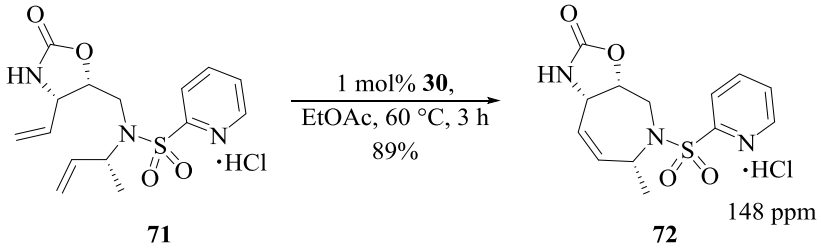

71 **72**

Scheme 14. RCM of cathepsin K inhibitor precursor.

The final scaling up of the reaction was performed with yet another derivative. Cyclization of oxazolidionone diene **73** with 0.25 mol% loading of **30** proceeded smoothly in toluene, reaching completion within 2 h at 80 °C.

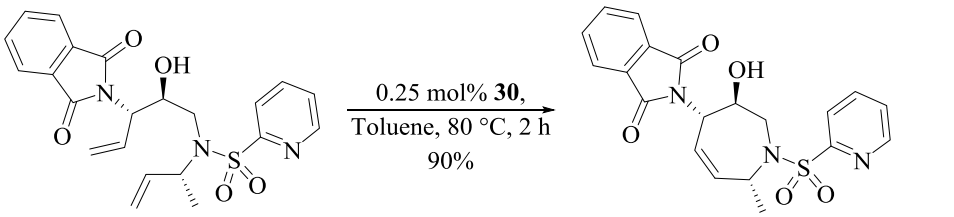

73 **74**

Scheme 15. Scale-up of the RCM cathepsin K inhibitor precursor.

The obtained product had very low solubility in toluene and crystallized from the reaction mixture upon formation. A simple filtration afforded **74** in 90% yield contaminated with 121 ppm of ruthenium.[96]

As presented above, decomposition of the catalyst is accepted for the sake of facilitated product purification. Even though E-factor is low, recycling of the catalyst is economically dispensable when value of the product substantially exceeds that of the catalyst. Only the metal may later be recovered and recycled.

1.2.2. PURIFICATION METHODS APPLICABLE TO MODIFIED CATALYSTS

To enhance its recyclability, modifications of a classical metathesis catalyst were undertaken. Ruthenium complexes are amenable to the introduction of additional

functional group in a few distinct positions. Tags can be connected (Figure 13) through non-labile ligands (pointed in black), or through labile ones (marked in red).

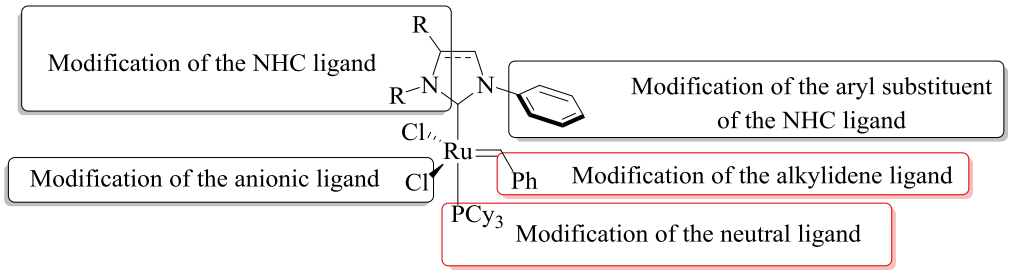

Figure 13. Possible position of tagging ruthenium catalyst based on **29**.

Ruthenium catalysts have been bound to different tags, including: (a) insoluble polymers; (b) inorganic materials (e.g. silica gel); (c) ionic liquid (IL) functionalities; (d) perfluorinated hydrocarbons; (e) soluble polymers or small-molecule functionalities. In an ideal case, modified catalysts can be easily retrieved from the reaction mixture by either filtration (nanofiltration) when considering (a), (b) and (e) above, or extraction into IL in the case (c), fluorous phase in the case (d) and non-polar solvent in the case (e).

I divided the catalysts in two main groups: heterogeneous and homogenous, and then based on material that have been bound to the complex. Within every group I present examples of different placement of tag connection.

1.2.2.1. HETEROGENEOUS COMPLEXES

The immobilization of known homogeneous ruthenium catalysts on different resins or silica was proposed as a modification aiming to facilitate purification. Heterogeneous catalysts have several advantages such as easy handling and recyclability, which lead to its utilization in multiple batches of the reaction. Catalyst stability also should be improved by inhibition of intermolecular interactions, simultaneously preventing undesirable bimolecular decomposition pathways. However, solid-phase catalysts often suffer from disadvantages like low activity compared to parent catalysts, high price of the solid support and, the most important, their recyclability is largely theoretical, since the catalyst is rapidly inactivated in successive cycles.

1.2.2.1.1. IMMOBILIZATION ON INORGANIC MATERIALS

The immobilization of ruthenium catalyst on various supports can be performed using two main approaches: covalent binding and adsorption. Inorganic materials offer excellent mechanical and thermal stability and low costs. They are compatible with almost all solvents and they are resistant to swelling.

The first and most straightforward approach of immobilization is the utilization of the phosphine solid support as an anchor. Complex **75** immobilized on mesoporous material MCM-41 (0.96 wt% Ru) was active in RCM of DEDAM. Conversions of 71% have been obtained in 30 min at RT with 5 mol% of **75**. This result was much poorer compared to the parent catalyst **27** (98%). Minor leaching has been observed, with 1.2 % (172 ppm) Ru contamination in the product.[97]

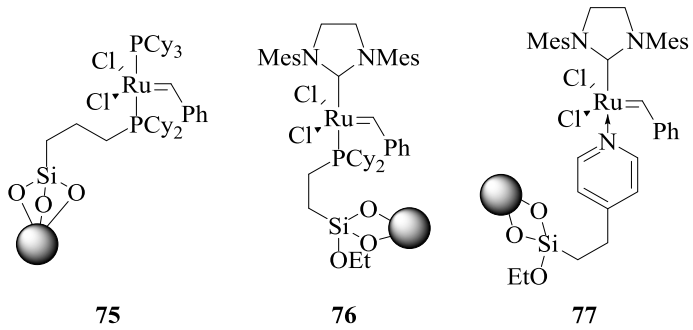

75 **76** **77**

Figure 13. Different possibility of tagging through neutral ligands based on Grubbs type complexes.

Hynek *et al.* presented immobilization of second (**76**) and third (**77**) generation of Grubbs type of catalyst on mesoporous molecular sieves MCM-41.[98] Both catalysts are active in the model RCM reaction with DEDAM, and after 5 h in 80 °C in toluene with 0.4 mol% of **76** and **77**, 90% and 60% of the conversions have been achieved, respectively. Catalyst **76** was found to be much more active compared to **77**, which after achieving 60% of conversion was probably deactivated. Nevertheless, leaching of ruthenium is much lower in the case of **77** than **76**, with 3.7 ppm and 105 ppm of ruthenium contamination, respectively. Tests of reusability of **76** in 6 cycles have been performed. After the first cycle conversion dropped to 76% then 70%, 56%, 48% and 29% of conversion have been achieved. On the other hand, **78** can be recycled multiple times very efficiently without leaching ruthenium (starting loading 0.75 mol%), and ICP-

MS analysis of the reaction solution shows < 5 ppb of ruthenium contamination after each cycle. These results encouraged authors to synthesize *p*-*N*-aryl anchoring derivative **79**, which was found to be less active compared to **78**. Nevertheless, **79** presented the same ruthenium leaching as analogue **78**. Complex **78** was found to be 2 – 3 times less active compared to the parent catalyst **30**. Differences in the activity between **78** and **79** can be caused by a steric interaction between the support and the active site.[99]

Chung reported ruthenium complex anchored to the siliceous mesostructured cellular foam (MCF). Obtained **80** presented high activity towards RCM of *N*,*N*-diallyl-4-methylbenzenesulfonamide. Complex showed almost no decrease in activity and leaching as after seven cycles with 5 mol% of **80** isolated product yields of 93 – 88% were achieved, with only 0.4 – 1.3 ppm of ruthenium content.[100]

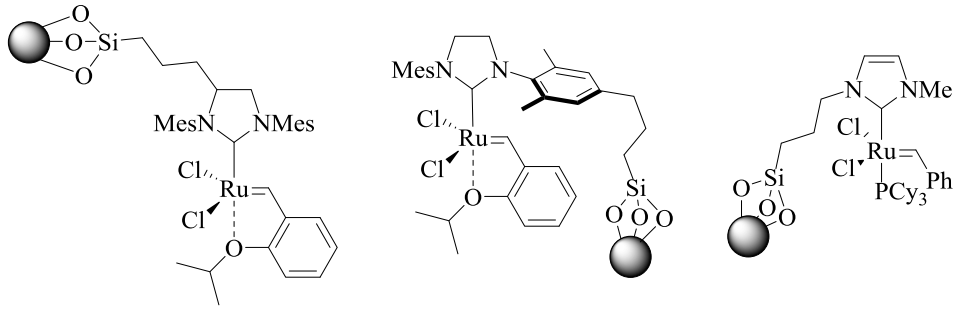

78 **79** **80**

Figure 14. Immobilization through NHC ligand.

Tagging through an anionic ligand was developed by Mol,[101] and optimized by Buchmeiser.[54b,c,102] This approach was also employed by groups of Grela and Hynek, who showed that **81** can be recycled in only two cycles, but with ruthenium contamination level in product as low as 17 ppm, while the activity of **81** was comparable to its homogenous analogue.[103] Lately Marciniec *et al.* presented grafting of **30** homologue on Aerosil 300.[104] Two plausible grafted species have been proposed with either one (**82b**) or two (**82a**) Ru-O bonds formed by substitution of one or both ionic ligands. The obtained mixture of complexes presented much lower activity towards DEDAM compared to the parent catalyst. These phenomena can be explained by the increased steric hindrance surrounding the ruthenium catalytic center. Nevertheless, these species were found to be very stable and could be reused within 15 cycles without significant loss of activity and leaching.

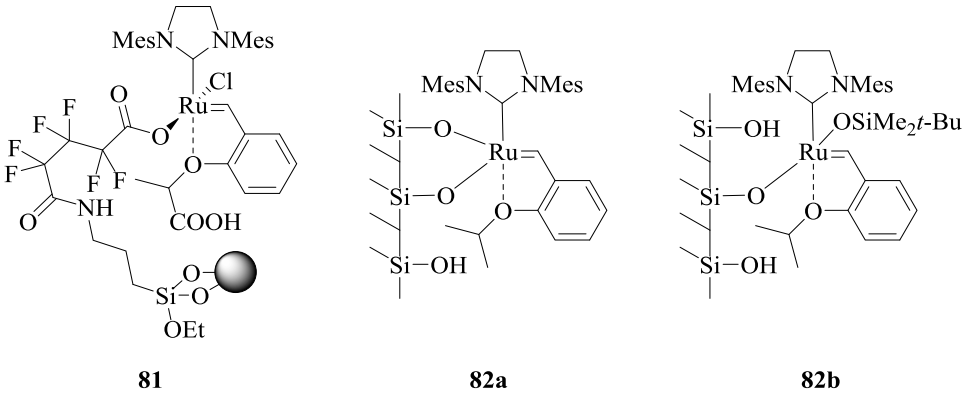

81 **82a** **82b**

Figure 15. Immobilization through ionic ligand.

Immobilization through modification of the benzylidene ligand is the easiest approach but also the most labile during catalytic cycle. Few approaches have been proposed thus far.[105] Blechert *et al.* presented simple modification of the benzylidene ligand followed by immobilization on LiChroprep Si 60®.[106] The obtained complex presented similar catalytic activity as the parent complex. Reusability of **83** has also been investigated, and with 0.15 mol% loading the complex could be reused two times without significant loss of activity. Ruthenium contamination in the product has been decreased to 32 ppm and 12 ppm in each cycle, respectively.

Lately Lee *et al.* presented complex immobilized on MCF, which can be considered as a complex of interconnected nanoreactors where catalyst is immobilized inside, on the "reactor wall".[107] Most of immobilized catalysts are isolated from the bulk of environment and conduct the reactions in nanopores.

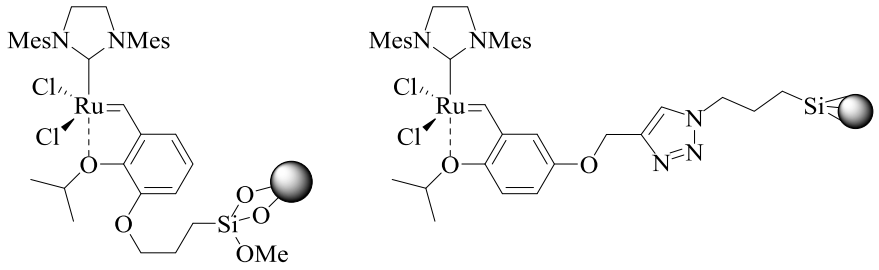

83 **84**

Figure 17. Immobilization through benzylidene ligand.

Complex **84** was tested in variety of RCM reactions, with good yields and higher activity towards macrocyclic RCM than the homogenous analogue **20.** Complex can be reused up to 10 times without significant decreasing of activity and with ruthenium

contamination of the product at low level of 3 to 8 ppm. RCM reaction under flow conditions in a circulating system have been investigated with **84** in a packed bed reactor. Almost quantitative conversions have been obtained after 1 h, but surprisingly contamination in the product was much higher – 607 ppm compared to batch conditions of 17 – 115 ppm. Further investigation led to the conclusion that tagging through benzylidene ligand is unsuitable for continuous flow conditions. Higher leaching of ruthenium compared to the batch system is due to the dominant dynamic release-return pathway[108] along with a lower emission of ethylene.[109]

1.2.2.1.2. NON-COVALENT IMMOBILIZATION

The non-covalent immobilization has been proposed as a simple alternative to the traditional immobilization. There is only one drawback of this method – strength of the bond between complex and the surface, which depends on the reaction conditions (temperature, substrate, solvent).

This method is based on the previous research published by Hoveyda[32] and Fogg,[110] where catalysts were easily recovered from the reaction mixture by a column chromatography. Instead of recovery after reaction, Jacobs *et al*. decided to mix first the catalyst with silica gel and then to conduct metathesis reaction. Catalyst **40** anchored on silica was found to be active in metathesis reaction. When the reaction was conducted in non-polar solvents as hexane, leaching of the catalyst was around 7 ppb, but when the solvent was exchanged to more polar like diethyl ether, the rate of leaching of the catalyst significantly increased.[111] The same effect can be observed in aromatic solvents or DCM.[112] The positive effect of the pore size in mesoporous molecular sieves on the activity of supported catalyst have been also demonstrated.[113] Thus far a variety of homogenous catalysts have been immobilized on different porous silica supports.[114] Catalyst that show extraordinary affinity to silica gel are the most suitable in this method.[115]

Latest research shows that the weak physisorption-based interaction between catalyst and complex can be responsible for the increased catalyst leaching; modification to promote stronger interactions such as, for example, forces between ammonium and silanol groups can prevent catalyst leaching even in polar systems.[113]

Recently this type of complexes has been used in continuous flow conditions[116] as well as in the tube-in-tube reactor.[58] Both applications present high selectivity and activity of the examined catalysts, similar or better than those obtained in the batchwise mode.

1.2.2.1.3. IMMOBILIZATION ON POLYMER SUPPORT

Polymers as a solid support are widely used in organic chemistry. Ruthenium complexes are mostly immobilized on polystyrene-divinylbenzene (PS-DVB), polyethylene, polypropylene and various of resins. These types of supports have been explored at the beginning of the studies on immobilized ruthenium complexes. Now, polymer supports are dominated by a variety of silica supports. The biggest drawback of polymers is their incompatibility with many common solvents. Moreover the properties of the immobilized catalyst can be completely different from those of the homogenous version.

The first example of immobilization of the ruthenium complex on polymer was presented in 1995. Complex **85** appeared to catalyze CM reaction 150 times slower compared to its homogeneous analogue.[117] Buchmeiser *et al.* presented immobilization of the Grubbs analogue onto monolite material. Complex **86** efficiently promoted RCM and is known only in heterogeneous variant, as homogenous analogue could not be formed.[54a] Later on *N*-substituent anchored Grubbs analogue **87** has been synthesized. Both complexes were deployed as fixed beds in a cartridge for applications in combinatorial or flow chemistry of various reaction including RCM, ROCM and enyne metathesis. The ruthenium contamination in the product was found to be approximately 70 ppm.

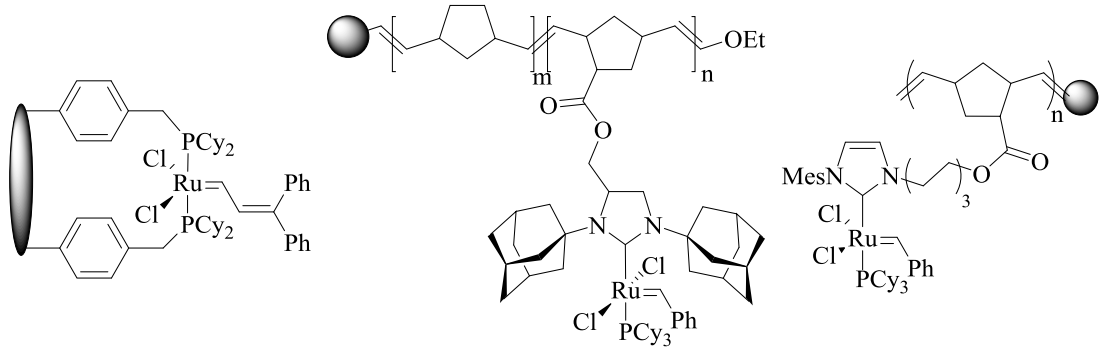

85 **86** **87**

Figure 18. Examples of immobilization of Grubbs type complexes.

Anchoring through the alkylidene ligand was firstly reported by Barrett and co-workers,[118] and then modified by Nolan,[119] Blechert,[120] Hoveyda,[121] Dowden,[122] Grela,[123] and many others.[124] This type of catalyst could be reused for up to 20 cycles without a significant loss of activity, but the ruthenium contamination in the product is high in most cases (above 300 ppm). Complex **84** that was anchored on MCF exhibits extraordinary activity, but when immobilized on TentaGel-support it showed sluggish initiation and prolonged reaction times.[107a]

1.2.2.1.4. IMMOBILIZATION ON MAGNETIC NANOPARTICLES

Magnetic nanoparticles (MNPs) have attracted a great interest due to their high stability, size and the simplicity of the separation by magnetic attraction.[125] Up to date only few examples of MNP-supported ruthenium complexes have been described. All of the modifications that have been utilized rely on labile benzylidene ligands. Zhu[126] and Che[127] reported independently utilization of magnetically-retrievable metathesis catalysts. **88** conducted the RCM reaction of a variety of substrates with excellent yields and could be recycled up to 22 cycles with almost no loss of activity.[127] On the other hand, activity of **89** was evaluated in oleo metathesis reactions with results comparable to the performance of **29**. It could be recycled up to 5 cycles without considerable loss in catalytic efficiency, with less than 3 ppm of ruthenium leaching.

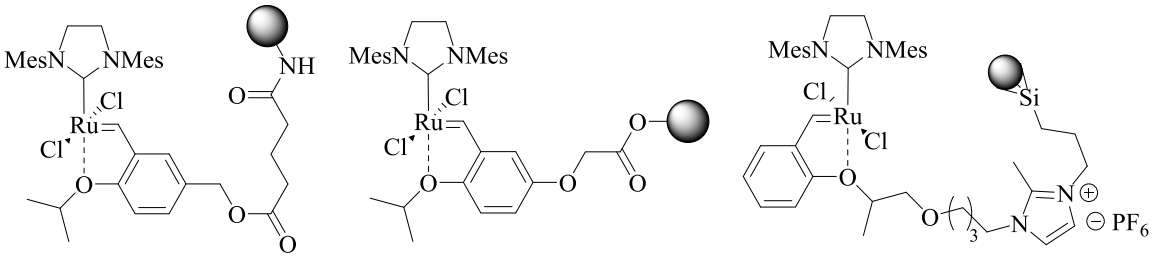

88 **89** **90**

Figure 19. Magnetically recoverable ruthenium complexes.

The latest modification utilized imidazolium salt linker.[128] Catalyst **90** exhibits excellent activity in RCM and CM reactions with loading lower than 1 mol%. Catalyst can be easy recovered and reused within 6 cycles without significant loss of catalytic activity. Leaching of the ruthenium is much higher compared to the previously described catalyst **88** and **89**, with 50 ppm compared to 3 ppm, respectively. During the first three cycles 54% of ruthenium leached from the support.

1.2.2.2. HOMOGENOUS CATALYSTS

Introduction of a tag into the structure of catalyst to modify solubility of the corresponding complex within special environment leads to the efficient recyclability and recovery of the catalyst.

1.2.2.2.1. IONIC GROUP TAGGING

In the early experiments ionic tags were utilized to increase solubility of such catalysts in water.[129] Unfortunately, **91** and **92** have been unstable and air-sensitive.[130]

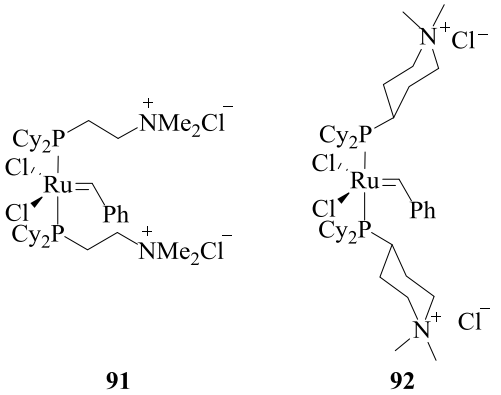

91 **92**

Figure 20. First attempts in ionic tagged water soluble complexes.

Another approach exploiting catalysts with ionic tags is conducting reaction in ionic liquids.[131] IL have recently received increasing attention as an environmentally preferable organic solvent alternative. They are nonflammable, low toxic, recoverable solvents with very low vapour pressure, and easy modulation of viscosity.[132] Most used room temperature IL are based on iminium or piridinium salts (Figure 21).

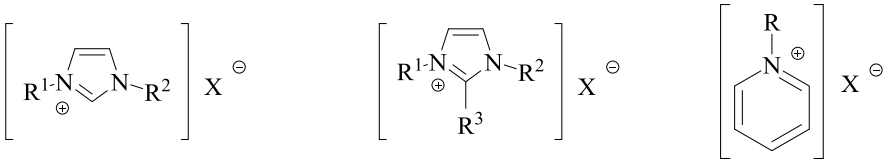

[emim]=R^1=Me, R^2=Et
[bmim]=R^1=Me, R^2=*n*-Bu
[hmim]=R^1=Me, R^2=*n*-C_6H_{13}
[omim]=R^1=Me, R^2=*n*-C_8H_{17}

[bdmim]=R^1=Me, R^2=*n*-Bu, R^3=Me

X= BF_4, PF_6, CH_3COO, CF_3SO_3, NTf_2

Figure 21. IL with possible counterions.

Dixneuf *et al.* presented the first efficient utilization of IL in metathesis reaction.[133] Cationic ruthenium-allenylidene **93** was found to be soluble in IL and active in biphasic conditions of [bdmim]/toluene. Both catalyst and IL could be reused. To improve solubility in the IL, catalysts with imidazolium motif as an ionic tag within benzylidene ligand have been designed.[134] These systems exhibit excellent reactivity, and the catalyst could be recovered, up to 10 cycles in a biphasic CH_2Cl_2/[bmim]PF_6 medium. **94** has been recovered up to 8 times, with 22 ppm of ruthenium contamination in the product.

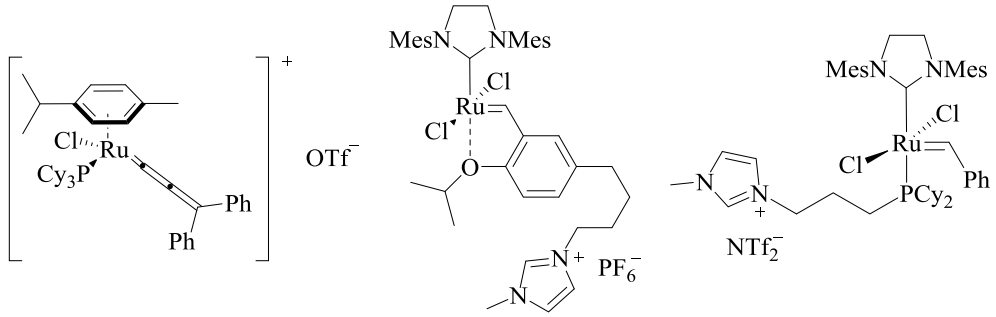

93 **94** **95**

Figure 22. IL immobilized complexes.

Consorti and Dupont presented similar concept, an ionophilic Ru complex **95** with an IL tagged to a phosphine ligand.[135] This approach enabled efficient recovery and reuse of the catalyst in up to 8 cycles, with <2 ppm of Ru contamination in the product at 0.25 mol% loading. Unfortunately, the catalyst is suitable only for simple substrates.

The new concept has been proposed by groups of Grela[136] and Mauduit[137] whereby an electron-withdrawing group was tagged to the benzylidene ligand. Pyridinium and ammonium moieties was responsible for an electronic activation of the catalysts, and high solubility in IL. Leaching of ruthenium was very low, and after simple filtration through a pad of silica Ru contents of 12 – 59 ppm for **96** and 25 – 173 ppm for **97** were determined. However, these catalysts are efficient only during the first cycles, with a significant loss of the activity in subsequent runs.

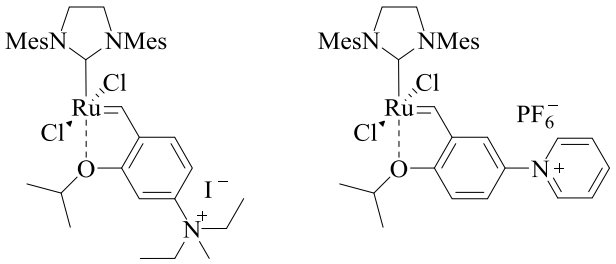

96 **97**

Figure 23. Ruthenium complexes with ionic tag.

Furthermore, complexes have been utilized in a variety of conditions such as: anchoring onto Raschig rings,[138] or onto an ionic polymer (SLIP),[51a,e,56a,139] continuous flow[140] with CO_2 as a transport vector[141] with good results and very low leaching even down to 0.03 ppm ruthenium content in the product.

Ionic tagging exhibits also other properties, as pH-responsive phase tag,[142] which leads to product contaminated with up to 10 ppm of ruthenium content. High affinity to silica (for example **38** or **40**) has been presented by Skowerski[143] and Grela.[144] They are easily removed from the reaction mixture by simple filtration through silica plug, to reduce ruthenium contamination even to <0.004 ppm.

1.2.2.2.2. FLUOROUS TAGGING

Fluorous techniques are useful methods for high-throughput synthesis because fluorous media constitute a liquid phase immiscible with other liquid phases. Reaction of a fluorous-tagged compound with organic compounds are conducted at higher temperature (monophasic) and the separation is pursued at lower temperature (biphasic).[131b,145] This approach has become popular because of its potential as a new paradigm of green chemistry.[146] Purification of the desired product can be achieved either via filtration through a short pad of fluorous-phase silica or by fluorous-phase extraction. Curran synthesised catalyst **98** which was found to be very active, and could be reused with up to 7 cycles. In each cycle, only 65 – 88 % of the catalyst could be recovered, so after seventh cycle, only 10 % of the original catalyst was retrieved. Ru contamination in the product was estimated at around 500 ppm.[147]

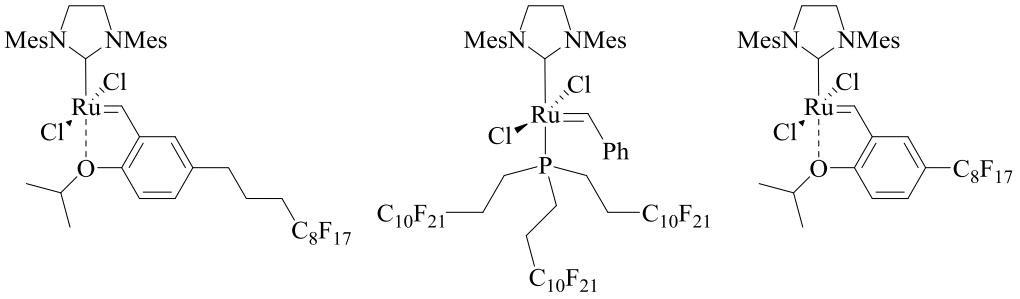

98 **99** **100**

Figure 24. Catalysts with fluorinated tags.

Catalyst **99** could be used under monophasic or biphasic conditions, although the catalyst is much more active under the latter conditions. It could be recycled up to three times without significant loss of activity. Recovery of the catalyst was not quantitative (first cycle – 90 %, second – 85 % and third – 57 %).[148]

Straightforward connection of a fluorous tag to a benzylidene ligand have been proposed by Matsugi (**100**). This modification not only simplifies the purification process but also improves the catalytic activity through the electron electron-withdrawing nature of the perfluoroalkyl chain. It could be recycled up to 5 cycles by fluorous solid phase extraction with minimal loss in reactivity.[149]

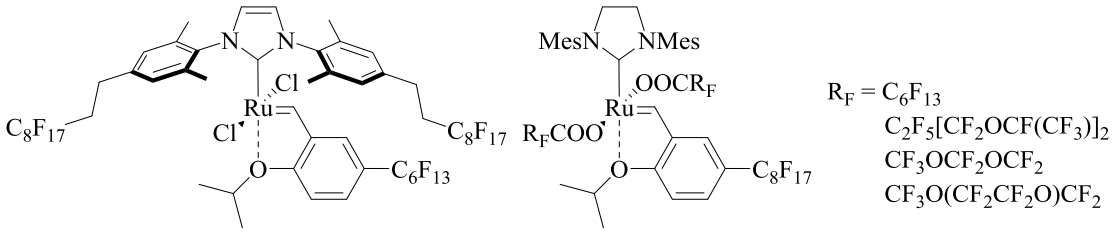

101 **102**

Figure 25. Catalysts with fluorinated tags synthetized by Kvíčala.

Based on work of Matsugi[149] and Curran[147] Kvíčala *et al.* proposed tagging through non-labile NHC and ionic ligands. Although **101** contains three fluorinated tags, its fluorophilicity is still too low to be regarded as a heavy fluorous and be efficiently recycled from the reaction mixture by fluorous/toluene liquid extraction. **101** was found to be less active than **100** and **30**. Next, a family of polyfluorinated complexes (**102**) have been synthesized with tagging via ionic ligands. Even though fluorophilicity of the complexes increased, activity and stability decreased rapidly with the size of the ionic tag.[150]

1.2.2.2.3. SOLUBLE POLYMER TAGGING

Soluble polymer-supported synthesis utilizes polymers that are soluble in a variety of organic solvents. The reaction is conducted in solution. For purification and recovery of the catalyst addition of solvent in which polymer is insoluble followed by simple filtration is sufficient. [151]

The first soluble polymer that has been used was as a tag in a ruthenium complex was hydrophilic poly(ethylene glycol) (PEG). PEG polymers are soluble in DMF, DCM, toluene, acetonitrile, water and methanol, but insoluble in diethyl ether, tert-butyl methyl ether, isopropanol, and cold ethanol. Complexes with PEG tagging were designed to be soluble in water, unfortunately most of them aggregate in micelles which decreases their catalytic activity.[42e,129,152] When utilized in organic solvent **39** (Figure 8) shows similar activity to **30**. After dissolving the crude product in diethyl ether and extracting several times with water ruthenium contamination decreasing to 41 ppm. Additional 24 h of stirring with activated carbon reduce the Ru content below detection limit (0.04 ppm).[42f,153] Other approach of PEG tagging have been also presented, mostly by anchoring through benzylidene ligand. This type of modified catalysts could be reused up to 17 cycles. Unfortunately contamination of the product was mostly not determined.[42d,154]

Based on previous work,[155] Bergbreiter *et al.* presented opposite approach, in which they utilized lipophilic polyisobutylene (PIB) oligomers as tags.[156] The resulting complex **103** was soluble only in heptane, and could be easily recovered by simple liquid/liquid or liquid/solid separation.[157] This particular catalyst is very active and stable, it could be recycled up to 5 cycles without significant loss of activity. RCM of DEDAM was carried out in heptane and then the product was extracted with acetonitrile; it was contaminated with 430 ppm of ruthenium. Within catalyst **104** the PIB tag was attached to the NHC ligand, which led to a 10-fold reduction in Ru contamination in comparison to **103**, with only 40 – 77 ppm of ruthenium content.[158] Moreover, **104** could be recycled up to 20 times. Latest results present utilization of both complexes in ROMP polymerization with good results.[159]

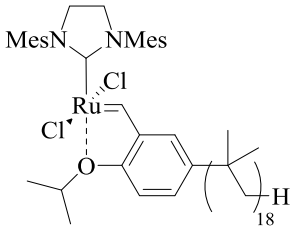

103

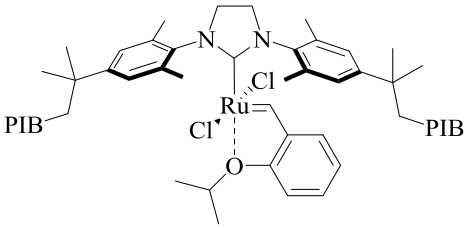

104

Figure 26. Catalysts with non-polar tags.

Termomorphic polyethylene is soluble in hot nonpolar solvents, but completely insoluble at room temperature in any solvent.[160] Bazzi and Bergbreiter utilized this property and presented complex **105** which could be recovered up to 5 times without significant loss of activity in RCM reaction. Purification procedure that has been used relied upon cooling the reaction mixture to room temperature to precipitate **105**, followed by washing up with toluene. This procedure led to 77 ppm of ruthenium content in the product.[161]

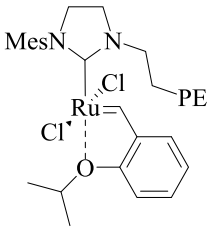

105

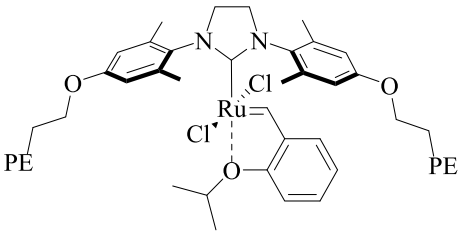

106

Figure 27. Catalysts with termomorphic tag.

Lower hindrance of *N*-alkyl substituted NHC in **105** led to faster decomposition of the corresponding complex, which explains slightly lower recyclability and stability of **105** in comparison to previously described complexes. To confirm this hypothesis catalyst **106** has been synthesised. It was found to be much more stable and could be recycled up to 8 times with 43 ppm of ruthenium contamination in the product.

1.3. MEMBRANE PROCESSES

Membrane processes, well-known separation processes, are pressure driven membrane-based separation techniques where an incoming feed stream is separated into two components referred to as the permeate (solvent and solutes able to pass through the membrane), and retentate (solvent and solutes unable to pass through membrane).[162] The separation driving force is the pressure difference, the so called transmembrane pressure (TMP), between the two sides of the membrane acting as a physical barrier useful for separation.

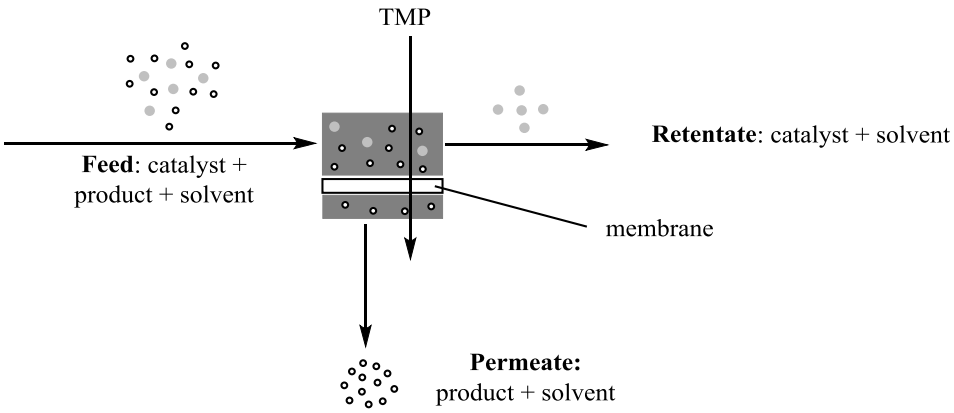

Figure 28. Principle of NF (nanofiltration) separation in the case of filtration of media containing solvent, catalyst and final products of reaction.

Membrane processes have found numerous industrial applications such as water and dairy purification, sea and brackish water desalination, waste water reclamation, food and beverage production, gas and vapour separation, energy conversion and storage, air pollution separation. Lately it became more and more popular in purification of organic solvent mixtures. The scope of the applications of membrane technology is still extending as they offer the advantages of highly selective separation, continuous, automatic and economical operation at ambient temperature, and simple integration into existing production processes, as well as appreciable energy savings.[163]

According to pressure required for the separation (bar), size of the pore (nm) and molecular weight cut off (MWCO) (g/mol) membrane processes have been classified into: microfiltration (MF), ultrafiltration (UF), nanofiltration (NF), and reversed osmosis (RO).

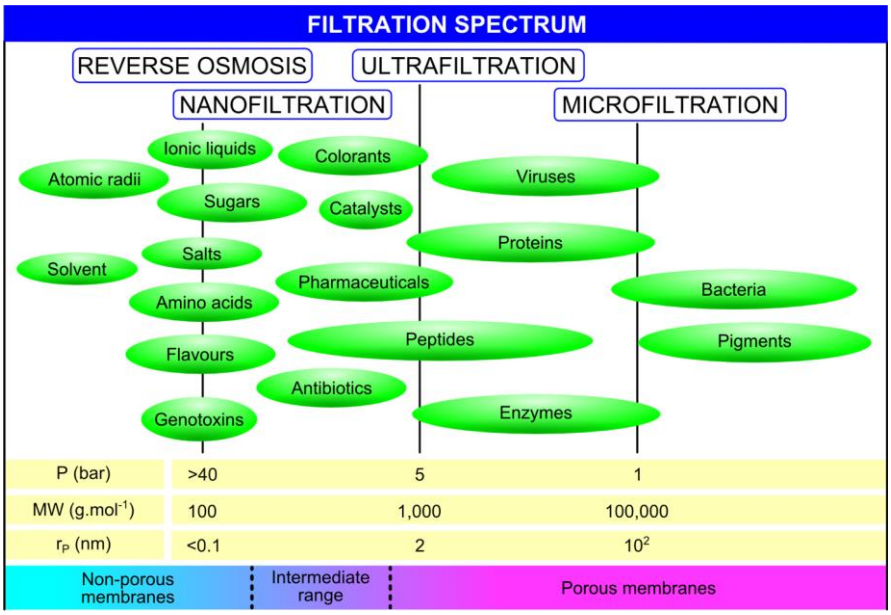

Figure 29. Classification of membrane processes according to operating pressure, pore size, MWCO, transport mechanism with examples of application. (Reproduced with permission from ref. 164. Copyright 2014 American Chemical Society)[164]

The term "nanofiltration" have been proposed in 1984 for the reverse osmosis process that selectively allows ionic solutes in feed water to permeate through a membrane.[165] "Organic solvent nanofiltration" (OSN) or alternatively "solvent resistant nanofiltration" (SRNF) or "organophilic nanofiltration" refers to membrane processes in organic solvents. NF require 5 to 40 bar pressure for the separation and is applicable for compounds up to 2 nm.

1.3.1. CLASSIFICATION OF THE MEMBRANES

OSN membranes are based on polymeric and inorganic materials which have high mechanical, chemical and thermal stability. Polymer membranes suffer from flux decline due to aging and compaction whereas ceramic ones do not compact under pressure, do not swell in organic solvent but their scaling up is much more difficult. Ceramic membranes have no pores so there is no risk of leaching, MWCO is much higher than polymer ones. Wide range of membranes are already commercially available such as Starmem, DuraMem, PuraMem.[166]

Table 1. Commercially available OSN membranes.

Entry	Membrane name	Manufacturer	MWCO	Solvent stability	Membrane type and material
1	MPF-50	Koch Membrane System (USA)	700 Da (based on rejection of Sudane)	Alcohol, ketones, esters, alkyl halides, alkenes	TFC, comprising a dense silicone top layer on a porous cross-linked PAN-based support
2	MPF-44	Koch Membrane System (USA)	250 Da (based on rejection of glucose in water)	Aqueous mixture of lower alcohols, hydrocarbons, chlorinated solvents (DCM, chloroform), aromatics (toluene, xylene), ketones (MEK), diethyl acetate, cyclohexane, propylene oxide, acetonitrile, THF, 1,4-dioxane	TFC, comprising a dense silicone top layer on a porous cross-linked PAN-based support
3	Starmem 120, 122, 228, 240	Grace-Davison (USA), distributed by Evonik MET (UK)	200, 220, 280, 400 Da (based on series on *n*-alkanes in toluene)	Alcohols (butanol, ethanol, and isopropanol), alkenes (hexane, heptane), aromatics (toluene, xylene), ethers (methyl tertbutyl ether), ketones, and others (butyl acetate, andethyl acetate)	Integrally skinned asymmetric membranes with active surfaces based on PI (pore size <5 nm)
4	PuraMem S380	Evonik MET (UK)	600 Da	Heptane, hexane	TFC with cross-linked PDMS layer on polyimide ultrafiltration support
5	DuraMem PuraMem 280	Evonik MET (UK)	150-900 Da	Acetone, ethanol, methanol, THF, DMF, DMSO, dimethylacetaamide, isopropanol, acetonitrile, methylethylketone, ethyl acetate	Integrally skinned asymmetric cross-linked polyimide-based membrane
6	Inopor 0.9 nm TiO_2	Inopor GmbH	450 Da	Methanol, isopropanol, THF, DMF	TiO_2
7	Inopor 3 nm Zr	Inopor GmbH	600 Da	Apolar solvents	ZrO_2

Membrane can be produced in flat sheet (polymer) or tubular shape (ceramic). For practical, industrial applications membranes have to be configured into modules as for example shown in Figure 29.

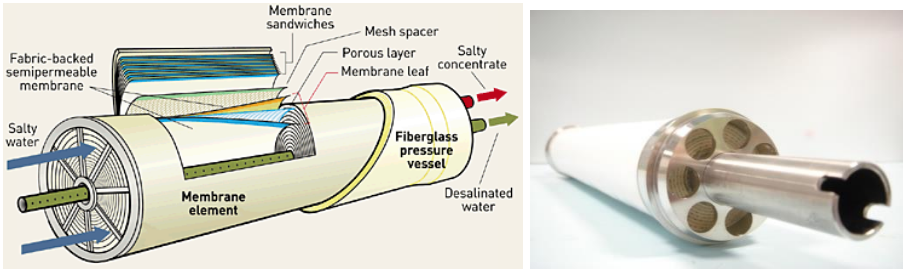

Figure 30. Spiral-wound module used in industry. (Reproduced with permission from ref. 167. Copyright Evonik MET) [167]

Membrane functional properties are characterized by two parameters: flux (or permeability) and rejection (or selectivity).[168]

The permeate flux is defined as the volume of solvent passing through a unit area of membrane per unit of time, and is usually expressed in terms of $Lm^{-2}h^{-1}$, while permeability is normalized to the applied pressure in terms of $Lm^{-2}h^{-1}bar^{-1}$. The flux is expressed by the following equation (*1*) where J is the flux, V_p is the volume of permeate collected.[169]

$$J = \frac{V_p}{A \cdot t} \qquad (1)$$

Rejection is a measure of the membrane separation performance and it is defined as the percentage of the molecules that are unable to pass the membrane. The rejection can be calculated according to equation (*2*) where R_i is the rejection of species i and C_i is the concentration in the feed (f) and permeate (p) solution respectively.[169]

$$R_i = 100\left(1 - \frac{C_{i,p}}{C_{i,f}}\right) \qquad (2)$$

The separation performance of membrane can also be expressed by its molecular weight cut-off (MWCO). It is defined as the molecular weight for which 90% of given solute is rejected by the membrane. This values are commonly supplied by the manufacturer to provide an indication of the membrane operating range. The MWCO can

be derived from a MWCO-curve (Figure 31) featuring the membrane's rejection for analytes with increasing MW.

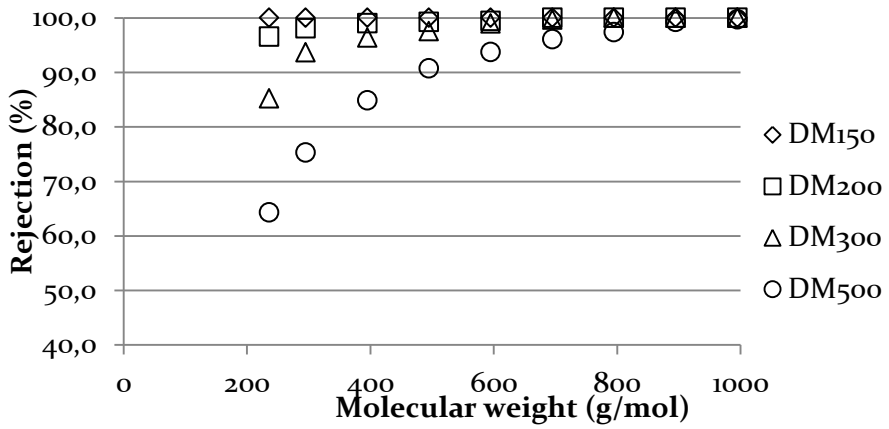

Figure 31. MWCO curves for DuraMem™ 150, 200, 300 and 500 on polyester support material in acetone, 30 bar and 30 °C.[167]

It should be kept in mind that different factors can influence the permeability of the membrane, such as pore-size distribution, charge effect, hydrophilicity, hydrophobicity, polarity of the solvent.[170] The molecular shape is also very important factor. It was demonstrated that branched molecules had higher rejection than their linear equivalents.[171] MWCO is highly dependent on the solvent solute system used, so caution must be applied before relying on this value.[172]

1.3.2. MEMBRANE FILTRATION CONDITIONS

Nowadays, the membrane setups use can be divided in two categories: the dead-end and cross-flow unit. In dead-end filtration the feed is forced through the membrane by pressure perpendicular on the membrane surface, whereas in cross-flow mode, the feed flows parallel to the membrane surface.

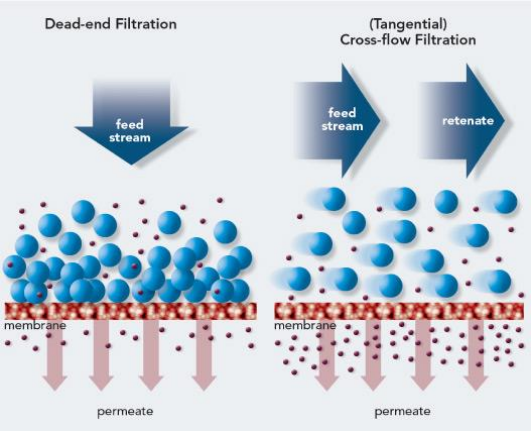

Figure 32. Dead-end filtration versus cross-flow filtration. (Copyright 2010 WCG)[173]

The majority of the applications of the nanofiltration reported in the literature have been applied in dead-end filtration mode on lab-scale set-up (batch system), while industrial membrane application generally run in cross-flow mode (continuous system).

It should be keep in mind that short-term OSN performance reported by academic groups will not necessarily be reproductive in long-term cross-flow testing. To contrast dead-end filtration involves pressurization of the feed with gas whereas flux in cross-flow module is generated by hydrodynamics feed.

In case of dead end systems we have to consider a few drawbacks as membrane fouling and concentration polarization. This phenomena cause extra resistance on the top of the membrane and slow down the transport even to 1% of the initial flux value.[174] Fouling of the membrane refers to the accumulation of the retained molecules in the pores of the membrane or at the membrane surface. Whereas concentration polarization referring to the accumulation of the retained solutes at the membrane boundary layer which might induce further fouling. There are many ways to avoid both phenomena, e. g. increasing cross-flow velocity, permeate pulsing or ultrasound treatment.[163c,175]

1.3.3. APPLICATION OF NANOFILTRATION IN CATALYTIC PROCESSES

Combination of homogeneous catalytic processes and catalyst recovery by OSN brings economical and process efficiency.[163c,176] This methodology has been already used in purification and recycling of the Co-Jacobsen's catalyst,[177] Heck and Suzuki reactions,[178] hydrogenation catalysts[176f,179] and many others.[180]

The size of homogenous catalyst is usually in the same order of magnitude as the substrates they convert. To increase rejection of the catalyst by membrane filtration they have to be molecular weight enlarged (MWE). MWE systems are generally achieved by attaching catalyst or ligand to molecular weight enlargement unit. It has to fulfil a few requirements, such as thermal and kinetic stability, inactivity in catalytic reaction, no interaction with other functional group in attached catalyst. Preparation of the MWE system should be simple, clean and cost-efficient. As MWE decoration dendrimers, dendrons, soluble polymers, hyper branched polymers, dendronized polymers, polyhedral oligomeric silsesquioxanes (POSS) and many more could be used (Figure 33). All these soluble supports have their own set of advantages and disadvantages, so great care has to be taken in selecting an appropriate support.[181]

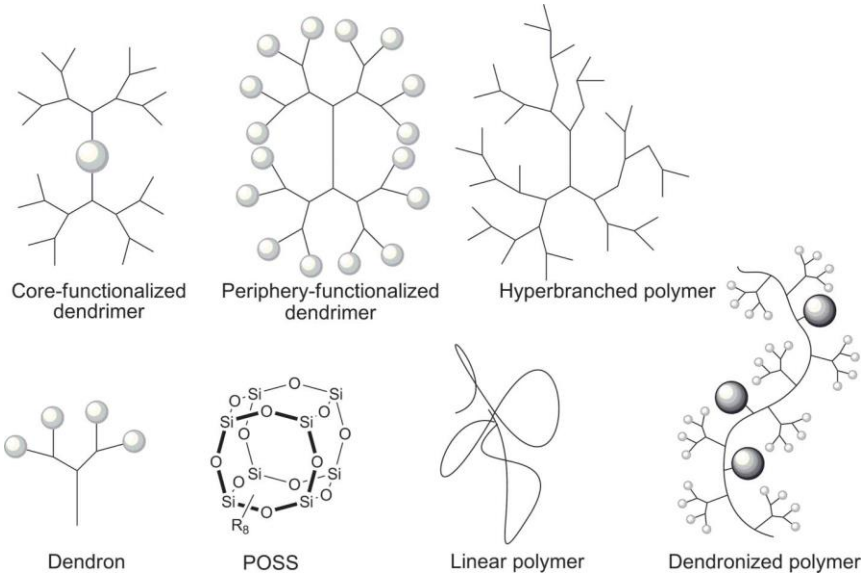

Figure 33. Molecular weight enlargement units used in homogenous catalysts. (Reproduced with permission from ref. 181b. Copyright 2011 Royal Society of Chemistry)[181b]

Few attempts in utilization of OSN of unmodified catalysts (without MWE) have been also described.[177,182] In most cases, retention of the catalyst was lower compared to MWE-modified analogue.

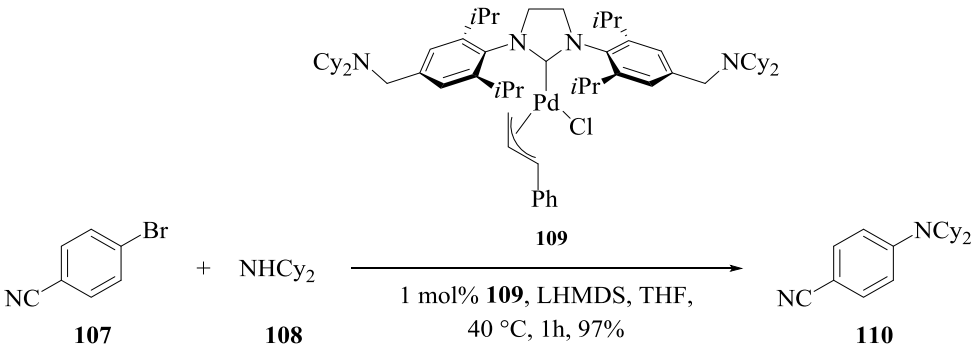

Scheme 16. Buchwald-Hartwig amination of 4-benzobromonitrile with dicyclohexyl amine.

A nice example of utilization of OSN in homogenous catalysis presented Plenio *et. al*. MWE modified palladium complex **109** has been utilized in Buchwald-Hartwig amination reaction with excellent yields. Shortly after reaction crude product was transferred to the OSN reactor with GKSS PDMF membrane (05/069) and pressurized to 5 bar resulting in flow of 2.5 mL/min. Only 3.5 ppm of Pd was detected in the coupling product after second filtration.[183]

1.3.3.1. APPLICATION OF NANOFILTRATION IN METATHESIS REACTION

The OSN of metathesis catalysts has been firstly reported by van Koten *et al.*[184] RCM reaction of DEDAM with dendric enlarged **111** was performed in an OSN reactor (SelRO nanofiltration membrane MPS-60; MWCO 400 Da). At 20% conversion, the catalyst was found to decompose, forming a black precipitate in the vessel. It was thought that decomposition of **111** was facilitated by the membrane surface, even though leaching of the catalyst through membrane did not appear to occur (colorless permeate). In classical conditions full conversion was obtained after 30 min.

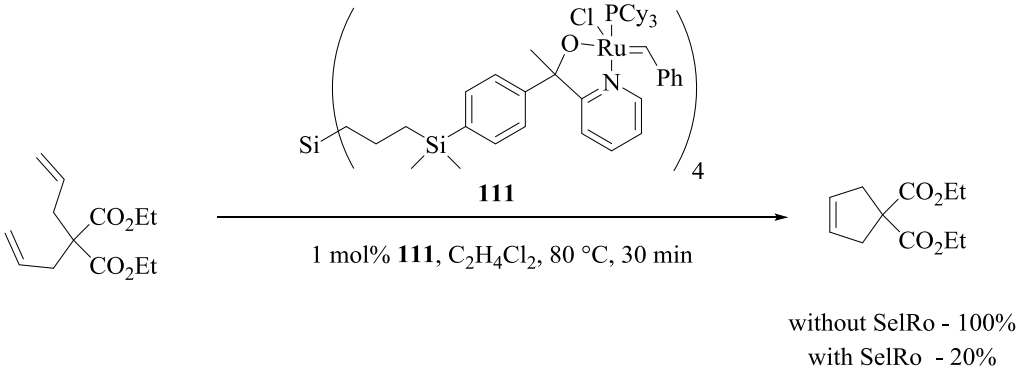

Scheme 17. RCM reaction of DEDAM with catalyst **111**.

Later, this experiment has been repeated by Vosloo, who concluded that low conversion of **111** was most probably due to the short lifetime of the catalyst, instead of the lack of stability of it on the membrane.[185]

Rabiller-Baudry *et al.* synthesised a variety of analogues of **30** with different molecular weights, ranging from 625 to 2195 g/mol,[182] in which the MWE unit was tagged to the benzylidene ligand. For OSN tests laboratory-made setup with cross-flow filtration (25 °C, 25 bar, flow 0.8 mL min^{-1}) and StarMem® 228 membrane (MWCO 280 Da) has been applied. Utilization of the cross-flow unit was supposed to avoid polarization concentration effect and fouling of the membrane. Initial screening of the catalysts showed that Ru fouling increased slightly with the catalyst's molecular mass. This result can be explained by the adsorption of the heaviest molecules on the membrane surface.[171] Further RCM experiments with **112** showed that dimethyl carbonate (DMC) is a much better solvent for the RCM reaction than toluene, as the complex was more stable and, subsequently, could be recycled 5 times without compromising catalytic activity, compared to 3 cycles in toluene. Retention of the catalyst was very low, only 90% after each cycle. After fifth filtration there was only 65% of the initial amount of **112**. Such low retention is caused by fully drained nanofiltration cell (and the membrane) after each cycle.

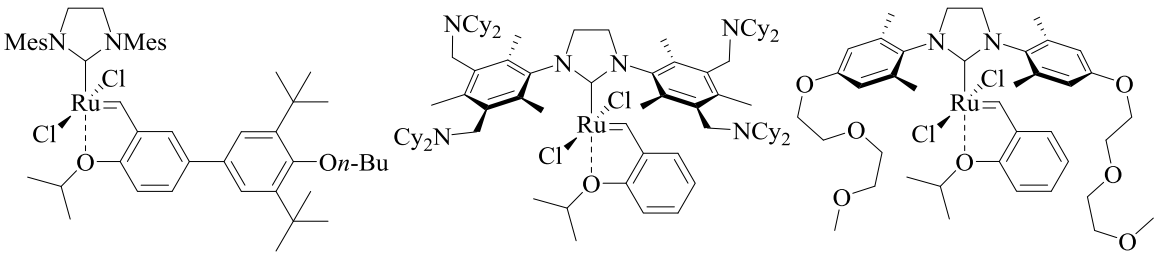

Figure 34. Different MWE tagging.

An MWE attached to the NHC ligand was described by Plenio.[186] Catalysts tagged in this way turned out to be more easily recovered than their alkylidene-tag counterparts. Complex **113** has been utilized in RCM and CM reactions in almost quantitative yield at 40 °C with 0.1 mol% catalyst loading. For OSN experiments GKSS PDMF 05/069 membrane has been used in Millipore cell pressurized to 5 bar which gives 1.67 mL min^{-1}

flow. 4 ppm Ru content in permeate in the case of dead-end filtration was detected. Moreover, RCM of DEDAM in a continuous flow system has been conducted. The experiment was carried out for 500 min, during this time samples were collected to determine the Ru contamination, which was less than 7 ppm. The highest conversion was only moderate, around 37% after 120 min and then started to drop, reaching only 6% after 500 min, due to rapid catalyst deactivation. The probable cause was the interaction of the catalyst with the membrane surface. These phenomena could be explained by addition of pieces of the membrane to the solution of the catalyst, or filtering solution of the catalyst through the membrane. Unfortunately authors did not try such experiments.

Fischermeister and Rabiller-Baudry continued to investigate the application of OSN in metathesis purification. Based on Plenio's research, they presented NHC tagged ruthenium catalysts which they tested in OSN conditions along with **30**.[187] RCM reaction with 0.5 mol% catalyst loading was conducted in the stainless steel MET-cell setup (40 bar, 30 °C) with StarMem 122 membrane (MWCO 220 Da). After full conversion reaction mixture was pressurized to 40 bar to start filtration. Because of dead volume of the setup (100 mL) only 2/3 of total amount of the reaction was filtrated. To the rest a new portion of substrate solution (200 mL) have been added and the reaction have been continued. After second cycle only 17% of yield in case of **30** and 64% in case of **114**, 230 and 329 TON, respectively, have been obtained. Catalysts probably decomposed during second cycle. ICP-OES measurements of the permeates present the ruthenium content on level 20 ppm in case of **30** and 14 ppm in case of **114**. There is very low difference in leaching between unmodified and modified catalyst which mean there is no point in modification of the catalyst when MWCO = 220 Da.

Based on previous work[188] Gebbink *et al*. presented recycling based on dialysis, by utilization of commercially available dialysis membrane (MWCO = 2000 Da). Catalyst **115** was placed in the dialysis bag and then along with solution of DEDAM in the vessel. After 6 h only 2% of substrate had reacted, and after one week – 16%.[189] Such low yield was due to driving forces in the system. The transport of the substrate and the product in and out of the membrane bag occurs by diffusion, which was intensified by a magnetic stirring bar at the bottom of the vessel. This force was too weak to let the substrate migrate into the membrane bag, in which it could interact with the catalyst and be converted to the product.

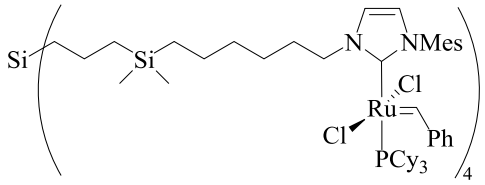

MW: 3703 g/mol

115

Figure 35. Dendritic modified Grubbs catalyst.

Combination of two concepts: catalytic membrane reactor (CMR)[190] and supported ionic phases (SILP)[191] has been reported by Fischemeister and Rabiller-Baudry in 2010. The modification was achieved in two steps, first by the absorption of the IL ([bmim][PF_6]) on the membrane, and then dispersion of **116** onto the IL supported membrane.[192] The permeability of the modified membrane was two times higher than a untreated one (0.35 L m^{-2} h^{-1} bar^{-1} – Starmem® 228 compared to 0.67 L m^{-2} h^{-1} bar^{-1} – IL StarMem® 228). The activity of the system was subsequently evaluated by performing RCM of *N*,*N*-diallyltosylamine (DATA). For OSN experiments the dead-end filtration cell pressurized to 15 bar have been utilized. The catalyst could be recycled 3 times before any decrease of activity was observed. After each cycle the cell was fully drained to avoid inhibition of **116** by too high concentration of the product.

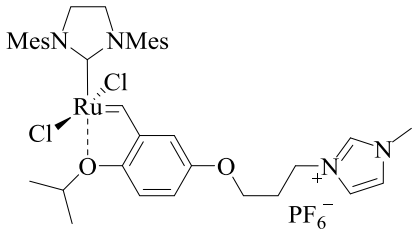

MW: 912 g/mol

116

Figure 35. IL tagged complex immobilized onto membrane.

In 2010 Vosloo *et al.* presented utilization of OSN in the purification of self-metathesis of 1-dodecene conducted with commercially available **26** or **117**.[185] The separation was achieved with the commercially available StarMem™ 120, 122, 228, 240 membranes (MWCO: 200, 220, 280, 400 Da). The best results have been obtained with StarMem™ 228 achieving high retention and flux, with up to 99% of each of the catalysts retained on the membrane. Complex **117** was recycled four times without significant loss of activity, but it deactivated completely after 60 h (overall TON = 5500).

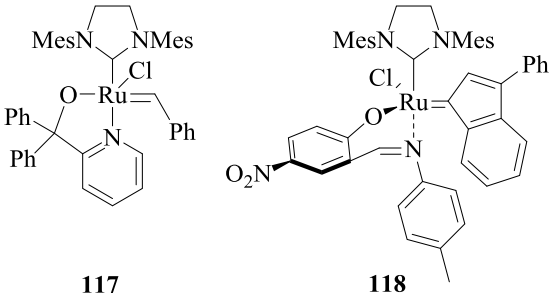

117 **118**

Figure 37. Commercially available catalysts purified by OSN.

Other commercially available catalysts have also been tested in OSN conditions. In 2014 Jensen and O'Neal presented utilization of continuous-flow system with nanofiltration module (PuraMem 280, MWCO = 280 Da, 45 bar, flux = 21.3 L m^{-2} h^{-1}) for recycling of **30**. RCM of DEDAM catalyzed by **30** with continuous addition of solution of DEDAM has been running for 10 h, reaching 1300 TON. The obtained product contained less than 0.5 ppm of ruthenium.[193] The results achieved were much better than previously described by Fishermeister (TON = 230).[187] Different membrane and what was the most important – utilization of the Teflon AF-2400 tubing, which constantly remove ethylene from the system, was crucial, as ethylene is a known inhibitor of the Ru based catalysts.[194]

In 2013 Ormerod et al. presented screening of RCM reaction conducted by variety of catalysts in OSN conditions.[195] The dead-end filtration unit and cross-flow continuous unit have been utilized along with three different membranes: polymeric hydrophobic DuraMem 200 (MWCO = 200 Da), ceramic hydrophilic Inopour 0.9 nm TiO_2 (MWCO = 450 Da) and ceramic modified with C_8 alkene group Inopour 1 nm TiO_2 (MWCO = 1500 Da). First tests of recyclability of **27** (1 mol%, RT, 4 h) in dead-end unit in DCM showed that recyclability is much higher in case of utilization of Inopour 0.9 nm TiO_2 membrane (4 cycle) than with StarMem® 200 (3 cycle). Comparing the MWCO of both membranes, results should be opposite, because StarMem® is tighter of the two. This phenomenon could be explained by the fact that DCM is not suitable for StarMem® 200 membrane.[176d,196] Rejection of **27** in this conditions was very low – only 35%, which means that 65% of the starting amount of the catalyst passed through the membrane during 3 cycles. Whereas, rejection of **27** in case of Inopour 0.9 nm TiO_2 was 80%, so only 20% of total amount of catalyst passes through the membrane during 4 cycles (Table 2, Entry 1 and 2). Comparing rejections of the catalyst and the product we can assume

that the ideal situation would be when rejection of the catalyst was as high as possible whereas rejection of the product was as low as possible.

Table 2. Influence of the solvent on rejection of the membrane.

Entry	Membrane	Catalyst	Time	Conv. (%)	Solvent	Rejection (%)		
						Catalyst	Substrate	Product
1	DM200	**27**	3 x 4 h	99 50 20	DCM	35	1	10
2	0.9 nm TiO_2	**27**	4 x 4 h	99 75 40 30	DCM	80	53	48
3	0.9 nm TiO_2	**27**	16 h	65	DCM	80	90	87
4	0.9 nm TiO_2	**31**	16 h	45	DCM	94-83	70-78	73-83
5	0.9 nm TiO_2	**31**	16 h	83	Acetone	99-88	40-57	57-64
6	DM200	**31**	16 h	87	Acetone	99	98	97
7	1 nm C_8	**31**	16 h	83	Acetone	85-78	35-38	30-40
8	1 nm C_8	**118**	16 h	-	Acetone	90-96	55-59	45-50

When the reaction has been performed in a cross-flow continuous unit (membrane 0.9 nm TiO_2) conversion of the RCM decreased rapidly (65% after 16 h vs 98% after 4 h in dead-end unit). This phenomenon could be explained by higher concentration of ethylene in the system. When solvent was exchanged to acetone, which could coordinate to the metal center to increase its stability and thus longevity, conversion increased. Not only conversion (from 45% to 83% in case of **31**) but also rejection of the catalyst increased whereas rejection of the substrate decreased. Moreover, other membranes were tested in acetone, in case of DuraMem rejection of the catalyst was very high, which is good, but rejection of the product also increased. Compared to other membranes 1 nm TiO_2 C_8 membrane works in acetone very well, rejection of **31** is moderately high while rejection of the product is much lower compared to other membranes. When the experiment was repeated with catalyst **118** rejection of the catalyst was higher but also rejection of the product increased (Table 2, Entry 8).

Another very important issue was washing out the reaction product from the reactor. This was carried out as a constant volume diafiltration using fresh solvent.

Unfortunately, catalyst was also washing out from the reactor. The more diafiltration volumes required to wash out the product, the more of the catalyst will be leaching out to the permeate. Number of volumes required to wash the product out of the system depends on the membrane and the solvent.

1.4. SUMMARY

Numerous techniques have been devised to purify metathesis products and to recycle the catalyst. Most of them require modification of the catalyst's structure, by attaching various tags, or by anchoring it to organic or inorganic supports. Despite this, there are only few strategies that are currently suitable for industrial applications. However, the situation is rapidly changing, as more immobilized catalysts are being developed and patented, though there may be many more avenues that remain to be explored.

A number of OSN membranes is now commercially available, but in this field there is still a lot to do. The latest results conclude that most of the membranes commercially available are too tight. Great care has to be taken in selecting appropriate solvent, because MWCO, provided by supplier, is highly dependent on the solvent. There is a great need to improve the membranes, their robustness towards swelling and leaching, multipurpose, selectivity and higher MWCO. This technology is still too expensive and optimization of the process is time consuming, so when it comes to overall process efficiency and overall costs simpler methods of purification are more attractive to the industry.

"Problems can't be solved at the same

level of awareness that created them"

Albert Einstein

PART 2 – RESULTS AND DISCUSSION

2.1. INTRODUCTION

My interest in studying the metathesis reaction in the context of Green Chemistry stems from a project devoted to the optimisation of self-metathesis of 1-dodecene which has been executed in cooperation with Nalco company. The main task of the project was to obtain as high an efficiency of the process as possible with low cost of the purification of the product. Even though self-metathesis of 1-dodecene looked simple, a mixture of side olefins could be formed due to alternative processes, which were caused by the products of decomposition of the catalyst. [197]

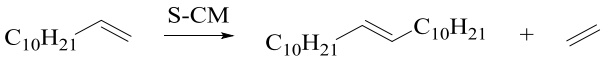

Scheme 18. Self-metathesis of 1-dodecene.

Scrupulous optimisation of the reaction conditions led to an increase in the conversion and selectivity from 7% and 50%, respectively, to an almost quantitative formation of the desired product catalysed by only 20 ppm of a catalyst. According to the process needs, as defined by Nalco, such a low amount of ruthenium contamination did not need to be removed from the product. This specific approach is suitable for simple linear alkenes[198] in other cases, especially drugs, where harsh regulation established by EMEA have to be met.

To implement the metathesis reaction into industrial processes a universal method of purification along with a simple method of recovery and reuse of the catalyst should be proposed. In chapter 1.2.1.3 a modern approach to the purification of the desired product

utilised in the industry has been described. Workup procedures allow the decomposition of the catalyst for the sake of the more expensive product.

Membrane processes are widely utilised in industrial procedures (ch.1.3). Lately they have also been adopted to the purification of the products of catalytic processes. In my research I decided to apply nanofiltration along with MWE catalyst modification as an easy and economical way of the purification of the product of the metathesis reaction. This method of purification allows to recover the expensive ruthenium catalyst and reuse it without further purification.

2.2. MODIFICATION OF THE CATALYST

In chapter 1.3.3. I described a wide range of molecular enlargement units that have been so far applied in OSF catalysis processes. Among them the POSS moiety gained my attention because of its unique three-dimensional cage structure composed of silicon and oxygen. The POSS molecule contains a basic polyhedral silicone-oxygen nanostructured skaffold or cage, with a precisely defined Si-Si distance of 0.5 nm. The cage may contain eight (T_8) (a cube-like cage), ten (T_{10}) or twelve (T_{12}) Si atoms in it, surrounded by eight, ten or twelve organic groups, respectively. The ratio of Si:O is 2:3. The Si atoms are located at the corners of the cage (at the surface of the basic cage structure).

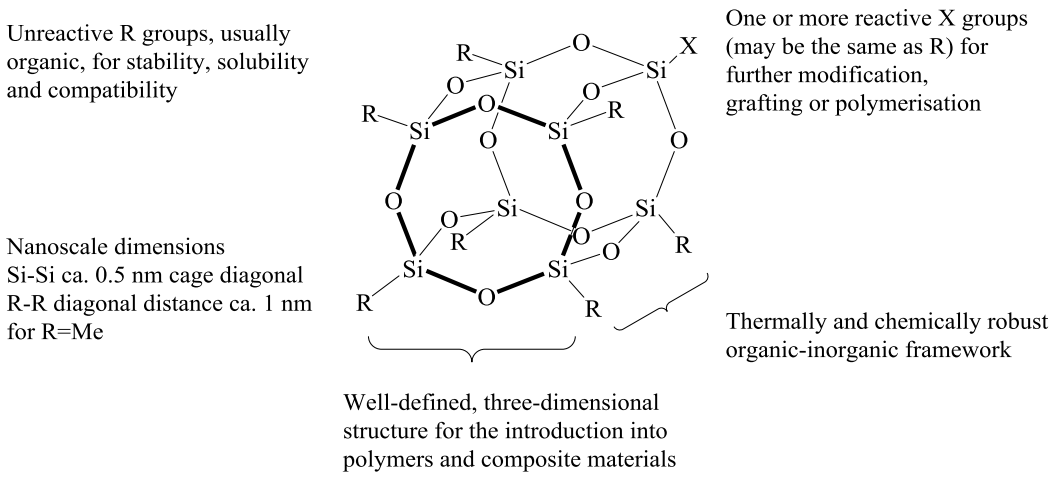

Figure 38. The general features of a cubic (T_8) polyhedral silsesquioxane.

It is possible to attach any chemical to the silica-like core. Customisation of POSS is simple and can be easily controlled. Based on the type of R group (e.g. hydrogen, alkyl, alkylene or aryl arylene), there is potentially an unlimited number of POSS types such as

alkyls, olefins, alcohols, esters, anhydrides, acids, amines, imides, epoxides, thiols, sulfonates, fluoroalkyls, silanols, and siloxides. This universality and multiplicity combined with the low price and thermal stability of the structures makes POSS an ideal candidate for a MWE unit.[199]

2.2.1. MODIFICATION OF THE NHC LIGAND

The first type of modification that I decided to undertake was the introduction of the POSS tag to the NHC ligand. NHC is a nonlabile ligand, which means that during the catalytic cycle it does not dissociate from the metal. Such approach should lead to full recovery of the modified complex. NHC ligands are synthesised from the corresponding imidazolium salts by deprotonation.

2.2.1.1. *N*-ALKYL SUBSTITUTED POSS-C_3-NHC

According to the literature,[181a] the connection between the MWE unit and the ligand should be achieved by a high yielding and clean reaction. Keeping this in mind I decided to synthesise an NHC ligand bearing an *N*-alkyl substituted POSS moiety, which would give me the opportunity to examine the influence of the POSS tag on the activity and stability of the complex.

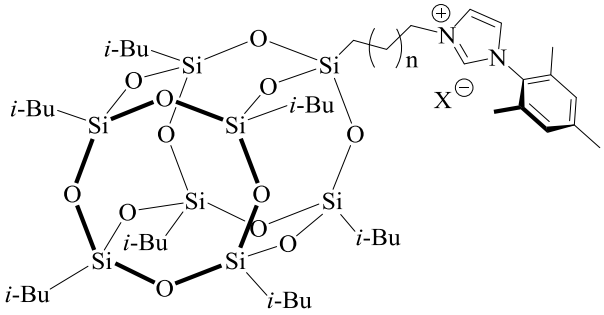

Figure 39. Imidazolium salt with *N*-alkyl substituted POSS(T_8) moiety.

The synthesis of the modified NHC salt started with mesitylimidazole **122.** Based on Zhang procedure,[200] commercially available 2,4,6-trimethylaniline (**120**) was treated with an aqueous solution of glyoxal (**121**) in MeOH. Next, paraformaldehyde, NH_4Cl and H_3PO_4 were added and the reaction was refluxed over 10 h. After completion, the reaction mixture was basified with 40% KOH to pH 9. Extraction followed by purification by column chromatography and crystallisation led to mesitylimidazole in 73% yield.

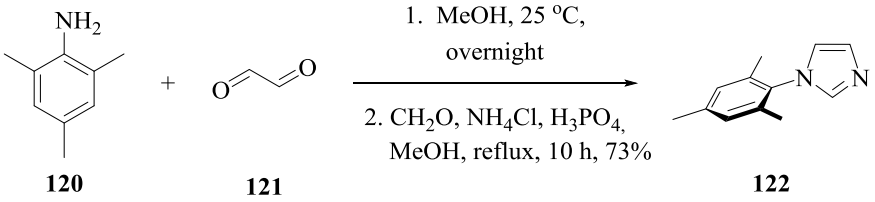

Scheme 19. The synthesis of *N*-mesitylimidazole.

The first trials of connecting imidazole and POSS have been performed as a two-step synthesis (Scheme 20). Such procedure has been chosen because of Trisilanol-heptaisobutylPOSS moiety (**125**) obtained from HybridCatalysis.[201] Corner-capping of trisilanol **125** is performed by using a trialkoxysilane.[202] Usually the reaction needs water and a base as catalyst ($Et_4N^+OH^-$) to fully or partially hydrolyze the trialkoxysilane to silanetriol, which subsequently condenses with trisilanol. But when the trialkoxysilane is connected with an imidazolium moiety (**124**), the corner-capping reaction is probably self-catalysed by **124**. Evaporation of the reaction mixture yields 3-(3-heptaisobutylPOSS(T_8)-propyl)-1-mesityl-1*H*-imidazolium iodide in 81% yield.

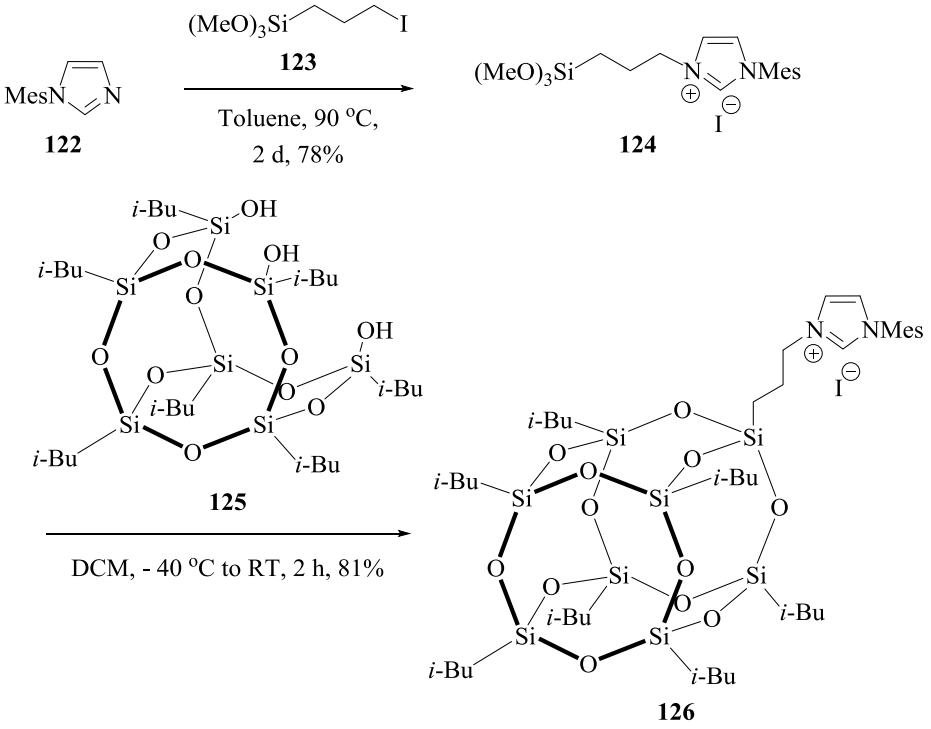

Scheme 20. Two step synthesis of 3-(3-heptaisobutylPOSS(T_8)-propyl)-1-mesityl-1*H*-imidazolium iodide (**126**).

The limiting factor of the generality of this procedure is compound **123**. There are only a few trialkoxysilane compounds like **123** available on the market. I decided to

change the strategy after obtaining heptaisobutylPOSS(T_8) cages with halogenated spacers such as 3-iodopropyl-heptaisobutylPOSS(T_8) **127**, from HybridCatalysis. Overnight refluxing in xylene led to **126** in almost quantitative yield. The structure of **126** was confirmed by ^{1}H NMR and MS with the peak at m/z = 1043.5. The characteristic signal of the imidazolium salt C2-H was found at δ = 10.17 ppm.

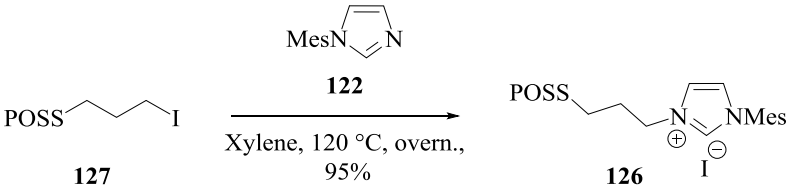

Scheme 21. Straightforward synthesis of imidazolium salt **126**.

Ruthenium complexes with unsaturated NHC ligands bearing unsymmetrical *N*-alkyl substituents are known in the literature. They are usually less active and less stable compared to those with symmetrical NHC ligands with both *N*-substituents aromatic.[161] Being aware of the possible lower stability I decided to synthesise the corresponding ruthenium complexes anyway.

The synthesis of the second generation ruthenium complexes started with the deprotonation of **126** with potassium *t*-amylate to generate NHC **128**. Next, a Shlenk flask with the reaction mixture was placed in a preheated oil bath and the first generation ruthenium catalyst (Scheme 22) was added. The progress of the metalation was monitored by TLC.

In the case of the Grubbs-type catalyst the product was observed by TLC, but during the purification the complex decomposed. A few trials were carried out, with the same result. The Grubbs complex with the unsymmetrical NHC ligand was apparently too unstable to allow isolation. Further implementation of nanofiltration requires a stable catalyst, which apparently in the case of the Grubbs-type complex was impossible to achieve.

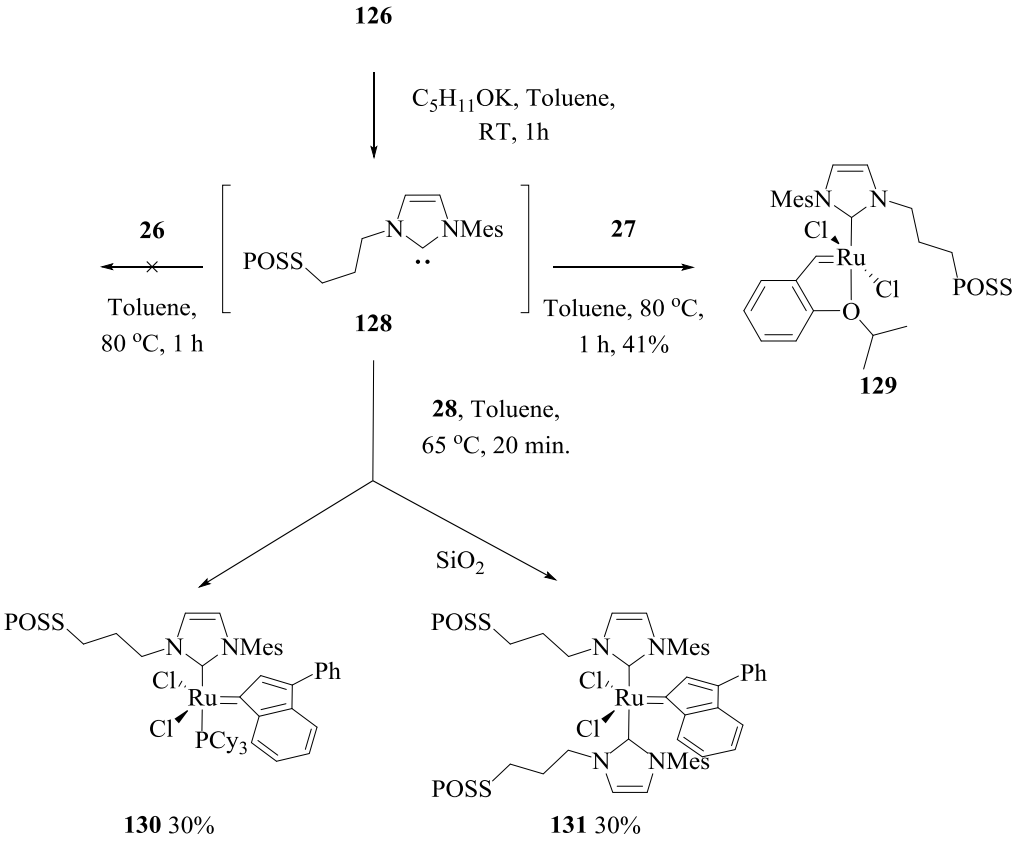

Scheme 22. The synthesis of ruthenium catalysts bearing a POSS-tagged NHC ligand.

Metalation of a Hoveyda I generation complex (**27**) was performed at 80 °C in toluene. The reaction was monitored by TLC. After completion, the reaction mixture was cooled and transferred to silica. During the purification a pale green product was collected, which was concentrated *in vacuo*. After recrystallisation from a mixture of DCM/MeOH catalyst **129** was obtained in moderate 41% yield.

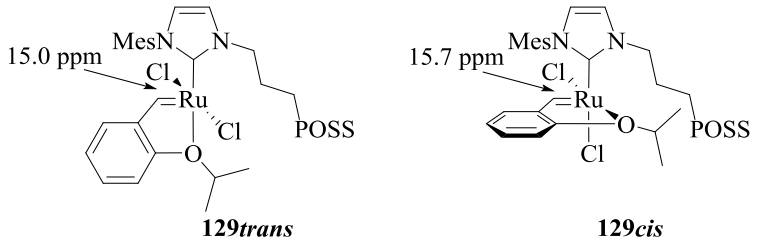

Figure 40. Two possible isomers of **129**.

In the ^{1}H NMR spectra of **129** I observed two signals in the region of benzylidene proton (Ru=CH) resonance in the ratio 1:10 (Figure 41). According to the literature[203] the benzylidene signal of the *cis* isomer is deshielded compared to the *trans* isomer. In the

case of **129** the signal at δ = 15.7 ppm comes from the *cis* isomer and the signal at δ = 15.0 ppm from the *trans* isomer (Figure 40, 41). Other signals from the benzylidene ligand are also doubled in the ratio of 1:10, which confirms the presence of two isomers.

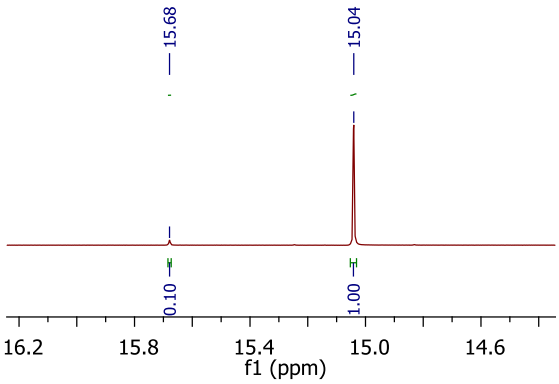

Figure 41. Benzylidene signals of **129**.

Crystals of the catalyst suitable for X-ray diffraction were obtained through the crystallisation from a mixture of DCM and MeOH at 4 °C.

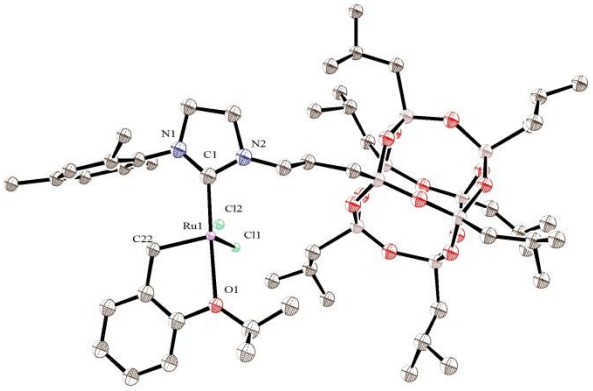

Figure 42. ORTEP representation of the molecular structure of **129**. Hydrogen atoms and disordered solvent molecules are omitted for clarity.

Complex **129** crystallises in the monoclinic $P2_1/n$ space group with one molecule in the asymmetric part of the unit cell, whereas analogous complexes **132**[189] and **133**[204] crystallise in the monoclinic $P2_1/c$ space group.

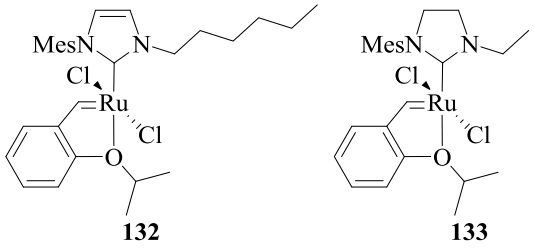

132 **133**

Figure 43. Parent catalysts chosen for discussion.

The distance between the Ru atom and C(1) is slightly longer (2.01 Å) than that in **132** (1.983 Å). A comparison between other relevant bond distances in **129** and **132** indicate that the two structures are very similar. Changes of the geometry of **129** are visible mainly in bond angles near the catalytic center. The Cl(1)–Ru(1)–Cl(2) angle (155.7°) is slightly wider than the corresponding angle in the parent **132** (151.62°). Also O(1)-Ru(1)-C(1) exhibits the same tendency, 174° compared to 179.36° in the case of **132**.

Table 3. Comparison of selected bond distances (Å) and angles (°) of complexes **129** with **132**, **133** and **30**.

Bond distance (Å)	**129**	**132**	**133**	**30**
Ru(1)-C(1)	2.01 (3)	1.983(2)	1.966	1.981
Ru(1)-C(22)	1.84(4)	1.834(2)	1.817	1.828
Ru(1)-O(1)	2.26(2)	2.2764(16)	2.269	2.2612
N(2)-C(1)	1.20(4)	1.369(3)	1.341	1.351
N(1)-C(1)	1.52(4)	1.363(3)	1.455	1.350
Bond angle (°)				
Ru(1)-C(1)-N(2)	124(3)	121.73(18)	118.4	120.8
Ru(1)-C(1)-N(1)	127(3)	134.49(18)	134.4	131.6
C(1)-Ru(1)-C(22)	104(1)	100.27(10)	102.46	101.5
O(1)-Ru(1)-C(1)	174(1)	179.36(8)	177.46	176.2
Cl(1)-Ru(1)-Cl(2)	155.7(2)	151.62(3)	151.11	156.5

Treatment of the indenylidene complex **28** with carbene **128** led to the substitution of one of the phosphines with the NHC ligand. The reaction was monitored by TLC, where only one product was observed. After full conversion the reaction mixture was

cooled to room temperature and purified by column chromatography on silica. During the purification two products have been obtained in 30% yield each. It appeared that SiO_2 used for chromatography might have catalysed the substitution of the second phosphine with the NHC. This hypothesis was confirmed by the treatment of the reaction mixture with SiO_2 over 15 min. After purification I obtained only one product – **131** in 31% yield.

The structure of **131** was confirmed by the ^{1}H NMR and MS spectra. The complexation of two carbene ligands to the Ru centre was confirmed by MS by the peak at m/z = 2506.7 $[M+H]^+$ and by ^{1}H NMR by the lack of signals from PCy_3 ligand in the region around δ = 1.5 ppm, as well as the lack of any signals in ^{31}P NMR. The ratio between the signal of Ru=C-CH of δ = 7.98 ppm and N-CH_2- of the spacer at δ = 5.04 ppm was 1:4, which also confirmed the presence of two NHC ligands in the complex.

Optimisation of the procedure was started with changing the base used. When potassium *t*-amylate was exchanged for KHMDS, an inseparable mixture of products was obtained. I was not satisfied by this result, and decided to examine a variety of stationary phases used in column chromatography. The most interesting results were obtained when column chromatography was conducted on Florisil as tha stationary phase. In these conditions **130** was obtained in 60% yield. Al_2O_3 was found to be unsuitable in this case. **131** was not observed but **130** was obtained in 10% yield.

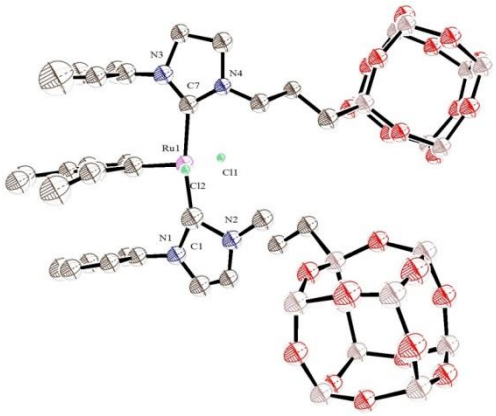

Figure 44. ORTEP representation of the molecular structure of **131**. Hydrogen atoms and isobutyl groups are omitted for clarity.

Crystals of catalyst **131** were obtained through the crystallisation from a mixture of DCM and MeOH at 4 °C. The obtained material led to confirmation of the topology of

the studied compound by X-ray structural analysis. Unfortunately, I was unable to grow crystals with better quality to recollect X-ray diffraction data.

Compound **131** crystallises in the triclinic P1 space group, whereas analogous complexes **134**[205] and **135**[206] , known in the literature, crystallise in the monoclinic C2/*c* space group and in the monoclinic $P2_1/c$ space group, respectively.

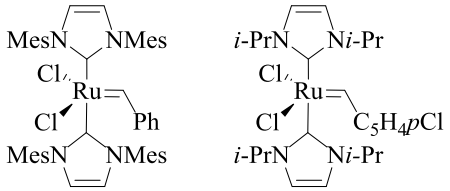

134 **135**

Figure 45. Parent catalysts known in the literature.

Table 4. Comparison of selected bond distances (Å) and angles (°) of complexes **131** with **134** and **135**.

Bond distance (Å)	**131**	**134**	**135**
Ru(1)-C(1)	2.05(4)	2.117(3)	2.115(3)
Ru(1)-C(7)	1.91(4)	2.108(3)	2.107(3)
Ru(1)-C(22)	1.90(3)	1.829(3)	1.821
N(1)-C(1)	1.33(4)	1.372(4)	1.366(4)
N(2)-C(1)	1.33(5)	1.373(4)	1.368(4)
N(3)-C(7)	1.48(6)	1.375(4)	1.364(4)
N(4)-C(7)	1.56(4)	1.368(4)	1.367(4)
Bond angle (°)			
C(1)-Ru(1)-C(22)	100(1)	96.80(13)	94.48(12)
C(7)-Ru(1)-C(22)	92(1)	98.00	100.92(13)
C(1)-Ru(1)-C(7)	168(2)	164.41(22)	163.68
Cl(1)-Ru(1)-C(7)	84(1)	89.03(8)	88.26(8)
Cl(1)-Ru(1)-C(1)	91(1)	91.91(9)	94.76(8)
Cl(2)-Ru(1)-C(7)	94(1)	88.51(8)	89.21(8)
Cl(2)-Ru(1)-C(1)	85(1)	86.87(9)	85.14(8)
Cl(1)-Ru(1)-C(22)	98.1(6)	104.88(10)	98.37(10)

Cl(2)-Ru(1)-C(22)	111.4(6)	88.96(10)	91.14(10)
Cl(1)-Ru(1)-Cl(2)	150.5(1)	166.16(3)	170.32(3)

Confirming the structure of **130** starts with NMR spectroscopy. In the region of Ru=C-CH I observed three groups of signals (Figure 46) in ^{1}H NMR spectra, which means that **130** has three forms which could be observed by NMR (Figure 47).

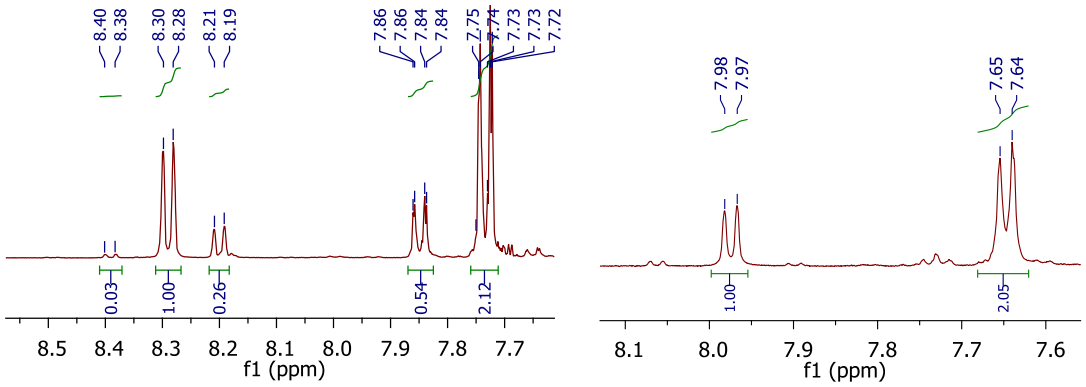

Figure 46. Characteristic signals of **130** (left) and **131** (right) ^{1}H NMR in CD_2Cl_2.

Characterisation of these three forms started with the main structure in which the signal from the Ru=C-CH was at δ = 8.29 (**130a**, Figure 45). The mesityl ring was situated above the indenylidene ligand. Such position could be subsequently stabilised by π-π stacking[207] between the mesityl ring and the indenylidene ligand. Additionally, such interaction was confirmed by signals from the methyl group of mesityl which were upfield δ = 1.63; 1.36; 1.08. In ^{1}H NMR I observed a set of signals from the methyl group of the mesityl ring lying on the other side, above Cl ligands (no π-π stacking) which were observed downfield at δ =1.89; 1.86; 1.72. The ratio between both groups of methyl signals was 1:0.25 the same as between the two signals of Ru=C-CH at δ = 8.29; 8.20 (Figure 46). According to the data discussed above I assumed that the second form of **130** was probably a rotamer (second structure, Figure 47). In the ^{31}P NMR I observed two signals δ = 31.00; 30.84 in the ratio of 0.04:1 which was similar to the ratio of Ru=C-CH in ^{1}H NMR spectra. The additional signal observed in ^{31}P NMR might be associated with the *cis* isomer of **130.**

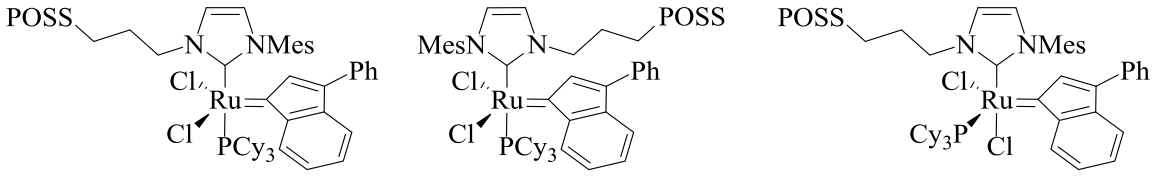

1:0.25:0.03

Figure 47. Three forms of **130**.

When ^{1}H NMR was repeated in benzene-d$_6$ the signal of the probable *cis* isomer was not observed (Figure 48), nor was the signal δ = 31.00 in ^{31}P NMR.

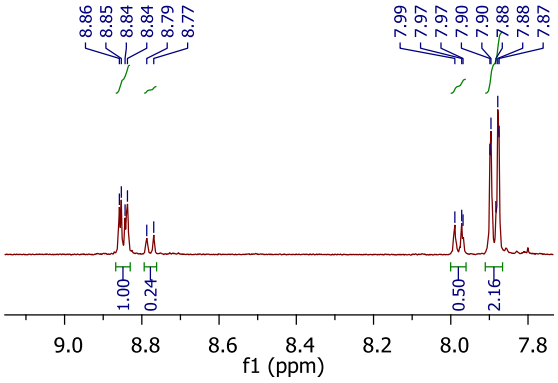

Figure 48. ^{1}H NMR of characteristic region Ru=C-CH of **130** in benzene-d$_6$.

Crystals of the catalyst suitable for X-ray diffraction were obtained through crystallisation from a mixture of DCM and MeOH at 4 °C.

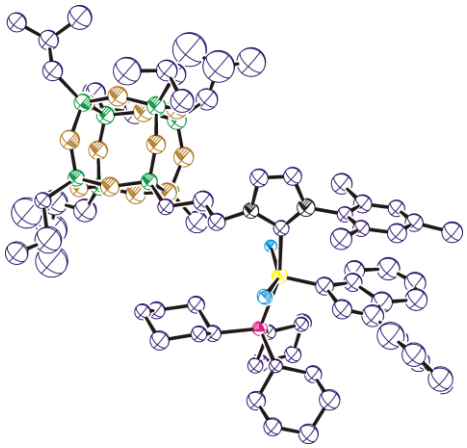

Figure 49. ORTEP representation of the molecular structure of **130**. Hydrogen atoms and disordered solvent molecules are omitted for clarity.

Complex **130** crystallises in the triclinic P1 space group with two molecules in the asymmetric part of the unit cell, whereas parent complex **136**[35] crystallises in the monoclinic $P2_1/c$ space group.

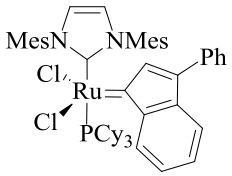

136

Figure 50. Parent catalyst **136** chosen for discussion.

The distance between the Ru atom and C(22) is slightly longer (1.80 Å) than that in **136** (1.7932 Å). In contrast, Ru(1)–C(1) bond length of 2.06 Å is shorter than that observed in complex **136** (2.0893 Å). A comparison between other relevant bond distances in **130** and **136** indicates that the two structures are very similar. Changes of the geometry of **130** are visible mainly in bond angles near the catalytic center. The Cl(1)–Ru(1)–Cl(2) angle (156.8°) is slightly smaller than the corresponding angle in the parent **136** (170.979°). Also P(1)-Ru(1)-C(1) exhibits the same tendency, 162.7° compared to 168.76° in the case of **136**. This might explain the extraordinary activity of **130**.

Table 5. Comparison of selected bond distances (Å) and angles (°) of complexes **130** with **136**.

Bond distance (Å)	**130**	**136**
Ru(1)-C(1)	2.06(4)	2.0893(12)
Ru(1)-C(22)	1.80(3)	1.7932(13)
Ru(1)-P(1)	2.42(1)	2.4107(4)
N(2)-C(1)	1.39(4)	1.3683(15)
N(1)-C(1)	1.32(4)	1.3651(15)
Bond angle (°)		
Ru(1)-C(1)-N(2)	121(2)	126.93(8)
Ru(1)-C(1)-N(1)	135(2)	129.93(8)
C(1)-Ru(1)-C(22)	98(1)	98.89(5)
P(1)-Ru(1)-C(1)	162.7(9)	168.76(3)
Cl(1)-Ru(1)-Cl(2)	156.8(3)	170.979(12)

Having the three complexes in hand, I attempted to examine their efficiency. To accomplish this, I chose a model RCM reaction of DEDAM (**8**) (Scheme 23).

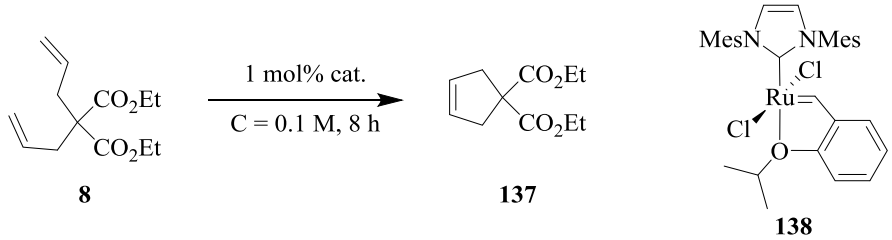

8 **137** **138**

Scheme 23. Model RCM reaction and parent catalyst utilised in its examination.

All reactions were analysed by GC, using dodecane as an internal standard to ensure that the proper product was obtained. To quench the reaction after given time intervals I utilised ethyl vinyl ether. I compared the catalytic activity of all tagged catalysts with parent complexes **136** (Figure 50) and **138** (Scheme 23).

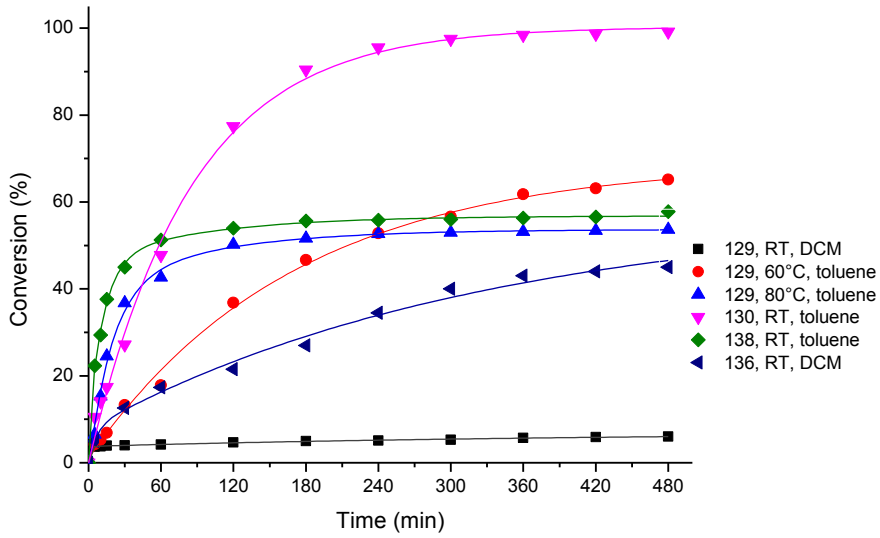

Figure 51. Reaction profile measurements of **129** and **130** compared to the parent complexes **134** and **135**.

Catalyst **129** was found to be very latent. After 8 h at room temperature it reached only 6% conversion. Increasing the temperature to 60 °C led to an increase of the conversion to 65% after 8 h and 81% after 24 h. At 80 °C the catalyst started decomposing reaching only 55% conversion. These results fall in line with known examples of catalysts bearing NHC ligands with a similar structure.[189]

Catalyst **131** bearing two NHC ligands was inactive in the RCM reaction at room or elevated temperature. Tasked with developing active, easily synthesised catalysts, I decided to abandon further investigations concerning this complex.

Surprisingly, the activity of complex **130** was considerably higher than that of the parent complex **136**. It reached 95% conversion after 2 h, whereas **136** needed elevated temperature to reach full conversion.

2.2.1.2. *N*-ALKYL SUBSTITUTED POSS-C_n-NHC

A simple and straightforward procedure (Scheme 21) of the synthesis of unsaturated unsymmetrical NHC salts has, in my opinion, a great potential, as a variety of NHC salts could be synthesised. The only limitation is the availability of the POSS moiety, which is increasing rapidly. Having a set of a set of halogenated POSS moieties in hand, obtained from Hybrid Catalysis, I decided to examine the universality of the procedure.

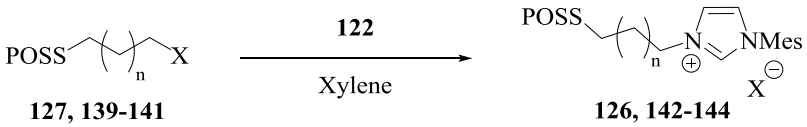

127, 139-141 **126, 142-144**

	n	X		oil bath 120 °C, 24 h	MW, 150 °C, 4 h
127	1	I	**126**	95%	99%
139	1	Br	**142**	77%	90%
140	3	Br	**143**	74%	83%
141	9	Br	**144**	66%	85%

Scheme 24. The synthesis of imidazolium salts tagged with POSS.

All imdazolium salts were obtained in good yield. To increase the efficiency of the reaction I decided to utilise MW irradiation which shortened the reaction time to 4 h and significantly increased the yield of the reaction.

To confirm the structure of the imidazolium salt ^{1}H NMR was applied. The characteristic signal of C2-H imidazole ring appeared above δ = 10 ppm in all cases.

In the case of 3-(4-heptaisobutylPOSS(T_8)-benzyl)-1-mesityl-1*H*-imidazolium chloride (**146**) the classical procedure gave a much higher yield (83%) compared to the reaction in MW conditions (31%).

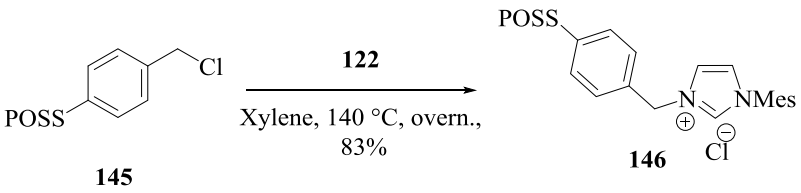

Scheme 25. The synthesis of **146** in classical conditions.

Salt **146** was characterised by ^{1}H NMR, which showed a characteristic signal of C2-H imidazole ring at δ = 10.87 ppm and two characteristic protons of the linker C_6H_4-$\underline{CH_2}$-N at δ = 5.96 ppm compared to the substrate C_6H_4-$\underline{CH_2}$-Cl at δ = 5.41 ppm.

The classical procedure was more efficient also in the case of 3-(5-(bisheptaisobutylPOSS(T_8)(methylsilyl)pentyl)-1-mesityl-1*H*-imidazolium iodide (**148**) with 85% yield compared to 66%.

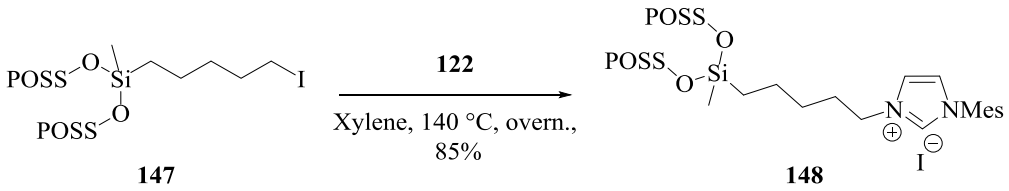

Scheme 26. The synthesis of **148** in classical conditions.

Salt **148** was characterised by ^{1}H NMR, which showed a characteristic signal of C2-H imidazole ring at δ = 10.19 ppm and by MS at *m/z* = 2087.58 $[M-H]^+$ compared to calculated *m/z* = 2087.57.

Additionally, I examined this procedure with bis(5-bromopentyl)octaphenyl POSS(T_{10}) (**149**) which contains two bromides per one POSS moiety. In this case both procedures gave similar yields: 80% (classical conditions) and 83% (MW).

Salt **150** was characterissed by NMR and MS. ^{1}H NMR showed a characteristic signal of C2-H imidazole ring at δ = 9.98 ppm, whereas MS contains *m/z* = 1742.4 $[M-Br]^+$ compared to calculated *m/z* = 1741.3.

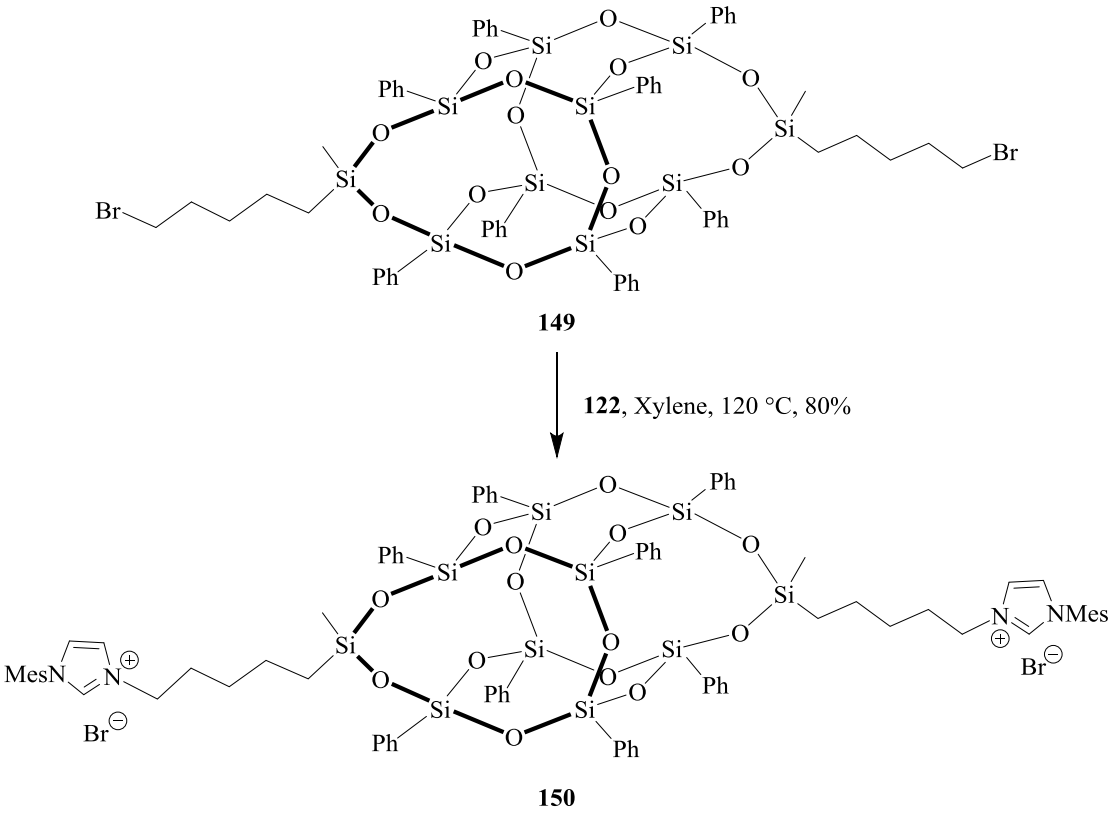

Scheme 27. The synthesis of bis(5-(1-mesityl-1*H*-imidazolium)pentyl)octaphenylPOSS (T_{10})-dibromide (**150**).

Promising results obtained with catalyst **130** encouraged me to synthesise other analogues of **130**. At the same time I wanted to examine if there is any relation between the activity of the indenylidene catalyst and the distance between the NHC ligand and the POSS moiety. For this purpose, I utilised the previously synthesised imidazolium salts **126, 142-144**. I synthetised the ruthenium complexes using a standard procedure: deprotonation of the appropriate imidazolium salt followed by substitution of the phosphine ligand with the obtained NHC.

The catalyst bearing the C3 linker (**130**) was obtained in 60% yield while the one with C5 linker (**151**) was obtained in 49% yield. Surprisingly I was not able to obtain the catalyst with C_{11} linker (**152**). A different procedure of deprotonation of the imidazolium salt was utilised and the spot of the product was observed on the TLC plate, but I was unable to isolate it because of its fast decomposition.

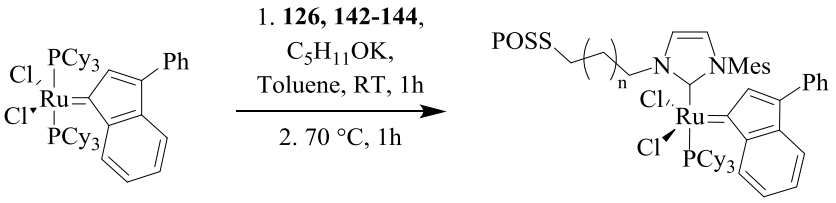

28 **130**, **151**, **152**

imidazolium salt	n	catalyst	yield
126	1	**130**	60%
142	1	**130**	60%
143	3	**151**	49%
144	9	**152**	0%

Scheme 28. The synthesis of indenylidene complexes bearing NHC-C_n-POSS(T_8) ligand.

I also examined if there are any differences in the yield of the synthesis of the ruthenium complex depending on the counterion in the imidazolium salt. Two salts with I and Br counterions were examined. In both cases catalyst **130** was obtained in 60% yield (Scheme 28).

Catalyst **151** was obtained as a mixture of three isomers. According to ^{1}H NMR and ^{31}P NMR of **151** compared with previously described **130** I was able to characterise two out of three isomers. The major isomer (Ru=C-CH δ = 8.29) and the minor isomer (δ = 8.21) have a similar structure to the previously described two main isomers of **130**. The third isomer with Ru=C-CH at δ = 8.32 has Ar-H mesityl signals downfield (δ = 6.25 and 5.83) compared to the main isomer (δ = 6.43 and 6.03), which means that there is a lack of π-π stacking which stabilises the structure.

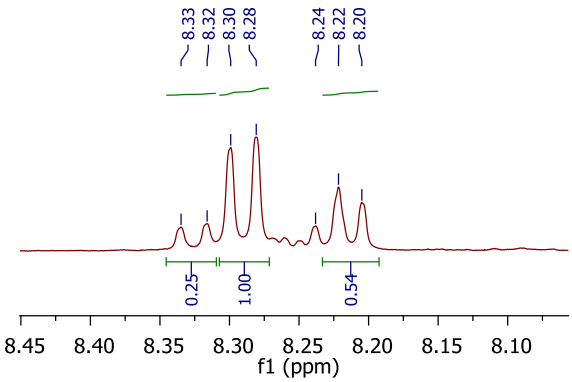

Figure 52. ^{1}H NMR of **151**, the characteristic region of Ru=C-CH (in CD_2Cl_2).

To conclude the investigation on the relationship between the distance of NHC-POSS in the ligand and the activity of the catalyst I synthesised salt **146** with a benzyl linker. The synthesis of the appropriate complexes was achieved using the procedure employing KHMDS as the base. Catalyst **153** was obtained in 35% yield.

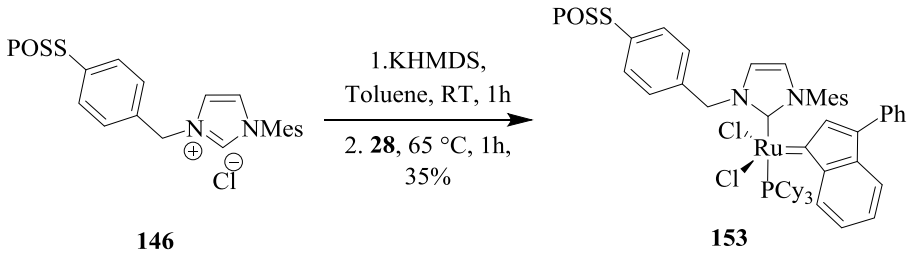

146 **153**

Scheme 29. The synthesis of catalyst **153** bearing NHC with benzyl linker.

The reactivity of the POSS-modified indenylidene catalysts **130**, **151** and **153** in the model RCM reaction of DEDAM (**8**) was compared with that of **136**. The reaction was performed in toluene at room temperature, according to the previously described procedure.

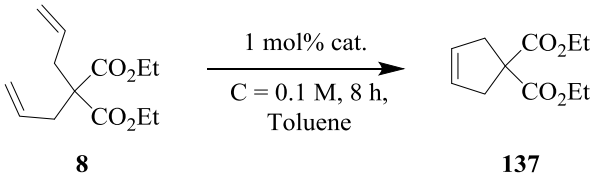

8 **137**

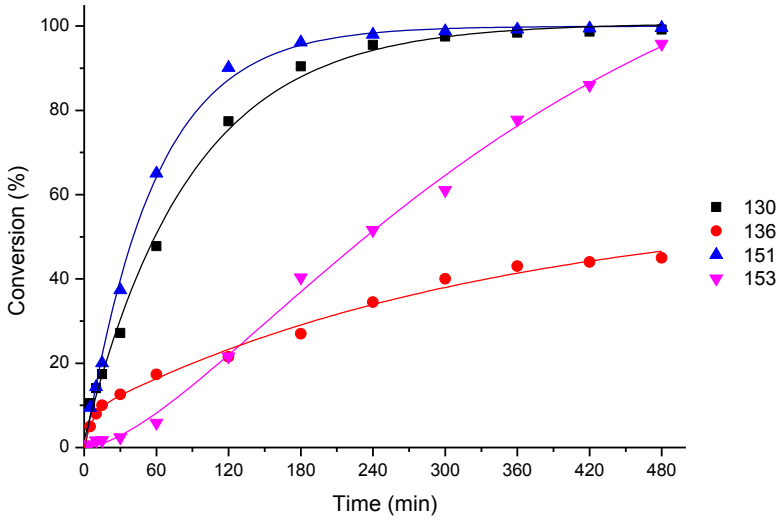

Figure 53. Reaction profile measurements of **130**, **151**, and **153** compared to the parent complex **136**.

As previously, all examined complexes were found to be much more active than the parent catalyst **136**. According to Figure 51 we can assume that the activity of the examined complexes increases with the length of the linker between the NHC and the POSS. Catalyst **153**, with a slightly different structure of the NHC ligand exhibited a different shape of the reaction profile. Such difference could be explained by longer activation time of the catalyst. The curve did not reach a plateau which means that the catalyst was still active.

I decided also to investigate if there is any relationship between the activity of the catalyst and the size of the POSS moiety attached to the NHC ligand. Having salt **139** in hand I was able to prepare the appropriate complex **154** in 50% yield.

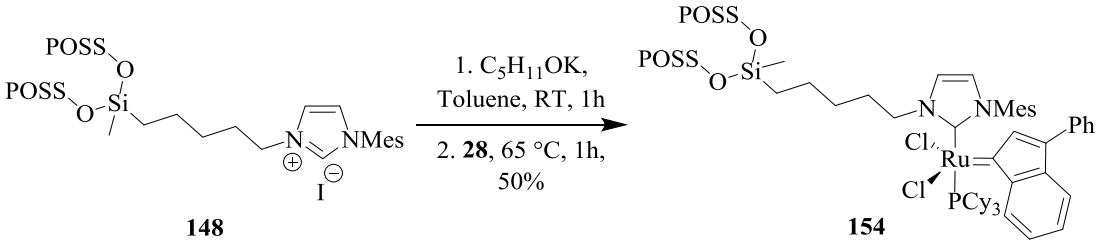

148 **154**

Scheme 30. Catalysts bearing NHC with two POSS moiety.

The influence of the size of the POSS tag on activity of the catalyst was examined in the RCM reaction of DEDAM (**8**). The reaction was performed in toluene at room temperature, according to the previously described procedure.

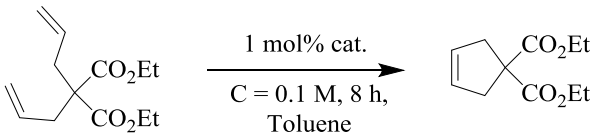

8 **137**

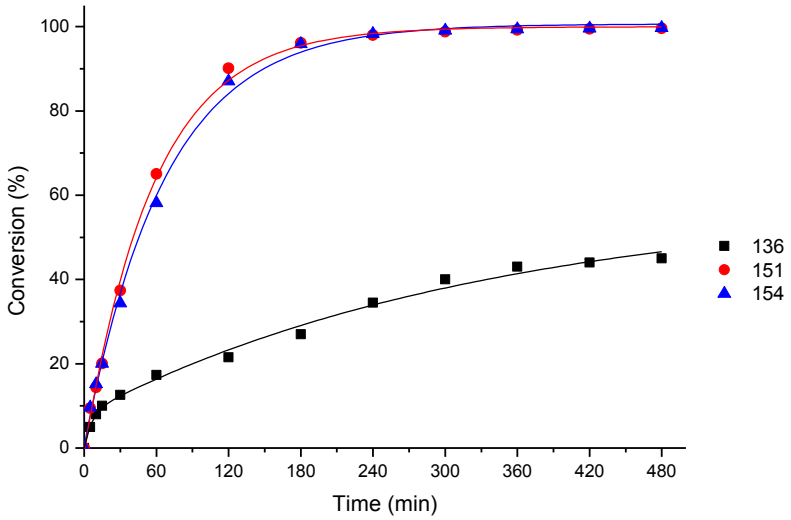

Figure 54. Reaction profile measurements of **151**, and **154** compared to the parent complex **136**.

There was almost no influence of the size of the POSS on the activity of the examined catalysts. I did not observe any relationship between the size of POSS and the activity.

2.2.1.3. CONCLUSIONS

A variety of NHC-modified ruthenium complexes have been synthesiszed. All of the newly synthesised indenylidene catalysts were found to be much more active in the model RCM reaction than the parent complex **136**. The most promising results were achieved with complex **130**, which I obtained with the highest yield among all the described complexes.

I was unable to purify and analyse the Grubbs-type catalyst as well as the indenylidene complexes containing NHC ligands prepared from **143** and **144** imidazolium salts.

The Hoveyda-type catalyst with the modified NHC ligand (**129**) had much lower activity towards DEDAM in comparison with the parent catalyst **138**. The catalyst needed elevated temperature to catalyse the metathesis reaction.

For further tests I chose catalyst **130**, which exhibited high activity towards the model reaction along with the highest yield of its synthesis.

2.2.2. MODIFICATION OF THE ANIONIC LIGAND

Anionic ligands are widely utilised as a site for tagging the ruthenium complexes, which was described in the first part of this dissertation. Anionic ligands can be exchanged with carboxylate groups, phenoxyl groups, alkoxyl groups and others.[208]

Carboxylate complexes, such as **155**, possess a unique ability of being activated by the exchange of the internal ionic ligand with the acid. They have been already examined as tagged with surfactants[208b] or immobilised on mesoporous molecular sieves.[103b] This type of catalyst exhibits high stability and can be utilised in aqueous emulsions.[208b] The classical carboxylate complex **155** has one disadvantage, as during the opening of the carboxylate ring in the complex with an acid, simultaneous disproportionation occurs which leads to a mixture of three complexes **156**, **157** and **158** (Scheme 31).

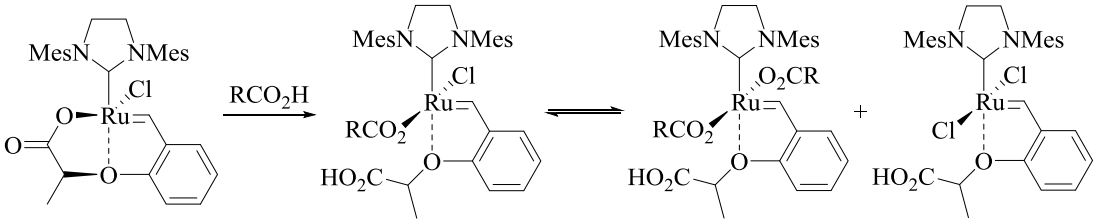

155 R = C_8F_{17} **156** 74% **157** 13% **158** 13%

Scheme 31. Disproportionation of **155**.

The desired complex **156** is the major product (74%), but there are two additional products **157** and **158**, 13% of each.[208a] When such mixture would be nanofiltered through a membrane with MWCO=500, complex **158** would pass through the membrane.

Disproportionation can be avoided when the chloride ligand is changed to trifluoroacetate (Scheme 32).

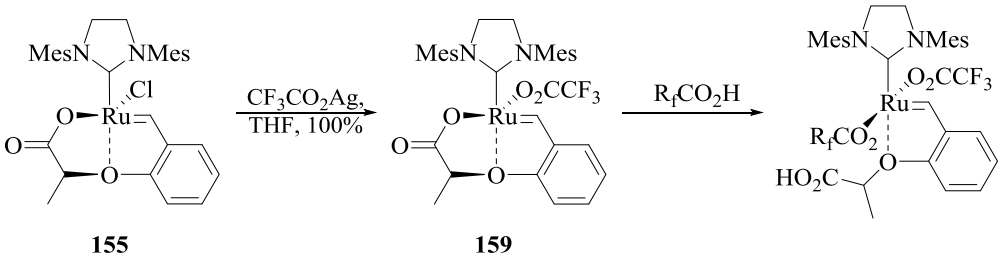

155 **159**

Scheme 32. The synthesis of complex with two perfluorinated ionic ligands.

Based on the described procedure, I prepared a POSS moiety with a hexafluoroglutaric linker by mixing 3-aminopropyl-heptaisobutylPOSS(T_8) (**160**) with hexafluoroglutaric anhydride. The product was obtained in quantitative yield without any purification.

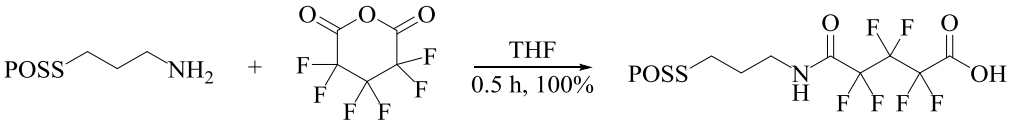

160 **161** **162**

Scheme 33. A POSS moiety with a hexafluoroglutaric linker.

The structure of the 2,2,3,3,4,4-hexafluoro-5-oxo-5-((3-(heptaisobutylPOSS(T_8)) propyl)amino)pentanoic acid **162** was confirmed by ^{1}H NMR. The characteristic signal of COO<u>H</u> was found at δ = 11.24 and MS with the signal at *m/z* = 1096.5 $[M]^+$ compared to calculated *m/z* = 1096.6.

Tagging of a ruthenium complex utilising the procedure described above is very simple, straightforward and what is most important, quantitative. The perfluorinated catalyst **159** was mixed with **162** in THF for a few minutes, and then the solvent was evaporated.

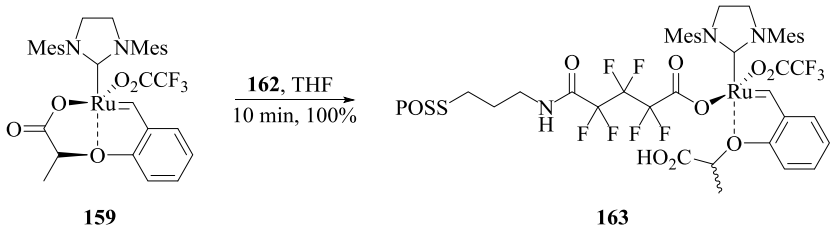

159 **163**

Scheme 34. The synthesis of the **163**.

The exchange of the ionic ligand was confirmed by ^{1}H NMR. The benzylidene proton Ru=<u>CH</u> of **159** was observed at δ = 16.85. After treatment of **159** with **162** I

observed two signals in the region of the benzylidene proton δ = 17.11; 17.04 in the ratio 1:1. Probably catalyst **163** exists in two forms. I did not observe disproportionation of **163**. Confirmation of disproportionation would be the third signal in the region of benzylidene proton at δ = 17.01 which comes from the carboxylate complex with two trifluoroacetic ligands.

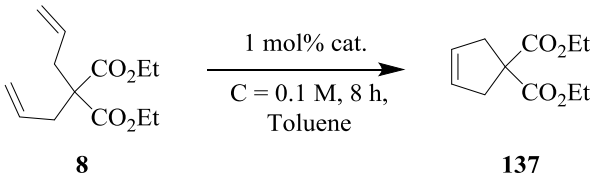

8 **137**

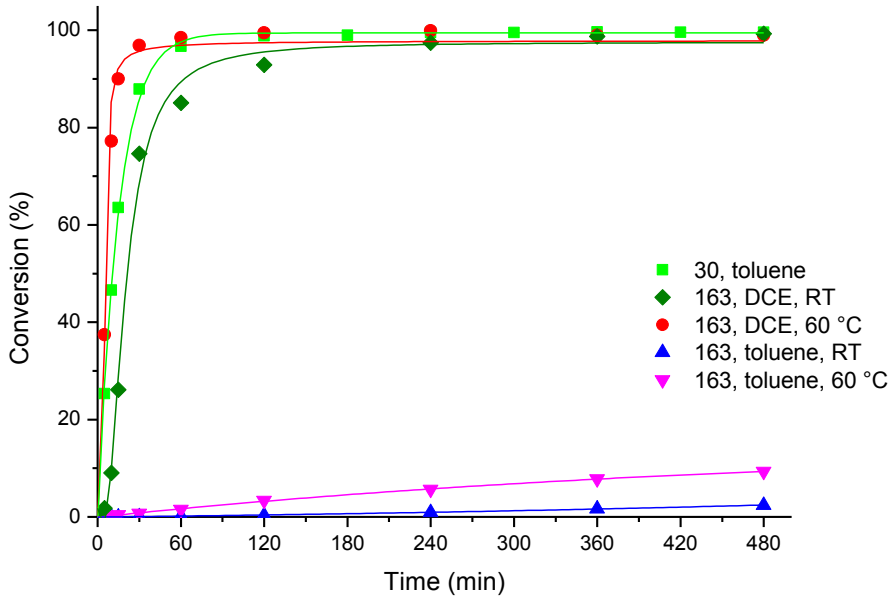

Figure 55. Reaction profile measurements of **163** compared to the parent complex **30**.

I performed the examination of its catalytic activity using the model RCM reaction of DEDAM in toluene and DCE at room and elevated temperatures. The reaction was conducted according to the previously described procedure.

Complex **163** was found to be slightly less active than the parent complex **30**. Surprisingly, when the chlorinated solvent was exchanged with toluene the activity of the catalyst decreased drastically. Bearing in mind that the nanofiltration test would be performed in toluene, catalyst **163** was not be suitable for further investigation.

The results obtained for DCE are in agreement with the literature. Usually complexes with perfluorinated ionic ligands are less active than those with chlorides. This trend is vividly shown by reaction profile measurements of complex **30** and its two analogues with acetate and trifluoroacetate as ionic ligands.

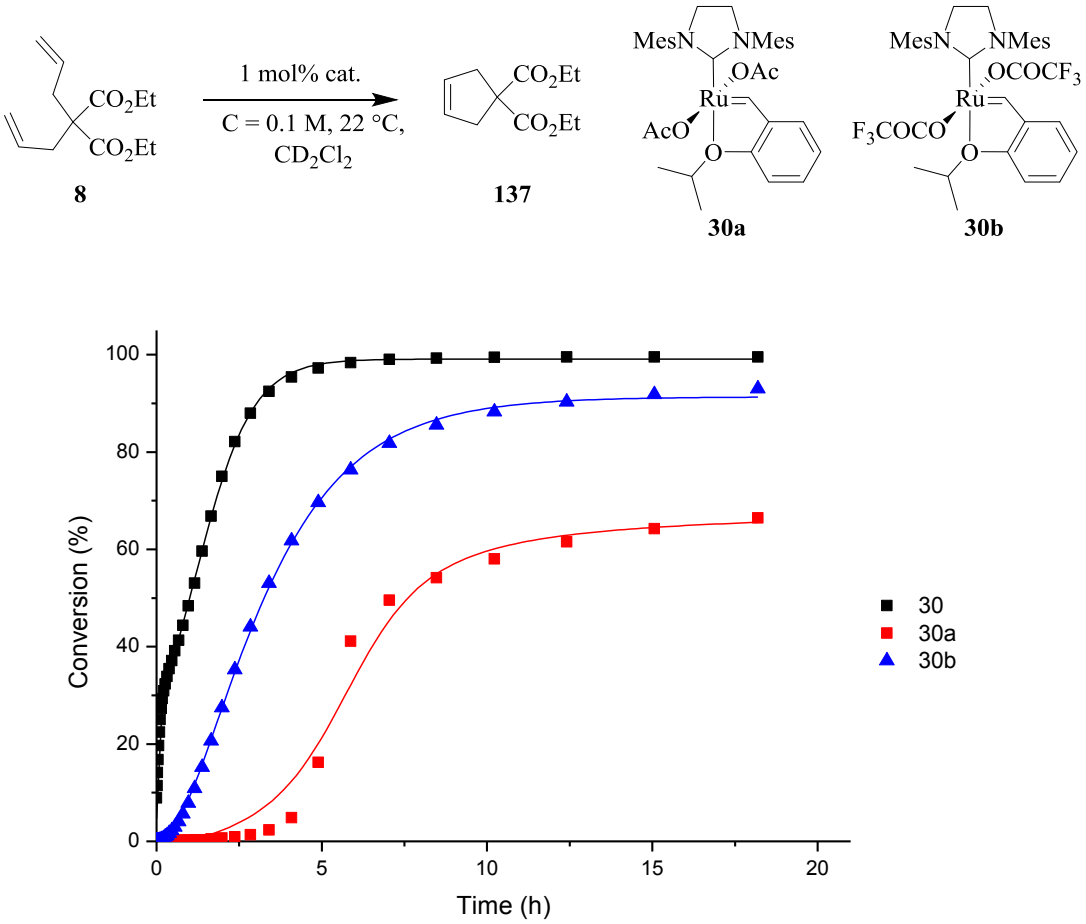

Figure 56. Reaction profile measurements of **30** and its analogues **30a** and **30b**.

During the research on the carboxylate complex I found that the complex with iodide ligands is much more stable than those with chloride or TFA ligands and can be stored in solution for months.[208a] Encouraged by this fact, I decided to synthesise an iodide analogue of **163**. The synthetic pathway was simpler compared to that of complex **163**.

Complex **155** was dissolved in acetone and treated with an excess of KI. The obtained product **164** was much darker than **155** and in ^{1}H NMR I observed the benzylidene signal at δ = 15.85, compared to δ = 16.45 in **155**. Based on the previously described procedure, complex **164** was mixed with acid **162** to obtain **165** in quantitative

yield. The structure of **165** was confirmed by ^{1}H NMR. In the characteristic region of the benzylidene ligand I found a signal at δ = 16.00. Over time I did not observe the formation of any additional signal in the benzylidene region which confirmed the lack of undesired disproportionation.

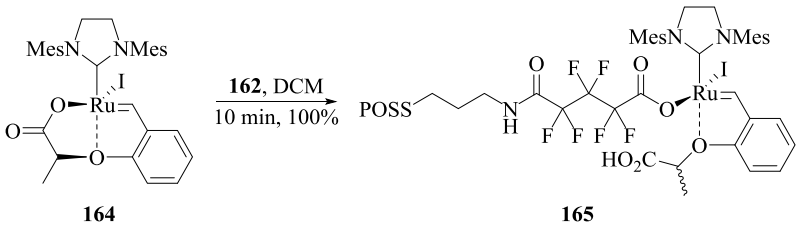

164 **165**

Scheme 35. The synthesis of iodide complex **165**.

The activity of the catalyst was examined in RCM of DEDAM and compared to the commercially available **30**. The reaction was performed in toluene and DCE, according to the previously described procedure.

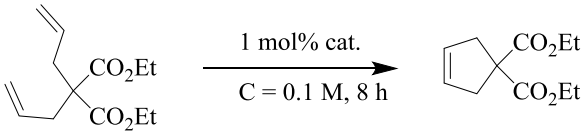

8 **137**

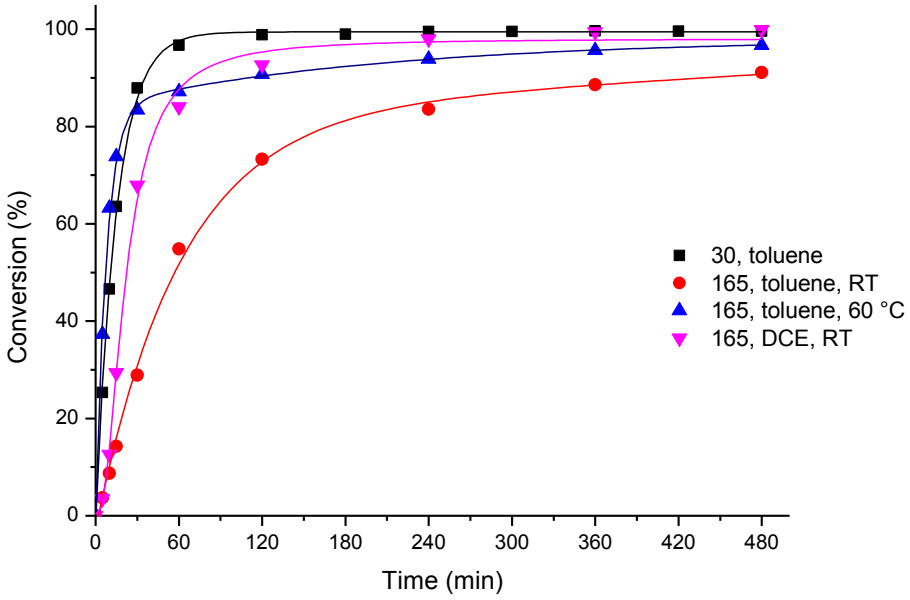

Figure 57. Reaction profile measurements of **165** as compared to the parent complex **30**.

Complex **165** was found to have the same activity towards DEDAM in DCE as the previously described **163**. According to literature, iodide complexes are supposed to be less active in comparison with the parent chloride complex and more active than complexes with perfluorocarboxylic acids as ionic ligands.[44a,209]

I observed a minor influence of the solvent on the activity of the examined complex. In toluene initialization of **165** was a bit slower compared to DCE and activity slightly decreased, whereas for **163** the differences were much greater.

2.2.2.1. CONCLUSIONS

I prepared two complexes with modified ionic ligands. Both of them were found to be active in the model RCM reaction. Both complexes have been examined in nanofiltration conditions.

2.2.3. MODIFICATION OF THE BENZYLIDENE LIGAND

The third modification that I decided to examine was the modification of the benzylidene ligand. This method of tagging has been already utilised with good results, which was described in the first part of this dissertation. The benzylidene ligand may dissociate during the catalytic cycle, but this is determined by the nature of the catalyst and conditions of the reaction. Being aware that this method of tagging could cause leaching during nanofiltration I decided to try such a modification.

2.2.3.1. CARBAMATE LINKER

The first concept that I decided to try was an urethane bond. Such a linking bond was chosen taking into account the easy accessibility of the POSS moiety with an isocyanate group. The benzylidene ligand was prepared according to a simple procedure which starts with commercially available 2-(4-hydroxyphenyl)acetic acid **166**. Esterification of the acid followed by alkylation, bromination, Stille coupling and reduction led to 2-(4-isopropoxy-3-vinyl-phenyl)ethanol **172**. Finally, POSS moiety **173** was attached to the benzylidene through an urethane linkage. The coupling was carried out in the presence of a catalytic amount of dibutyltin dilaurate. Ligand **174** was synthesised in 66% overall yield.

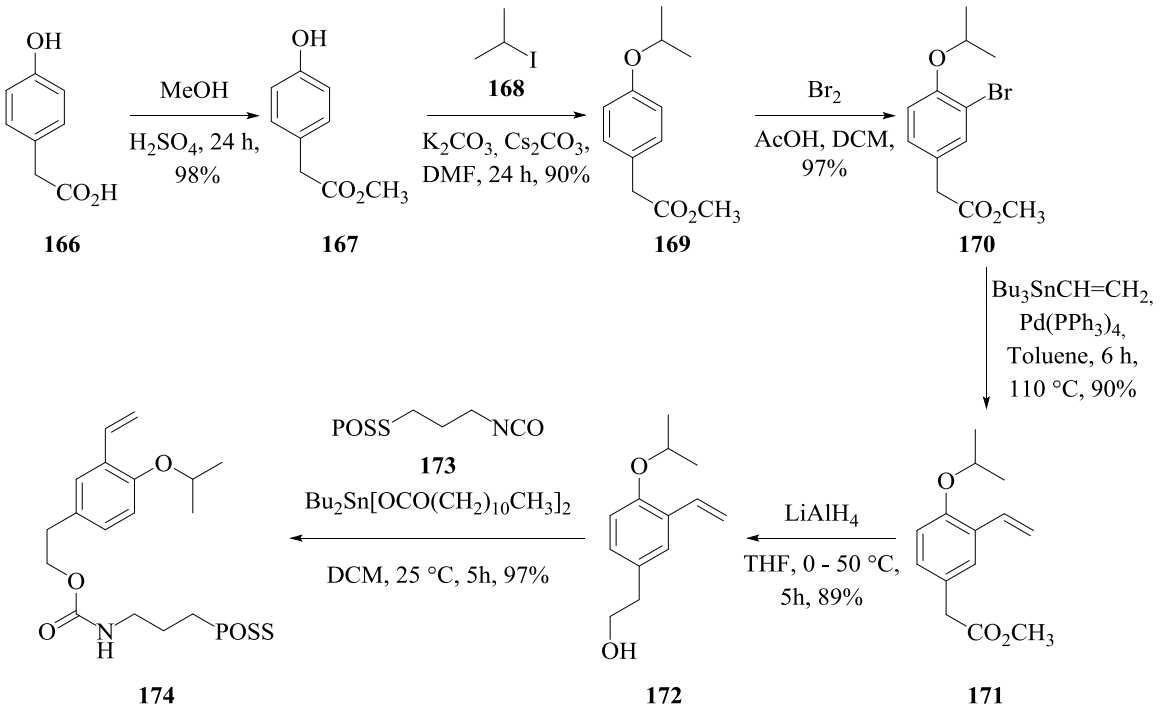

Scheme 36. The synthesis of 4-isopropoxy-3-vinylphenethyl (3-heptaisobutylPOSS(T_8)-propyl) carbamate **174**.

Having modified the benzylidene ligand, a Hoveyda-type catalyst was prepared from appropriate second generation indenylidene complexes **31** or **136**.

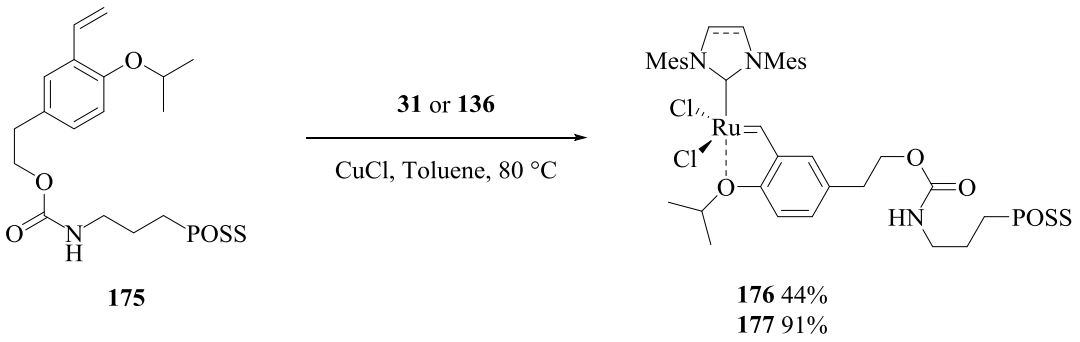

Scheme 37. The synthesis of Hoveyda type catalysts bearing an urethane linkage.

Catalyst **176** with an unsaturated NHC ligand was obtained in much lower 44% yield, compared to 91% in the case of **177** (with the saturated NHC ligand).

The structure of **176** and **177** was confirmed by ^{1}H NMR and MS. The characteristic signals from the benzylidene proton (Ru=CH) were found at δ = 16.67 ppm and 16.59 ppm, respectively. The composition of the complexes was confirmed by MS with the signals at *m/z* = 1571.3 and 1569.4, compared to calculated *m/z* = 1571.3 and 1569.4, respectively.

A crystal of **177** was obtained by crystallisation from a mixture of DCM/MeOH. I was not able to obtain a crystal of **176**.

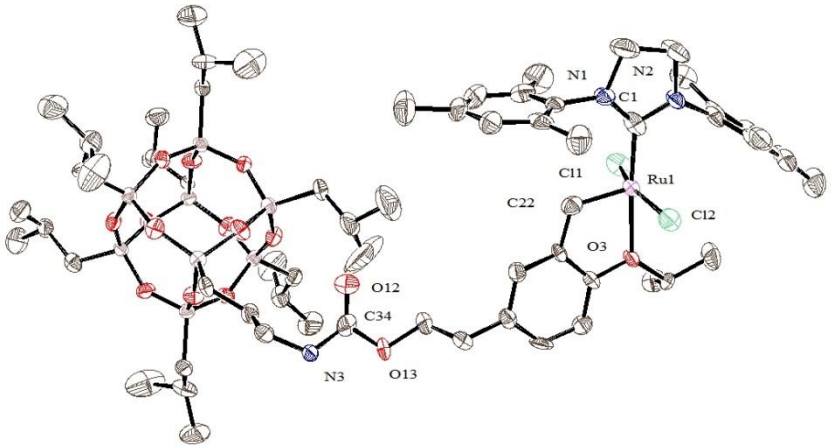

Figure 58. ORTEP representation of the molecular structure of **177**. Thermal ellipsoids at 50% level of probability.

Molecules of **177** crystallised in monoclinic $P2_{1/c}$ space group with one molecule in the asymmetric unit, whereas the parent complex **30** crystalised in monoclinic $P2_{1/n}$ space group also with one molecule in the asymmetric unit.

Table 6. Comparison of selected bond distances (Å) and angles (°) of complexes **177** and **30**.

Bond distance (Å)	177	30
Ru(1)-C(1)	1.980(4)	1.981(5)
Ru(1)-C(22)	1.827(4)	1.828(5)
Ru(1)-O(1)	2.244(4)	2.261(3)
N(2)-C(1)	1.349(6)	1.351(6)
N(1)-C(1)	1.349(6)	1.350(5)
Bond angle (°)		
Ru(1)-C(1)-N(2)	133.7(3)	120.8(3)
Ru(1)-C(1)-N(1)	118.8(3)	131.6(3)
C(1)-Ru(1)-C(22)	102.6(2)	101.5(14)
O(1)-Ru(1)-C(1)	177.0(1)	176.2(14)
Cl(1)-Ru(1)-Cl(2)	160.90(4)	156.5(5)

The ruthenium atom is pentacoordinated. The five-membered ring formed by Ru(1)C(22)C(23)C(24)O(3) is almost flat. The torsion angle Ru(1)C(22)C(23)C(24) is equal to -5.3(5)°. The angle between the ruthenium atom and two chloride atoms is 160.91(4)°. The Ru(1)-C(1) and Ru(1)-C(22) bond lengths are: 1.980(4)Å and 1.827(4)Å, respectively. The geometry of the catalyst part remains nearly unchanged in comparison to the earlier reported geometry of **30**. The most significant discrepancy is the conformation of the NHC ligand - the C(1)N(1)C(4), C(1)N(2)C(13) angles are 123.8(4)° and 129.2(4)° in **177**, whereas in the structure of **30** they are equal to: 126.9(1)° and 126.6(1)°, respectively. Furthermore, in the crystal structure **177**, the Ru(1)-O(1) bond is elongated to 2.244(4)Å.

The activity of the catalysts was compared with the commercially available Hoveyda 2nd generation catalyst (**30**) in the RCM reaction of DEDAM (**8**). The reaction was performed in toluene and DCM at room temperature, according to the previously described procedure.

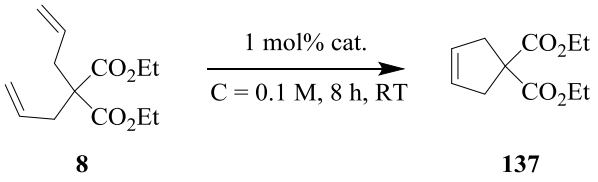

8 **137**

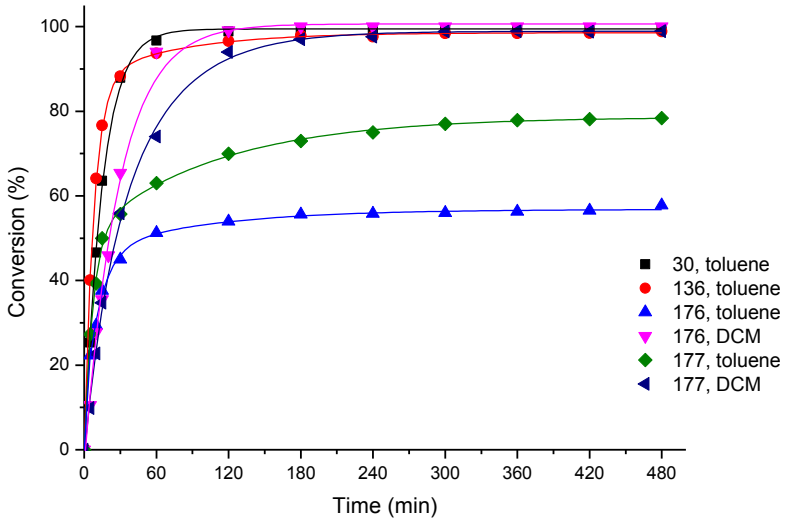

Figure 59. Reaction profile measurements of **176**, **177**, compared to the parent complexes **30** and **135**.

Both catalysts were found to be active in the model RCM reaction of DEDAM performed in DCM, but when solvent was changed to toluene, the activity of both complexes decreased drastically. This phenomenon surprised me, because I did not find any data in the literature concerning similar behaviour. Another very important thing that should be considered was that nanofiltration was to be performed in toluene. Bearing this in mind I decided to find a linker which would not interfere with the activity of the examined catalyst.

Catalyst **176** is less active compared to **177**, which did not surprise me. Hoveyda-type catalysts bearing unsaturated NHC ligands are usually less active than those with saturated NHC ligands.[37c] Bearing in mind the criteria of "ideal MWE tagged catalyst" I decided that in the case of benzylidene modification part I will focus on the catalyst bearing the saturated NHC ligand.

2.2.3.2. AMIDE LINKER

The amide group has been chosen as a promising and easily synthesised linking bond. Based on a protocol described by Dowden[122] I prepared the appropriate secondary alcohol **179** starting with commercially available δ-caprolactone (**178**) which was attached to the benzylidene ligand by Mitsunobu reaction.

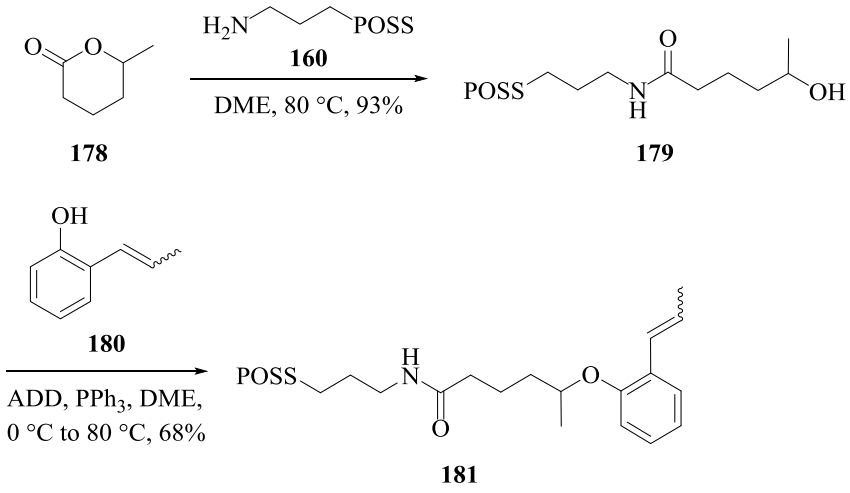

Scheme 38. The synthesis of *N*-(3-heptaisobutylPOSS(T_8)-propyl)-5-(2-(prop-1-en-1-yl) phenoxy)hydroxyhexanamide **181**.

A simple two-step protocol led to the POSS-tagged benzylidene ligand **181** in 63% overall yield. Next, **181** was attached to ruthenium via standard procedure of ligand exchange with 69% yield.

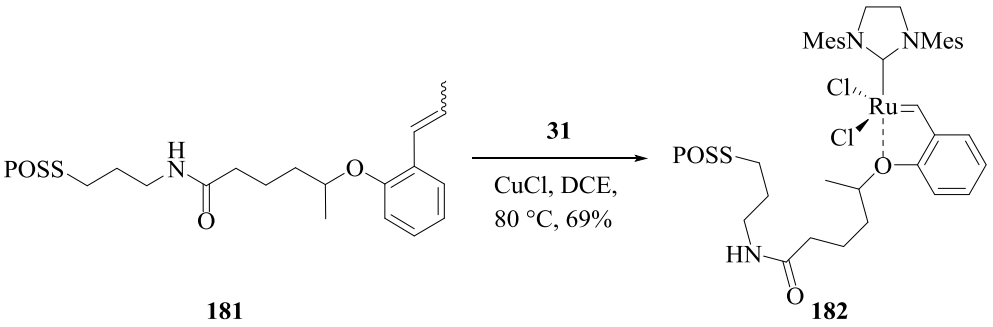

Scheme 39. The synthesis of Hoveyda-type catalyst with amide linker.

In the ^{1}H NMR spectrum of **182** I observed a singlet in the region of benzylidene proton (Ru=CH) resonance at δ = 16.60 ppm which confirmed the structure.

The activity of the complex has been examined in the model RCM reaction of DEDAM in toluene and DCM and compared with the parent catalyst **30**.

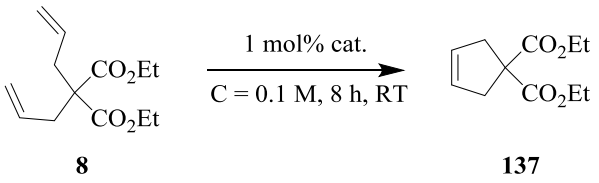

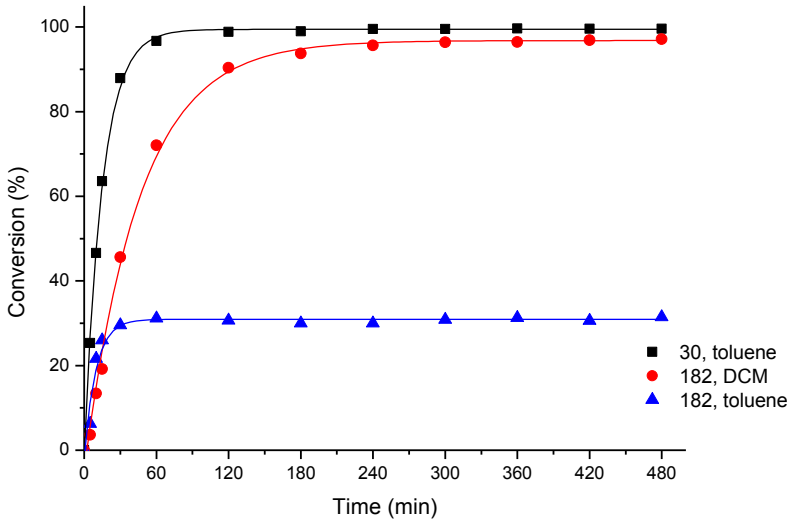

Figure 60. Reaction profile measurements of **182** in toluene and DCM compared to the parent complex **30**.

The influence of the solvent on the activity of the examined catalyst was observed also in this case. The decrease of the activity of the examined complex in toluene was even greater compared to the previously described complexes **176** and **177**. Because

nanofiltration must be conducted in toluene, complex **182** was inappropriate for further tests.

2.2.3.3. ESTER LINKER

The ester group attracted my attention because of a wide range of methods of its synthesis. The synthesis of the ligand started with commercially available 5-bromosalicylaldehyde (**183**) which was alkylated followed by Wittig reaction. 4-Bromo-1-isopropoxy-2-(prop-1-enyl)benzene (**185**) was transformed to the appropriate carboxylate analogue by a two-step procedure.[210] In the first step **185** was transformed to a Grignard reagent which was reacted with copper iodide to obtain the appropriate cuprate. The reaction of β-propiolactone with the cuprate afforded 3-(4-isopropoxy-3-(prop-1-enyl)phenyl)propanoic acid (**186**) in good yield. Compound **186** was coupled[211] with 5-hydroxypentyl-heptaisobutylPOSS(T_8) (**187**) to obtain the benzylidene ligand with ester linking bond (**188**).

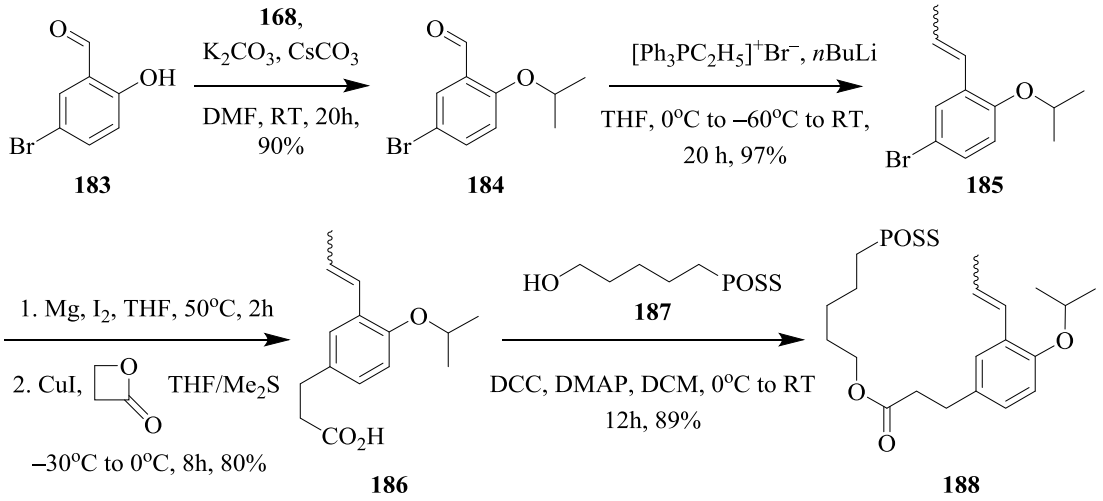

Scheme 40. The synthesis of 5-heptaisobutylPOSS(T_8)pentyl-3-(4-isopropoxy-3-(prop-1-enyl)phenyl)propanoate (**188**).

According to the previously described procedure, I prepared catalyst **189** from **31** in 65% yield. The structure of the catalyst was confirmed by ^{1}H NMR the characteristic signal of the benzylidene proton (Ru=CH) was found at δ = 16.52 ppm. The composition of **189** was confirmed by MS with the signal at *m/z* = 1584.3 compared to calculated *m/z* = 1584.4.

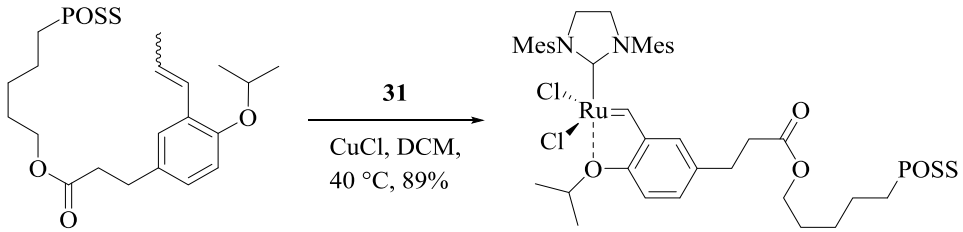

Scheme 41. The synthesis of catalyst **189** with an ester linking group.

The obtained complex was examined in the model RCM reaction of DEDAM in toluene, DCM and DCE according to the previously described procedure. The activity of the complex was compared with the parent catalyst **30**.

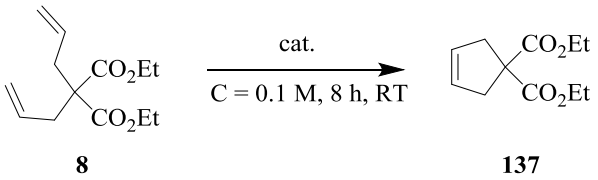

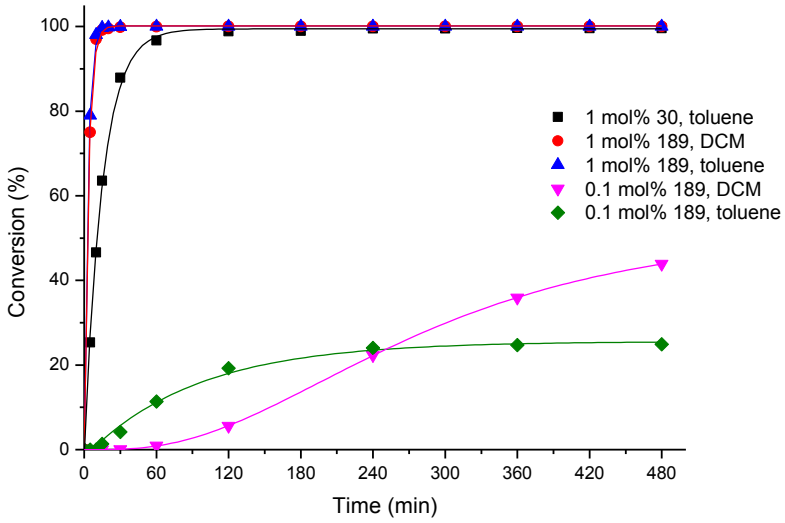

Figure 61. Reaction profile measurements of **189** in toluene and DCM compared to the parent complex **30**.

Complex **189** was found to be much more active than the parent complex **30**. In the case of catalyst loading of 1 mol% catalyst **189** had similar activity towards DEDAM in DCM as in toluene. I did not observe any influence of the solvent on the activity of the examined catalyst. When catalyst loading was decreased to 0.1 mol% I observed differences in the initiation of the examined complex in DCE and toluene. In toluene I

noticed faster initiation of the catalyst than in DCM, but after 4 h the reaction reached a plateau. In the case of DCE the initiation of **189** was much slower but after 8 h the reaction profile curve did not reach a plateau, which means that the catalyst was still active. The reason of this phenomenon could be better stabilization of the $14e^-$ species in the chlorinated solvent than in toluene.

Comparing complexes with different linkers **182**, **177** and **189** I observed that the cause of different activity in toluene compared to DCM might be the proton connected to the urethane and amide group. In the case of **189**, there is no proton. To confirm this hypothesis I decided to synthesise a complex with a liner not containing any heteroatom.

2.2.3.4. HYDROCARBON LINKER

The connection between the benzylidene ligand and the POSS moiety by a hydrocarbon chain could be constructed by applying various methods of coupling. Having 4-bromo-1-isopropoxy-2-(prop-1-enyl)benzene (**185**) and it's magnesium derivative in hand I decided to utilise the Kumada coupling. This type of coupling has many advantages such as low cost, high selectivity and mild conditions. Originally it was catalysed by nickel(II) or palladium(II) catalysts. To date a wide range of procedures and catalysts have been applied in the Kumada coupling.

The first trials of the Kumada coupling I performed based on the Beller procedure[212] with $Pd(OAc)_2$ as catalyst. I obtained only 20% yield of **190**. Due to lower the than expected yield of the reaction, further optimization of this process was performed by varying the catalyst source, solvent, base and other reaction conditions. Selected results are collected on Scheme 42. Replacement of $Pd(OAc)_2$ with PEPSI palladium catalyst resulted in decrease in yield of the desired product. The exchange of the catalyst to $FeCl_3$ according to protocol described by Nakamura[213] did not change the efficiency of the procedure. I obtained **190** with only 20% yield. $Fe(acac)_3$ applied as the catalyst, according to Cahiez[214] procedure, was found to be inactive in this transformation, as well as $CoCl_2$[215]. I obtained surprisingly low yield of **190** with $CuCl_2$[216] (11%). Finally, I obtained the best results when $Co(acac)_3$ was applied as catalyst.[217]

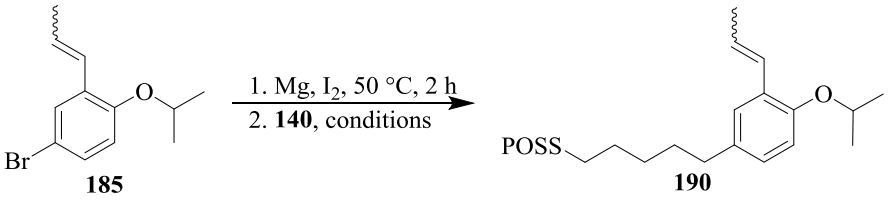

Conditions	yield
$Pd(OAc)_2$, PCy_3, THF/NMP, RT, 20 h	20%
$FeCl_3$, TMEDA, THF, 0 °C then RT, 20 h	20%
$Fe(acac)_3$, TMEDA, HMTA, THF, 0 °C then RT, 10 h	0%
$CuCl_2$, THF, -50 °C, 5h	11%
$CoCl_2$, TMEDA, LiI, THF, 10 °C then RT, 10 h	0%
Pd-PEPPSI, THF/DME, 0 °C to RT, 20 h	2%
$Co(acac)_2$, THF, RT, 20 h	40%

Scheme 42. Optimization of the Kumada coupling.

Further improvements of the Cahiez procedure with $Co(acac)_3$ as the catalyst led to 99% yield of **190**.

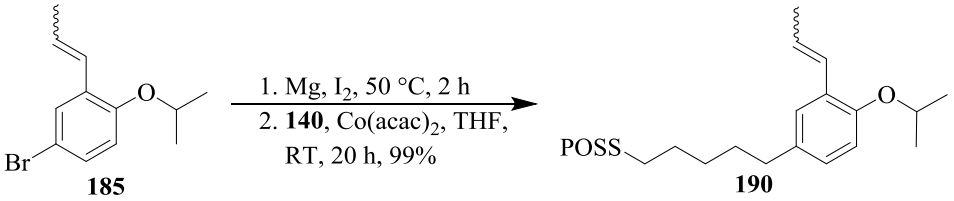

Scheme 43. The synthesis of the benzylidene ligand with C_5 hydrocarbon linker.

According to the previously described procedure I prepared catalyst **191** from **31** with 70% yield. The structure of the catalyst was confirmed by ^{1}H NMR, which showed the characteristic signal of the benzylidene proton (Ru=CH) at δ = 16.46 ppm. The composition of **191** was confirmed by MS with the signal at *m/z* = 1512.3 which was exactly as calculated *m/z* = 1512.3.

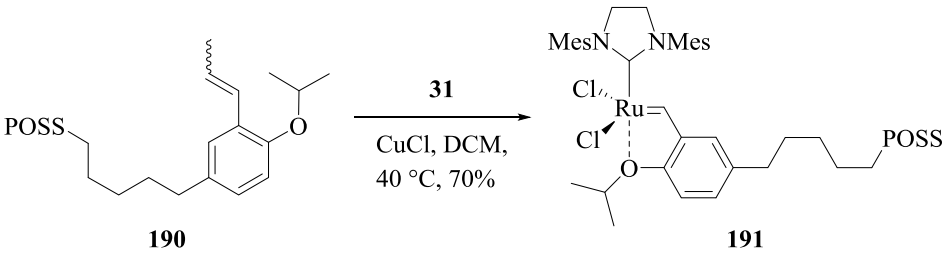

Scheme 44. The synthesis of **191**.

A crystal of **191** suitable for X-ray diffraction was obtained from a mixture of DCM/MeOH at 4 °C. The molecule of **191** crystallised in monoclinic $P2_{1/c}$ space group

with one molecule in the asymmetric unit, whereas parent complex **30** crystallised in $P2_{1/n}$ space group.

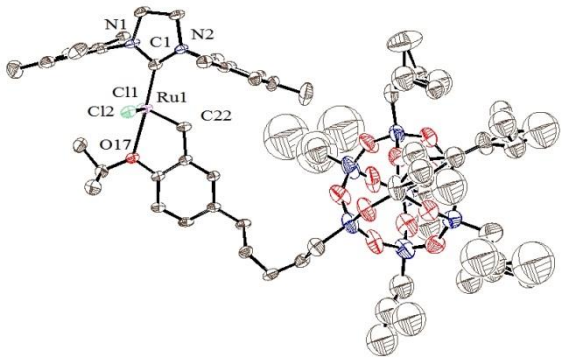

Figure 62. ORTEP representation of the molecular structure of **191**.

The distance between the Ru atom and C(1) was slightly shorter (1.976 Å) than in **30** (1.981 Å). Also Ru(1)–O(1) bond length of 2.227 Å was shorter than that observed in complex **30** (2.261 Å). A comparison between other relevant bond distances in **191** and **30** indicated that these two structures are very similar. The Cl(1)–Ru(1)–Cl(2) angle (159.54°) is slightly wider than the corresponding angle in the parent **30** (156.5°). This might explain the slightly higher activity of **191** compared to the parent catalyst **30**.

Table 7. Comparison of selected bond distances (Å) and angles (°) of complexes **191** and **30**.

Bond distance (Å)	191	30
Ru(1)-C(1)	1.976(6)	1.981(5)
Ru(1)-C(22)	1.829(7)	1.828(5)
Ru(1)-O(1)	2.227(4)	2.261(3)
N(2)-C(1)	1.347(7)	1.351(6)
N(1)-C(1)	1.352(8)	1.350(5)
Bond angle (°)		
Ru(1)-C(1)-N(2)	132.9(5)	120.8
Ru(1)-C(1)-N(1)	119.5(5)	131.6
C(1)-Ru(1)-C(22)	102.8(3)	90.69
O(1)-Ru(1)-C(1)	176.2(2)	176.06(5)
Cl(1)-Ru(1)-Cl(2)	159.54(6)	156.251(15)

Having the complex in hand, I attempted to examine its efficiency in toluene and DCM at room temperature in the model RCM reaction of DEDAM. The activity of the complex was compared with that of the parent catalyst **30**.

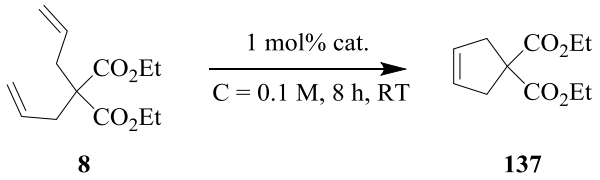

8 **137**

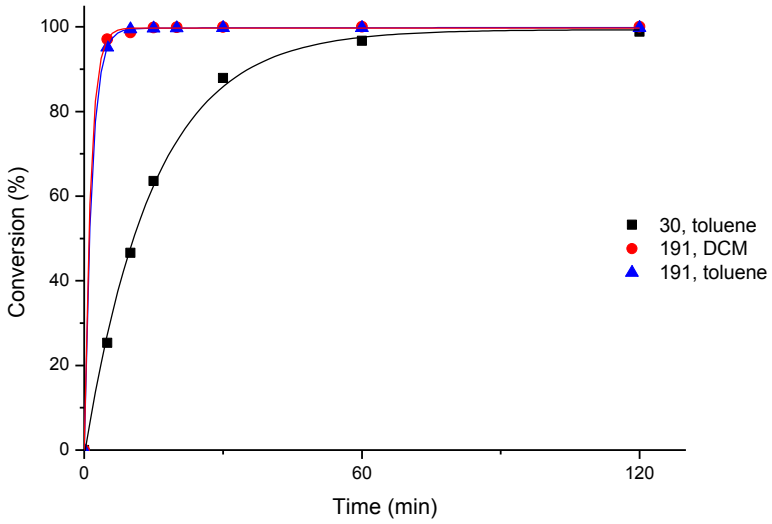

Figure 63. Reaction profile measurements of **191** in toluene and DCM compared to the parent complex **30**.

The examined complex was found to be much more active in the model RCM reaction in comparison to the parent complex **30**. I did not observe any influence of solvent on the activity of the examined catalyst. In toluene as well as in DCM catalyst **191** exhibited similar activity. This result confirms the earlier prediction that some tagging bonds (urethane, amide) interfere with the activity of the examined catalysts in the case of reactions conducted in toluene.

2.2.3.5. MODYFICATION OF THE ISOPROPOXY GROUP

Encouraged by the fact that the ester group in the linker does not interfere with the activity of the ruthenium complex and by earlier work of Bieniek[218] who activated the ruthenium catalyst by modification of the isopropoxy moiety, I decided to prepare one more modification. Originally,[219] the isopropoxy group was exchanged by methyl

propanoate group which coordinates to the metal. Based on the described procedure I esterified acid **192** with 5-hydroxypentyl-heptaisobutylPOSS(T_8) (**187**) which led to ligand precursor **193** with almost quantitative yield (Scheme 45).

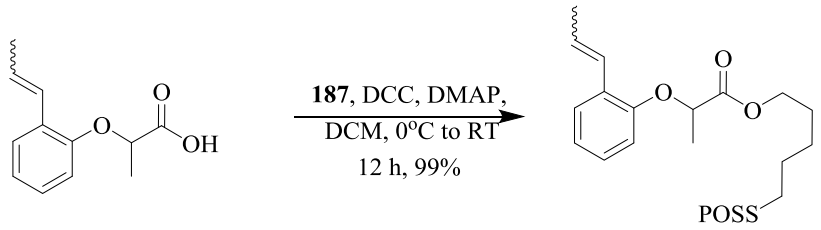

192 **193**

Scheme 45. The synthesis of benzylidene ligand **193**.

Compound **193** was coordinated to ruthenium by exchange with **31** and CuCl in refluxing DCM (Scheme 46). The structure of the catalyst was confirmed by ^{1}H NMR. The characteristic signal of the benzylidene proton (Ru=CH) was found at δ = 16.51 ppm. The composition of **194** was confirmed by MS with the signal at *m/z* = 1542.3 compared to calculated *m/z* = 1542.4.

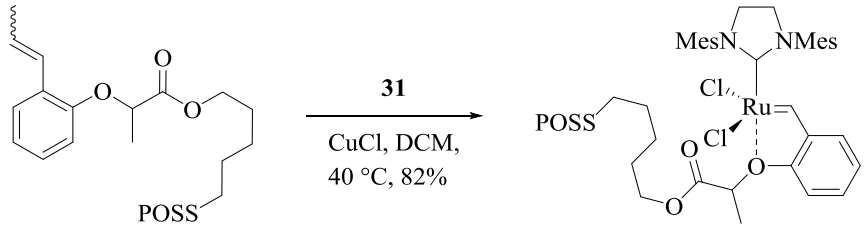

193 **194**

Scheme 46. The synthesis of complex **194**.

The activity of the catalyst was examined in the model RCM reaction of DEDAM (**8**) and compared to the parent catalyst **30**. The reaction was performed in toluene and DCE at room temperature, according to the previously described procedure.

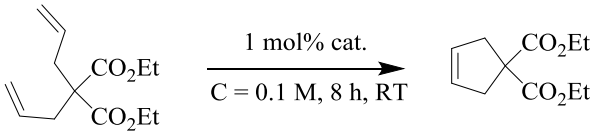

8 **137**

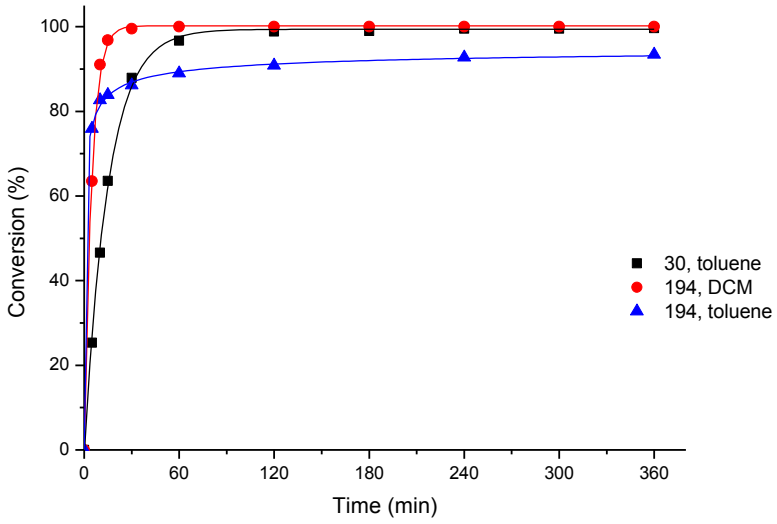

Figure 64. Reaction profile measurements of **194** in toluene and DCE compared to the parent complex **30**.

Complex **194** was found to be very active in DCE. After 10 min it reached almost full conversion. This result was in agreement with earlier results of Bieniek,[219-220] where the newly synthetised catalyst was found to be more active than the parent catalyst **30**. When the solvent was changed to toluene a slight decrease of activity of **194** was observed.

2.2.3.6. CONCLUSIONS

I synthesised five catalysts with modified benzylidene ligands. Two of them were found to have much lower activity in toluene than in a chlorinated solvent. I was not able to explain this phenomenon. I could only suspect that the cause of such changes in the activity is the linker. In the case of urethane and amide linker I observed a decrease of activity whereas in the case of ester or hydrocarbon linker the differences in activity were almost intangible. Catalyst **194** which was supposed to be very active and stable according to previous research[219] was found to demonstrate different activity in toluene than in the chlorinated solvent.

2.3. BATCH NANOFILTRATION

As a starting point for the screening of nanofiltration of the metathesis postreaction mixture, the batch version was chosen because of its simplicity. This method of filtration has a few drawbacks which have been described in the first part of this dissertation. Nevertheless, for optimisation and membrane selection the batch mode was the best model. As model complexes for these tests the most representative catalysts were chosen: **129**, **130**, **163** and **177**. A wide range of catalysts with a variety of tagging bonds chosen for this part of research were intended to help to determine the best connection between POSS and catalyst. I conducted this part of the research in cooperation with the group of prof. Livingston at the Imperial College of London.

2.3.1. MEMBRANES USED

Three commercial organic solvent nanofiltration (OSN) membranes Starmem 228, Starmem 240 and Duramem 500 were purchased from Evonic Membrane Extraction Technology, UK. The molecular weight cut offs (MWCO) (according to the supplier) are as follows: for Starmem 228 – 280 $g \cdot mol^{-1}$; for Starmem 240 – 400 $g \cdot mol^{-1}$and for Duramem 500 – 500 $g \cdot mol^{-1}$. Solvents used for MWCO determination as provided by the suppliers are: toluene for Starmem 228 and Starmem 240; DMF and acetone for Duramem 500.

2.3.2. MEMBRANE PRE-CONDITIONING

All the commercial and home-made membranes selected for this study were treated with pure solvent prior to filtering of the reaction mixture in order to remove any preserving agents from the membrane pores. Pure solvent was passed through the membranes until steady state flux was achieved.

2.3.3. ORGANIC SOLVENT NANOFILTRATION SETUP AND PROCEDURE FOR BATCH EXPERIMENTS

All batch nanofiltration experiments were carried out in a Sepa ST dead end filtration cell (Figure 7) (Osmonics USA), at 3×10^6 Pa and at 30 °C. A disk of the desired membrane (dia. 14 cm^2) was fitted into a stainless steel filtration cell with the active side of the membrane facing towards the reaction mixture. A stainless steel sintered plate was

placed below the membrane to provide mechanical support for the membrane during the filtration. Finally, the filtration cell was closed by clamping the cell base against the body with a set of high pressure clamps.

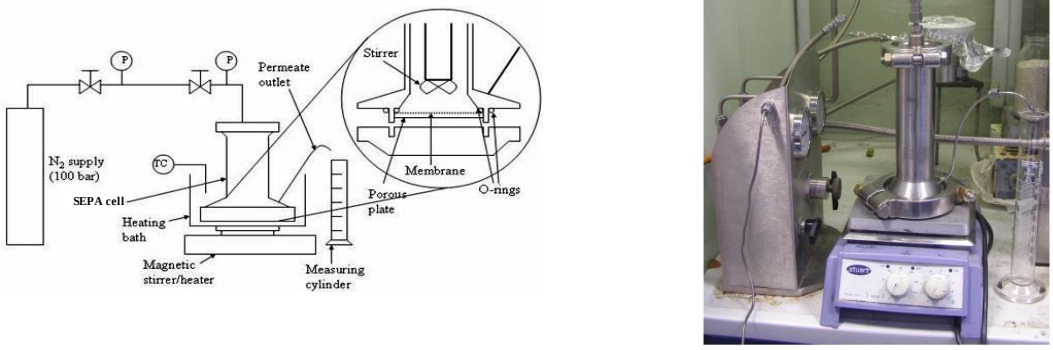

Figure 65. Dead end cell for catalyst recovery by nanofiltration.

The reactions were performed in a Carousel 12 (Radleys Discovery Technologies), and then the post-reaction mixture was transferred to the dead end cell for catalyst recovery. Pressure was applied by connecting the filtration system to a pressurised nitrogen cylinder. Continuous stirring was applied to avoid concentration polarization. After the pressurising of the cell, fresh solvent was introduced to the filtration cell with the help of a HPLC pump at the same rate as the permeate was being generated.

2.3.4. MEMBRANE AND CATALYST SCREENING

Initial screening of the membrane was performed by separating the previously chosen complexes from their post-reaction mixture. The model reaction of RCM of DEDAM (**8**) was performed with 1 mol% catalyst loading. Upon completion of the reaction, the post-reaction mixture was transferred into the filtration cell and pressurised.

Table 7. Screening of the membranes with chosen ruthenium complexes.

Entry	Catalyst	Conditions	Conversion	Membrane	% Rejection
1	**163**	Toluene, 80 °C, 6 h	39%	Duramem 500	73
2	**177**	DCM, RT, 3 h	96%	Duramem 500	71
3	**177**	Toluene, 30 °C, 3 h	94%	Starmem 240	77
4	**177**	Toluene, RT, 5 h	92%	Starmem 240	72
5	**177**	Toluene, RT, 5 h	92%	Starmem 228	100
6	**163**	Toluene, 60 °C, overn.	65%	Starmem 240	100
7	**129**	Toluene, 60 °C, overn.	60%	Starmem 240	100
8	**130**	Toluene, 60 °C, overn.	100%	Starmem 240	77

The first tests of the membranes gave very promising results. Starmem 228 and 240 membranes showed 100% rejection of the examined catalyst (Entry 5 – 7).

After completion of the filtration the filtration cell was opened and the membrane was removed to examine the physical appearance of the surface of the membrane.

Table 8. Physical appearance of the surface of the examined membranes, entry numbers are the same as in the Table 7.

Entry/Membrane/Solvent	Picture of the membrane	Physical appearance
2 Duramem 500 DCM	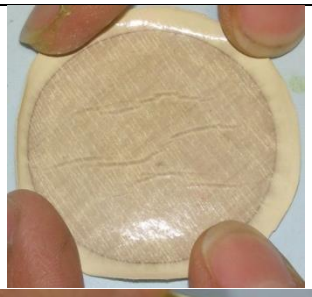	Creases at the surface as a result of swelling
3 Starmem 240 Toluene		Creases at the surface as a result of swelling
4 Starmem 240 Toluene	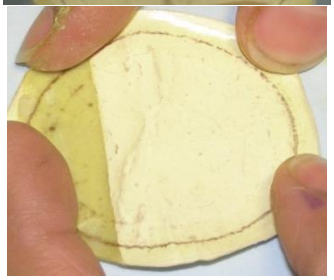	Creases at the surface as a result of swelling

5 Starmem 228 Toluene		Smooth surface
6 Starmem 240 Toluene		Smooth surface, but ruthenium black on the surface
7 Starmem 240 Toluene	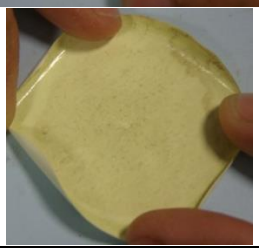	Smooth surface, but ruthenium black on the surface

As we can see in Table 8 only Starmem 228 presents good quality of the surface, which means that this membrane does not swell during filtration. Surface of the Starmem 240 (Entry 6 and 7) was also smooth, but in this case the catalyst decomposed during filtration. On the surface I was able to observe ruthenium black. The cause of decomposition of the examined complexes was unknown, but the reasons could be: the interaction between $14e^-$ Ru species and the membrane surface, the stability of the $14e^-$ Ru species, the interaction between the catalyst and the solvent. According to the supplier, Starmem 228 and Starmem 240 are the most suitable for separations in toluene, which were therefore used as the reaction/separation media. The reaction/separation with Duramem 500 was performed in DCM. According to the supplier, Duramem 500 is a cross-linked membrane stable in chlorinated solvents. The results indicates that only Starmem 228 shows stable separation performance with a catalyst rejection of approximately 100% and product rejection in the range of 10%.

At the same time I examined the influence of the transmembrane pressure (TMP), the driving force of the separation, on the rejection of the catalyst.

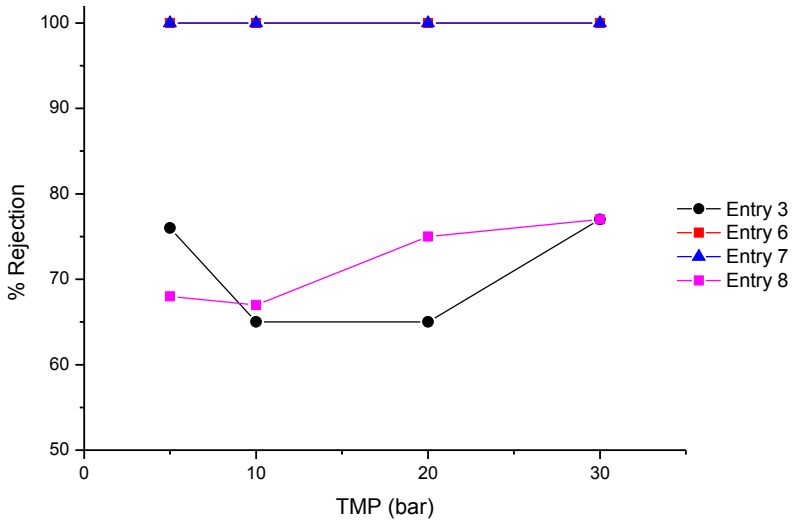

Figure 66. Effect of TMP on % rejection of the examined catalyst from the post-reaction mixture, entry numbers are the same as in Table 7.

The data shows that rejection increases with the pressure for almost all examined membranes. These results are in agreement with the literature. For the rest of the trials, 30 bar was chosen as TMP.

2.3.5. RECYCLING AND REUSE OF THE CATALYST

In the next step of the investigation I decided to check whether it is possible to recycle and reuse the catalysts. In this study Starmem 228 membrane was utilised. The model RCM reaction was performed according to the previously described procedure (toluene, 60 °C, overnight), after which the post-reaction mixture was transferred into the filtration cell. The system was pressurised, and fresh solvent was added at the same rate at which permeate was being collected, to keep the volume of the solvent in the cell at the same level. Fresh solvent was added to the system upon full removal of the product. Next, the solution of the catalyst was transferred back into the carousel tube and fresh substrate was added for the next reaction cycle.

The data presented in Table 9 shows that MWE catalysts have better rejection compared to the commercially available **31**. Having proven the concept, the next step was optimization of the conditions and finding the best way of recycling and reusing catalyst.

Table 9. Study of catalyst recycling and reuse in batch mode with MWE enlargement ruthenium complexes in comparison with commercially available **31**.

Entry no	Cat.	Cycle	Conv. (%)[a)]	% rejection (Catalyst) [b)]	Flux $L \cdot m^{-2} \cdot h^{-1}$	% rejection (product) [c)]	No of vol. passed [d)]
1	**129**						
		1	69	100	4.3	65	7
		2	55	100	3.8	58	7
		3	40	100	2.1	49	7
2	**130**						
		1	100	100	4.5	90	7
		2	95	100	3.8	88	7
		3	87	100	2.6	65	7
3	**163**						
		1	70	98	4.6	70	5
		2	63	99	3.5	60	7
		3	62	98	2.3	60	7
4	**177**						
		1	100	100	4.4	99	2
		2	90	100	3.4	89	3
		3	78	100	2.5	70	5
5	**31**						
		1	100	82	4.2	90	2
		2	89	83	3.1	81	3
		3	73	85	2.4	65	7

[a)] % conversion is based on GC analysis; [b)] % rejection of catalyst is based on UV analysis; [c)] % rejection of product is based on GC analysis for initial permeate collected; [d)] No of vol passed are calculated from diafiltration to remove product until constant value

2.4. NANOFILTRATION IN CONTINUOUS FLOW SYSTEM

Since ruthenium MWE enlargement complexes have been tested in batch nanofiltration mode, the next step was their application in continuous flow nanofiltration reactor. This part of research I established in cooperation with the group of prof. Dieter Vogt in the University of Technology Eindhoven.

The continuous flow nanofiltration reactor consists of one loop. The reactor can be filled with the aid of a syringe or a HPLC pump. The reaction mixture flows along the loop operated by a centrifugal pump and passes through the membrane chamber, in which the reaction mixture is partially separated from the MWE catalyst. The permeate is collected and analysed continuously, enabling constant monitoring of the flux through the membrane and conversion of the reaction. In this system a cross-flow filtration setup has been applied. I will omit details of the construction and modification of the setup. This

was the subject of work of Eng. Atilla Asar who built the setup and optimised the continuous process. I will focus on the reaction details.

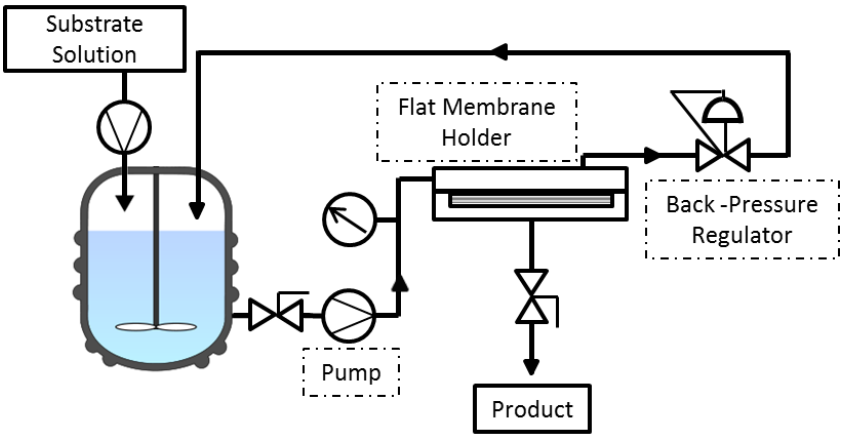

Figure 67. Home-made continuous mini-plant designed and built in the group of prof. Vogt.

RCM of DEDAM (**8**) has been chosen as the model reaction for this part of research. Among all catalysts chosen for the nanofiltration test in batch mode **130** was found to fulfil all the requirements of the ideal NME catalyst, such as straightforward synthesis, high activity, and high retention.

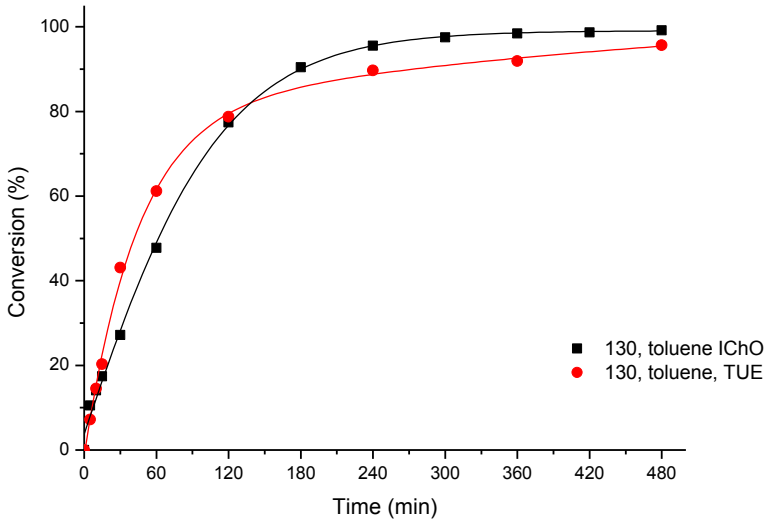

Figure 68. Reaction profile measurements of **130** in differently purified toluene.

130 was very active in the model RCM reaction in toluene, but it was worth to know if there is any relationship between the activity of **130** and the method of

purification of toluene. In Warsaw I used toluene distilled over Na whereas in TUE toluene was purified with alumina filled argon flushed column and degassed before use.

As we can observe in Figure 68 there is very small influence of the method of the solvent purification on the activity of **130**.

The feed rate and the permeate flow should be equal. This guarantees a constant volume in the set-up during the experiment. The feed rate is calculated according to the kinetic model of the metathesis reaction. According to literature[44a,45a] metathesis the reaction proceeds with pseudo 1st order kinetics.

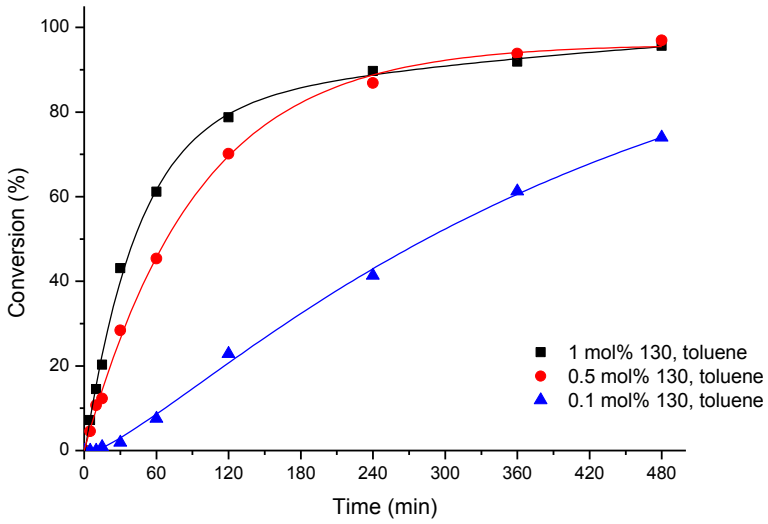

Figure 69. Reaction profile measurements of different loading of **130** in toluene.

The rate law for a first order reaction, combined with the mol balance:

$$-\frac{d[alkene]}{dt} = k[alkene] \qquad (3)$$

Since the reactor is operated isothermally the differential equation can be solved:

$$-\ln(1-X) = kt \qquad (4)$$

in which X is conversion.

A plot of -ln(1-X) as a function of time should give a straight line with slope k. From the Figure 70 it was concluded that k = 0.01012 h^{-1}.

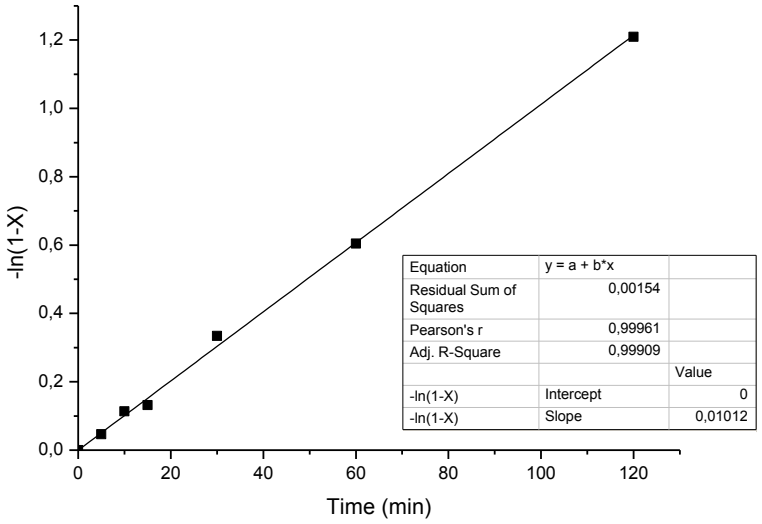

Figure 70. Ln(1-X) in time plot of **130** that demonstrates pseudo first order kinetics.

Applying the equation to CSTR in combination with a first order rate law equation we I able to calculate the flow rate of the reactor:

$$\upsilon_0 = \frac{V \cdot k}{X} \qquad (5)$$

in which *V* is the volume of the CSTR, υ_0 is the flow of the substrate into the reactor.

I was able to calculate how many times the volume of the reactor will be exchanged in time:

$$\tau = \frac{V}{\upsilon_0} \qquad (6)$$

The first version of the home-made continuous reactor was simple (Figure 69) as it consists of a syringe pump and a Schlenk flask connected by metal tubing with a membrane holder. The reaction mixture was circulated in the metal tubing by the pump and pressurised by back-pressure regulator.

Figure 71. First version of the home-made continuous mini-plant designed and built in the group of prof. Vogt.

In the beginning I decided to examine whether the catalyst would be active in such a setup. The reaction was initiated in a round bottom Schlenk flask. After completion of the reaction the flask was connected with the mini-plant. Fresh solution of DEDAM was added at the same rate as the flow rate of the membrane, which was 0.119 mL/min. As the membrane, I decided to use Duramem with MWCO = 300 previously pretreated with toluene, which was pressurised to 10 bar.

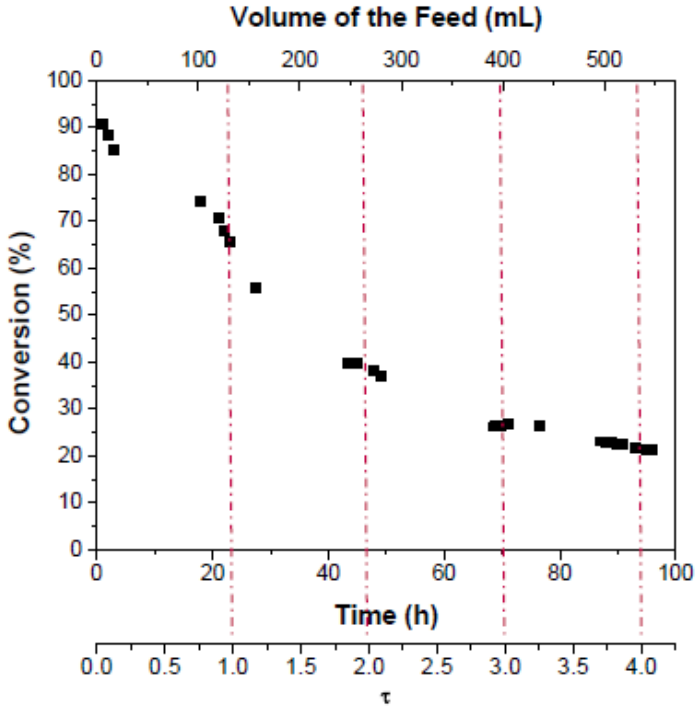

Figure 72. Reaction profile measurements of **130** in toluene in continuous system.

Reaction time was 96 h, we exchanged reaction volume four times, and TON reached 480 (Figure 72).

Next, a freshly dissolved portion of the catalyst was added to the solution of DEDAM which was circulated in the setup. Fresh solution of DEDAM was added at the rate of 0.075 mL/min. As the membrane, as previously, we utilised Duramem with MWCO = 300, which was pressurised to 2.5 bar.

The reaction has been performed for 70 h, during which time I exchanged the volume of the reaction five times (Figure 73). The highest conversion of 80% was reached after 10 h. The catalyst reached TON = 250. The permeate was collected to examine the amount of ruthenium contamination which was as high as 167 ppm according to ICP MS.

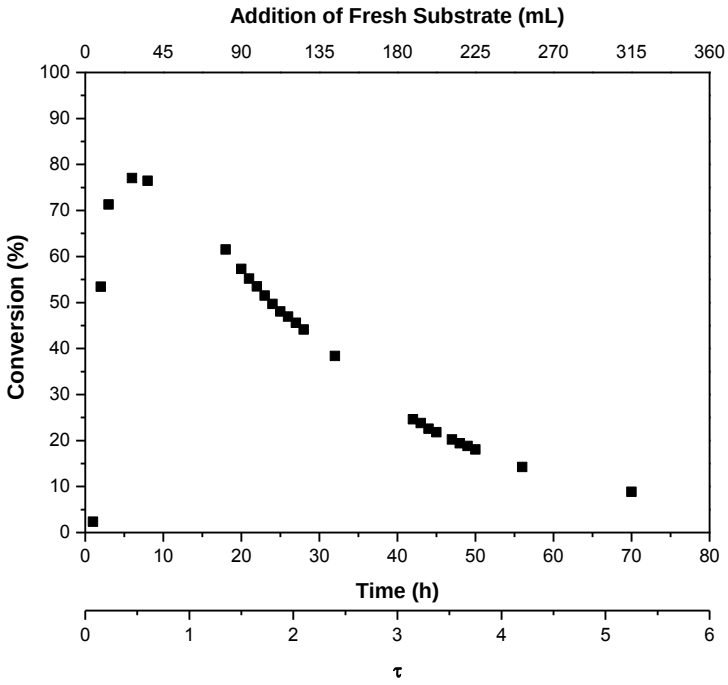

Figure 73. Reaction profile measurements of **130** in toluene in continuous system with Duramem membrane.

After completion of the reaction the filtration cell was opened and the membrane was taken out to examine the physical appearance of its surface. It appeared that membrane had creases on the surface, which can explain the rather high ruthenium contamination in the permeate.

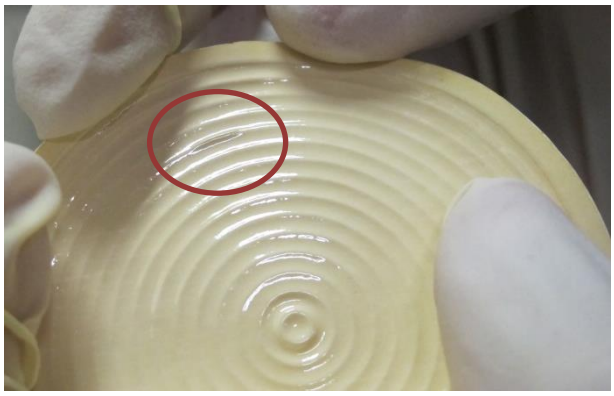

Figure 74. Membrane cracking.

I decided to exchange the previously utilised Duramem to PuraMem S380 (MWCO = 600). PuraMem membranes are designed especially for toluene solutes. At the same time the reactor was rebuilt to lower the total volume (Figure 75).

Figure 75. Second version of the home-made continuous mini-plant.

I performed the reaction with 0.5 mol% loading of **130**. Fresh solution of DEDAM was added at the rate of 0.085 mL/min. The membrane (PuraMem S380) was pressurised to 3 bar. The reaction has been run for 86 h, during which time I exchanged the volume of the reactor seven times.

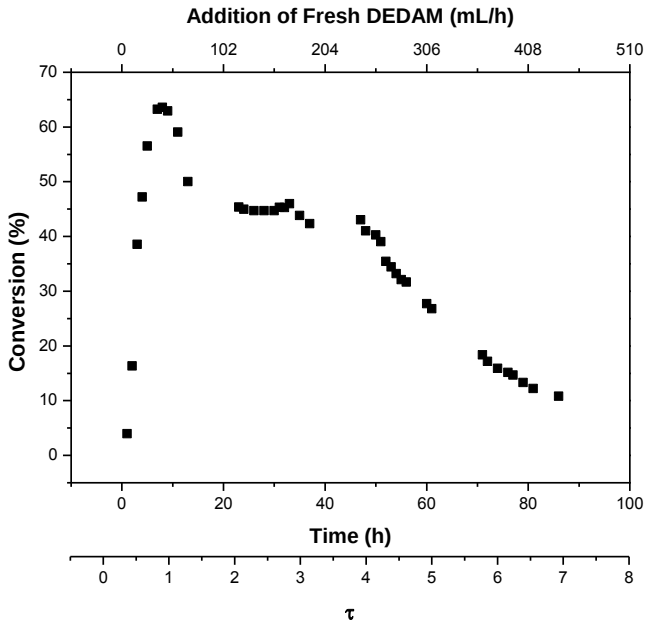

Figure 76. Reaction profile measurements of **130** in toluene in continuous system with PuraMem S280.

The highest 65% conversion was reached after 10 h. The catalyst reached TON = 637. The permeate was collected to examine the amount of ruthenium contamination. During the first 47 h of reaction ruthenium contamination reached 30 ppm (according to ICP MS), during the next 39 h of reaction ruthenium contamination slightly increased and reached 39 ppm (according to ICP MS).

As we can observe in Figure 76, the reaction reached a plateau after 10 h and continued over 20 h. During this time the catalyst was active even though conversion did not reach 100%. After 40 h of the reaction conversion started to decrease which means that the catalyst probably started to decompose. This was the first time when a metathesis reaction was conducted over such a long period of time with only 0.5 mol% catalyst loading. In the literature the longest time during which a metathesis reaction was conducted in continuous system was 10 h. [186,193]

These promising results encouraged me to examine complex **165**. In the previous part of this dissertation I recounted that **165** had much higher activity in toluene than **163**. Bearing in mind the requirements of the ideal NME catalyst I decided to exchange **163** previously examined in batch nanofiltration to **165**.

In analogy to the previously described measurement of **130**, I calculated ln(1-X) of **165** according to the reaction profile measurement and feed rate.

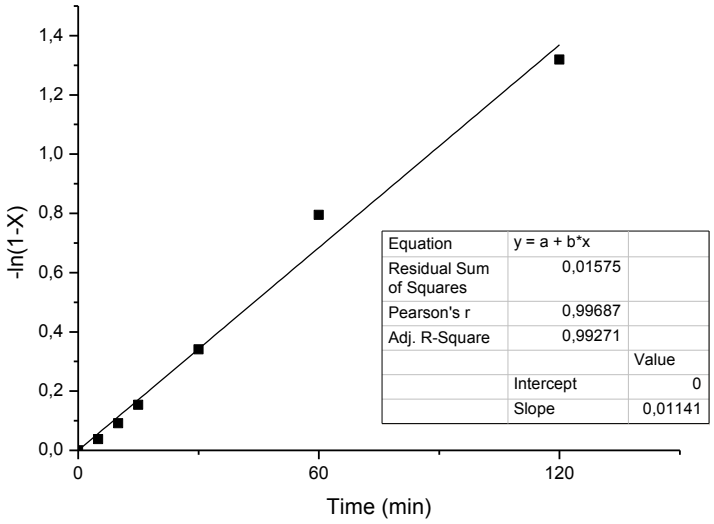

Figure 77. Ln(1-X) in time plot of **165**.

Before started the reaction the setup was slightly changed – the syringe pump was exchanged for a HPLC pump.

Figure 78. Modified home-made continuous mini-plant designed and built in the group of prof. Vogt.

I performed the reaction with 1 mol% loading of **165**. Fresh solution of DEDAM was added at the rate of 4.1 mL/h. The membrane (PuraMem S380) was pressurised to 5 bar. The reaction has been performed for 165 h.

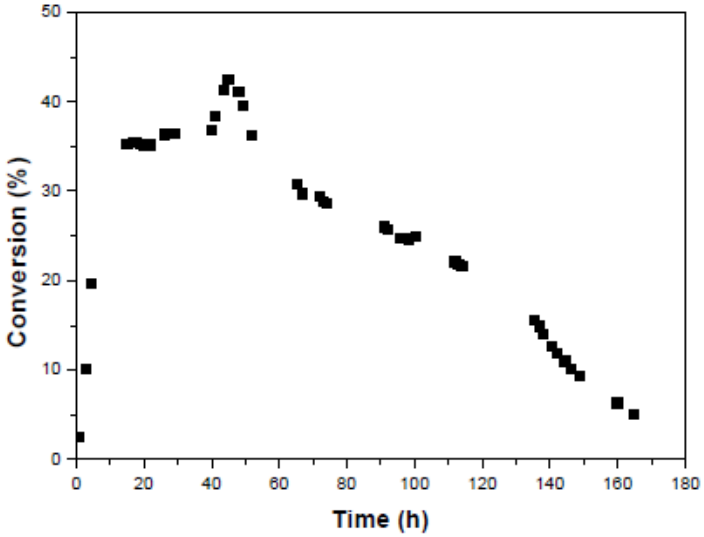

Figure 79. Reaction profile measurements of **165** in toluene in continuous system with PuraMem S280.

The highest 45% conversion was reached after 70 h. The catalyst reached TON = 659. The permeate was collected to examine the amount of ruthenium contamination. During the first 52 h the ruthenium contamination reached 19 ppm (according to ICP MS), during the next 91 h it slightly increased and reached 34 ppm (according to ICP MS).

Unfortunately, during the reaction fluctuations of the system appeared which did not allow to calculate how many times the volume of the reactor was exchanged, even though we obtained the lowest ruthenium contamination in the permeate.

2.5. CONCLUSION OF RESULTS AND DISCUSSION

To summarize, fourteen new Ru catalysts bearing POSS tag were synthesized. The linked MWEs were tag to NHC ligand, benzylidene ligand or to ionic ligands to examine which kind of connection is the most suitable for recovery and reuse of the Ru catalysts after metathesis reaction.

I was found that almost all of newly synthesised catalysts were more active in the model RCM reaction compared to the parent complexes. At this stage of research it was observed that some linking bonds (urethane, amide) interfere with the catalytic activity of the examined complexes when metathesis was performed in toluene. This phenomenon made some catalysts (**176**, **177**, **182**) inappropriate for the next part of the research.

Next, four catalysts (**129**, **130**, **163**, **177**) were chosen and their recovery after metathesis reaction by nanofiltration in batch system were examined. At the same time filtration procedures were optimised. Among all catalysts chosen for initial screening **130** was found to have the highest retention during nanofiltration. This part of my research was performed in cooperation with prof. Livingstone from Imperial College of London.

Additionally, I utilized catalyst **130** in metathesis of DEDAM performed continuously. To the continuous setup charged with catalyst **130** I continuously added solution of the substrate and at the same time collected reaction mixture after filtration. Under these conditions I was able to exchange volume of the system over seven times in over 80 h. Encouraged by this result I repeated the procedure for catalyst **165**. This part of research I established in cooperation with the group of prof. Dieter Vogt in the University of Technology Eindhoven.

Summing up, I synthesised catalysts which could be recovered and reused after metathesis reaction. I optimised nanofiltration process of purification of the metathesis reaction in batch and continuous mode. Examined catalysts were found to be active in model reaction. The results I obtained show that there is still a great deal to be done in this area. This procedure should be explored to further proliferation to the industry.

"It's not easy being green"

Kathrine Sanderson

PART 3 - EXPERIMENTAL SECTION

3.1 GENERAL INFORMATION

3.1.1. APPARATUS AND ANALYTICAL METHODS

Reactions were monitored by TLC on silica gel 60 F_{254}, (E. Merc, Darmstadt) and spots were detected either by UV-absorption or by charring with H_2SO_4/4-methoxybenzaldehyde in methanol.

Flash column chromatography was performed using silica gel 60 (E. Merck; 230–400 mesh), Florisil (Fluka, 60-100 mesh) or size exclusion gel (BioBeads S-X1 200-400 mesh).

^{1}H NMR and ^{13}C NMR spectra were recorded on *Varian AC*-200 (200 MHz), *Varian AC*-400 (400 MHz), Agilent 400-MR DD2 (400 MHz), *Bruker AM*-500 (500 MHz) *Varian AC*-600 (600 MHz) spectrometers in $CDCl_3$ if not otherwise noted. Chemical shift values of ^{1}H spectra are reported as values in ppm relative to residual $CDCl_3$ (δ 7.26 ppm), CD_2Cl_2 (δ 5.32 ppm) while chemical shift values of ^{13}C NMR spectra are reported relative to $CDCl_3$ (δ 77.16 ppm), CD_2Cl_2 (δ 53.84 ppm) as internal standard if not otherwise noted. Chemical shift values of ^{31}P spectra are reported relative to 85% $H_3PO_{4(aq.)}$ (δ 0.00 ppm) Multiplicities are described using the following abbreviations: s = singlet, d = doublet, t = triplet, q = quartet, m = multiplet, br = broad. Coupling constants (*J*) are quoted in Hz.

MS (ESI) were recorded on Mariner Perseptive Biosystems, Inc. MS (EI, LSIMS) spectra were recorded on AMD 604 Intectra GmbH instrument. Ion mass (*m/z*) signals are reported as values in atomic mass units followed, in parentheses, by the peak intensities relative to the base peak (100%).

Gas chromatography (GC) was conducted using GC HP 6890 with HP 5 column and Perkin-Elmer Clarus 680 chromatograph using dodecene as an internal standard.

IR analysis were conducted using Perkin-Elmer Spectrum 2000 FT-IR, wavenumbers in cm^{-1}.

Microanalyses were provided by the Institute of Organic Chemistry, Polish Academy of Sciences, Warsaw.

Melting points of new synthesised compounds were measured on Boetius apparatus.

3.1.2 MODEL SUBSTRATES, SOLVENTS, AND OTHER CHEMICALS

Unless otherwise noted, all metathesis reactions were carried out under an argon atmosphere, using standard Schlenk techniques and vacuum line. The solvents were dried by distillation over the following drying agents and were transferred under argon: THF, Et_2O (K/benzophenone), toluene (Na), *n*-pentane, *n*-hexane, DCM (CaH_2), MeOH (Mg). The following solvents were used as received: DMF, MeCN, ethanol, and acetone. *c*-Hexane and ethyl acetate were purified by distillation.

Catalysts **26**, **27** and **28** were purchased from Aldrich, Strem or Apeiron and used as received. Catalysts **29**, **30**, **31**, **155**, **136** and **138** were prepared according to literature methods. All other commercially available reagents were used as received.

POSS derivatives **125**, **127**, **139**, **140**, **141**, **145**, **147**, **149**, **160**, **173** and **187** were donated by HybridCatalysis and used as received.

3.2. MODIFICATIONS OF NHC LIGAND

3.2.1. SYNTHESIS OF 1-MESITYL-1*H*-IMIDAZOLE (122)

A 1 L around bottom flask was charged with 2,4,6-trimethylaniline (**120**) (10.8 g; 11.2 mL; 80 mmol; 1 equiv.), MeOH (50 mL) and 30% aq. glyoxal (**121**) (9.18 mL; 80 mmol). The reaction mixture was stirred for 16 h at room temperature. A yellowish slurry was formed. Solid NH_4Cl (7.7g; 144 mmol; 1.8 equiv.) was added followed by 37% aq formaldehyde (11.9 mL; 160 mmol; 2 equiv.). The mixture was diluted with MeOH (300 mL) and the resulting mixture was refluxed for 1 h. H_3PO_4 (9.8 mL, 85%; 144 mmol; 1.8 equiv.) was added over a period of 10 min. The resulting mixture was then stirred at reflux for further 4 – 8 h. The reaction progress was monitored by TLC. After removal of the solvent, the dark residue was poured onto ice (300 g) and alkalized with aq. 40% KOH solution until pH 9. The resulting mixture was extracted with Et_2O. The organic phases were combined and washed with H_2O, brine and dried ($MgSO_4$). The solvent was removed and the residue was chromatographed on silica gel (c-hexane–EtOAc). The product was obtained as a colourless solid after being recrystallized from EtOAc; (11.4 g; 61.2 mmol; 77%); Spectral data are in agreement with those reported in the literature.[200] Mp. 107 – 108 °C

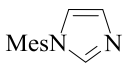

122

^{1}H NMR ($CDCl_3$, 400 MHz): δ 7.45 (t, J = 1.0 Hz, 1H), 7.23 (t, J = 1.0 Hz, 1H), 6.96 (d, J = 0.5 Hz, 2H), 6.89 (t, J = 1.2 Hz, 1H), 2.33 (s, 3H), 1.98 (s, 6H).

^{13}C NMR ($CDCl_3$, 50 MHz): δ 138.95, 137.51, 135.49, 133.43, 129.52, 129.07, 120.15, 21.11, 17.42.

3.2.2. SYNTHESIS OF 1-MESITYL-3-(3-(TRIMETHOXYSILYL)PROPYL)-1*H*-IMIDAZOLIUM IODIDE (124)

A 25 mL Schlenk flask was charged with 1-mesityl-1*H*-imidazole (**122**) (559 mg; 3 mmol; 1 equiv.) and flushed with argon. Toluene (5 mL) followed by (3-iodopropyl) trimethoxysilane (**123**) (958 mg; 3.3 mmol; 1.1 equiv.) was added and the resulting solution was heated at 80 °C for 3 days. After cooling to room temperature the solvent was evaporated *in vacuo*. Washing with Et_2O (2 x 20 mL) and drying of the residue *in vacuo* afforded 1-mesityl-3-(3-(trimethoxysilyl)propyl)-1*H*-imidazolium iodide (**124**)

(1.35 g; 2.33 mmol; 78 %) as a pale yellow oily solid; Spectral data are in agreement with those reported in the literature.[221] Mp 103 – 106 °C

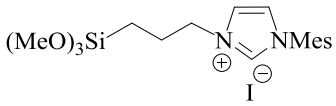

^{1}H NMR ($CDCl_3$, 400 MHz): δ 9.99 (t, J = 1.5 Hz, 1H), 7.77 (t, J = 1.8 Hz, 1H), 7.23 (t, J = 1.8 Hz, 1H), 7.02 (s, 2H), 4.72 (t, J = 7.2 Hz, 2H), 3.59 (s, 9H), 2.35 (s, 3H), 2.10 (s, 6H), 2.08 (m, 2H), 0.72 (t, J = 8.0 Hz, 2H).

^{13}C NMR ($CDCl_3$, 100 MHz): δ 141.41, 137.35, 134.15, 130.43, 129.87, 123.12, 52.12, 50.77, 24.32, 21.05, 5.56.

IR (KBr, cm^{-1}): v 3381, 3123, 3063, 2942, 2839, 1743, 1608, 1563, 1546, 1486, 1455, 1412,1379, 1356, 1328, 1203, 1162, 1071, 968, 934, 857, 817, 774, 729, 698, 668, 636, 578, 552, 444, 419.

3.2.3. SYNTHESIS OF 3-(3-HEPTAISOBUTYLPOSS(T_8)-PROPYL)-1-MESITYL-1*H*-IMIDAZOLIUM IODIDE (**126**)

A 25 ml Schlenk flask was charged with 1-mesityl-3-(3-(trimethoxysilyl)propyl)-1*H*-imidazolium iodide (**124**) (1.90 g; 4 mmol) and flushed with argon. DCM (40 mL) followed by trisilanol-heptaisobutyl POSS **125** (3.16 g; 4 mmol) was added and the resulting mixture was stirred for 2 h. Afterwards all manipulations were performed without an inert gas atmosphere. The solvent was evaporated and the residue was dried *in vacuo*. Crude product was purified by column chromatography using 2 % MeOH in DCM as an eluent. After evaporation of solvents and drying *in vacuo* 3-(3-heptaisobutylPOSS(T_8)-propyl)-1-mesityl-1*H*-imidazolium iodide (**126**) was obtained as a colourless solid (3.80 g; 3.24 mmol; 81%). Mp 195 – 205 °C (DCM/MeCN)

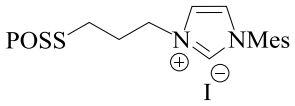

^{1}H NMR ($CDCl_3$, 400 MHz): δ 10.08 (t, J = 1.5 Hz, 1H), 7.56 (t, J = 1.7 Hz, 1H), 7.22 (t, J = 1.8 Hz, 1H), 7.00 (d, J = 0.5 Hz, 2H), 4.71 (t, J = 6.8 Hz, 2H), 2.33 (s, 3H), 2.08 (s, 6H), 2.07 – 2.00 (m, 2H), 1.90 – 1.78 (m, 7H), 0.98 – 0.90 (m, 42H), 0.64 – 0.55 (m, 16H).

^{13}C NMR ($CDCl_3$, 100 MHz): δ 141.62, 137.93, 134.31, 130.56, 130.05, 129.46, 123.36, 122.54, 52.72, 25.80, 25.79, 25.77, 24.40, 23.99, 23.92, 22.53, 22.51, 21.22, 17.93, 17.42, 8.85.

IR (DCM, cm^{-1}): *v* 2954, 2928, 2908, 2870, 1609, 1562, 1546, 1465, 1402, 1382, 1366, 1332, 1229, 1204, 1108, 1037, 952, 837, 742, 670, 577, 482, 431.

MS (ESI^+) *m/z* calcd for $C_{43}H_{83}N_2O_{12}Si_8$ $[M-I]^+$ 1043.4; found: 1043.5.

HR MS (TOF MS ESI^+) *m/z* calcd for $C_{43}H_{83}N_2O_{12}Si_8$ $[M-I]^+$ 1043.4100; found: 1043.4083.

Elemental analysis calcd for $C_{43}H_{83}IN_2O_{12}Si_8$: C, 44.08; H, 7.14; N, 2.39; I, 10.83; found: C, 44.32; H, 7.18; N, 2.33; I, 10.61.

3.2.4. SYNTHESIS OF 3-(3-HEPTAISOBUTYLPOSS(T_8)-PROPYL)-1-MESITYL-1*H*-IMIDAZOLIUM BROMIDE (**142**)

To a 20 mL round bottom flask charged with 3-bromopropyl-heptaisobutyl POSS(T_8) (**139**) (1220 mg; 1.3 mmol; 1.3 equiv.) and 1-mesityl-1*H*-imidazole (**122**) (186 mg; 1 mmol; 1.0 equiv.) a few drops of xylene was added. The reaction flask was placed in MW and heated at 150 °C for 4 h. Before cooling down 5 mL of toluene was added. The mixture was transferred straight onto a column containing silica gel. Column chromatography was performed using first 10% EtOAc in *c*-hexane, and then 2% MeOH in DCM as an eluent. The product 3-(3-heptaisobutylPOSS(T_8)-propyl)-1-mesityl-1*H*-imidazolium bromide (**142**) was obtained as a colourless solid after being recrystallized from acetonitrile (1.01 g; 0.9 mmol; 90%). Mp 208 – 211 °C (DCM/MeCN)

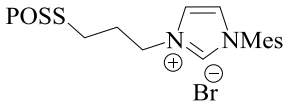

^{1}H NMR ($CDCl_3$, 400 MHz): δ 10.45 (s, 1H), 7.58 (t, *J* = 1.6 Hz, 1H), 7.17 (t, *J* = 1.7 Hz, 1H), 6.99 (d, *J* = 0.4 Hz, 2H), 4.72 (t, *J* = 7.2 Hz, 2H), 2.33 (s, 3H), 2.07 (s, 6H), 1.99 – 1.90 (m, 2H), 1.90 – 1.78 (m, 7H), 0.99 – 0.91 (m, 42H), 0.72 – 0.43 (m, 16H).

^{13}C NMR ($CDCl_3$, 100 MHz): δ 141.55, 138.90, 134.33, 130.73, 130.05, 123.15, 122.02, 52.49, 25.82, 25.79, 24.42, 24.02, 23.95, 22.56, 22.53, 21.23, 17.77, 8.88.

IR (DCM, cm^{-1}): *v* 3030, 2954, 2928, 2908, 2870, 1609, 1561, 1546, 1488, 1465, 1402, 1383, 1366, 1332, 1277, 1229, 1207, 1168, 1108.

MS (ESI^+) *m/z* calcd for $C_{43}H_{83}N_2O_{12}Si_8$ $[M-Br]^+$ 1043.4; found: 1043.5.

HR MS (ESI$^+$) *m/z* calcd for $C_{43}H_{83}N_2O_{12}Si_8$ $[M-Br]^+$ 1043.4100; found: 1043.4072.

Elemental analysis calcd for $C_{43}H_{83}BrN_2O_{12}Si_8$: C, 45.92; H, 7.44; N 2.49; Br, 7.10; found: C, 46.18; H, 7.40; N, 2.56; Br, 7.10.

3.2.5. SYNTHESIS OF 3-(5-HEPTAISOBUTYLPOSS(T_8)-PENTYL)-1-MESITYL-1*H*-IMIDAZOLIUM BROMIDE (**143**)

To a 20 mL round bottom flask charged with 5-bromopentyl-heptaisobutyl POSS(T_8) (**140**) (384 mg; 0.398 mmol; 1.3 equiv.) and 1-mesityl-1*H*-imidazole (**122**) (57 mg; 0.306 mmol; 1.0 equiv.) a few drops of xylene were added. The reaction flask was placed in MW and heated at 160 °C for 4 h. Before cooling down 2 mL of toluene was added. The reaction mixture was transferred straight onto a column containing silica gel. Column chromatography was performed using 10% EtOAc in *c*-hexane, and then 2% MeOH in DCM as an eluent. 3-(5-heptaisobutylPOSS(T_8)-pentyl)-1-mesityl-1*H*-imidazolium bromide (**143**) was obtained as a colourless solid after being recrystallized from acetonitrile (293 mg; 0.254 mmol; 83%). Mp 195 – 198 °C (DCM/MeCN).

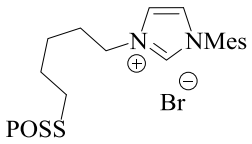

^{1}H NMR ($CDCl_3$,400 MHz): δ 10.45 (s, 1H), 7.58 (t, J = 1.6 Hz, 1H), 7.17 (t, J = 1.7 Hz, 1H), 6.99 (d, J = 0.4 Hz, 2H), 4.72 (t, J = 7.2 Hz, 2H), 2.33 (s, 3H), 2.07 (s, 6H), 2.00 – 1.90 (m, 2H), 1.90 – 1.78 (m, 7H), 1.49 – 1.35 (m, 4H), 0.98 – 0.91 (m, 42H), 0.63 – 0.54 (m, 16H).

^{13}C NMR ($CDCl_3$, 101 MHz): δ 141.50, 138.64, 134.31, 130.76, 130.03, 123.20, 122.37, 50.62, 30.37, 29.51, 25.82, 25.80, 24.01, 23.96, 22.61, 22.59, 22.46, 21.23, 17.77, 12.16.

IR (DCM, cm^{-1}): ν 2953, 2930, 2907, 2869, 1609, 1561, 1546, 1464, 1401, 1383, 1366, 1332, 1265, 1229, 1203, 1168, 1100, 1038, 838, 742, 562, 479, 431.

MS (ESI$^+$) *m/z* calcd for $C_{45}H_{87}N_2O_{12}Si_8$ $[M-Br]^+$ 1071.44; found 1071.44.

HR MS (ESI$^+$) *m/z* calcd for $C_{45}H_{87}N_2O_{12}Si_8$ $[M-Br]^+$ 1071.4413; found: 1071.4407.

Elemental analysis calcd for $C_{45}H_{87}BrN_2O_{12}Si_8$: C, 46.89; H, 7.61; N, 2.43; Br, 6.93; found: C, 46.65; H, 7.58; N, 2.41; Br, 6.90.

3.2.6. SYNTHESIS OF 3-(11-HEPTAISOBUTYLPOSS(T_8)-UNDECYL)-1-MESITYL-1*H*-IMIDAZOLIUM BROMIDE (**144**)

To a 20 mL round bottom flask charged with 11-bromoundecyl-heptaisobutyl POSS(T_8) (**141**) (1366 mg; 1,3 mmol; 1.3 equiv.) and 1-mesityl-1*H*-imidazole (**122**) (186 mg; 1 mmol; 1.0 equiv.) a few drops of xylene were added. Reaction flask was placed in MW and heated at 160 °C for 4 h. Before cooling down 5 mL of toluene was added. The reaction mixture was transferred straight onto a column containing silica gel. Column chromatography was performed using first 10% EtOAc in *c*-hexane, and then 2% MeOH in DCM as an eluent. 3-(11-heptaisobutylPOSS(T_8)-undecyl)-1-mesityl-1*H*-imidazolium bromide (**144**) was obtained as a colourless solid after being recrystallized from acetonitrile (1.06 g; 0.853 mmol; 85%). Mp 164 – 166 °C (DCM/CH_3CN)

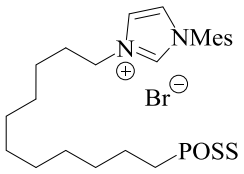

^{1}H NMR ($CDCl_3$, 400 MHz): δ 10.44 (t, J = 1.4 Hz, 1H), 7.64 – 7.62 (m, 1H), 7.16 (t, J = 1.7 Hz, 1H), 6.99 (d, J = 0.5 Hz, 2H), 4.71 (t, J = 7.2 Hz, 2H), 2.33 (s, 3H), 2.07 (s, 6H), 2.02 – 1.92 (m, 2H), 1.88 – 1.78 (m, 7H), 1.40 – 1.20 (m, 18H), 0.96 – 0.90 (m, 42H), 0.62 – 0.54 (m, 16H).

^{13}C NMR ($CDCl_3$, 101 MHz): δ 141.31, 138.46, 134.17, 130.63, 129.86, 123.01, 122.29, 50.51, 32.71, 30.52, 29.57, 29.52, 29.46, 29.29, 29.09, 26.14, 25.65, 23.84, 23.82, 22.63, 22.48, 22.45, 21.06, 17.61, 11.97.

IR (DCM, cm^{-1}): v 3415, 2953, 2925, 2868, 1609, 1564, 1545, 1464, 1401, 1383, 1366, 1332, 1230, 1204, 1104, 1038, 956, 838, 742, 577, 481, 432.

MS (ESI^+) *m/z* calcd for $C_{51}H_{99}N_2O_{12}Si_8$ $[M-Br]^+$ 1155.54; found: 1156.53.

HR MS (ESI^+) *m/z* calcd for $C_{51}H_{99}N_2O_{12}Si_8$ $[M-Br]^+$ 1155.5352; found: 1155.5326.

Elemental analysis calcd for $C_{51}H_{99}BrN_2O_{12}Si_8$: C, 49.52; H, 8.07; N, 2.26; Br, 6.46; found: C, 49.52; H, 8.15; N, 2.15; Br, 6.52.

3.2.7. SYNTHESIS OF 3-(4-HEPTAISOBUTYLPOSS(T_8)-BENZYL)-1-MESITYL-1*H*-IMIDAZOLIUM CHLORIDE (**146**)

To a 50 mL round bottom flask charged with 4-(heptaisobutylPOSS(T_8))-benzyl chloride (**145**) (10.4 g; 11 mmol; 1.1 equiv.) a few drops of xylene were added followed by 1-mesityl-1*H*-imidazole (**122**) (1.86 g; 10 mmol; 1 equiv.). The reaction flask was placed in oil bath preheated to 140 °C. The mixture was stirred for 48 h. Before cooling down 5 mL of toluene was added. The reaction mixture was transferred straight to a column containing silica gel. Column chromatography was performed using first 10% EtOAc in *c*-hexane, and then 2% MeOH in DCM as an eluent. 3-(4-heptaisobutylPOSS(T_8)-benzyl)-1-mesityl-1*H*-imidazolium chloride (**146**) was obtained as a colourless solid after being recrystallized from acetonitrile (9.34 g; 8.28 mmol; 83%). Mp 253 – 254 °C (DCM/MeCN)

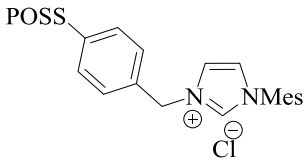

^{1}H NMR ($CDCl_3$, 400 MHz): δ 10.87 (t, J = 1.5 Hz, 1H), 7.69 (d, J = 8.0 Hz, 2H), 7.57 (t, J = 1.7 Hz, 1H), 7.54 (d, J = 8.1 Hz, 2H), 7.08 (t, J = 1.8 Hz, 1H), 6.94 (s, 2H), 5.96 (brs, 2H), 2.29 (s, 3H), 2.01 (s, 6H), 1.76 – 1.90 (m, 7H), 0.97 – 0.87 (m, 42H), 0.62 – 0.57 (m, 14H).

^{13}C NMR ($CDCl_3$, 101 MHz): δ 141.39, 138.90, 135.61, 135.19, 134.25, 133.50, 130.83, 129.95, 129.07, 128.33, 123.13, 122.44, 77.48, 77.16, 76.84, 53.61, 25.80, 25.78, 23.95, 22.57, 22.47, 21.19, 17.68, 17.41.

IR (DCM, cm^{-1}): v 3402, 2955, 2928, 2908, 2871, 2628, 1609, 1548, 1466, 1402, 1384, 1367, 1333, 1231, 1106, 1037, 1024, 952, 837, 742, 683, 579, 483.

MS (ESI^+) *m/z* calcd for $C_{47}H_{83}N_2O_{12}Si_8$ $[M-Cl]^+$ 1091.41; found: 1091.41.

HRMS (ESI^+) *m/z* calcd for $C_{47}H_{83}N_2O_{12}Si_8$ $[M-Cl]^+$ 1091.4100; found: 1091.4065.

Elemental analysis calcd for $C_{47}H_{83}ClN_2O_{12}Si_8$: C, 50.03; H, 7,41; Cl, 3.14; N, 2.48; found: C, 49.37; H, 7.40; Cl, 3.12; N, 2.40.

3.2.8. SYNTHESIS OF 3-(5-(BISHEPTAISOBUTYLPOSS(T_8)(METHYLSILYL)PENTYL)-1-MESITYL-1H-IMIDAZOLIUM IODIDE (**148**)

To a 50 mL round bottom flask charged with 5-iodopentyl-methylsilane-bis(heptaisobutylPOSS(T_8)) (**147**) (4.19 g; 2.2 mmol; 1.1 equiv.) a few drops of xylene were added followed by 1-mesityl-1*H*-imidazole (**122**) (373 mg; 2 mmol; 1 equiv.), and the reaction mixture was placed in oil bath preheated to 130 °C. The reaction mixture was stirred for 24 h. Before cooling down 5 mL of toluene was added. The reaction was transferred straight to a column containing silica gel. Column chromatography was performed using first 10% EtOAc in *c*-hexane, and then 2% MeOH in DCM. 3-(5-(bisheptaisobutylPOSS(T_8)(methylsilyl)pentyl)-1-mesityl-1*H*-imidazolium iodide (**148**) was obtained as a white solid after being recrystallized from acetonitrile (3.55 g; 1.79 mmol; 85%) Mp 175 – 177 °C (DCM/MeCN)

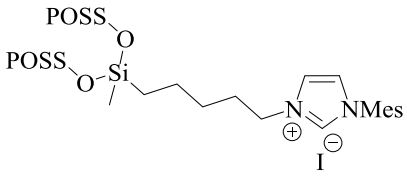

^{1}H NMR ($CDCl_3$, 400 MHz): δ 10.19 (t, J = 1.5 Hz, 1H), 7.49 (t, J = 1.7 Hz, 1H), 7.16 (t, J = 1.8 Hz, 1H), 6.98 (s, 2H), 4.68 (t, J = 7.3 Hz, 2H), 2.32 (s, 3H), 2.07 (s, 6H), 1.98 – 1.92 (m, 2H), 1.88 – 1.76 (m, 14H), 1.44 – 1.35 (m, 4H), 0.99 – 0.85 (m, 84H), 0.61 – 0.49 (m, 30H), 0.09 (s, 3H).

^{13}C NMR ($CDCl_3$, 101 MHz): δ 141.64, 137.94, 134.28, 130.53, 130.05, 123.17, 122.38, 50.89, 30.37, 29.76, 25.86, 25.83, 25.80, 25.78, 23.94, 23.89, 22.55, 22.53, 22.48, 22.23, 21.21, 17.98, 16.63, −1.38.

IR (DCM, cm^{-1}): v 2954, 2928, 2907, 2871, 2627, 1562, 1545, 1465, 1401, 1383, 1366, 1333, 1260, 1229, 1202, 1169, 1113, 1066, 954, 837, 742, 632, 561, 482, 433.

MS (ESI^+) *m/z* calcd for $C_{74}H_{153}N_2O_{26}Si_{17}$ $[M-I]^+$ 1963.68; $C_{74}H_{153}IN_2O_{26}Si_{17}$ $[M-H]^+$ 2087.57; found: 1963.69; 2087.58.

HR MS (ESI^+) *m/z* calcd for $C_{74}H_{153}N_2O_{26}Si_{17}$ $[M-I]^+$ 1961.6789; $C_{74}H_{153}IN_2O_{26}Si_{17}$ $[M-H]^+$ 2087.5756; found: 1961.6797; 2087.5769.

Elemental analysis calcd for $C_{74}H_{153}IN_2O_{26}Si_{17}$: C, 42.50; H, 7.37; N, 1.34; I, 6.07; found: C, 42.38; H, 7.31; N, 1.41; I, 6.16.

3.2.9. SYNTHESIS OF BIS(5-(1-MESITYL-1*H*-IMIDAZOL-3-IUM)PENTYL)-OCTAPHENYLPOSS(T_{10})DIBROMIDE (**150**)

To the 20 mL round bottom flask charged with bis(5-bromopentyl) octaphenylPOSS(T_{10}) (**149**) (1452 mg; 1 mmol; 1 equiv.) a few drops of xylene were added followed by 1-mesityl-1*H*-imidazole (**122**) (745 mg; 4 mmol; 4 equiv.), and the mixture was placed in microwave. The reaction mixture was stirred for 4 h in 160 °C. Before cooling down 5 mL of toluene was added. The reaction mixture was transferred to the top of the chromatographic column containing silica gel, and product was eluted using first DCM, and then 2% MeOH in DCM. Bis(5-(1-mesityl-1*H*-imidazolium) pentyl)octaphenylPOSS(T_{10})-dibromide (**150)** was obtained as a colourless solid after being recrystallized from diethyl ether (1519 mg; 0.832 mmol; 83%). Mp 215 °C (DCM/Et_2O)

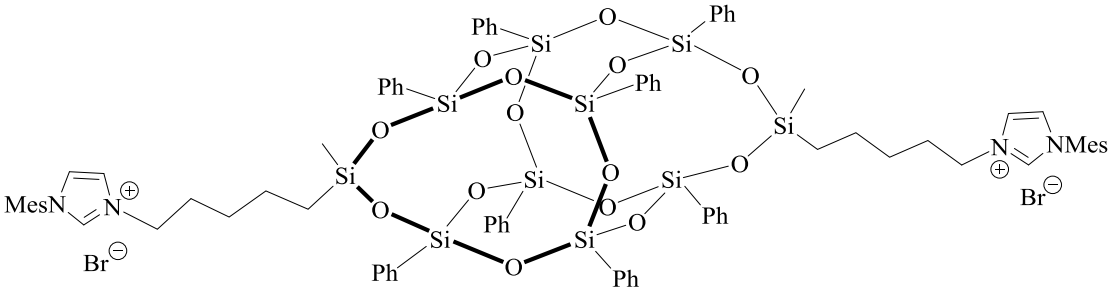

^{1}H NMR ($CDCl_3$, 400 MHz): δ 10.18 (d, J = 1.2 Hz, 2H), 7.53 – 7.16 (m, 40H), 6.93 (d, J = 0.5 Hz, 4H), 6.92 – 6.88 (m, 3H), 6.73 (t, J = 1.8 Hz, 1H), 4.37 – 4.30 (m, 4H), 2.32 (s, 6H), 1.96 (d, J = 3.6 Hz, 12H), 1.73 – 1.62 (m, 4H), 1.46 (dd, J = 15.5, 7.4 Hz, 4H), 1.30 (dd, J = 14.9, 7.6 Hz, 4H), 0.77 – 0.68 (m, 4H), 0.30 (d, J = 9.9 Hz, 6H).

^{13}C NMR ($CDCl_3$, 126 MHz): δ 141.40, 141.33, 138.16, 138.00, 134.18, 134.07, 133.97, 133.95, 131.91, 131.86, 131.31, 131.11, 130.88, 130.83, 130.72, 130.69, 130.65, 130.58, 129.93, 128.24, 128.08, 128.05, 128.04, 128.00, 127.98, 127.95, 127.92, 127.82, 123.02, 122.71, 122.23, 122.12, 50.21, 50.15, 30.10, 30.01, 29.81, 29.18, 29.04, 22.34, 22.27, 21.20, 17.70, 17.67, 16.54, 16.40, 0.11, −0.64, −0.68.

IR (DCM, cm^{-1}): v 3402, 3071, 3027, 2927, 2860, 1962, 1890, 1824, 1774, 1594, 1561, 1546, 1487, 1487, 1458, 1430, 1380, 1263, 1201, 1130, 1095, 1029, 998, 853, 823, 730, 699, 672, 609, 573, 492, 447.

MS (ES^+) *m/z* calcd for $C_{84}H_{94}N_4O_{14}Si_{10}{}^{79}Br$ $[M-Br]^+$ 1741.36; found: 1742.4

HR MS (ES^+) *m/z* calcd for $C_{84}H_{94}N_4O_{14}Si_{10}$ $[M-2Br]^{2+}$ 831.222; found: 831.722

Elemental analysis calcd for $C_{84}H_{94}Br_2N_4O_{14}Si_{10}$: C, 55,30; H, 5,19; Br, 8.76; N, 3.07; found: C, 55.06; H, 5.20, N, 3.00, Br, 8.79.

3.2.10. SYNTHESIS OF COMPLEX **129**

A 50 ml Schlenk flask was charged with 3-(3-heptaisobutylPOSS(T_8)-propyl)-1-mesityl-1*H*-imidazolium iodide (**126**) (1.2 equiv.; 0.18 mmol; 211 mg) and argonated. Toluene (5 mL) followed by potassium *t*-amylate (1.2 equiv.; 1.7 mol/l; 0.106 mL) were added and the resulting solution was stirred for 1 h at RT. Then the Schlenk flask was placed in preheated oil bath (65 °C) and stirred for 10 min. Next, **27** (1 equiv., 0.15 mmol, 90.1 mg) was added and the reaction was stirred for 1 h. The reaction was monitored by TLC. After reaching full conversion the reaction mixture was cooled down and placed on Florisil. Column chromatography was performed with 3% Et_2O in pentane as an eluent. The resulting product was concentrated *in vacuo*, and the green solid was dissolved in DCM (5 mL). MeOH (10 mL) was added and DCM was slowly removed under vacuum. The precipitated product was collected by filtration, washed with cold MeOH (10 mL), and dried *in vacuo* to afford **129** as green crystals (90 mg, 0.066 mmol, 44%).

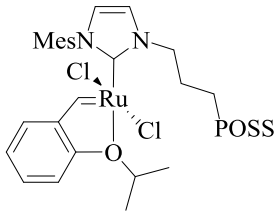

^{1}H NMR ($CDCl_3$, 400 MHz): δ 16.23 (*cis*, d, *J* = 3.9 Hz, 0.1 x 1H), 15.06 (*trans*, s, 0.9 x 1H), 7.68 (*cis*, dd, *J* = 12.6, 8.2 Hz, 0.1 x 1H), 7.56 (*trans*, dd, *J* = 11.2, 4.4 Hz, 0.9 x 1H), 7.18 (d, *J* = 2.1 Hz, 1H), 7.08 (s, 1H), 7.04 – 6.96 (m, 2H), 6.93 (d, *J* = 2.1 Hz, 1H), 6.88 (t, *J* = 7.4 Hz, 1H), 5.42 (*cis*, t, *J* = 5.9 Hz, 0.1 x 1H), 5.33 (*trans*, dt, *J* = 12.0, 6.0 Hz, 0.9 x 1H), 4.53 – 4.45 (m, 2H), 2.49 (s, 3H), 2.27 – 2.18 (m, 2H), 2.17 (s, 6H), 1.95 – 1.81 (m, 15H), 1.02 – 0.94 (m, 42H), 0.68 – 0.58 (m, 16H).

^{1}H NMR (CD_2Cl_2, 400 MHz): δ 15.68 (*cis*, s, 0.1 x 1H), 15.04 (*trans*, s, 0.9 x 1H), 7.66 – 7.60 (m, 1H), 7.23 (d, *J* = 2.1 Hz, 1H), 7.11 (s, 2H), 7.08 – 7.01 (m, 2H), 6.98 (d, *J* = 2.1 Hz, 1H), 6.96 – 6.90 (m, 1H), 4.51 – 4.44 (m, 2H), 2.49 (s, 3H), 2.28 – 2.17 (m, 2H), 2.14 (s, 6H), 1.96 – 1.83 (m, 13H), 1.79 – 1.72 (m, 2H), 0.97 (dt, *J* = 13.2, 9.2 Hz, 42H), 0.88 – 0.80 (m, 2H), 0.70 – 0.57 (m, 14H).

^{13}C NMR (CD_2Cl_2, 101 MHz): δ 284.74, 174.19, 153.46, 144.01, 140.25, 137.94, 137.55, 129.97, 129.71, 126.30, 122.87, 122.68, 121.04, 113.96, 76.66, 55.36, 36.08, 35.48, 32.27, 32.10, 31.82, 31.70, 28.31, 28.22, 27.55, 27.43, 27.18, 26.90, 26.87, 26.77, 26.07, 26.03, 26.01, 24.54, 24.44, 24.03, 22.98, 22.95, 22.89, 21.49, 20.12, 9.99.

IR (DCM, cm^{-1}): v 2952, 2926, 2870, 2852, 1589, 1567, 1466, 1451, 1403, 1383, 1366, 1332, 1285, 1228, 1169, 1110, 1037, 957, 896, 837, 743, 688, 567, 482, 432.

HR MS (ASAP$^+$) *m/z* calcd for $C_{53}H_{94}{}^{35}Cl_2N_2O_{13}{}^{102}RuSi_8$ $[M]^+$ 1362.3331; found: 1362.3329.

3.2.11. SYNTHESIS OF COMPLEX **130**

A 50 ml Schlenk flask was charged with 3-(3-heptaisobutylPOSS(T_8)-propyl)-1-mesityl-1*H*-imidazolium iodide (**126**) (193 mg; 0.165 mmol; 1.1 equiv.) and argonated. Toluene (5 mL) followed by solution of potassium t-amylate 1.7 M in toluene (0.097 mL; 1.1 eqiv) were added and the resulting solution was stirred for 1 h at RT. Then the Schlenk flask was placed in a preheated oil bath (65 °C) and stirred for 10 min. Next, **28** (138 mg; 0.15 mmol) was added and the reaction was stirred for 1 h. The progress of the reaction was monitored by TLC. After reached full conversion reaction was cooled down and placed on Florisil. Column chromatography was performed with 3% Et_2O in pentane as an eluent. The resulting product was concentrated *in vacuo*, and the red solid was dissolved in DCM (5 mL). MeOH (10 mL) was added and DCM was slowly removed under vacuum. The precipitated product was collected by filtration, washed with cold MeOH (10 mL), and dried *in vacuo* to afford **129** as red crystals (160 mg; 0.095 mmol, 63%)

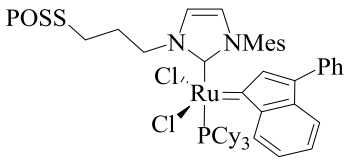

^{1}H NMR (CD_2Cl_2, 500 MHz): δ 8.21 (d, J = 7.4 Hz, 0.8 x 1H), 8.13 – 8.10 (m, 0.2 x 1H), 7.79 – 7.73 (m, 0.2 x 2H), 7.65 (d, J = 11.0 Hz, 0.7 x 2H), 7.49 – 7.41 (m, 1H), 7.33 (t, J = 7.6 Hz, 2H), 7.22 – 7.12 (m, 2H), 7.10 – 7.05 (m, 1H), 7.02 – 6.97 (m, 2H), 6.88 (s, 0.2 x 1H), 6.80 (d, J = 1.6 Hz, 0.2 x 1H), 6.72 (dd, J = 3.8, 1.5 Hz, 0.2 x 1H), 6.70 (d, J = 1.9 Hz, 0.8 x1H), 6.33 (s, 1H), 5.93 (s, 1H), 4.96 (dt, J = 14.7, 7.4 Hz, 1H), 4.91 – 4.83 (m, 1H), 2.54 (s, 0.2 x 3H), 2.48 (d, J = 11.6 Hz, 0.2 x 2H), 2.33 – 2.19 (m, 2H + 0.2 x 3H), 1.99 (s, 0.2 x 3H), 1.86 – 1.79 (m, 10H), 1.78 (s, 3H), 1.70 – 1.66 (m, 2H), 1.64 (s,

3H), 1.63 – 1.26 (m, 17H), 1.20 – 0.98 (m, 16H), 0.93 – 0.81 (m, 42H), 0.61 – 0.45 (m, 14H).

^{13}C NMR (CD_2Cl_2, 126 MHz): δ 292.68, 184.38, 183.77, 144.50, 143.20, 142.37, 141.30, 138.66, 138.48, 138.23, 138.13, 138.00, 137.96, 137.47, 137.29, 136.90, 136.72, 136.45, 136.41, 136.04, 130.00, 129.80, 129.52, 129.35, 128.85, 128.79, 128.65, 128.16, 127.99, 127.64, 127.19, 126.83, 126.58, 125.52, 124.93, 123.88, 120.96, 120.48, 118.27, 116.70, 34.98, 34.84, 34.49, 34.37, 33.59, 33.47, 30.94, 30.78, 30.54, 30.27, 30.22, 29.84, 29.55, 28.97, 28.47, 28.39, 28.32, 28.24, 27.20, 26.93, 26.06, 25.29, 24.56, 24.47, 23.69, 23.45, 23.03, 22.99, 22.60, 20.03, 19.83, 19.32, 18.81, 18.63, 18.60, 10.12, 9.28.

^{31}P NMR (162 MHz, CD_2Cl_2) δ 31.00, 30.84.

IR (DCM, cm^{-1}): *v* 3055, 2953, 2928, 2869, 2852, 1539, 1488, 1465, 1445, 1404, 1382, 1366, 1332, 1228, 1168, 1111, 1037, 916, 886, 846, 837, 774, 752, 741, 696, 647, 617, 583, 481, 431.

MS (FD) *m/z* calcd for $C_{76}H_{125}{}^{35}Cl_2N_2O_{12}P^{102}RuSi_8$ 1686.4618; found: 1686.4529.

HR MS (ES^+) *m/z* calcd for $C_{76}H_{125}{}^{35}Cl_2N_2O_{12}P^{102}RuSi_8$ 1684.5545; found: 1684.5527.

Elemental analysis calcd for $C_{76}H_{125}Cl_2N_2O_{12}PRuSi_8$: C, 54.13; H, 7.47; Cl, 4.20; N, 1,66; found: C, 54.03; H, 7.45; Cl, 4.16; N, 1.57.

3.2.12. SYNTHESIS OF COMPLEX **131**

A 50 ml Schlenk flask was charged with 3-(3-heptaisobutylPOSS(T_8)-propyl)-1-mesityl-1*H*-imidazolium iodide **126** (2 equiv.; 0.29 mmol; 339 mg) and argonated. Toluene (10 mL) followed by potassium tert-pentoxide (2 equiv.; 1.7 mol/l; 0.29 mmol; 0.17 mL) were added and the resulted solution was stirred for 1 h in RT. Then **28** (1 equiv., 0.145 mmol, 134 mg) was added. The reaction mixture was placed in preheated oil bath and stirred at 65 °C for 20 min. The progress of the reaction was monitored by TLC. After reaching full conversion the reaction mixture was cooled down and silica gel (2.4 g) was added. The reaction was stirred for additional 2 h. Column chromatography was performed with *c*-hexane as an eluent. The resulting product was concentrated *in vacuo*, affording **133** as a red solid (110 mg, 0.045 mmol, 31%).

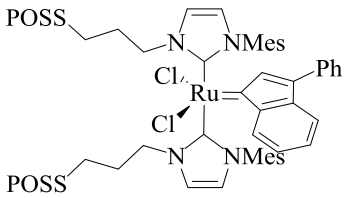

^{1}H NMR ($CDCl_3$, 500 MHz): δ 7.97 (d, J = 7.4 Hz, 1H), 7.65 (d, J = 7.2 Hz, 2H), 7.51 (d, J = 7.4 Hz, 1H), 7.40 (t, J = 7.7 Hz, 2H), 7.18 (d, J = 1.9 Hz, 2H), 7.10 (t, J = 7.4 Hz, 1H), 7.07 (s, 1H), 7.03 (t, J = 7.5 Hz, 1H), 6.79 (d, J = 7.5 Hz, 1H), 6.69 (d, J = 1.8 Hz, 2H), 6.23 (s, 2H), 5.79 (s, 7H), 5.04 (dd, J = 14.4, 6.6 Hz, 4H), 1.97 – 1.81 (m, 32H), 1.78 (s, 6H), 1.65 (s, 5H), 1.01 – 0.95 (m, 82H), 0.68 – 0.60 (m, 16H).

^{13}C NMR ($CDCl_3$, 126 MHz): δ 299.50, 188.19, 144.51, 140.42, 138.35, 137.57, 136.70, 136.56, 136.53, 136.38, 136.31, 135.97, 135.83, 135.73, 133.01, 130.65, 129.43, 129.10, 128.98, 128.86, 128.38, 127.94, 127.56, 127.48, 126.83, 126.73, 126.57, 126.52, 126.44, 125.25, 124.67, 123.17, 122.87, 121.75, 120.21, 115.35, 54.02, 35.78, 35.30, 30.34, 28.06, 27.87, 27.35, 27.15, 27.05, 26.76, 26.52, 26.50, 26.32, 25.95, 25.89, 25.86, 25.18, 24.42, 24.09, 24.02, 23.99, 23.32, 23.11, 23.03, 22.68, 22.60, 22.26, 22.17, 21.01, 19.54, 19.35, 19.29, 18.37, 9.62, 1.17, 0.15.

IR (DCM, cm^{-1}): v 3424, 2954, 2926, 2870, 1711, 1609, 1488, 1464, 1447, 1403, 1382, 1366, 1332, 1280, 1229, 1168, 1110.

MS (FD) *m/z* calcd for $C_{101}H_{175}{}^{35}Cl_2N_4O_{24}{}^{102}RuSi_{16}$ $[M+H]^+$ 2450.4850; found: 2450.4875.

3.2.13. SYNTHESIS OF COMPLEX **151**

A 25 ml Schlenk flask was charged with 3-(11-heptaisobutylPOSS(T_8)-undecyl)-1-mesityl-1*H*-imidazolium bromide (**143**) (380 mg; 0.33 mmol; 1.1 equiv.) and argonated. Toluene (6 mL) followed by potassium *t*-amylate 1.7 mol/L in toluene (0.194 mL; 0.33 mmol; 1.1 equiv.) were added and the resulting solution was stirred for 1 h at RT. Then the Schlenk flask was placed in a preheated oil bath (70 °C) and stirred for 10 min. Next, **28** (277 mg; 0.3 mmol; 1 equiv.) was added and reaction mixture was stirred for 0.5 h. The progress of the reaction was monitored by TLC. After completion of the reaction all manipulations were performed without an inert gas atmosphere. The reaction mixture was cooled to room temperature and the crude product was purified by column chromatography on Florisil using 10% EtOAc in *c*-hexane as an eluent. The resulting product was concentrated *in vacuo*, and the residue was dissolved in DCM (5 mL).

MeOH (10 mL) was added and DCM was slowly removed under vacuum. The precipitated product was collected by filtration, washed with MeOH (10 mL), and dried *in vacuo* to afford **151** as deep red crystals (250 mg; 0.146 mmol; 49%).

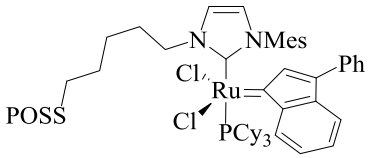

^{1}H NMR (CD_2Cl_2, 400 MHz): δ 8.21 (d, J = 6.6 Hz, 0.3 x 1H), 7.85 (dd, J = 7.5, 6.2 Hz, 0.3 x 2H), 7.77 – 7.67 (m, 0.7 x 2H), 7.60 – 7.49 (m, 1H), 7.45 – 7.38 (m, 2H), 7.32 – 7.22 (m, 2H), 7.19 – 7.11 (m, 1H), 7.10 – 7.05 (m, 2H), 6.97 (d, J = 5.5 Hz, 0.7 x 1H), 6.93 (t, J = 3.0 Hz, 0.3 x 1H), 6.80 (d, J = 1.8 Hz, 0.3 x 1H), 6.78 (d, J = 1.9 Hz, 0.7 x 1H), 6.82 – 6.77 (m, 1H), 6.42 (s, 1H), 6.01 (s, 1H), 5.07 – 4.90 (m, 0.7 x 2H), 4.91 – 4.79 (m, 0.3 x 2H), 2.63 (s, 0.3 x 3H), 2.44 (dd, J = 23.8, 12.0 Hz, 0.3 x 2H), 2.36 (s, 0.3 x 3H), 2.22 (dt, J = 15.3, 7.5 Hz, 2H), 2.08 (s, 0.3 x 3H), 1.94 – 1.82 (m, 13H), 1.80 – 1.73 (m, 2H), 1.72 (s, 3H), 1.70 – 1.56 (m, 17H), 1.53 (s, 3H), 1.50 – 1.36 (m, 2H), 1.50 – 1.36 (m, 16H), 1.30 – 1.10 (m, 15H), 1.01 – 0.93 (m, 42H), 0.70 – 0.55 (m, 14H).

^{13}C NMR (CD_2Cl_2, 101 MHz): δ 144.45, 142.31, 141.24, 138.22, 137.92, 137.40, 136.66, 136.35, 129.79, 129.50, 128.81, 128.62, 128.16, 127.64, 126.80, 126.64, 124.92, 121.13, 116.69, 51.66, 34.50, 34.35, 33.58, 33.42, 32.27, 32.10, 31.82, 31.70, 30.80, 30.63, 30.49, 30.21, 30.15, 29.78, 28.45, 28.35, 28.31, 28.21, 27.55, 27.43, 27.13, 26.90, 26.78, 26.03, 26.02, 26.01, 24.52, 24.48, 24.45, 23.39, 22.99, 22.97, 21.32, 19.99, 19.30, 18.61, 18.57, 12.62.

^{31}P NMR (CD_2Cl_2, 162 MHz): δ 31.43, 31.29, 30.54.

IR (DCM, cm^{-1}): v 3056, 2952, 2925, 2851, 1710, 1589, 1487, 1464, 1446, 1403, 1383, 1365, 1332, 1267, 1228, 1168, 1112, 1038, 1006, 917, 888, 837, 774, 743, 696, 617, 564, 482, 431.

HR MS (ES^+) m/z calcd for $C_{78}H_{129}{}^{35}Cl_2N_2O_{12}{}^{102}RuPSi_8$ $[M]^+$ 1712.5858; found: 172.5898.

Elemental analysis calcd for $C_{78}H_{130}Cl_2N_2O_{12}RuPSi_8$: C, 54.61; H, 7.64; Cl, 4.13; N, 1.63; found C, 54.56; H, 7.52; N, 1.58.

3.2.14. SYNTHESIS OF COMPLEX **153**

A 25 ml Schlenk flask was charged with 3-(4-heptaisobutylPOSS(T_8)-benzyl)-1-mesityl-1*H*-imidazolium chloride (**146**) (564 mg; 0. 5 mmol; 1 equiv.) and argonated. Toluene (20 mL) followed by KHMDS 0.5M solution in toluene (1.2 ml; 0.6 mmol; 1.2 equiv.) were added and the resulted solution was stirred at room temperature for 1 h. Then the Schlenk flask was placed in a preheated oil bath (70 °C) and stirred for 10 min. Next, **28** (462 mg; 0.5 mmol; 1 equiv.) was added and the reaction was stirred for 1 h. The progress of the reaction was monitored by TLC. After completion all manipulations were performed without an inert gas atmosphere. The reaction was cooled to room temperature and the crude product was purified by column chromatography on Florisil using 10% EtOAc in *c*-hexane as an eluent. The resulting product was concentrated *in vacuo*, and the residue was dissolved in DCM (5 mL). MeOH (10 mL) was added and DCM was slowly removed under vacuum. The precipitated product was collected by filtration, washed with MeOH (10 mL), and dried *in vacuo* to afford **153** as deep red crystals (400 mg; 0.231 mmol; 46%).

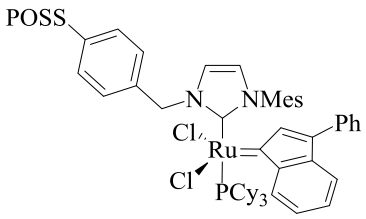

^{1}H NMR (CD_2Cl_2, 400 MHz): δ 8.21 (d, J = 7.2 Hz, 1H), 8.12 – 8.08 (m, 1H), 7.79 – 7.73 (m, 6H), 7.68 – 7.52 (m, 2H), 7.49 – 7.41 (m, 1H), 7.33 – 7.19 (m, 4H), 7.10 – 7.01 (m, 3H), 6.98 – 6.87 (m, 1H), 6.85 – 6.76 (m, 1H), 6.64 – 6.59 (m, 1H), 6.42 – 6.39 (m, 1H), 6.25 – 6.20 (m, 1H), 6.17 (s, 1H), 1.99 (s, 3H), 1.86 – 1.79 (m, 10H), 1.78 (s, 3H), 1.64 (s, 3H), 1.62 – 1.20 (m, 17H), 1.18 – 0.98 (m, 16H), 0.95 – 0.85 (m, 42H), 0.71 – 0.35 (m, 14H).

^{13}C NMR (CD_2Cl_2, 126 MHz): δ 292.68, 184.38, 183.77, 144.50, 143.20, 142.37, 141.30, 138.66, 138.48, 138.23, 138.13, 138.00, 137.96, 137.47, 137.29, 136.90, 136.72, 136.45, 136.41, 136.04, 130.00, 129.80, 129.52, 129.35, 128.85, 128.79, 128.55, 128.16, 127.99, 127.69, 127.17, 126.88, 126.58, 125.55, 124.93, 123.89, 120.96, 120.48, 118.27, 116.70, 34.98, 34.84, 34.49, 34.37, 33.59, 33.47, 30.94, 30.78, 30.54, 30.27, 29.84, 29.55, 28.97, 28.47, 28.32, 28.24, 26.93, 26.06, 25.29, 24.56, 24.47, 23.69, 23.45, 23.03, 22.99, 22.60, 20.03, 19.83, 19.39, 18.81, 18.63, 10.15, 9.28.

^{31}P NMR (162 MHz, CD_2Cl_2) δ 34.83.

IR (DCM, cm^{-1}): *v* 3056, 2928, 2850, 1540, 1487, 1445, 1356, 1267, 1229, 1216, 1200, 1173, 1112, 1027, 1005, 916, 887, 848, 774, 755, 736, 697, 665, 583, 510, 489.

MS (FD^+) calcd for $C_{80}H_{125}Cl_2N_2O_{12}PRuSi_8$ $[M]^+$ 1734.52; found: 1734.3.

HR MS (ES+) calcd for $C_{80}H_{125}{}^{35}Cl_2N_2O_{12}P^{108}RuSi_8$ $[M]^+$ 1732.5545; found 1732.5533.

3.2.15. SYNTHESIS OF COMPLEX **154**

A 25 ml Schlenk flask was charged with 3-(5-(bisheptaisobutylPOSS(T_8) (methylsilyl)pentyl)-1-mesityl-1*H*-imidazolium iodide (**148**) (230 mg; 0.11 mmol; 1.1 equiv.) and argonated. Toluene (5 mL) followed by potassium *t*-amylate 1.7 mol/L in toluene (0.07 mL; 0.12 mmol; 1.2 equiv.) were added and the resulting solution was stirred for 1 h at RT. Then the Schlenk flask was placed in a preheated oil bath (70 °C) and stirred for 10 min. Next, **28** (92.4 mg; 0.12 mmol; 1 equiv.) was added and the reaction mixture was stirred for 1 h. The progress of the reaction was monitored by TLC. After completion all manipulations were performed without an inert gas atmosphere. The reaction was cooled to room temperature and the crude product was purified by column chromatography on Florisil using 5% EtOAc in *c*-hexane as an eluent. The resulting product was concentrated *in vacuo*, and the residue was dissolved in DCM (5 mL). MeOH (10 mL) was added and DCM was slowly removed under vacuum. The precipitated product was collected by filtration, washed with MeOH (10 mL), and dried *in vacuo* to afford **154** as deep red crystals (130 mg; 0.0499 mmol; 50%).

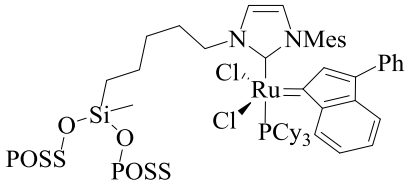

^{1}H NMR (CD_2Cl_2, 400 MHz): δ 8.39 (d, *J* = 6.5 Hz, 0.5 x 1H), 8.32 (d, *J* = 6.7 Hz, 0.5 x 1H), 8.29 (d, *J* = 6.9 Hz, 0.5 x 1H), 8.21 (d, *J* = 6.7 Hz, 0.5 x 1H), 8.04 – 7.93 (m, 1H), 7.90 – 7.82 (m, 1H), 7.77 – 7.68 (m, 1H), 7.68 – 7.61 (m, 1H), 7.57 – 7.46 (m, 2H), 7.45 – 7.33 (m, 2H), 7.29 – 7.19 (m, 2H), 7.11 – 7.00 (m, 2H), 6.92 – 6.84 (m, 1H), 6.79 – 6.77 (m, 0.5 x 1H), 6.71 – 6.67 (m, 0.5 x 1H), 6.45 – 6.19 (m, 2H), 6.05 – 5.95 (m, 1H), 5.82 – 5.75 (m, 1H), 5.08 – 4.90 (m, 2H), 2.63 (s, 0.5 x 3H), 2.36 (s, 0.5 x 3H), 2.08 (s, 0.5 x 3H), 1.94 – 1.82 (m, 13H), 1.80 – 1.73 (m, 2H), 1.72 (s, 3H), 1.78 – 1.49 (m, 17H), 1.43 (s, 3H), 1.40 – 1.36 (m, 2H), 1.50 – 1.36 (m, 16H), 1.30 – 1.10 (m, 15H), 1.03 – 0.87 (m, 84H), 0.72 – 0.54 (m, 28H), 0.09 (s, 3H).

^{13}C NMR (CD_2Cl_2, 101 MHz): δ 144.43, 142.37, 141.25, 137.92, 137.40, 136.66, 136.35, 129.79, 129.50, 128.89, 128.16, 127.64, 126.80, 126.20, 124.92, 121.13, 116.69, 51.66, 34.50, 34.35, 33.58, 33.42, 32.27, 32.10, 31.82, 31.70, 30.80, 30.63, 30.49, 30.21, 30.15, 29.61, 28.45, 28.35, 28.31, 28.21, 27.55, 27.43, 27.13, 26.94, 26.82, 26.29, 26.26, 26.17, 25.48, 25.42, 25.40, 23.82, 23.76, 22.32, 22.27, 21.32, 19.99, 19.30, 18.61, 18.57, 12.62, −1.77.

^{31}P NMR (CD_2Cl_2, 162 MHz): δ 34.19, 33.36, 32.82.

IR (DCM, cm^{-1}): ν 2954, 2927, 2871, 1488, 1465, 1402, 1383, 1366, 1333, 1260, 1229, 1206, 1169, 1116, 1066, 954, 837, 773, 742, 696, 561, 483, 431.

MS (ES+) calcd for $C_{107}H_{195}{}^{35}Cl_2N_2O_{26}P^{102}RuSi_{17}$ $[M]^+$ 2602.83; found 2602.86.

3.3. ANIONIC LIGAND MODIFICATION

3.3.1. SYNTHESIS OF METHYL 2-(2-(PROP-1-EN-1-YL)PHENOXY)PROPANOATE

To a 200 mL round bottom flask charged with K_2CO_3 (8.3 g; 60 mmol; 1.5 equiv.) and Cs_2CO_3 (2.6 g; 8 mmol; 0.2 equiv.) 100 mL of *N*,*N*-dimethylformamide was added followed by E/Z mixture of 2-propenylphenol (5.14 ml; 40 mmol; 1 equiv.). After stirring for 30 min at room temperature, methyl 2-bromopropionate (4.9 ml; 44 mmol; 1.1 equiv.) was added, and the reaction mixture was stirred for 24 h at room temperature. The reaction mixture was poured onto water (300 mL) and extracted with diethyl ether (3x50 mL). The combined extracts were washed with brine and water and dried ($MgSO_4$). The solvent was evaporated to give the crude product as a yellow oil. It was distilled to afford methyl 2-(2-(prop-1-en-1-yl)phenoxy)propanoate as a colourless oil (7.64 g; 34.7 mmol; 87%). Spectral data are in agreement with those reported in the literature.[218b] Mixture of isomers: *E*/*Z* = 7:3

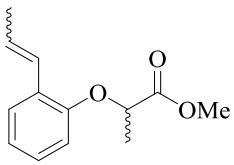

^{1}H NMR ($CDCl_3$, 400 MHz): δ 7.43 (dd, *J* = 7.7, 1.7 Hz, 0.7 x 1H), 7.30 (dd, *J* = 7.5, 1.7 Hz, 0.3 x 1H), 7.20 – 7.08 (m, 1H), 6.99 – 6.91 (m, 1H), 6.82 – 6.76 (m, 1H), 6.71 (dd, *J* = 8.2, 1.0 Hz, 0.7 x 1H), 6.62 (dd, *J* = 11.6, 1.8 Hz, 0.3 x 1H), 6.25 (dq, *J* = 15.9, 6.6 Hz, 0.7 x 1H), 5.85 (dq, *J* = 11.6, 7.1 Hz, 0.3 x 1H), 4.76 (p, *J* = 6.7 Hz, 1H), 3.75 (s, 3H), 1.91 (dd, *J* = 6.7, 1.8 Hz,

0.7 x 3H), 1.85 (dd, *J* = 7.1, 1.9 Hz, 0.3 x 3H), 1.65 (d, *J* = 6.8 Hz, 0.7 x 3H), 1.62 (d, *J* = 6.8 Hz, 0.3 x 3H).

^{13}C NMR ($CDCl_3$, 101 MHz): δ 172.85, 155.30, 154.32, 130.57, 127.99, 127.87, 127.69, 127.10, 126.69, 125.54, 125.20, 121.84, 121.27, 113.09, 73.47, 73.39, 52.36, 18.74, 18.57, 14.83.

3.3.2. SYNTHESIS OF 2-(2-(PROP-1-EN-1-YL)PHENOXY)PROPANOIC ACID

To a 100 ml round bottom flask charged with methyl 2-(2-(prop-1-en-1-yl)phenoxy)propanoate (1806 mg; 8.2 mmol) in THF/H_2O (50 mL; 9:1 v/v) LiOH (393 mg; 16.4 mmol; 2 equiv.) was added. The mixture was stirred in reflux for 24 h, cooled to room temperature, and acidified with diluted HCl aq. THF was removed *in vacuo*, and the residue was extracted with AcOEt (3 x 50 mL). The combined extracts were washed with brine and water and dried ($MgSO_4$). The solvent was evaporated to give the crude product as a yellow oil. Purification by silica gel chromatography with 10% EtOAc in *c*-hexane as an eluent afforded 2-(2-(prop-1-en-1-yl)phenoxy)propanoic acid as a colourless crystalline solid (1590 mg; 7.71 mmol; 94 %). Spectral data are in agreement with those reported in the literature.[103a,222] Mixture of isomers: E/Z = 7:3.

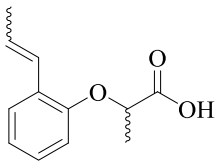

^{1}H NMR ($CDCl_3$, 400 MHz): δ 11.09 (brs, 1H), 7.43 (dd, *J* = 7.7, 1.7 Hz, 0.7 x 1H), 7.30 (dd, *J* = 7.6, 1.7 Hz, 0.3 x 1H), 7.22 – 7.11 (m, 1H), 7.03 – 6.93 (m, 1H), 6.84 – 6.72 (m, 0.85 x 2H), 6.58 (dd, *J* = 11.6, 1.7 Hz, 0.3 x 1H), 6.25 (dq, *J* = 15.9, 6.6 Hz, 0.7 x 1H), 5.86 (dq, *J* = 11.6, 7.1 Hz, 0.3 x 1H), 4.78 (p, *J* = 6.8 Hz, 1H), 1.91 (dd, *J* = 6.6, 1.7 Hz, 0.6 x 3H), 1.83 (dd, *J* = 7.1, 1.8 Hz, 0.3 x 1H), 1.69 (d, *J* = 6.9 Hz, 0.6 x 3H), 1.66 (d, *J* = 6.9 Hz, 0.3 x 1H).

^{13}C NMR ($CDCl_3$, 101 MHz): δ 177.80, 154.82, 153.91, 130.76, 128.15, 128.04, 127.81, 127.72, 127.65, 127.16, 126.91, 125.36, 125.02, 122.25, 121.81, 113.61, 113.26, 73.21, 72.94, 19.10, 18.60, 14.85.

3.3.3. SYNTHESIS OF COMPLEX **155**

To a 20 ml Schlenk flask charged with 2-(2-(prop-1-en-1-yl)phenoxy)propanoic acid (359 mg; 1.74 mmol; 1.5 equiv.) dissolved in DCM (25 mL), **34** (1101 mg; 1.16 mmol;1 equiv.) was added under an argon atmosphere. The mixture was stirred for 5 min,

and CuCl (172 mg; 1.74 mmol; 1.5 equiv.) was added. The mixture was heated to reflux for 1 h. The reaction mixture was allowed to cool to room temperature and concentrated *in vacuo*. From this point, all manipulations were carried out in air with reagent-grade solvents. The product was purified by silica gel chromatography (10% EtOAc in *c*-hexane). The solvent was evaporated *in vacuo* and the residue was dissolved in DCM (5 mL). MeOH (10 mL) was added and DCM was slowly removed under vacuum. The precipitated product was collected by filtration, washed with MeOH (10 mL), and dried *in vacuo* to afford complex **155** as a green microcrystalline solid (478 mg; 0.77 mmol; 66%). Spectral data are in agreement with those reported in the literature.[103a]

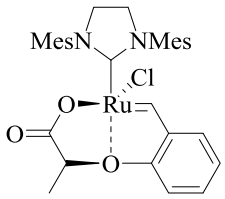

^{1}H NMR (CD_2Cl_2, 400 MHz): δ 16.45 (s, 1H), 7.56 (ddd, J = 8.2, 7.4, 1.7 Hz, 1H), 7.13 – 6.99 (m, 7H), 4.59 (t, J = 7.0 Hz, 1H), 4.21 (s, 4H), 2.45 (brs, 6H), 2.40 (s, 6H), 2.34 (s, 6H), 1.15 (d, J = 7.0 Hz, 3H).

^{13}C NMR ($CDCl_3$, 125 MHz): δ 293.3, 210.3, 181.5, 154.6, 146.7, 139.3, 138.8, 130.0, 129.6, 129.4, 126.6, 122.2, 119.1, 84.1, 51.4, 21.0, 19.00, 18.8, 18.5.

3.3.4. SYNTHESIS OF COMPLEX **164**

To a 20 ml round bottom flask charged with complex **155** (447 mg; 0.72 mmol; 1 equiv.) reagent-grade acetone (10 mL) in air, followed by KI (1195 mg; 7.2 mmol; 10 equiv.) were added. The mixture was stirred for 30 min and then filtered. The addition of KI and stirring for 30 min was repeated twice more. The mixture was filtered, and the solvent was evaporated *in vacuo*. The residue was dissolved in DCM (5 mL), passed through a pad of silica, and washed with EtOAc (10 mL). The solvents were evaporated in vacuo, and the residue was dissolved in DCM (5 mL). MeOH was added (10 mL), and DCM was slowly removed under vacuum. The precipitated product was collected by filtration, washed with MeOH (5 mL), and dried *in vacuo* to afford complex **164** as a dark green microcrystalline solid (456 mg; 0.641 mmol; 89%). Spectral data are in agreement with those reported in the literature.[103b,222]

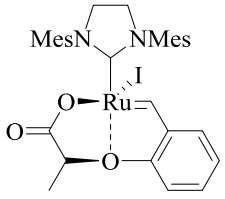

^{1}H NMR (CD_2Cl_2, 400MHz,): δ 15.85 (d, J = 0.9 Hz), 7.65 – 7.58 (m, 1H), 7.08 (s, 4H),7.06 (d, J = 4.2 Hz, 3H), 4.72 (q, J = 7.0 Hz, 1H),

4.20 (s, 4H), 2.47 (brs, 6H), 2.40 (d, J = 6.0 Hz, 12H), 1.17 (d, J = 7.0 Hz, 3H).

^{13}C NMR (CD_2Cl_2, 101 MHz): δ 291.49, 212.14, 181.06, 154.89, 147.21, 139.80, 130.78, 130.12, 130.08, 127.16, 122.76, 119.43, 84.60, 30.27, 21.38, 19.58, 19.47.

3.3.5. SYNTHESIS OF COMPLEX **159**

To a 20 ml round bottom flask charged with complex **155** (248 mg; 0.4 mmol; 1 equiv.) reagent-grade DCM (10 mL) in air, followed by and silver trifluorocetate (92.8 mg; 0.42 mmol; 1.05 equiv.) were added. The mixture was stirred for 30 min in the dark and then filtered through a pad of celite. The solvent was evaporated *in vacuo*. The residue was dissolved in DCM (1 mL), EtOAc (1 mL) was added and DCM was slowly removed under vacuum. The precipitated product was collected by filtration, and dried *in vacuo* to afford complex **159** as a dark purple microcrystalline solid (168 mg; 0.241 mg; 60%). Spectral data are in agreement with those reported in the literature.

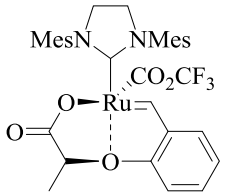

^{1}H NMR (CD_2Cl_2, 400 MHz): δ 16.85 (d, *J* = 0.9 Hz, 1H), 7.53 (ddd, *J* = 8.2, 7.4, 1.6 Hz, 1H), 7.16 – 7.10 (m, 4H), 7.05 (dd, *J* = 7.6, 1.6 Hz, 1H), 6.99 (d, *J* = 8.2 Hz, 1H), 4.60 (q, *J* = 7.0 Hz, 1H), 4.22 – 4.15 (m, 4H), 2.42 (s, 6H), 2.33 (s, 6H), 2.30 (s, 6H), 1.16 (d, *J* = 7.0 Hz, 3H).

^{13}C NMR (CD_2Cl_2, 101 MHz): δ 303.62, 303.42, 209.32, 180.81, 161.58 (q, *J* = 36.7 Hz), 155.78, 146.76, 140.11, 139.63, 139.35, 135.19, 131.04, 130.32, 130.06, 127.10, 122.96, 118.99, 114.78 (q, *J* = 290.1 Hz), 84.73, 52.07, 21.42, 19.23, 18.37, 18.26.

^{19}F NMR (CD_2Cl_2, 376 MHz): δ −74.47.

3.3.6. SYNTHESIS OF 2,2,3,3,4,4-HEXAFLUORO-5-OXO-5-((3-(HEPTAISOBUTYLPOSS(T_8))PROPYL)AMINO)PENTANOIC ACID (**162**)

A 25 ml Schlenk flask was charged with 3-aminopropyl-heptaisobutylPOSS(T_8) (**160**) (1749 mg; 2 mmol) and argonated. THF (15 mL) followed by perfluoroglutaric anhydride (**161**) (444 mg; 0.268 ml; 2 mmol) were added and the reaction mixture was stirred for 30 min. Solvent was evaporated to afford 2,2,3,3,4,4-hexafluoro-5-oxo-5-((3-(HeptaisobutylPOSS(T_8))propyl)amino)pentanoic acid in quantitative yield.

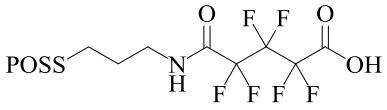

^{1}H NMR ($CDCl_3$, 400 MHz): δ 11.24 (s, 1H), 6.66 (s, 1H), 3.39 – 3.32 (m, 2H), 1.90 – 1.77 (m, 7H), 1.72 – 1.61 (m, 2H), 1.01 – 0.87 (m, 42H), 0.64 – 0.55 (m, 16H).

^{13}C NMR ($CDCl_3$, 101 MHz): δ 162.17 (m), 159.05 (t, J = 25.9 Hz), 111.85 (t, J = 30.7 Hz), 110.54 (t, J = 30.7 Hz), 109.19 (t, J = 32.0 Hz), 42.62, 29.83, 29.53, 25.86, 25.74, 24.04, 24.01, 22.66, 22.63, 22.53, 22.42, 9.33.

^{19}F NMR ($CDCl_3$, 376 MHz): δ −118.71, −119.95, −125.74.

IR (DCM, cm^{-1}): v 3444, 3333, 2954, 2928, 2906, 2871, 2627, 1768, 1713, 1542, 1465, 1402, 1384, 1366, 1332, 1230, 1169, 1108, 1039, 953, 920, 838, 805, 742, 689, 562, 482, 432.

MS (EI^+) *m/z* calcd for $C_{36}H_{71}F_6NO_{15}Si_8$ $[M]^-$ 1096.63; found: 1096.5.

HR MS (ES^-) *m/z* calcd for $C_{36}H_{70}F_6NO_{15}Si_8$ $[M-H]^-$ 1094.2804; found: 1094.2781.

Elemental analysis calcd for $C_{36}H_{71}F_6NO_{15}Si_8$: C, 39.43; H, 6.53; N, 1.28; F,10.39; found: C, 39.46; H, 6.57; N, 1.25; F, 10.34.

3.3.7. SYNTHESIS OF COMPLEX **163**

2,2,3,3,4,4-Hexafluoro-5-oxo-5-((3-heptaisobutylPOSS(T_8))propyl)amino) pentanoic acid (**162**) (69.8 mg, 0.1 mmol) was added to a solution of complex **159** (110 mg, 0.1 mmol) in dry THF (5 mL). The reaction mixture was stirred for 20 min. The reaction mixture was evaporated and dried *in vacuo* to give a purple complex **163** as microcrystalline solid (179 mg; 0.1 mmol; quant.). Mixture of isomers: 1:1

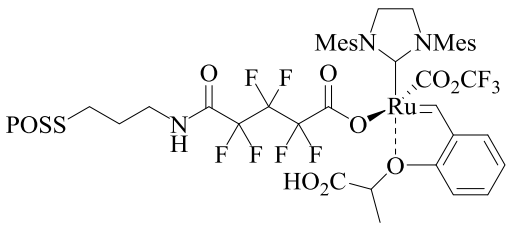

^{1}H NMR (CD_2Cl_2, 600 MHz): δ 17.11 (s, 0.5 x 1H), 17.04 (t, J = 4.0 Hz, 0.5 x 1H), 8.75 (brs, 1H), 7.61 – 7.54 (m, 1H), 7.20 – 7.10 (m, 5H), 7.10 – 7.04 (m, 1H), 7.05 – 6.97 (m, 1H), 6.53 (s, 0.5 x 1H), 6.39 (t, J = 5.6 Hz, 0.5 x 1H), 4.75 – 4.67 (m, 1H), 4.25 – 4.17 (m, 4H), 3.76 (ddd, J = 6.6, 4.2, 2.6 Hz, 1H), 3.37 – 3.31 (m, 1H), 3.24 – 3.13 (m, 1H), 2.47 – 2.39 (m, 6H), 2.33 (d, J = 6.3 Hz, 6H), 2.30 – 2.24 (m,

6H), 1.91 – 1.81 (m, 7H), 1.71 – 1.63 (m, 1H), 1.58 – 1.50 (m, 1H), 1.21 – 1.15 (m, 3H), 0.98 – 0.91 (m, 42H), 0.66 – 0.59 (m, 16H).

^{13}C NMR (CD_2Cl_2, 101 MHz): δ 306.44, 306.11, 208.65, 208.61, 182.90, 163.06 (t, J = 25.9 Hz), 161.74 (q, J = 37.0 Hz), 158.64 (t, J = 25.6 Hz), 155.76, 155.69, 146.79, 146.67, 140.27, 140.19, 139.61, 139.53, 139.39, 139.38, 135.16, 135.05, 131.50, 131.42, 130.37, 130.32, 130.20, 130.17, 127.35, 127.27, 123.18, 123.10, 119.09, 118.89, 114.73 (q, J = 290.0 Hz), 110.59 (t, J = 37.1 Hz), 109.59 (t, J = 31.1 Hz), 108.59 (t, J = 32.1 Hz), 84.58, 52.11, 42.90, 42.75, 30.64, 30.28, 26.04, 26.00, 25.97, 25.88, 24.60, 24.50, 24.49, 24.47, 24.46, 23.51, 22.98, 22.92, 22.88, 22.45, 21.47, 21.45, 19.16, 19.04, 18.36, 18.24, 18.19, 9.80, 9.75, 1.37.

^{19}F NMR (CD_2Cl_2, 376 MHz): δ −74.47, −118.86, −120.25, −125.30.

IR (DCM, cm^{-1}): v 3332, 2954, 2926, 2907, 2871, 1704, 1661, 1599, 1543, 1486, 1455, 1402, 1383, 1366, 1332, 1268, 1229, 1187, 1169, 1109, 1037, 951, 920, 882, 838, 803, 744, 576, 481, 432.

HR MS (ES$^+$) m/z calcd for $C_{67}H_{105}N_3O_{18}F_6NaSi_8{}^{102}Ru$ [M−CO_2CF_3−H+Na]+ 1702.4393; found: 1702.4363.

Elemental analysis calcd for $C_{69}H_{106}F_9N_3O_{20}RuSi_8$: C, 46.19; H, 5.95; N, 2.34; F, 9.53; found: C, 46.04; H, 5.90; N, 2.16; F, 9.64.

3.3.8. SYNTHESIS OF COMPLEX **165**

2,2,3,3,4,4-Hexafluoro-5-oxo-5-((3-heptaisobutylPOSS(T_8))propyl)amino) pentanoic acid (**162**) (142 mg; 0.2 mmol) was added to a solution of complex **164** (219 mg; 0.2 mmol) in DCM (5 mL). The reaction mixture was stirred for 20 min. The product was precipitated by the addition of *n*-pentane (3 mL), collected by filtration, and dried *in vacuo* to give a green microcrystalline solid (362 mg; 0.2 mmol; quant.).

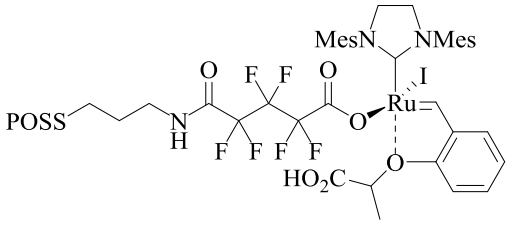

^{1}H NMR (CD_2Cl_2, 400 MHz): δ 16.00 (d, J = 0.7 Hz, 1H), 9.08 (brs, 1H), 7.65 (ddd, J = 8.3, 5.2, 3.8 Hz, 1H), 7.11 – 7.01 (m, 8H), 6.58 (s, 1H), 4.82 (q, J = 7.0 Hz, 1H), 4.21 (s, 4H), 3.33

(dd, *J* = 13.0, 6.6 Hz, 2H), 2.44 – 2.32 (m, 16H), 1.93 – 1.79 (m, 9H), 1.71 – 1.60 (m, 2H), 1.17 (d, *J* = 7.0 Hz, 3H), 0.98 – 0.93 (m, 42H), 0.63 – 0.59 (m, 16H).

^{13}C NMR (CD_2Cl_2, 101 MHz): δ 294.24, 211.28, 183.19, 158.91 (t, *J* = 29.4 Hz), 154.65, 147.14, 140.16, 139.92, 139.52, 139.37, 138.96, 135.14, 131.22, 130.30, 130.13, 127.39, 122.90, 119.51, 84.33, 52.08, 42.89, 30.61, 30.26, 29.93, 26.02, 26.00, 25.97, 25.95, 24.46, 24.44, 24.43, 23.48, 23.27, 22.95, 22.89, 22.85, 22.41, 21.45, 21.37, 19.48, 19.33, 19.03, 18.36, 18.22, 14.46, 9.73, 1.34.

IR (DCM, cm^{-1}): *v* 3334, 2954, 2926, 2871, 1763, 1715, 1655, 1606, 1596, 1542, 1483, 1466, 1453, 1401, 1383, 1366, 1332, 1269, 1229, 1169, 1110, 1037, 1020, 951, 920, 881, 838, 802, 745, 643, 578, 482, 432.

^{19}F NMR (CD_2Cl_2, 376 MHz): δ −118.93, −120.19, −125.54.

HR MS (ES^+) *m/z* calcd for $C_{67}H_{106}F_6IN_3O_{18}{}^{102}RuSi_8$ $[M-H+2Na]^+$ 1852.3335; found: 1852.3312.

Elemental analysis calcd for $C_{67}H_{106}F_6IN_3O_{18}RuSi_8$: C, 44.50; H, 5.91; N, 2.32; I, 7.02; F, 6.30; found: C, 44.32; H, 5.93; N, 2.30; I, 6.74; F, 6.47.

3.4. BENZYLIDENE MODIFICATION

3.4.1. CARBAMATE LINKER

3.4.1.1. SYNTHESIS OF METHYL 2-(4-HYDROXYPHENYL)ACETATE (**167**)

To a 500 ml round bottom flask charged with solution of the 2-(4-hydroxy-phenyl)-acetic acid (**166**) (4.41g; 29.0 mmol) in MeOH (120 mL) 1.5 mL of H_2SO_4 was added and the reaction mixture was refluxed overnight. Then the solvent was evaporated and the residue was dissolved in TBME, washed with saturated $NaHCO_3$, water and brine (50 mL each). The organic layer was dried over $MgSO_4$ and evaporated under reduced pressure. The product obtained (yellow oil, 4.72 g; 28.4 mmol; 98 % yield) was directly used for the next reaction without further purification. NMR spectra were consistent with those described in the literature.

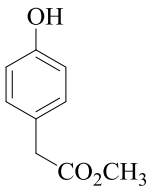

^{1}H NMR ($CDCl_3$, 200 MHz): δ 7.09 (d, J = 8.7 Hz, 2H), 6.76 (d, J = 8.7 Hz, 2H), 5.20 (brs, 1H), 3.70 (s, 3H), 3.56 (s, 2H).

3.4.1.2. SYNTHESIS OF METHYL 2-(4-ISOPROPOXYPHENYL)ACETATE (169)

To a 200 mL round bottom flask charged with methyl 2-(4-hydroxyphenyl)acetate (**167**) (4.65 g; 28.0 mmol; 1 equiv.), K_2CO_3 (7.74 g; 56.0 mmol; 2 equiv.), Cs_2CO_3 (1.82 g; 5.60 mmol; 0.2 equiv.) and 120 mL of DMF were added and stirred for one hour at room temperature. Isopropyl iodide (**168**) (9.52 g; 5.60 mL; 56.0 mmol; 2 equiv.) was added and the stirring was continued for 16 hours. Then the reaction mixture was poured onto 50 mL of water, extracted with TBME (3 x 50 mL), washed with 50 mL of water and 50 mL of brine, dried over $MgSO_4$, and evaporated. The residue was purified on the column chromatography (30% of EtOAc in *c*-hexane) giving methyl 2-(4-isopropoxyphenyl)acetate (**189**) as a colourless oil (5.25 g; 25.2 mmol; 90%).

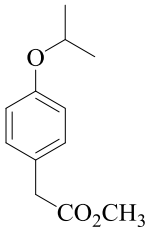

^{1}H NMR ($CDCl_3$, 400 MHz): δ 7.14 – 7.20 (m, 2H), 6.81 – 6.88 (m, 2H), 4.52 (sept., J = 6.0 Hz, 1H), 3.69 (s, 3H), 3.56 (s, 2H), 1.33 (d, J = 6.0 Hz, 6H).

^{13}C NMR ($CDCl_3$, 100 MHz): δ 172.4, 157.0, 130.2, 125.8, 115.9, 69.8, 51.9, 40.2, 22.0.

IR (DCM, cm^{-1}): v 3456, 3034, 2978, 2952, 2935, 2029, 1959, 1889, 1740, 1613, 1581, 1511, 1436, 1384, 1373, 1335, 1296, 1243, 1183, 1158, 1139, 1121, 1014, 955, 891, 861, 817, 786, 730, 690, 624, 553, 519, 478.

MS (ESI^+) *m/z* calcd for $C_{12}H_{16}O_3Na$ $[M+Na]^+$ 231.25; $C_{42}H_{32}O_6Na$ $[2M+Na]^+$, 439.5; found: 231.2; 439.3.

Elemental analysis calcd for $C_{12}H_{16}O_3$: C, 69.21; H, 7.74; found: C, 69.22; H, 7.71.

3.4.1.3. SYNTHESIS OF METHYL 2-(3-BROMO-4-ISOPROPOXYPHENYL)ACETATE (170)

To the solution of methyl 2-(4-isopropoxyphenyl)acetate (**169**) (5.14 g; 24.7 mmol) in DCM (80 mL), 50 μL of acetic acid, bromine (3.95 g; 1.27 mL; 24.7 mmol)

were added dropwise at 0 °C and the mixture was stirred for three hours at room temperature. After completion of the reaction (monitored by TLC), the reaction mixture was quenched with 10 mL of saturated aqueous solution of $Na_2S_2O_5$, then was poured onto 20 mL of water and extracted with diethyl ether (3 x 50 mL). The combined organic layers were washed with water (50 mL), dried over anhydrous $MgSO_4$ and evaporated to give methyl 2-(3-bromo-4-isopropoxyphenyl)acetate as colourless oil, (6.94 g; 24.2 mmol; 97%).

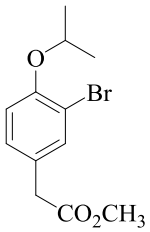

^{1}H NMR ($CDCl_3$, 400 MHz): δ 7.44 – 7.48 (m, 1H), 7.11 – 7.16 (m, 1H), 6.84-6.88 (m, 1H), 4.52 (sept., J = 6.0 Hz, 1H), 3.69 (s, 3H), 3.53 (s, 2H), 1.37 (d, J = 6.0 Hz, 6H).

^{13}C NMR ($CDCl_3$, 100 MHz,): δ 171.8, 153.7, 134.1, 129.1, 127.5, 115.6, 113.6, 72.2, 52.1, 39.8, 22.0.

IR (DCM, cm^{-1}): v 3457, 2979, 2952, 2935, 2843, 1740, 1605, 1567, 1493, 1466, 1452, 1435, 1407, 1385, 1374, 1337, 1281, 1255, 1217, 1195, 1154, 1139, 1110, 1047, 1015, 953, 903, 877, 850, 814, 728, 671, 629, 578, 502, 441.

MS (ESI^+) *m/z* calcd for $C_{12}H_{15}{}^{79}BrO_3Na$ $[M+Na]^+$ 309.14; found: 309.1.

Elemental analysis calcd for $C_{12}H_{15}BrO_3$: C, 50.19; H, 5.27; Br, 27.83; found: C, 50.46; H, 5.13; Br, 27.74.

3.4.1.4. SYNTHESIS OF METHYL 2-(4-ISOPROPOXY-3-VINYLPHENYL)ACETATE (**171**)

In a flame dried Schlenk flask, methyl 2-(3-bromo-4-isopropoxyphenyl)acetate (**170**) (1.72 g; 6.00 mmol; 1 equiv.) and tetrakis(triphenylphosphine)palladium(0) (347 mg; 0.300 mmol; 0.05 equiv.) were dissolved in 35 mL of anhydrous toluene under argon. To the reaction mixture tributyl(vinyl)tin (2.28 g; 2.10 mL; 7.20 mmol; 1.2 equiv.) was added and the reaction mixture was stirred at 110 °C for 18 hours. After that the reaction mixture was cooled down to ambient temperature and stirred with an aqueous solution of KF for an hour. The reaction mixture was filtered through a celite plug and the filtrate was extracted with DCM (3 x 20 mL). Combined organic phases were washed with 20 mL of water, dried over $MgSO_4$ and evaporated *in vacuo*. The residue was purified by

chromatography column (0 – 5 % of EtOAc in *c*-hexane) giving methyl 2-(4-isopropoxy-3-vinylphenyl)acetate as a colourless oil (1.26 g; 5.38 mmol; 90%).

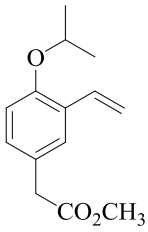

^{1}H NMR ($CDCl_3$, 400 MHz): δ 7.38 (d, J = 2.4 Hz, 1H), 7.12 (dd, J = 2.4, 8.4 Hz, 1H), 7.03 (dd, J = 11.2, 17.6 Hz, 1H), 6.83 (d, J = 8.4 Hz, 1H), 5.74 (dd, J = 1.6, 17.6 Hz, 1H), 5.24 (dd, J = 1.6, 11.2 Hz, 1H), 4.52 (sept., J = 6.0 Hz, 1H), 3.69 (s, 3H), 3.56 (s, 2H), 1.34 (d, J = 6.0 Hz, 6H).

^{13}C NMR ($CDCl_3$, 100 MHz,): δ 172.3, 154.3, 131.7, 129.4, 127.9, 127.4, 125.9, 114.2, 114.1, 70.9, 52.0, 40.4, 22.2.

IR (DCM, cm^{-1}): v 3463, 3086, 3023, 2978, 2952, 2935, 2843, 1740, 1625, 1608, 1578, 1492, 1466, 1452, 1435, 1384, 1373, 1336, 1308, 1248, 1196, 1154, 1138, 1119, 1054, 1015, 1015, 999, 957, 909, 855, 816, 709, 657, 630, 585, 422.

MS (ES^+) *m/z* calcd for $C_{14}H_{18}O_3Na$ $[M+Na]^+$ 257.28; found: 257.2.

Elemental analysis calcd for $C_{14}H_{18}O_3$: C, 71.77; H, 7.74; found: C, 71.90; H, 7.82.

3.4.1.5. SYNTHESIS OF 2-(4-ISOPROPOXY-3-VINYL-PHENYL)-ETHANOL (**172**)

A solution of methyl 2-(4-isopropoxy-3-vinylphenyl)acetate (**171**) (1.22 g; 5.20 mmol; 1 equiv.) in 52 mL of dry THF was cooled to 0 °C. A suspension of $LiAlH_4$ (6.68 ml; 5.72 mmol; 1.1 equiv.) in dry THF was added dropwise and the mixture was stirred for one hour at 0 °C. Then the reaction mixture was brought to ambient temperature and was stirred for further hour at the same temperature. After that the mixture was diluted with diethyl ether (50 mL) and 2 mL of water; then the mixture was filtered through a celite plug. Filtrate was evaporated and the residue was purified by column chromatography (10 – 20% of EtOAc in *c*-hexane) resulting in the 2-(4-isopropoxy-3-vinyl-phenyl)-ethanol as a colorless oil (960 mg; 4.63 mmol; 89%).

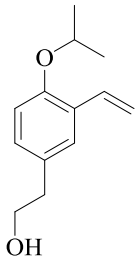

^{1}H NMR ($CDCl_3$, 400 MHz): δ 7.33 (d, J = 2.4 Hz, 6H), 7.00-7.09 (m, 2H), 6.84 (d, J = 8.4 Hz, 1H), 5.74 (dd, J = 1.6, 18.0 Hz, 1H), 5.24 (dd, J = 1.6, 11.2 Hz, 1H), 4.50 (sept, J = 6.0 Hz, 1H), 3.83 (t, J = 6.6 Hz, 2H), 2.81 (t, J = 6.6 Hz, 2H), 1.34 (d, J = 6.0 Hz, 6H).

^{13}C NMR ($CDCl_3$, 100 MHz): δ 153.9, 131.8, 130.3, 129.2, 127.9, 127.0,

114.5, 114.0, 71.0, 63.7, 38.4, 22.2.

IR (DCM, cm^{-1}): *v* 3356, 3085, 3026, 2977, 2933, 2873, 1681, 1625, 1608, 1577, 1491, 1452, 1426, 1384, 1372, 1335, 1286, 1246, 1148, 1137, 1119, 1046, 999, 957, 907, 814, 606.

MS (ESI^+) *m/z* calcd for $C_{13}H_{19}O_2$ $[M+H]^+$ 207.29; $C_{13}H_{18}O_2Na$ $[M+Na]^+$ 229.27; found 207.2; 229.4.

Elemental analysis calcd for $C_{13}H_{18}O_2$ C, 75.69; H, 8.80; found: C, 75.41; H, 8.97.

3.4.1.6. SYNTHESIS OF 4-ISOPROPOXY-3-VINYLPHENETHYL (3-HEXAISOBUTYLPOSS(T_8)-PROPYL) CARBAMATE (**174**)

To a 50 mL Schlenk flask charged with 2-(4-isopropoxy-3-vinyl-phenyl)-ethanol (**172**) (227 mg; 1.10 mmol; 1.1 equiv.) and 3-isocyanatopropylhexaisobutylPOSS(T_8) (**173**) (901 mg; 1 mmol; 1 equiv.) under argon 35 mL of dry DCM was added. Ten drops of dibutyl tin dilaurate was added and the reaction mixture was stirred in room temperature for eighteen hours. The solvent was evaporated and the residue was purified by column chromatography (0 – 5% of EtOAc in c-hexane) providing 4-isopropoxy-3-vinylphenethyl (3-heptaisobutylPOSS(T_8)-propyl) carbamate as a white solid (1.08 g; 0.978 mmol; 97%). Mp 97 – 98 °C (DCM/MeCN).

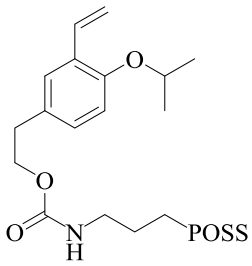

^{1}H NMR ($CDCl_3$, 400 MHz): δ 7.32 (d, *J* = 2.0 Hz, 1H), 6.98 – 7.10 (m, 2H), 6.81 (d, *J* = 8.4 Hz, 1H), 5.72 (dd, *J* = 1.6, 17.6 Hz, 1H), 5.22 (dd, *J* = 1.6, 11.2 Hz, 1H), 4.68 (brs, 1H), 4.50 (sept., *J* = 6.0 Hz, 1H), 4.24 (t, *J* = 7.0 Hz, 2H), 3.12 – 3.20 (m, 2H), 2.86 (t, *J* = 7.0 Hz, 2H), 1.79 – 1.86 (m, 7H), 1.54 – 1.64 (m, 2H), 1.34 (d, *J* = 6.0 Hz, 6H), 0.98 – 0.92 (m, 42H), 0.58 – 0.64 (m, 16H).

^{13}C NMR ($CDCl_3$, 100 MHz): δ 156.4, 153.9, 131.9, 129.9, 129.0, 127.8, 126.9, 114.4, 113.9, 70.9, 65.4, 43.2, 34.8, 31.9, 25.7, 25.6, 23.9, 23.8, 22.5, 22.4, 22.2, 14.1, 9.0.

IR (DCM, cm^{-1}): *v* 3340, 2954, 2930, 2907, 2870, 1696, 1625, 1529, 1492, 1465, 1401, 1383, 1366, 1332, 1280, 1246, 1230, 1168, 1109, 1038, 957, 905, 838, 742, 688, 563, 482, 431.

MS (ESI$^+$) *m/z* calcd for $C_{45}H_{87}NO_{15}Si_8$ $[M+H]^+$ 1106.4; found: 1106.8.

Elemental analysis calcd for $C_{45}H_{87}NO_{15}Si_8$: C, 48.83; H, 7.92; N, 1.27; found: C, 48.58; H, 7.88; N, 1.14.

3.4.1.7. SYNTHESIS OF COMPLEX **177**

To a 20 ml Schlenk flask charged with 4-isopropoxy-3-vinylphenethyl (3-heptaisobutylPOSS(T_8)-propyl) carbamate (**174**) (0.398 mg; 0.36 mmol; 1.2 equiv.), copper(I) chloride (59.4 g; 0.600 mmol; 1.2 equiv.) and **34** or **134** (0.30 mmol; 1 equiv.) under argon anhydrous toluene (10 mL) was added. The mixture was heated in 80 °C for 40 minutes, then cooled down to ambient temperature, and the solvent was evaporated *in vacuo*. The mixture was then purified utilizing column chromatography (5 – 10% of EtOAc in *c*-hexane). The solvent was evaporated *in vacuo* and the residue was dissolved in DCM (5 mL). MeOH (10 mL) was added and DCM was slowly removed under vacuum. The precipitated product was collected by filtration, washed with cold MeOH (10 mL), and dried *in vacuo* to afford green crystals (44 – 91%).

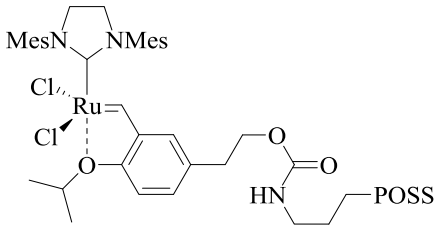

177, 91%;

^{1}H NMR ($CDCl_3$, 400 MHz): δ 16.51 (s, 1H), 7.35 (dd, *J* = 2.0, 8.4 Hz, 1H), 7.07 (s, 4H), 6.69-6.76 (m, 2H), 4.86 (sept., *J* = 6.0 Hz, 1H), 4.61 – 4.70 (m, 1H), 4.19 (t, *J* = 6.8 Hz, 2H), 4.18 (s, 4H), 3.14 – 3.21 (m, 2H), 2.89 (t, *J* = 6.8 Hz, 2H), 2.47 (s, 12H), 2.40 (s, 6H), 1.78 – 1.90 (m, 7H), 1.55 – 1.64 (m, 2H), 1.25 (d, *J* = 6.0 Hz, 6H), 0.98 – 0.91 (m, 42H), 0.58 – 0.62 (m, 16H).

^{13}C NMR ($CDCl_3$, 100 MHz,): δ 297.1, 211.4, 156.3, 151.0, 145.3, 138.8, 131.7, 129.7, 129.3, 122.9, 120.1, 112.8, 74.9, 65.1, 51.5, 43.3, 34.1, 25.7, 25.6, 23.8, 23.8, 23.2, 22.4, 22.4, 21.1, 21.0, 9.2.

IR (DCM, cm^{-1}): *v* 3345, 2954, 2926, 2908, 2870, 1726, 1596, 1486, 1465, 1419, 1400, 1383, 1366, 1332, 1259, 1228, 1168, 1104, 1036, 950, 920, 837, 807, 774, 742, 578, 482, 432.

MS (FD) *m/z* calcd for $C_{65}H_{111}{}^{35}Cl_2N_3O_{15}{}^{102}RuSi_8$ $[M]^+$ 1571.3; found: 1571.3.

Elemental analysis calcd for $C_{65}H_{111}Cl_2N_3O_{15}RuSi_8$ C, 49.69; H, 7.21; Cl, 4.51; N, 2.67; found: C, 49.50; H, 7.10; Cl, 4.35; N, 2.41.

3.4.1.8. SYNTHESIS OF COMPLEX **176**

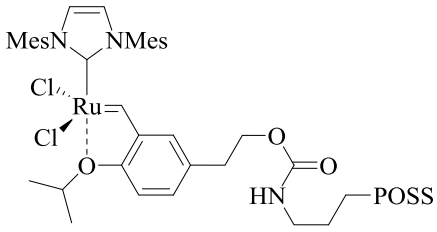

176, 44%

^{1}H NMR ($CDCl_3$, 400 MHz): δ 16.67 (s, 1H), 7.36 (dd, J = 2.0, 8.4 Hz, 1H), 7.26 – 7.28 (m, 1H), 7.11 – 7.14 (m, 5H), 6.82 (d, J = 2.0 Hz, 1H), 6.73 (d, J = 8.4 Hz, 1H), 4.89 (sept., J = 6.0 Hz, 1H), 4.65 – 4.70 (m, 1H), 4.21 (t, J = 7.0 Hz, 2H), 3.14 – 3.22 (m, 2H), 2.92 (t, J = 7.0 Hz, 2H), 2.46 (s, 6H), 2.27 (s, 12H), 1.78 – 1.90 (m, 7H), 1.56 – 1.64 (m, 2H), 1.34 (d, J = 6.0 Hz, 6H), 0.98 – 0.91 (m, 42H), 0.58 – 0.64 (m, 16H).

^{13}C NMR ($CDCl_3$, 100 MHz): δ 293.0, 175.7, 156.3, 151.1, 145.5, 139.5, 138.0, 135.8, 131.8, 129.0, 124.7, 122.4, 112.8, 75.0, 65.1, 43.3, 34.2, 25.6, 23.8, 23.7, 23.3, 22.4, 22.3, 21.1, 21.0, 19.1, 9.2.

IR (DCM, cm^{-1}): v 3346, 2954, 2926, 2870, 1725, 1488, 1465, 1401, 1383, 1366, 1319, 1292, 1228, 1168, 1105, 1037, 923, 837, 742, 695, 578, 481, 431.

MS (FD) *m/z* calcd for $C_{65}H_{109}{}^{35}Cl_2N_3O_{15}{}^{102}RuSi_8$ $[M]^+$ 1569.4; found: 1569.4.

Elemental analysis calcd for $C_{65}H_{109}Cl_2N_3O_{15}RuSi_8$: C, 49.75; H, 7.00; Cl, 4.52; N, 2.65; found: C, 49.46; H, 7.01; Cl, 4.56; N, 2.58.

3.4.2. AMIDE LINKER

3.4.2.1. SYNTHESIS OF *N*-(3-HEPTAISOBUTYLPOSS(T_8)-PROPYL)-5-HYDROXYHEXANAMIDE (**179**)

To a Schlenk tube charged with 3-aminopropyl-heptaisobutylPOSS(T_8) (**160**) (7.89 g; 9.02 mmol), DME (40 mL) followed by δ-caprolactone (**178**) (1.03 g; 0.993 mL; 9.02 mmol) were added and the reaction mixture was heated to 80 °C for 72 h. After completion the reaction mixture was cooled down, solvent was evaporated *in vacuo* and product was purified on colum chromatography with 30% of EtOAc in *c*-hexane as an

eluent. *N*-(3-HeptaisobutylPOSS(T_8)-propyl)-5-hydroxyhexanamide was obtained as a colourless solid (8.27g; 8.36 mmol; 93%). Mp. 148 – 150 °C (DCM/MeCN)

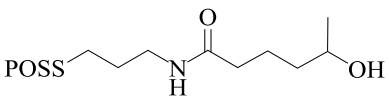

^{1}H NMR ($CDCl_3$, 400 MHz): δ 5.64 (brs, 1H), 3.80 (dd, *J* = 12.4, 6.2 Hz, 1H), 3.24 (dd, *J* = 12.8, 6.8 Hz, 2H), 2.22 (td, *J* = 7.2, 4.3 Hz, 2H), 2.14 (s, 2H), 1.91 – 1.78 (m, 7H), 1.73 (dd, *J* = 14.6, 7.3 Hz, 2H), 1.64 – 1.53 (m, 2H), 1.47 (dt, *J* = 9.4, 6.5 Hz, 2H), 1.19 (d, *J* = 6.2 Hz, 3H), 0.98 – 0.91 (m, 42H), 0.64 – 0.56 (m, 16H).

^{13}C NMR ($CDCl_3$, 101 MHz): δ 173.13, 67.53, 41.96, 38.66, 36.32, 25.83, 24.03, 23.99, 23.71, 23.15, 22.62, 22.59, 21.73, 9.61.

IR (DCM, cm^{-1}): *v* 3298, 2954, 2930, 2907, 2869, 1646, 1555, 1465, 1401, 1383, 1366, 1332, 1230, 1198, 1169, 1110, 1038, 954, 838, 743, 563, 481, 431.

MS (ESI^+) *m/z* calcd for $C_{37}H_{82}NO_{14}Si_8$ $[M+H]^+$ 988.38; $C_{37}H_{81}NO_{14}Si_8Na$ $[M+Na]^+$ 1010.37; found: 988.39; 1010.37.

HR MS (ESI^+) *m/z* calcd for $C_{37}H_{81}NO_{14}Si_8Na$ $[M+Na]^+$ 1010.3709; found: 1010.3689.

Elemental analysis calcd for $C_{37}H_{81}NO_{14}Si_8$: C, 44, 95; H, 8.26; N, 1.42; found: C, 44.88; H, 8.25; N, 1.29.

3.4.2.2. SYNTHESIS OF *N*-(3-HEPTAISOBUTYLPOSS(T_8)-PROPYL)-5-(2-(PROP-1-EN-1-YL)PHENOXY)HYDROXYHEXANAMIDE (**181**)

To a Schlenk tube charged with *O*-(prop-1-enyl)phenol (**180**) (124 mg; 1 mmol; 1 equiv.), *N*-(3-heptaisobutylPOSS(T_8)-propyl)-5-hydroxyhexanamide (**160**) (1186 mg; 1.2 mmol; 1.2 equiv.), triphenylphosphine (315 mg; 1.2 mmol; 1.2 equiv.) and dry toluene (14 mL) were added. Reaction was cooled down to 0 °C and ADD (315 mg; 1.2 mmol; 1.2 equiv.) was added and the reaction mixture was stirred for 18 h allowing to warm up to room temperature. Then the mixture was placed at 80 °C for 24h. The reaction mixture was cooled down, the precipitation was filtered off and the residue was purified by column chromatography with 5 % of EtOAc in *c*-hexane as an eluent. *N*-(3-heptaisobutylPOSS(T_8)-propyl)-5-(2-(prop-1-en-1-yl)phenoxy)hydroxyhexanamide was obtained as a colourless solid (750 mg; 0.679 mmol; 68%). Mixture of isomers: E/Z = 8:2. Mp 113 – 115 °C (DCM/MeCN).

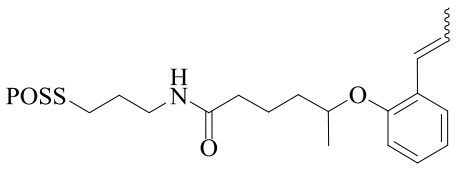

^{1}H NMR ($CDCl_3$, 400 MHz): δ 7.40 (dd, J = 7.6, 1.6 Hz, 1H), 7.21 – 7.09 (m, 1H), 6.88 (dd, J = 13.1, 7.9 Hz, 2H), 6.71 (dd, J = 15.9, 1.7 Hz, 0.8 x 1H), 6.54 (d, J = 9.8 Hz, 0.2 x 1H), 6.20 (dq, J = 15.9, 6.6 Hz, 0.8 x 1H), 5.79 (dd, J = 11.6, 7.1 Hz, 0.2 x 1H), 5.52 – 5.35 (m, 1H), 4.39 (dd, J = 11.2, 5.7 Hz, 1H), 3.22 (dd, J = 13.0, 6.1 Hz, 2H), 2.20 (dd, J = 12.4, 7.0 Hz, 2H), 1.92 – 1.72 (m, 12H), 1.72 – 1.51 (m, 4H), 1.34 – 1.25 (m, 2H), 0.98 – 0.91 (m, 42H), 0.64 – 0.55 (m, 16H).

^{13}C NMR ($CDCl_3$, 101 MHz): δ 172.60, 154.67, 130.47, 128.29, 127.92, 127.76, 126.56, 126.43, 126.04, 125.97, 125.79, 120.82, 120.12, 114.07, 113.83, 74.33, 41.90, 36.74, 36.06, 25.84, 25.83, 24.04, 23.99, 23.20, 22.62, 22.59, 22.01, 19.96, 19.13, 14.85, 9.62.

IR (DCM, cm^{-1}): v 3298, 2954, 2931, 2908, 2870, 1642, 1596, 1552, 1484, 1465, 1453, 1401, 1383, 1366, 1332, 1230, 1197, 1169, 1109, 1038, 970, 838, 745, 564, 482.

MS (ESI^+) *m/z* calcd for $C_{46}H_{89}NO_{14}Si_8Na$ $[M+Na]^+$ 1126.43; found: 1126.4.

HR MS (ESI^+) *m/z* calcd for $C_{46}H_{89}NO_{14}Si_8Na$ $[M+Na]^+$ 1126.4335; found: 1126.4336.

Elemental analysis calcd for $C_{46}H_{89}NO_{14}Si_8$: C, 50.00; H, 8.12; N, 1.27; found: C, 49.96; H, 8.00; N, 1.28.

3.4.2.3. SYNTHESIS OF COMPLEX **182**

To a Schlenk flask charged with *N*-(3-heptaisobutylPOSS(T_8)-propyl)-5-(2-(prop-1-en-1-yl)phenoxy)hydroxyhexanamide (**181**) (211 mg; 0.2 mmol; 1 equiv.) and copper(I) chloride (29.7 mg; 0.3 mmol; 1.5 equiv.) under argon DCE (10 mL) was added followed by **31** (209 mg; 0.22 mmol; 1.1 equiv.). The mixture was heated to 80 °C for 15 minutes, then cooled down to ambient temperature, and the solvent was evaporated *in vacuo*. The mixture was then purified utilizing column chromatography (5 – 10% of EtOAc in *c*-hexane). The solvent was evaporated *in vacuo* and the residue was dissolved in DCM (5 mL). MeOH (10 mL) was added and DCM was slowly removed under vacuum. The precipitated product was collected by filtration, washed with cold MeOH (10 mL), and dried *in vacuo* to afford green crystals (215 mg; 0.138 mmol; 69%).

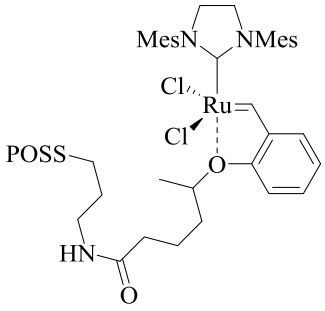

^{1}H NMR ($CDCl_3$, 400 MHz): δ 16.60 (s, 1H), 7.52 – 7.46 (m, 1H), 7.07 (d, J = 9.2 Hz, 4H), 6.93 – 6.84 (m, 2H), 6.78 (d, J = 8.4 Hz, 1H), 5.62 (s, 1H), 4.69 (d, J = 5.8 Hz, 1H), 4.15 (s, 4H), 3.28 – 3.17 (m, 1H), 3.17 – 3.06 (m, 1H), 2.59 – 2.32 (m, 18H), 2.02 (d, J = 4.7 Hz, 1H), 1.85 (tq, J = 13.3, 6.6 Hz, 10H), 1.68 – 1.44 (m, 6H), 1.27 (d, J = 6.1 Hz, 3H), 0.98 – 0.91 (m, 42H), 0.64 – 0.55 (m, 16H).

^{13}C NMR ($CDCl_3$, 101 MHz): δ 210.79, 172.79, 152.12, 145.38, 139.01, 129.91, 129.59, 122.98, 122.59, 113.30, 78.61, 51.69, 42.05, 36.86, 34.84, 25.83, 25.82, 24.01, 23.97, 23.16, 22.79, 22.61, 22.55, 21.30, 19.01, 9.64.

IR (DCM, cm^{-1}): v 3341, 2954, 2926, 2871, 1674, 1656, 1589, 1575, 1532, 1478, 1466, 1453, 1419, 1400, 1382, 1366, 1332, 1294, 1266, 1229, 1168, 1108, 1036, 951, 837, 798, 744.

MS (FD) *m/z* calcd for $C_{65}H_{111}{}^{35}Cl_2N_3O_{14}{}^{102}RuSi_8$ $[M]^+$ 1555.5; found: 1555.3.

Elemental analysis calcd for $C_{65}H_{111}Cl_2N_3O_{14}RuSi_8$: C, 50.28; H, 6.94; N, 2.73; Cl, 4.36; found: C, 50.20; H, 7.19; N, 2.70; Cl, 4.56.

3.4.3. ESTER LINKER

3.4.3.1. SYNTHESIS OF 5-BROMO-2-ISOPROPOXYBENZALDEHYDE (**184**)

To a 500 mL round bottom flask charged with K_2CO_3 (10.4 g; 75 mmol; 1.5 equiv.) and Cs_2CO_3 (3.26 g; 10 mmol; 0.2 equiv.) 200 mL of DMF was added followed by 5-bromo-2-hydroxybenzaldehyde (**183**) (10.1 g; 50 mmol; 1 equiv.). After stirring for 30 min at room temperature, 2-iodopropane (**168**) (4.99 ml; 50 mmol; 1 equiv.) was added, and the reaction mixture was stirred for 24 h at room temperature. The reaction mixture was poured onto water (300 mL) and extracted with diethyl ether (3 x 50 mL). The combined extracts were washed with brine and water and dried ($MgSO_4$). The solvent was evaporated to give the crude product as a yellow oil. The crude product was distilled to afford 5-bromo-2-isopropoxybenzaldehyde as a colourless oil (10.5 g; 43.3 mmol; 87%). NMR spectra were consistent with those described in the literature.[223]

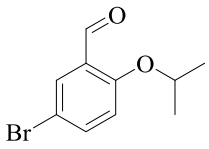

^{1}H NMR ($CDCl_3$, 400 MHz): δ 10.37 (s, 1H), 7.87 (dd, J = 4.6, 2.6 Hz, 1H), 7.59 – 7.53 (m, 1H), 6.87 (dt, J = 8.9, 2.7 Hz, 1H), 4.63 (dq, J = 12.1, 6.0 Hz, 1H), 1.40 (d, J = 6.0 Hz, 6H).

^{13}C NMR ($CDCl_3$, 101 MHz): δ 188.72, 159.51, 138.19, 130.92, 127.01, 116.09, 113.15, 71.70, 21.96.

3.4.3.2. SYNTHESIS OF 4-BROMO-1-ISOPROPOXY-2-(PROP-1-EN-1-YL)BENZENE (**185**)

To an argonated Schlenk tube charged with solution of ethyl triphenylphosphonium bromide (8.35 g; 22.5 mmol; 1.5 equiv.) in THF at 0 °C butyllithium 1.6 M solution in THF (14.1 mL; 11.5 mmol; 1.5 equiv.) was added to give red solution. The reaction mixture was allowed to stir at room temperature for 2 h prior to cooling to −60 °C. The solution of 5-bromo-2-isopropoxybenzaldehyde (3.65 g; 15 mmol) in 5 mL dry THF was slowly added over a period of 30 min while maintaining a temperature −60 °C. The reaction was then allowed to continue under argon atmosphere while slowly warming up to room temperature for 18 h. Upon reaction completion, the mixture was diluted with Et_2O, transferred to a separating funnel and extracted with saturated $NaHCO_3$ and brine. The organic layer was dried over Na_2SO_4 and evaporated to give the crude product as a yellow oil. The crude product was distilled to afford 4-bromo-1-isopropoxy-2-(prop-1-enyl)benzene (**185**) (3.72 g; 14.6 mmol; 97%) as a bright yellow oil. NMR spectra consistent with those described in the literature.[223]

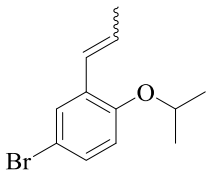

^{1}H NMR ($CDCl_3$, 400 MHz): δ 8.29 (d, J = 2.5 Hz, 1H), 8.05 (dd, J = 9.1, 2.9 Hz, 1H), 6.87 (d, J = 9.2 Hz, 1H), 6.66 (dq, J = 16.0, 1.6 Hz, 1H), 6.32(m, 1H), 4.69 (sept., J = 6.1 Hz, 1H), 1.93 (dd, J = 6.7, 1.7 Hz, 3H), 1.41 (d, J = 6.1 Hz, 6H).

3.4.3.3. SYNTHESIS OF 3-(4-ISOPROPOXY-3-(PROP-1-ENYL)PHENYL)PROPANOIC ACID (**186**)

A Schlenk flask was charged with Mg (176 mg; 7.25 mmol; 1.5 equiv.) which was activated by flame drying under a flow of inert gas and then suspended in 2 mL of THF. Solution of 4-bromo-1-isopropoxy-2-(prop-1-enyl)benzene (**185**) (1230 mg; 4.83 mmol; 1 equiv.) in 5 ml of dry THF was slowly added and the suspension was brought to a reflux. Upon completion of the addition of 4-bromo-1-isopropoxy-2-(prop-1-enyl)benzene, the

resulting suspension was cooled to RT and stirred for 1 h. Trituration was performed[2] to calculate the yield of Grignard reagent. Schlenk flask was charged with copper(I) iodide (419 mg; 2.20 mmol; 1.1 equiv.). After flushing with argon 10 ml of dry THF and 1 mL of Me_2S were added and the solution was cooled to −30°C. Solution of Grignard reagent was slowly added to this solution and the mixture was stirred for 30 min at this temperature. Then, a solution of oxetan-2-one (0.126 mL; 144 mg, 2 mmol) in 2 mL of THF was added dropwise to the flask. The mixture was stirred at the same temperature for 1 h and allowed to warm to 0 °C over 1 h. The reaction mixture was quenched by addition of 10 ml 3M HCl and then mixture was extracted with three 10 mL portions of 3M NaOH from the organic layer. The alkaline solution was acidified with 6M HCl to pH=1 and then extracted with ether. The etheral extracts were washed with brine and dried $MgSO_4$. Removal of the solvent from the filtrate *in vacuo* gave the crude product, which was purified by column chromatography with 10% of EtOAc in *c*-hexane as an eluent. 3-(4-isopropoxy-3-(prop-1-enyl)phenyl)propanoic acid was obtained as a pale yellow solid (397 mg; 1.6 mmol; 80 %). NMR spectra consistent with those described in the literature.[211] Mixture of isomers: E/Z = 95:5. Mp = 88 – 92 °C;

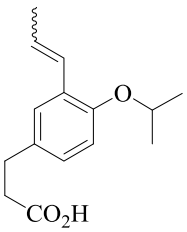

^{1}H NMR ($CDCl_3$, 400 MHz,): δ 7.24 (s, 1H), 6.99 (m, 1H), 6.79 (d, J = 8.4 Hz, 1H), 6.70 (d, *J* = 16.0 Hz, 1H, *E*), 6.20 (m, *J* = 6.4 Hz, 1H, *E*), 4.47 (m, *J* = 6.0 Hz, 1H), 2.88 (t, *J* = 7.6 Hz, 2H), 2.65 (t, *J* = 7.6 Hz, 2H), 1.90 (m, 3H), 1.34 (d, *J* = 6.0 Hz, 6H).

3.4.3.4. SYNTHESIS OF 5-HEPTAISOBUTYLPOSS(T_8)PENTYL-3-(4-ISOPROPOXY-3-(PROP-1-ENYL)PHENYL)PROPANOATE (**188**)

DCC (*N*,*N*'-dicyclohexylcarbodiimide) (413 mg; 2 mmol; 1 equiv.) and DMAP (4-dimethylaminopyridine) (489 mg; 4 mmol; 2 equiv.) were added to a solution of 3-(4-isopropoxy-3-propenyl-phenyl)-propionic acid (**186**) (497 mg, 2 mmol) and 5-hydroxypentyl-heptaisobutylPOSS(T_8) (2169 mg; 2.4 mmol; 1.2 equiv.) in 28 mL of anhydrous DCM at 0 °C. The reaction mixture was slowly warmed to room temperature and stirred for another 12 h at room temperature. Then the insoluble materials were

[2] 10 ml round-bottom flask equipped with magnetic stirring bar and septum was heated with heat gun under reduced pressure and cooled to room temperature under argon atmosphere. The dry flask was charged with accurately weighed I_2 (254 mg, 1mmol), stopped with rubber septum and flushed with argon. Sat. LiCl in THF (4 ml) was added and stirring was started. After the iodine was completely dissolved, the resulting brown solution was cooled to 0°C in an ice bath and the Grignard reagent was added dropwise via 1ml syringe until the brown color disappeared.

filtered out and the filtrate was concentrated *in vacuum*. The crude product was purified by column chromatography on silica using 5% ethyl acetate in *c*-hexane as the eluent to give pure 5-heptaisobutylPOSS(T_8)pentyl-3-(4-isopropoxy-3-(prop-1-enyl)phenyl) propanoate as colourless solid (1983 mg; 1.77 mmol, 89%). Mixture of isomers: E/Z = 97:3. Mp. = 116 – 117 °C

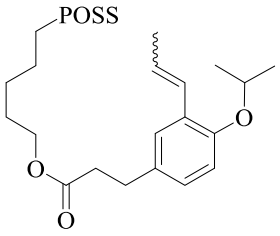

^{1}H NMR ($CDCl_3$, 500 MHz): δ 7.23 (d, J = 2.2 Hz, 1H), 6.96 (dd, J = 8.3, 2.2 Hz, 1H), 6.77 (d, J = 8.4 Hz, 1H), 6.68 (dd, J = 15.9, 1.7 Hz, 1H, *E*), 6.20 (dd, J = 15.9, 6.6 Hz, 1H, *E*), 4.51 – 4.42 (m, 1H), 4.05 (t, J = 6.8 Hz, 2H), 2.89 – 2.83 (m, 2H), 2.61 – 2.55 (m, 2H), 1.92 – 1.79 (m, 9H), 1.64 – 1.56 (m, 2H), 1.47 – 1.38 (m, 4H), 1.33 (d, J = 6 Hz, 6H), 0.98 – 0.91 (m, 42H), 0.66 – 0.55 (m, 16H).

^{13}C NMR ($CDCl_3$, 125 MHz): δ 173.26, 153.26, 132.78, 128.34, 127.45, 126.40, 126.04, 125.99, 114.69, 77.41, 77.16, 76.91, 71.14, 64.67, 36.41, 30.51, 29.09, 28.50, 25.85, 25.83, 24.05, 24.02, 22.67, 22.65, 22.60, 22.40, 19.07, 12.14.

IR (CH_2Cl_2, cm^{-1}): v 2954, 2931, 2908, 2869, 1738, 1492, 1465, 1401, 1383, 1366, 1332, 1230, 1169, 1107, 1038, 956, 838, 741, 565, 480, 431.

MS (ESI^+) *m/z* calcd for $C_{48}H_{93}O_{15}Si_8$ $[M+H]^+$ 1133.46; found: 1133.5.

Elemental analysis calcd. for $C_{48}H_{92}O_{15}Si_8$: C, 50.84; H, 8.18; found: C, 50.46 ; H, 8.15.

3.4.3.5. SYNTHESIS OF COMPLEX **189**

5-HeptaisobutylPOSS(T_8)-pentyl-3-(4-isopropoxy-3-(prop-1-enyl)phenyl) propanoate (**188**) (680 mg; 0.6 mmol), copper(I) chloride (89.1 mg; 0.9 mmol; 1.5 equiv.) and **31** (597 mg; 0.63 mmol; 1.05 equiv.) were placed in a Schlenk tube under argon and dissolved in 50 mL of DCM. The mixture was heated at 40 °C for 40 minutes, then cooled down to ambient temperature, and solvent was evaporated. The mixture was then purified utilizing column chromatography (5 – 10% of of EtOAc in *c*-hexane). Solvent was evaporated *in vacuo* and the residue was dissolved in DCM (10 mL). MeOH (20 mL) was added and DCM was slowly removed under vacuum. The precipitated product was collected by filtration, washed with cold MeOH (20 mL), and dried *in vacuo* to afford green crystals (850 mg; 0.536 mmol; 89%).

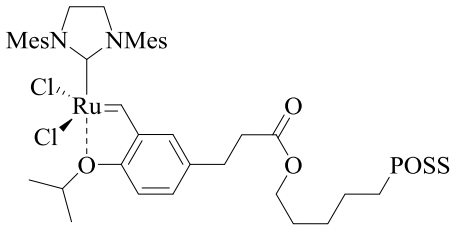

^{1}H NMR ($CDCl_3$, 500 MHz): δ 16.52 (s, 1H), 7.34 (dd, J = 8.4, 1.8 Hz, 1H), 7.07 (s, 4H), 6.73 (d, J = 1.8 Hz, 1H), 6.69 (d, J = 8.5 Hz, 1H), 4.90 – 4.81 (m, 1H), 4.17 (s, 4H), 4.06 (t, J = 6.9 Hz, 2H), 2.91 (t, J = 7.9 Hz, 2H), 2.57 – 2.51 (m, 2H), 2.48 (s, 12H), 2.41 (s, 6H), 1.91 – 1.80 (m, 9H), 1.67 – 1.59 (m, 2H), 1.48 – 1.32 (m, 4H), 1.25 (d, J = 6.1 Hz, 6H), 0.98 – 0.91 (m, 42H), 0.66 – 0.55 (m, 16H).

^{13}C NMR ($CDCl_3$, 125 MHz): δ 297.20, 173.01, 151.02, 145.45, 138.97, 134.48, 129.52, 129.43, 122.60, 112.96, 76.41, 75.09, 64.77, 52.04, 51.62, 36.25, 29.75, 29.09, 28.46, 27.41, 25.84, 24.02, 23.10, 22.66, 22.23, 21.23, 19.82, 19.68, 19.09, 12.15, 0.15.

IR (DCM, cm^{-1}): v 2954, 2927, 2870, 1737, 1595, 1487, 1466, 1418, 1400, 1383, 1366, 1332, 1293, 1260, 1229, 1168,1107, 1037, 951, 837, 810.

MS (FD) *m/z* calcd for $C_{67}H_{114}{}^{35}Cl_2N_2O_{15}{}^{102}RuSi_8$ $[M]^+$ 1584.4; found: 1584.3.

Elemental analysis calcd for $C_{67}H_{114}Cl_2N_2O_{15}RuSi_8$: C, 50.79; H, 7.25; N, 1.77; Cl, 4.48; found: C, 50.54; H, 7.56; N, 1.78; Cl, 4.48.

3.4.4. HYDROCARBON LINKER

3.4.4.1. SYNTHESIS OF 4-(5-HEPTAISOBUTYLPOSS(T_8)PENTYL)-1-ISOPROPOXY-2-(PROP-1-ENYL)BENZENE (**190**)

A Schlenk flask was charged with Mg (176 mg; 7.25 mmol; 1.5 equiv.), which was activated by flame drying under a flow of inert gas and suspended in 2 ml of THF. Solution of 4-bromo-1-isopropoxy-2-(prop-1-enyl)benzene (**185**) (1230 mg; 4.83 mmol) in 5 ml dry THF was slowly added and the suspension was brought to reflux. Upon completion of the addition of **185**, the resulting suspension was cooled to RT with stirring for 1h. Trituration was performed[3]. A Schlenk flask was charged with 10 mL of dry THF, $Co(acac)_3$ (162 mg; 0.45 mmol; 0.1 equiv.), 5-bromopentyl-heptaisobutylPOSS(T_8) (**140**) (4.41 g; 4.5 mmol) and TMEDA (0.1 mL; 78.4 mg; 0.675 mmol; 0.15 equiv.). The reaction mixture was cooled to 0 °C, then solution of Grignard reagent (1.5 equiv.) was

[3] 10 ml round-bottom flask equipped with magnetic stirring bar and septum was heated with heat gun under reduced pressure and cooled to room temperature under argon atmosphere. The dry flask was charged with accurately weighed I_2 (254 mg, 1 mmol), stopped with rubber septum and flushed with argon. Sat. LiCl in THF (4 ml) was added and stirring was started. After the iodine was completely dissolved, the resulting brown solution was cooled to 0 °C in an ice bath and the Grignard reagent was added dropwise via 1ml syringe until the brown color disappeared.

added by syringe pump at 2 ml/h. Reaction was stirred overnight. MeOH was added and the resulting mixture was concentrated in vacuo. The crude product was purified by column chromatography on silica using 1% ethyl acetate in c-hexane as an eluent to give pure 4-(5-heptaisobutylPOSS(T_8)-pentyl)-1-isopropoxy-2-(prop-1-enyl)benzene as colourless solid (4.72 g; 4.45 mmol, 99%). Mixture of isomers E/Z = 6:4. Mp. 89 – 90 °C

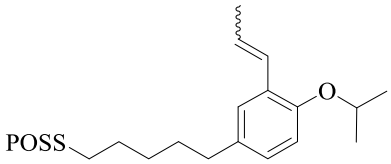

^{1}H NMR ($CDCl_3$, 500 MHz): δ 7.21 (d, J = 2.1 Hz, 0.6 x 1H), 7.08 (d, J = 2.1 Hz, 0.4 x 1H), 6.98 (dd, J = 8.4, 2.2 Hz, 0.4 x 1H), 6.94 (dd, J = 8.3, 2.2 Hz, 0.6 x 1H), 6.81 (d, J = 8.4 Hz, 0.4 x 1H), 6.77 (d, J = 8.4 Hz, 0.6 x 1H), 6.70 (dd, J = 15.9, 1.7 Hz, 0.6 x 1H), 6.54 (dd, J = 11.6, 1.8 Hz, 0.4 x 1H), 6.21 (dq, J = 15.9, 6.6 Hz, 0.6 x 1H), 5.78 (dq, J = 11.6, 7.1 Hz, 0.4 x 1H), 4.53 – 4.40 (m, 1H), 2.52 (dd, J = 16.0, 9.7 Hz, 2H), 1.93 – 1.79 (m, 10H), 1.59 (dd, J = 20.7, 5.7 Hz, 2H), 1.48 – 1.41 (m, 2H), 1.42 – 1.35 (m, 2H), 1.33 (dd, J = 10.0, 6.1 Hz, 6H), 0.98 – 0.91 (m, 42H), 0.62 – 0.58 (m, 16H).

^{13}C NMR ($CDCl_3$, 125 MHz): δ 153.78, 152.86, 135.19, 134.53, 130.33, 128.15, 127.71, 127.54, 127.50, 126.39, 126.26, 126.22, 126.02, 125.69, 114.70, 114.51, 71.23, 35.27, 35.20, 32.60, 32.57, 31.56, 31.52, 25.86, 24.06, 24.03, 23.12, 22.69, 22.67, 22.45, 22.26, 19.07, 14.92, 12.15, 0.16.

IR (DCM, cm^{-1}): v 2954, 2929, 2869, 1489, 1465, 1401, 1383, 1366, 1332, 1230, 1169, 1109, 1038, 956, 838, 742, 564, 481, 431.

MS (FD) *m/z* calcd for $C_{45}H_{88}O_{13}Si_8Na$ $[M+Na]^+$1083.43; found: 1083.4.

Elemental analysis calcd for $C_{45}H_{88}O_{13}Si_8$: C, 50.9; H, 8.36; found: C, 50.96; H, 8.35.

3.4.4.2. SYNTHESIS OF COMPLEX **191**

4-(5-HeptaisobutylPOSS(T_8)pentyl)-1-isopropoxy-2-(prop-1-enyl)benzene (**190**) (1044 mg; 1.1 mmol; 1.1 equiv.), copper(I) chloride (149 mg; 1.5 mmol; 1.5 equiv.) and **31** (1062 mg; 1 mmol) were placed in a Schlenk tube under argon and dissolved in 50 mL of DCM. The mixture was heated at 40 °C for 40 minutes, then cooled down to ambient temperature, and solvent was evaporated. The mixture was then purified utilizing column chromatography (5 – 10% of of EtOAc in *c*-hexane). Solvent was evaporated *in vacuo* and the residue was dissolved in DCM (5 mL). MeOH (10 mL) was added and DCM was

slowly removed under vacuum. The precipitated product was collected by filtration, washed with cold MeOH (10 mL), and dried *in vacuo* to afford green crystals (1.06 g; 0.701 mmol; 70%).

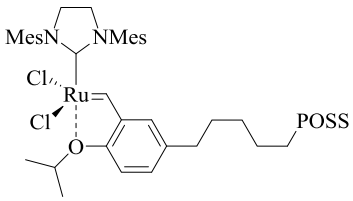

^{1}H NMR ($CDCl_3$, 500 MHz): δ 16.46 (s, 1H), 7.28 (dd, J = 8.4, 2.0 Hz, 1H), 7.07 (s, 4H), 6.69 (d, J = 2.0 Hz, 1H), 6.67 (d, J = 8.4 Hz, 1H), 4.89 – 4.81 (m, 1H), 4.18 (s, 4H), 2.58 – 2.53 (m, 2H), 2.48 (s, 12H), 2.40 (s, 6H), 1.92 – 1.81 (m, 9H), 1.51 (d, J = 7.7 Hz, 4H), 1.43 (dd, J = 15.3, 7.8 Hz, 2H), 1.40 – 1.34 (m, 2H), 1.25 (d, J = 6.1 Hz, 6H), 0.96 (dd, J = 6.6, 3.4 Hz, 42H), 0.61 (dd, J = 7.0, 5.8 Hz, 16H).

^{13}C NMR ($CDCl_3$, 125 MHz): δ 297.85, 211.98, 150.49, 145.24, 138.72, 136.43, 129.35, 122.35, 112.49, 74.69, 34.39, 32.42, 31.03, 25.69, 23.86, 22.52, 21.07, 12.01.

IR (DCM, cm^{-1}): v 2954, 2927, 2870, 1607, 1485, 1465, 118, 1400, 1383, 1366, 1332, 1265, 1228, 1168, 1106, 1037, 930, 836, 742, 578, 481, 431.

MS (FD) *m/z* calcd for $C_{64}H_{110}{}^{35}Cl_2N_2O_{13}{}^{102}RuSi_8$ $[M]^+$ 1512.46; found: 1512.3.

Elemental analysis calcd for $C_{64}H_{110}Cl_2N_2O_{13}RuSi_8$: C, 50, 83; H, 7.33; N, 1.85; Cl, 4.69; found: C, 50.82; H, 7.53; N, 1.69; Cl, 4.73.

3.4.5. MODIFICATION OF THE ISOPROPOXY MOIETY

3.4.5.1. SYNTHESIS OF 5-HEPTAISOBUTYLPOSS(T_8)-PENTYL 2-(2-(PROP-1-EN-1-YL)PHENOXY)PROPANOATE (**193**)

DCC (*N*,*N*'-dicyclohexylcarbodiimide) (124 mg; 0.6 mmol; 1 equiv.) and DMAP (4-dimethylaminopyridine) (147 mg; 1.2 mmol; 2 equiv.) were added to a solution of 3-(4-isopropoxy-3-propenyl-phenyl)-propionic acid (**192**) (124 mg, 0.6 mmol) and 5-hydroxypentyl-heptaisobutylPOSS(T_8) (**187**) (651 mg; 0.72 mmol; 1.2 equiv.) in 6 mL anhydrous DCM at 0 °C. The reaction mixture was slowly warmed to room temperature and stirred for another 12 h at room temperature. Then the insoluble materials were filtered out and the filtrate was concentrated under vacuum. The crude product was purified by column chromatography on silica using 5 % ethyl acetate in *c*-hexane as an eluent to give pure 5-heptaisobutylPOSS(T_8)-pentyl-2-(2-(prop-1-en-1-yl)phenoxy) propanoate as white solid (641 mg; 0.596 mmol; 99%). Mixture of isomers E/Z = 7:3. Mp 93 °C

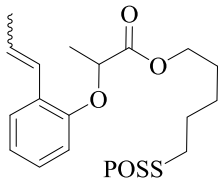

^{1}H NMR ($CDCl_3$, 400 MHz): δ 7.40 (dd, J = 7.7, 1.6 Hz, 0.7 x 1H), 7.27 (dd, J = 7.5, 1.5 Hz, 0.3 x 1H), 7.17 – 7.05 (m, 1H), 6.97 – 6.87 (m, 1H), 6.82 – 6.73 (m, 1H), 6.70 (dd, J = 8.2, 0.8 Hz, 0.7 x 1H), 6.60 (dd, J = 11.6, 1.5 Hz, 0.3 x 1H), 6.23 (dq, J = 15.9, 6.6 Hz, 0.7 x 1H), 5.82 (dq, J = 11.6, 7.1 Hz, 0.3 x 1H), 4.73 (p, J = 6.7 Hz, 1H), 4.19 – 4.03 (m, 2H), 1.92 – 1.77 (m, 10H), 1.62 (dd, J = 11.0, 6.8 Hz, 3H), 1.59 – 1.54 (m, 2H), 1.42 – 1.32 (m, 2H), 1.32 – 1.23 (m, 2H), 0.98 – 0.91 (m, 42H), 0.61 – 0.56 (m, 16H).

^{13}C NMR ($CDCl_3$, 101 MHz): δ 172.45, 172.44, 155.38, 154.41, 130.58, 128.00, 127.84, 127.65, 127.41, 127.05, 126.70, 126.60, 125.67, 125.31, 121.78, 121.17, 113.07, 73.43, 73.41, 65.35, 65.32, 28.92, 28.34, 25.85, 25.83, 24.05, 24.01, 23.19, 22.65, 22.63, 22.50, 22.12, 19.12, 18.82, 18.79, 14.88, 12.10.

IR (DCM, cm^{-1}): v 2954, 2931, 2907, 2869, 1758, 1737, 1693, 1599, 1486, 1465, 1401, 1383, 1366, 1332, 1276, 1230, 1169, 1106, 1039, 954, 838, 744, 615, 563, 480, 431.

MS (ESI^+) *m/z* calcd for $C_{45}H_{86}NaO_{15}Si_8$ $[M+Na]^+$ 1113.4; found: 1113.4.

HR MS (ES+) *m/z* calcd for $C_{45}H_{86}NaO_{15}Si_8$ $[M+Na]^+$ 1113.4019 found 1113.3997.

Elemental analysis calcd for $C_{45}H_{86}O_{15}Si_8$: C, 45,5; H, 7.94; found: C, 49.44; H, 7.99.

3.4.5.2. SYNTHESIS OF CATALYST **194**

5-HeptaisobutylPOSS(T_8)-pentyl 2-(2-(prop-1-en-1-yl)phenoxy)propanoate (**193**) (590 mg; 0.54 mmol; 1.2 equiv.), copper(I) chloride (66.8 mg; 0.675 mmol; 1.5 equiv.) and **31** (427 mg; 0.45 mmol) were placed in a Schlenk tube under argon and dissolved in 23 mL of DCM. The mixture was heated in 40 °C for 40 minutes, then cooled down to ambient temperature, and the solvent was evaporated. The mixture was then purified utilizing column chromatography (5 – 10% of EtOAc in *c*-hexane). The solvent was evaporated *in vacuo* and the residue was dissolved in DCM (5 mL). MeOH (10 mL) was added and DCM was slowly removed under vacuum. The precipitated product was collected by filtration, washed with cold MeOH (10 mL), and dried *in vacuo* to afford green crystals (567 mg; 0.36 mmol; 82%).

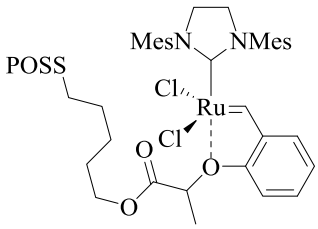

^{1}H NMR (CD_2Cl_2, 500 MHz): δ 16.51 (s, 1H), 7.56 – 7.50 (m, 1H), 7.07 (s, 4H), 7.01 – 6.95 (m, 2H), 6.66 (d, J = 8.2 Hz, 2H), 4.95 (q, J = 6.8 Hz, 1H), 4.13 (s, 4H), 4.06 – 3.96 (m, 2H), 2.45 (brs, 12H), 2.41 (s, 6H), 1.94 – 1.81 (m, 7H), 1.61 – 1.51 (m, 2H), 1.46 (d, J = 6.8 Hz, 3H), 1.41 (dd, J = 15.7, 8.2 Hz, 2H), 1.32 (dd, J = 15.3, 8.2 Hz, 2H), 0.97 (dd, J = 6.6, 1.3 Hz, 42H), 0.62 (dd, J = 7.0, 3.4 Hz, 16H).

^{13}C NMR (CD_2Cl_2, 126 MHz): δ 297.70, 210.49, 170.86, 151.95, 145.92, 139.45, 139.04, 129.84, 129.32, 124.15, 122.79, 113.08, 74.33, 66.58, 52.22, 29.47, 28.73, 26.71, 26.02, 25.23, 24.47, 23.74, 23.66, 23.44, 23.01, 22.57, 21.46, 19.83, 19.06, 17.85, 12.52.

IR (DCM, cm^{-1}): v 2954, 2927, 2908, 2870, 1762, 1736, 1606, 1593, 1574, 1478, 1466, 1453, 1416, 1400, 1383, 1366, 1332, 1294, 1263, 1229, 1168, 1108, 1037, 951, 920, 850, 837, 794, 742, 617, 579, 482, 431.

MS (FD) *m/z* calcd for $C_{64}H_{108}{}^{35}Cl_2N_2O_{15}{}^{102}RuSi_8$ $[M]^+$ 1542.4; found: 1542.3.

Elemental analysis calcd for $C_{64}H_{108}N_2O_{15}RuSi_8Cl_2$ C, 49.84; H, 7.06; Cl, 4.60; N, 1.82; found: C, 49.78; H, 7.08; N, 1.65; Cl, 4.39.

3.5. PROCEDURE OF RCM OF DEDAM FOR REACTION PROFILE MESUREMENT

DEDAM (**8**) (129 mg; 0.5 mmol) and dodecane (51 mg; 0.3 mmol; 0.6 equiv.) were dissolved in 5 mL of appropriate solvent under argon. Appropriate catalyst (0.005 mmol; 0.01 equiv.) was added and reaction mixture was stirred in appropriate temperature. Aliquots (0.1 mL) were taken in intervals and added to the solution of ethyl vinyl ether in DCM (2 M; 0.5 mL). The samples were shaken, then allowed to stand for 5 min, then analyzed by GC.

3.6. PROCEDURE OF BATCHWISE RCM OF DEDAM WITH NANOFILTRATION

A 20 mL glass tube was charged with DEDAM (**8**) (721 mg; 3 mmol), placed in a Carousel 12 (Radleys Discovery Technologies) set up preheated to appropriate temperature and flushed with nitrogen. 30 mL of appropriate solvent was added to the

glass tube under nitrogen. Appropriate catalyst (0.03 mmol; 0.01 equiv.) was added to the solution and reaction mixture was stirred within the time. The post-reaction solution was transferred to the Sepa ST dead end filtration cell (Osmonics USA) with disk of desired membrane on the bottom cell with active side of the membrane facing towards the reaction mixture. Finally, the filtration cell was closed by clamping the cell base against the body with a set of high pressure clamps. Pressure was applied by connecting the filtration system to pressurised nitrogen cylinder. Continuous stirring was applied to avoid concentration polarization. After pressurizing the cell, fresh solvent was introduced to the filtration cell with the help of HPLC pump at the same rate at which permeate was generated. The permeate was collected and monitored by GC till complete elution of the product.

3.7. PROCEDURE OF BATCHWISE RCM OF DEDAM WITH NANOFILTRATION AND REUSE OF THE CATALYST

A 20 mL glass tube was charged with DEDAM (**8**) (721 mg; 3 mmol), placed in a Carousel 12 (Radleys Discovery Technologies) set up preheated to appropriate temperature and flushed with nitrogen. 30 mL of appropriate solvent was added to the solution under nitrogen. Appropriate catalyst (0.03 mmol; 0.01 equiv.) was added and reaction mixture was stirred within the time. The post-reaction solution was transferred to the Sepa ST dead end filtration cell (Osmonics USA) with disk of desired membrane placed on the bottom of the filtration cell with active side of the membrane facing towards the reaction mixture. Finally, the filtration cell was closed by clamping the cell base against the body with a set of high pressure clamps. Pressure was applied by connecting the filtration system to pressurised nitrogen cylinder. Continuous stirring was applied to avoid concentration polarization. After pressurizing the cell, fresh solvent was introduced to the filtration cell with the help of HPLC pump at the same rate at which permeate was generated. After removal of the product from the mixture placed in Sepa cell, estimated from the product rejection data, the solution of the catalyst was transferred back into glass tube, fresh solution of the substrate was added for the next reaction cycle.

3.8. PROCEDURE OF RCM OF DEDAM IN CONTINUOUS SYSTEM

A 500 mL round bottom flask was charged with DEDAM (**8**) (2404 mg; 10 mmol), and flushed with argon. 100 mL of toluene was added under argon. Appropriate

(192) Keraani, A.; Rabiller-Baudry, M.; Fischmeister, C.; Bruneau, C. *Catal. Today* **2010**, *156*, 268.
(193) O'Neal, E. J.; Jensen, K. F. *ChemCatChem* **2014**, *6*, 3004.
(194) (a) Ulman, M.; Grubbs, R. H. *J. Org. Chem.* **1999**, *64*, 7202; (b) Scholz, J.; Loekman, S.; Szesni, N.; Hieringer, W.; Görling, A.; Haumann, M.; Wasserscheid, P. *Adv. Synth. Catal.* **2011**, *353*, 2701.
(195) Ormerod, D.; Bongers, B.; Porto-Carrero, W.; Giegas, S.; Vijt, G.; Lefevre, N.; Lauwers, D.; Brusten, W.; Buekenhoudt, A. *RSC Advances* **2013**, *3*, 21501.
(196) Darvishmanesh, S.; Degrève, J.; Van der Bruggen, B. *ChemPhysChem* **2010**, *11*, 404.
(197) Hong, S. H.; Sanders, D. P.; Lee, C. W.; Grubbs, R. H. *J. Am. Chem. Soc.* **2005**, *127*, 17160.
(198) Czaban, J.; Schertzer, B. M.; Grela, K. *Adv. Synth. Catal.* **2013**, *355*, 1997.
(199) Hartmann-Thompson, C. *Applications of Polyhedral Oligomeric Silsesquioxanes*; Springer Netherlands, 2011.
(200) Liu, J.; Chen, J.; Zhao, J.; Zhao, Y.; Li, L.; Zhang, H. *Synthesis* **2003**, *2003*, 2661.
(201) HybridCatalysis; http://www.hybridcatalysis.com/#capabilities.
(202) Gerritsen, G., Technische Universiteit Eindhoven, 2011.
(203) (a) Barbasiewicz, M.; Michalak, M.; Grela, K. *Chem. Eur. J.* **2012**, *18*, 14237; (b) Tzur, E.; Szadkowska, A.; Ben-Asuly, A.; Makal, A.; Goldberg, I.; Woźniak, K.; Grela, K.; Lemcoff, N. G. *Chem. Eur. J.* **2010**, *16*, 8726.
(204) Vehlow, K.; Maechling, S.; Blechert, S. *Organometallics* **2006**, *25*, 25.
(205) Conrad, J. C.; Yap, G. P. A.; Fogg, D. E. *Organometallics* **2003**, *22*, 1986.
(206) Weskamp, T.; Schattenmann, W. C.; Spiegler, M.; Herrmann, W. A. *Angew. Chem. Int. Ed.* **1998**, *37*, 2490.
(207) Meyer, E. A.; Castellano, R. K.; Diederich, F. *Angew. Chem. Int. Ed.* **2003**, *42*, 1210.
(208) (a) Gawin, R.; Grela, K. *Eur. J. Inorg. Chem.* **2012**, *2012*, 1477; (b) Gawin, R.; Czarnecka, P.; Grela, K. *Tetrahedron* **2010**, *66*, 1051.
(209) Wappel, J.; Urbina-Blanco, C. A.; Abbas, M.; Albering, J. H.; Saf, R.; Nolan, S. P.; Slugovc, C. *Beilstein J. Org. Chem.* **2010**, *6*, 1091.
(210) Kawashima, M.; Sato, T.; Fujisawa, T. *Tetrahedron* **1989**, *45*, 403.
(211) Liu, G.; Wang, J. *Angew. Chem. Int. Ed.* **2010**, *49*, 4425.
(212) Frisch, A. C.; Shaikh, N.; Zapf, A.; Beller, M. *Angew. Chem. Int. Ed.* **2002**, *41*, 4056.
(213) Nakamura, M.; Matsuo, K.; Ito, S.; Nakamura, E. *J. Am. Chem. Soc.* **2004**, *126*, 3686.
(214) Cahiez, G.; Habiak, V.; Duplais, C.; Moyeux, A. *Angew. Chem. Int. Ed.* **2007**, *46*, 4364.
(215) (a) Cahiez, G.; Chaboche, C.; Duplais, C.; Giulliani, A.; Moyeux, A. *Adv. Synth. Catal.* **2008**, *350*, 1484; (b) Nasielski, J.; Hadei, N.; Achonduh, G.; Kantchev, E. A. B.; O'Brien, C. J.; Lough, A.; Organ, M. G. *Chem. Eur. J.* **2010**, *16*, 10844.
(216) Cahiez, G.; Gager, O.; Buendia, J. *Synlett* **2010**, *2010*, 299.
(217) Cahiez, G. r.; Chaboche, C.; Duplais, C.; Moyeux, A. *Org. Lett.* **2008**, *11*, 277.
(218) (a) Bieniek, M., doctoral dissertation, 2008; (b) Bieniek, M.; Bujok, R.; Cabaj, M.; Lugan, N.; Lavigne, G.; Arlt, D.; Grela, K. *J. Am. Chem. Soc.* **2006**, *128*, 13652.
(219) Bieniek, M.; Samojłowicz, C.; Sashuk, V.; Bujok, R.; Śledź, P.; Lugan, N. l.; Lavigne, G.; Arlt, D.; Grela, K. *Organometallics* **2011**, *30*, 4144.
(220) Grela, K.; Michrowska, A.; Bieniek, M. *The Chemical Record* **2006**, *6*, 144.
(221) Dastgir, S.; Coleman, K. S.; Green, M. L. H. *Dalton T.* **2011**, *40*, 661.
(222) Gawin, R. doctoral dissertation, 2012.
(223) Bujok, R.; Bieniek, M.; Masnyk, M.; Michrowska, A.; Sarosiek, A.; Stępowska, H.; Arlt, D.; Grela, K. *J. Org. Chem.* **2004**, *69*, 6894.

REFERENCES

(1) Calderon, N.; Chen, H. Y.; Scott, K. W. *Tetrahedron Lett.* **1967**, *8*, 3327.

(2) (a) Nicola, T.; Brenner, M.; Donsbach, K.; Kreye, P. *Org. Proc. Res. Dev.* **2005**, *9*, 513; (b) Trnka, T. M.; Grubbs, R. H. *Acc. Chem. Res.* **2001**, *34*, 18; (c) Grubbs, R. H. *Tetrahedron* **2004**, *60*, 7117; (d) Vougioukalakis, G. C.; Grubbs, R. H. *Chem. Rev.* **2010**, *110*, 1746; (e) Grela, K. *Beilstein J. Org. Chem.* **2010**, *6*, 1089; (f) Grubbs, R. H. *Handbook of Metathesis*; Wiley-VCH: Weinheim, Germany, 2003.

(3) (a) Meek, S. J.; O'Brien, R. V.; Llaveria, J.; Schrock, R. R.; Hoveyda, A. H. *Nature* **2011**, *471*, 461; (b) Hoveyda, A. H.; Malcolmson, S. J.; Meek, S. J.; Zhugralin, A. R. *Angew. Chem. Int. Ed.* **2010**, *49*, 34; (c) Nicolaou, K. C.; Bulger, P. G.; Sarlah, D. *Angew. Chem. Int. Ed.* **2005**, *44*, 4490; (d) Morzycki, J. W. *Steroids* **2011**, *76*, 949.

(4) (a) Wallace, D. J.; Goodman, J. M.; Kennedy, D. J.; Davies, A. J.; Cowden, C. J.; Ashwood, M. S.; Cottrell, I. F.; Dolling, U.-H.; Reider, P. J. *Org. Lett.* **2001**, *3*, 671; (b) Lin, Y. A.; Chalker, J. M.; Davis, B. G. *ChemBioChem* **2009**, *10*, 959.

(5) de Weghe, P.; Eustache, J. *Curr. Top. Med. Chem.* **2005**, *5*, 1495.

(6) (a) Slugovc, C. *Macromol. Rapid Commun.* **2004**, *25*, 1283; (b) Buchmeiser, M. R. *Chem. Rev.* **2000**, *100*, 1565(c) Leitgeb, A.; Wappel, J.; Slugovc, C. *Polymer* **2010**, *51*, 2927; (d) Bielawski, C. W.; Grubbs, R. H. *Prog. Polym. Sci.* **2007**, *32*, 1; (e) Mol, J. C. *J. Mol. Catal. A: Chem.* **2004**, *213*, 39.

(7) (a) Calderon, N.; Ofstead, E. A.; Ward, J. P.; Judy, W. A.; Scott, K. W. *J. Am. Chem. Soc.* **1968**, *90*, 4133; (b) Mol, J. C.; Moulijn, J. A.; Boelhouw.C *Chem. Commun.* **1968**, 633; (c) Astruc, D. *New J. Chem.* **2005**, *29*, 42.

(8) Bradshaw, C. P. C.; Howman, E. J.; Turner, L. *J. Catal.* **1967**, *7*, 269.

(9) Calderon, N. *Acc. Chem. Res.* **1972**, *5*, 127.

(10) (a) Lewandos, G. S.; Pettit, R. *J. Am. Chem. Soc.* **1971**, *93*, 7087(b) Lewandos, G. S.; Pettit, R. *Tetrahedron Lett.* **1971**, 789.

(11) Grubbs, R. H.; Brunck, T. K. *J. Am. Chem. Soc.* **1972**, *94*, 2538.

(12) Hérisson, P. J.-L.; Chauvin, Y. *Makromol. Chem.* **1971**, *141*, 161.

(13) (a) Grubbs, R.; Tumas, W. *Science* **1989**, *243*, 907; (b) Gilliom, L. R.; Grubbs, R. H. *J. Am. Chem. Soc.* **1986**, *108*, 733; (c) Gilliom, L. R.; Grubbs, R. H. *Organometallics* **1986**, *5*, 721; (d) Schrock, R. R. *J. Organomet. Chem.* **1986**, *300*, 249; (e) Schrock, R. R. *Polyhedron* **1995**, *14*, 3177(f) Schwab, P.; France, M. B.; Ziller, J. W.; Grubbs, R. H. *Angew. Chem., Int. Ed. Engl.* **1995**, *34*, 2039; (g) Schwab, P.; Grubbs, R. H.; Ziller, J. W. *J. Am. Chem. Soc.* **1996**, *118*, 100; (h) Grubbs, R. H.; Miller, S. J.; Fu, G. C. *Acc. Chem. Res.* **1995**, *28*, 446; (i) Demonceau, A.; Stumpf, A. W.; Saive, E.; Noels, A. F. *Macromolecules* **1997**, *30*, 3127; (j) Banks, R. L.; Bailey, G. C. *Ind. Eng. Chem. Prod. Res. Dev.* **1964**, *3*, 170.

(14) Zukowska, K.; Grela, K. *Cross Metathesis* in *Olefin Metathesis: Theory and Practice, First Edition*, John Wiley & Sons, Inc., 2014, Chapter 2, 39-83.

(15) (a) Chatterjee, A. K.; Choi, T.-L.; Sanders, D. P.; Grubbs, R. H. *J. Am. Chem. Soc.* **2003**, *125*, 11360; (b) Zukowska, K.; Grela, K.; *Cross Metathesis* in *Comprehensive Organic Synthesis, Second Edition*, Elsevier B.V., 2014; Vol. 5, Chapter 5; (c) Zukowska, K.; Szadkowska, A.; Grela, K.; *Olefin Metathesis* in *Comprehensive Inorganic Chemistry II, Second Edition: From elements to aplications*, Elsevier B.V., 2013; Vol. 6, Chapter 5.

(16) (a) van Lierop, B. J.; Lummiss, J. A. M.; Fogg, D. E.; John Wiley & Sons, Inc., 2014; (b) Cossy, J.; Arseniyadis, S.; Meyer, C. *Metathesis in natural product synthesis : strategies, substrates and catalysts*; Wiley-VCH: Weinheim, 2010; (c) Monfette, S.; Fogg, D. E. *Chem. Rev.* **2009**, *109*, 3783.

(17) Ivin, K. J.; Mol, J. C. In *Olefin Metathesis and Metathesis Polymerization II*; Academic Press: London, 1997.

(18) (a) Wengrovius, J. H.; Schrock, R. R.; Churchill, M. R.; Missert, J. R.; Youngs, W. J. *J. Am. Chem. Soc.* **1980**, *102*, 4515; (b) Churchill, M. R.; Rheingold, A. L.; Youngs, W. J.; Schrock, R. R.; Wengrovius, J. H. *J. Organomet. Chem.* **1981**, *204*, C17; (c) Kress, J.; Osborn, J. A. *J. Am. Chem. Soc.* **1983**, *105*, 6346; (d) Kress, J.; Wesolek, M.; Osborn, J. A. *J. Chem. Soc., Chem. Commun.* **1982**, 514; (e) Kress, J.; Osborn, J. A.; Greene, R. M. E.; Ivin, K. J.; Rooney, J. J. *J. Am. Chem. Soc.* **1987**, *109*, 899; (f) Kress, J.; Aguero, A.; Osborn, J. A. *J. Mol. Catal.* **1986**, *36*, 1; (g) Youinou, M. T.; Kress, J.; Fischer, J.; Aguero, A.; Osborn, J. A. *J. Am. Chem. Soc.* **1988**, *110*, 1488; (h) Lefebvre, F.; Leconte, M.; Pagano, S.; Mutch, A.; Basset, J.-M. *Polyhedron* **1995**, *14*, 3209.

(19) (a) Couturier, J.-L.; Paillet, C.; Leconte, M.; Basset, J.-M.; Weiss, K. *Angew. Chem. Int. Ed. Engl.* **1992**, *31*, 628; (b) Quignard, F.; Leconte, M.; Basset, J.-M. *J. Chem. Soc., Chem. Commun.* **1985**, 1816.

(20) (a) Schrock, R. R.; DePue, R. T.; Feldman, J.; Yap, K. B.; Yang, D. C.; Davis, W. M.; Park, L.; DiMare, M.; Schofield, M. *Organometallics* **1990**, *9*, 2262; (b) Schrock, R. R.; Feldman, J.; Cannizzo, L. F.; Grubbs, R. H. *Macromolecules* **1987**, *20*, 1169; (c) Schaverien, C. J.; Dewan, J. C.; Schrock, R. R. *J. Am. Chem. Soc.* **1986**, *108*, 2771; (d) Schrock, R. R.; DePue, R. T.; Feldman, J.; Schaverien, C. J.; Dewan, J. C.; Liu, A. H. *J. Am. Chem. Soc.* **1988**, *110*, 1423.

(21) (a) Bazan, G. C.; Oskam, J. H.; Cho, H. N.; Park, L. Y.; Schrock, R. R. *J. Am. Chem. Soc.* **1991**, *113*, 6899; (b) Murdzek, J. S.; Schrock, R. R. *Organometallics* **1987**, *6*, 1373; (c) Schrock, R. R.; Murdzek, J. S.; Bazan, G. C.; Robbins, J.; DiMare, M.; O'Regan, M. *J. Am. Chem. Soc.* **1990**, *112*, 3875; (d) Bazan, G. C.; Khosravi, E.; Schrock, R. R.; Feast, W. J.; Gibson, V. C.; O'Regan, M. B.; Thomas, J. K.; Davis, W. M. *J. Am. Chem. Soc.* **1990**, *112*, 8378.

(22) (a) Hoveyda, A. H.; Zhugralin, A. R. *Nature* **2007**, *450*, 243; (b) Schrock, R. R.; Hoveyda, A. H. *Angew. Chem. Int. Ed.* **2003**, *42*, 4592; (c) Pietraszuk, C. In *Olefin metathesis*; Grela, K., Ed.; John Wiley & Sons, Inc., 2014; (d) Schrock, R. R. *Chem. Rev.* **2009**, *109*, 3211.

(23) Jiang, A. J.; Simpson, J. H.; Muller, P.; Schrock, R. R. *J. Am. Chem. Soc.* **2009**, *131*, 7770.

(24) Malcolmson, S. J.; Meek, S. J.; Sattely, E. S.; Schrock, R. R.; Hoveyda, A. H. *Nature* **2008**, *456*, 933.

(25) (a) Alexander, J. B.; La, D. S.; Cefalo, D. R.; Hoveyda, A. H.; Schrock, R. R. *J. Am. Chem. Soc.* **1998**, *120*, 4041; (b) La, D. S.; Alexander, J. B.; Cefalo, D. R.; Graf, D. D.; Hoveyda, A. H.; Schrock, R. R. *J. Am. Chem. Soc.* **1998**, *120*, 9720; (c) Zhu, S. S.; Cefalo, D. R.; La, D. S.; Jamieson, J. Y.; Davis, W. M.; Hoveyda, A. H.; Schrock, R. R. *J. Am. Chem. Soc.* **1999**, *121*, 8251; (d) Aeilts, S. L.; Cefalo, D. R.; Bonitatebus, J. P. J.; Houser, J. H.; Hoveyda, A. H.; Schrock, R. R. *Angew. Chem. Int. Ed.* **2001**, *40*, 1452; (e) Cortez, G. A.; Schrock, R. R.; Hoveyda, A. H. *Angew. Chem. Int. Ed.* **2007**, *46*, 4534; (f) Jiang, A. J.; Zhao, Y.; Schrock, R. R.; Hoveyda, A. H. *J. Am. Chem. Soc.* **2009**, *131*, 16630; (g) Ibrahem, I.; Yu, M.; Schrock, R. R.; Hoveyda, A. H. *J. Am. Chem. Soc.* **2009**, *131*, 3844; (h) Flook, M. M.; Jiang, A. J.; Schrock, R. R.; Müller, P.; Hoveyda, A. H. *J. Am. Chem. Soc.* **2009**, *131*, 7962; (i) Wang, C.; Yu, M.; Kyle, A. F.; Jakubec, P.; Dixon, D. J.; Schrock, R. R.; Hoveyda, A. H. *Chem. Eur. J.* **2013**, *19*, 2726; (j) Hoveyda, A. H. *J. Org. Chem.* **2014**, *79*, 4763; (k) Townsend, E. M.; Hyvl, J.; Forrest, W. P.; Schrock, R. R.; Muller, P.; Hoveyda, A. H. *Organometallics* **2014**, *33*, 5334; (l) Wang, C.; Haeffner, F.; Schrock, R. R.; Hoveyda, A. H. *Angew. Chem., Int. Ed.* **2013**, *52*, 1939; (m) Marinescu, S. C.; Levine, D. S.; Zhao, Y.; Schrock, R. R.; Hoveyda, A. H. *J. Am. Chem. Soc.* **2011**, *133*, 11512; (n) Zhang, H.; Yu, E. C.; Torker, S.; Schrock, R. R.; Hoveyda, A. H. *J. Am. Chem. Soc.* **2014**, *136*, 16493.

(26) (a) Michelotti, F. W.; Keaveney, W. P. *J. Polym. Sci., Part A* **1965**, *3*, 895; (b) Rinehart, R. E.; Smith, H. P. *J. Polym. Sci., Part B: Pol. Lett.* **1965**, *3*, 1049.

(27) (a) Nguyen, S. T.; Johnson, L. K.; Grubbs, R. H.; Ziller, J. W. *J. Am. Chem. Soc.* **1992**, *114*, 3974; (b) France, M. B.; Grubbs, R. H.; McGrath, D. V.; Paciello, R. A. *Macromolecules* **1993**, *26*, 4742.
(28) (a) Fu, G. C.; Grubbs, R. H. *J. Am. Chem. Soc.* **1993**, *115*, 3800; (b) Kinoshita, A.; Mori, M. *Synlett* **1994**, 1020; (c) Miller, S. J.; Grubbs, R. H. *J. Am. Chem. Soc.* **1995**, *117*, 5855; (d) Kanaoka, S.; Grubbs, R. H. *Macromolecules* **1995**, *28*, 4707; (e) Hillmyer, M. A.; Laredo, W. R.; Grubbs, R. H. *Macromolecules* **1995**, *28*, 6311.
(29) Nguyen, S. T.; Grubbs, R. H.; Ziller, J. W. *J. Am. Chem. Soc.* **1993**, *115*, 9858.
(30) Armstrong, S. K. *J. Chem. Soc.-Perkin Trans. 1* **1998**, 371.
(31) (a) Harrity, J. P. A.; Visser, M. S.; Gleason, J. D.; Hoveyda, A. H. *J. Am. Chem. Soc.* **1997**, *119*, 1488; (b) Harrity, J. P. A.; La, D. S.; Cefalo, D. R.; Visser, M. S.; Hoveyda, A. H. *J. Am. Chem. Soc.* **1998**, *120*, 2343.
(32) Kingsbury, J. S.; Harrity, J. P. A.; Bonitatebus, P. J.; Hoveyda, A. H. *J. Am. Chem. Soc.* **1999**, *121*, 791.
(33) J. Harlow, K.; F. Hill, A.; D. E. T. Wilton-Ely, J. *J. Chem. Soc., Dalton Trans.* **1999**, 285.
(34) (a) Furstner, A.; Liebl, M.; F. Hill, A.; D. E. T. Wilton-Ely, J. *Chem. Commun.* **1999**, 601; (b) Fürstner, A.; Grabowski, J.; Lehmann, C. W. *J. Org. Chem.* **1999**, *64*, 8275.
(35) Schanz, H.-J.; Jafarpour, L.; Stevens, E. D.; Nolan, S. P. *Organometallics* **1999**, *18*, 5187.
(36) (a) Fürstner, A.; Guth, O.; Düffels, A.; Seidel, G.; Liebl, M.; Gabor, B.; Mynott, R. *Chem. Eur. J.* **2001**, *7*, 4811; (b) Fürstner, A.; Radkowski, K.; Wirtz, C.; Goddard, R.; Lehmann, C. W.; Mynott, R. *J. Am. Chem. Soc.* **2002**, *124*, 7061; (c) Dragutan, V.; Dragutan, I.; Verpoort, F. *Platinum Met. Rev.* **2005**, *49*, 33.
(37) (a) Arduengo, A. J.; Krafczyk, R.; Schmutzler, R.; Craig, H. A.; Goerlich, J. R.; Marshall, W. J.; Unverzagt, M. *Tetrahedron* **1999**, *55*, 14523; (b) Arduengo, A. J. *Acc. Chem. Res.* **1999**, *32*, 913; (c) Samojłowicz, C.; Bieniek, M.; Grela, K. *Chem. Rev.* **2009**, *109*, 3708; (d) Hopkinson, M. N.; Richter, C.; Schedler, M.; Glorius, F. *Nature* **2014**, *510*, 485; (e) Vougioukalakis, G. C.; Grubbs, R. H. *Chem. Eur. J.* **2008**, *14*, 7545.
(38) (a) Frenzel, U.; Weskamp, T.; J. Kohl, F.; Schattenmann, W. C.; Nuyken, O.; Herrmann, W. A. *J. Organomet. Chem.* **1999**, *586*, 263; (b) Ackermann, L.; Fürstner, A.; Weskamp, T.; Kohl, F. J.; Herrmann, W. A. *Tetrahedron Lett.* **1999**, *40*, 4787; (c) Scholl, M.; Trnka, T. M.; Morgan, J. P.; Grubbs, R. H. *Tetrahedron Lett.* **1999**, *40*, 2247; (d) Huang, J.; Stevens, E. D.; Petersen, J. L.; Nolan, S. P. *J. Am. Chem. Soc.* **1999**, *121*, 2674.
(39) Gessler, S.; Randl, S.; Blechert, S. *Tetrahedron Lett.* **2000**, *41*, 9973.
(40) Grela, K.; Harutyunyan, S.; Michrowska, A. *Angew. Chem. Int. Ed.* **2002**, *41*, 4038.
(41) (a) Seiders, T. J.; Ward, D. W.; Grubbs, R. H. *Org. Lett.* **2001**, *3*, 3225; (b) Van Veldhuizen, J. J.; Garber, S. B.; Kingsbury, J. S.; Hoveyda, A. H. *J. Am. Chem. Soc.* **2002**, *124*, 4954; (c) Van Veldhuizen, J. J.; Gillingham, D. G.; Garber, S. B.; Kataoka, O.; Hoveyda, A. H. *J. Am. Chem. Soc.* **2003**, *125*, 12502; (d) Gillingham, D. G.; Kataoka, O.; Garber, S. B.; Hoveyda, A. H. *J. Am. Chem. Soc.* **2004**, *126*, 12288; (e) Van Veldhuizen, J. J.; Campbell, J. E.; Giudici, R. E.; Hoveyda, A. H. *J. Am. Chem. Soc.* **2005**, *127*, 6877; (f) Funk, T. W.; Berlin, J. M.; Grubbs, R. H. *J. Am. Chem. Soc.* **2006**, *128*, 1840; (g) Berlin, J. M.; Goldberg, S. D.; Grubbs, R. H. *Angew. Chem. Int. Ed.* **2006**, *45*, 7591; (h) Giudici, R. E.; Hoveyda, A. H. *J. Am. Chem. Soc.* **2007**, *129*, 3824.
(42) (a) Lynn, D. M.; Mohr, B.; Grubbs, R. H.; Henling, L. M.; Day, M. W. *J. Am. Chem. Soc.* **2000**, *122*, 6601; (b) Lynn, D. M.; Grubbs, R. H. *J. Am. Chem. Soc.* **2001**, *123*, 3187; (c) Rolle, T.; Grubbs, R. H. *Chem. Commun.* **2002**, 1070; (d) Varray, S.; Lazaro, R.; Martinez, J.; Lamaty, F. *Organometallics* **2003**, *22*, 2426; (e) Gallivan, J. P.; Jordan, J. P.; Grubbs, R. H. *Tetrahedron Lett.* **2005**, *46*, 2577; (f) Hong, S. H.; Grubbs, R. H. *J. Am. Chem. Soc.* **2006**, *128*, 3508; (g) Mwangi, M. T.; Runge, M. B.; Bowden, N. B. *J. Am. Chem. Soc.* **2006**, *128*, 14434; (h) Binder, J. B.; Guzei, I. A.; Raines, R. T. *Adv. Synth. Catal.* **2007**, *349*, 395.
(43) (a) Berlin, J. M.; Campbell, K.; T. Ritter, T.; Funk, T. W.; Chlenov, A.; Grubbs, R. H. *Org. Lett.* **2007**, *9*, 1339; (b) Stewart, I. C.; Ung, T.; Pletnev, A. A.; Berlin, J. M.; Grubbs, R. H.; Schrodi, Y. *Org. Lett.* **2007**, *9*, 1589.

(44) (a) Dias, E. L.; Nguyen, S. T.; Grubbs, R. H. *J. Am. Chem. Soc.* **1997**, *119*, 3887; (b) Sanford, M. S.; Love, J. A.; Grubbs, R. H. *J. Am. Chem. Soc.* **2001**, *123*, 6543; (c) Sanford, M. S.; Ulman, M.; Grubbs, R. H. *J. Am. Chem. Soc.* **2001**, *123*, 749.
(45) (a) Nelson, D. J.; Manzini, S.; Urbina-Blanco, C. A.; Nolan, S. P. *Chem. Commun.* **2014**, *50*, 10355; (b) Thiel, V.; Hendann, M.; Wannowius, K.-J.; Plenio, H. *J. Am. Chem. Soc.* **2012**, *134*, 1104.
(46) (a) Clavier, H.; Grela, K.; Kirschning, A.; Mauduit, M.; Nolan, S. P. *Angew. Chem. Int. Ed.* **2007**, *46*, 6786; (b) Goldup, S. M.; Pilkington, C. J.; White, A. J. P.; Burton, A.; Barret, A. G. M. *J. Org. Chem.* **2006**, *71*, 6185.
(47) (a) Guideline on the specification limits for residues of metal catalysts; http://www.ema.europa.eu/docs/en_GB/document_library/Scientific_guideline/2009/09/WC500003587.pdf; (b) Deraedt, C.; d'Halluin, M.; Astruc, D. *Eur. J. Inorg. Chem.* **2013**, *2013*, 4881.
(48) (a) Ley, S. V.; Baxendale, I. R. *Nat. Rev. Drug Discov.* **2002**, *1*, 573; (b) Szczepaniak, G.; Kosinski, K.; Grela, K. *Green Chemistry* **2014**, *16*, 4474.
(49) Skowerski, K.; Wierzbicka, C.; Grela, K. *Curr. Org. Chem.* **2013**, *17*, 2740.
(50) (a) Sheldon, R. A. *Green Chemistry* **2007**, *9*, 1273; (b) Anastas, P. T.; Warner, J. C. *Green chemistry : theory and practice*; Oxford University Press: Oxford, 1998.
(51) (a) Jas, G.; Kirschning, A. *Chem. Eur. J.* **2003**, *9*, 5708; (b) Burguete, M. I.; García-Verdugo, E.; Luis, S. V. *Beilstein J. Org. Chem.* **2011**, *7*, 1347; (c) Kirschning, A.; Jas, G. In *Immobilized Catalysts*; Kirschning, A., Ed.; Springer Berlin Heidelberg, 2004; Vol. 242; (d) Wegner, J.; Ceylan, S.; Kirschning, A. *Adv. Synth. Catal.* **2012**, *354*, 17; (e) Wegner, J.; Ceylan, S.; Kirschning, A. *Chem. Commun.* **2011**, *47*, 4583; (f) Hintermair, U.; Francio, G.; Leitner, W. *Chem. Commun.* **2011**, *47*, 3691; (g) Noel, T.; Buchwald, S. L. *Chem. Soc. Rev.* **2011**, *40*, 5010.
(52) Pashkova, A.; Greiner, L. *Chem. Ing. Tech.* **2011**, *83*, 1337.
(53) (a) Anastas, P. T.; Kirchhoff, M. M. *Acc. Chem. Res.* **2002**, *35*, 686; (b) Wiles, C.; Watts, P. *Green Chem.* **2012**, *14*, 38; (c) Vaccaro, L.; Lanari, D.; Marrocchi, A.; Strappaveccia, G. *Green Chem.* **2014**, *16*, 3680.
(54) (a) Mayr, M.; Mayr, B.; Buchmeiser, M. R. *Angew. Chem. Int. Ed.* **2001**, *40*, 3839; (b) Krause, J. O.; Lubbad, S. H.; Nuyken, O.; Buchmeiser, M. R. *Macromol. Rapid Commun.* **2003**, *24*, 875; (c) Yang, L.; Mayr, M.; Wurst, K.; Buchmeiser, M. R. *Chem. Eur. J.* **2004**, *10*, 5761.
(55) Kirschning, A.; Altwicker, C.; Dräger, G.; Harders, J.; Hoffmann, N.; Hoffmann, U.; Schönfeld, H.; Solodenko, W.; Kunz, U. *Angew. Chem. Int. Ed.* **2001**, *40*, 3995.
(56) (a) Kirschning, A.; Solodenko, W.; Mennecke, K. *Chem. Eur. J.* **2006**, *12*, 5972(b) Kunz, U.; Schönfeld, H.; Solodenko, W.; Jas, G.; Kirschning, A. *Ind. Eng. Chem. Res.* **2005**, *44*, 8458.
(57) Monfette, S.; Eyholzer, M.; Roberge, D. M.; Fogg, D. E. *Chem. Eur. J.* **2010**, *16*, 11720.
(58) Skowerski, K.; Czarnocki, S. J.; Knapkiewicz, P. *ChemSusChem* **2014**, *7*, 536.
(59) Yang, L.; Jensen, K. F. *Org. Proc. Res. Dev.* **2013**, *17*, 927.
(60) Maynard, H. D.; Grubbs, R. H. *Tetrahedron Lett.* **1999**, *40*, 4137.
(61) Cho, J. H.; Kim, B. M. *Org. Lett.* **2003**, *5*, 531.
(62) Ahn, Y. M.; Yang, K. L.; Georg, G. I. *Org. Lett.* **2001**, *3*, 1411.
(63) Paquette, L. A.; Schloss, J. D.; Efremov, I.; Fabris, F.; Gallou, F.; Méndez-Andino, J.; Yang, J. *Org. Lett.* **2000**, *2*, 1259.
(64) Balskus, E. P.; Méndez-Andino, J.; Arbit, R. M.; Paquette, L. A. *J. Org. Chem.* **2001**, *66*, 6695.
(65) Higham, L.; K. Whittlesey, M. *Chem. Commun.* **1998**, 1107.
(66) Grubbs, R. H.; Ferguson, M. L.; O'Leary, D. J. In *Organic Reactions*, 2004; Vol. 22.
(67) Haack, K.; Ahn, Y.; Georg, G. *Mol. Divers.* **2005**, *9*, 301.
(68) Knight, D. W.; Morgan, I. R.; Proctor, A. J. *Tetrahedron Lett.* **2010**, *51*, 638.
(69) Löber, A.; Verch, A.; Schlemmer, B.; Höfer, S.; Frerich, B.; Buchmeiser, M. R. *Angew. Chem. Int. Ed.* **2008**, *47*, 9138.

(70) (a) Katayama, H.; Urushima, H.; Nishioka, T.; Wada, C.; Nagao, M.; Ozawa, F. *Angew. Chem. Int. Ed.* **2000**, *39*, 4513; (b) Louie, J.; Grubbs, R. H. *Organometallics* **2002**, *21*, 2153; (c) Minenkov, Y.; Occhipinti, G.; Jensen, V. R. *Organometallics* **2013**, *32*, 2099.
(71) Liu, W.; Nichols, P. J.; Smith, N. *Tetrahedron Lett.* **2009**, *50*, 6103.
(72) Galan, B. R.; Kalbarczyk, K. P.; Szczepankiewicz, S.; Keister, J. B.; Diver, S. T. *Org. Lett.* **2007**, *9*, 1203.
(73) Winter, P.; Hiller, W.; Christmann, M. *Angew. Chem. Int. Ed.* **2012**, *51*, 3396.
(74) Szczepaniak, G.; Czarnocki, S. J.; Skowerski, K. *Use of metal scavengers for removal of ruthenium residues*, WO2014174501A2, 2014.
(75) (a) Yee, N. K.; Farina, V.; Houpis, I. N.; Haddad, N.; Frutos, R. P.; Gallou, F.; Wang, X.-j.; Wei, X.; Simpson, R. D.; Feng, X.; Fuchs, V.; Xu, Y.; Tan, J.; Zhang, L.; Xu, J.; Smith-Keenan, L. L.; Vitous, J.; Ridges, M. D.; Spinelli, E. M.; Johnson, M.; Donsbach, K.; Nicola, T.; Brenner, M.; Winter, E.; Kreye, P.; Samstag, W. *J. Org. Chem.* **2006**, *71*, 7133; (b) Farina, V.; Shu, C.; Zeng, X.; Wei, X.; Han, Z.; Yee, N. K.; Senanayake, C. H. *Org. Proc. Res. Dev.* **2009**, *13*, 250.
(76) (a) Ley, S. V.; Baxendale, I. R.; Bream, R. N.; Jackson, P. S.; Leach, A. G.; Longbottom, D. A.; Nesi, M.; Scott, J. S.; Storer, R. I.; Taylor, S. J. *J. Chem. Soc., Perkin Trans. 1* **2000**, 3815; (b) Kaldor, S. W.; Siegel, M. G. *Curr. Opin. Chem. Biol.* **1997**, *1*, 101; (c) Kirschning, A.; Monenschein, H.; Wittenberg, R. *Angew. Chem. Int. Ed.* **2001**, *40*, 650; (d) Parlow, J. J.; Devraj, R. V.; South, M. S. *Curr. Opin. Chem. Biol.* **1999**, *3*, 320.
(77) Westhus, M.; Gonthier, E.; Brohm, D.; Breinbauer, R. *Tetrahedron Lett.* **2004**, *45*, 3141.
(78) McEleney, K.; Allen, D. P.; Holliday, A. E.; Crudden, C. M. *Org. Lett.* **2006**, *8*, 2663.
(79) Pulko, I.; Sandholzer, M.; Kolar, M.; Slugovc, C.; Krajnc, P. *Tetrahedron Lett.* **2010**, *51*, 5827.
(80) Su, H.-L.; Hongfa, C.; Bazzi, H. S.; Bergbreiter, D. E. *Macromol. Sy.* **2010**, *297*, 25.
(81) French, J. M.; Caras, C. A.; Diver, S. T. *Org. Lett.* **2013**, *15*, 5416.
(82) (a) Liu, Q.; Xu, Z. *Langmuir* **1995**, *11*, 4617; (b) Ponder, S. M.; Darab, J. G.; Bucher, J.; Caulder, D.; Craig, I.; Davis, L.; Edelstein, N.; Lukens, W.; Nitsche, H.; Rao, L.; Shuh, D. K.; Mallouk, T. E. *Chem. Mater.* **2001**, *13*, 479; (c) Ponder, S. M.; Darab, J. G.; Mallouk, T. E. *Environ. Sci. Technol.* **2000**, *34*, 2564; (d) Cao, J.; Zhang, W.-X. *J. Hazard. Mater.* **2006**, *132*, 213; (e) Li, X.-q.; Elliott, D. W.; Zhang, W.-x. *Crit. Rev. Solid State Mater. Sci.* **2006**, *31*, 111; (f) Li, X.-q.; Zhang, W.-x. *J. Phys. Chem. C* **2007**, *111*, 6939.
(83) Macdonald, J. E.; Kelly, J. A.; Veinot, J. G. C. *Langmuir* **2007**, *23*, 9543.
(84) Macdonald, J. E.; Veinot, J. G. C. *Langmuir* **2008**, *24*, 7169.
(85) (a) S. AMIT & CO.; http://www.s-amit.com/home/default.asp; (b) SiliCycle Inc.; www.silicycle.com.
(86) Lambeth, R. H.; Pederson, S. J.; Baranoski, M.; Rawlett, A. M. *J. Polym. Sci., Part A: Polym. Chem.* **2010**, *48*, 5752.
(87) Pederson, R. L.; Fellows, I. M.; Ung, T. A.; Ishihara, H.; Hajela, S. P. *Adv. Synth. Catal.* **2002**, *344*, 728.
(88) Faucher, A.-M.; Bailey, M. D.; Beaulieu, P. L.; Brochu, C.; Duceppe, J.-S.; Ferland, J.-M.; Ghiro, E.; Gorys, V.; Halmos, T.; Kawai, S. H.; Poirier, M.; Simoneau, B.; Tsantrizos, Y. S.; Llinàs-Brunet, M. *Org. Lett.* **2004**, *6*, 2901.
(89) Dersch, W.; Samstag, W. *Process for the preparation of macrocyclic compounds by ruthenium complex catalyzed metathesis reaction*, WO2004089974A1, 2004.
(90) Gallou, F.; Saim, S.; Koenig, K. J.; Bochniak, D.; Horhota, S. T.; Yee, N. K.; Senanayake, C. H. *Org. Proc. Res. Dev.* **2006**, *10*, 937.
(91) Busacca, C. A.; Farina, V.; Gallou, F.; Haddad, N.; Wang, X.-J.; Wei, X.; Xu, J.; Xu, Y.; Yee, N. K.; Zhang, L. *Process for preparing nitrogen-containing macrocyclic compounds*, US20050209135A1, 2005.
(92) Shu, C.; Zeng, X.; Hao, M.-H.; Wei, X.; Yee, N. K.; Busacca, C. A.; Han, Z.; Farina, V.; Senanayake, C. H. *Org. Lett.* **2008**, *10*, 1303.

(93) (a) Grela, K. *Ruthenium Complexes as (Pre)catalysts for Metathesis Reactions, Boehringer Ingelheim International*: Germany, PCT Patent WO 2004/035596 A1, U.S. Patent 6,867,303, 2005; (b) Braun, M.; Busacca, C. A.; Chen, F.-J.; Gump, E. L.; Majeska, J. B.; Pennino, S.; Qiu, F.; Villagra, M. F. *Stabilized pharmaceutical formulations of a potent HCV inhibitor*, WO2013106506A1, 2013; (c) Busacca, C. A.; Gallou, F.; Haddad, N.; Hossain, A.; Kapadia, S. R.; Liu, J.; Senanayake, C. H.; Wei, X.; Yee, N. K. *Process for preparing macrocyclic compounds*, WO2006096652A2, 2006; (d) Busacca, C. A.; Frutos, R. P.; Haddad, N.; Kapadia, S. R.; Lorenz, J. C.; Saha, A.; Senanayake, C. H.; Wei, X. *Process for the preparation of 4-(4-prolyloxy)quinoline derivatives as HCV protease inhibitors*, US20050267151A1, 2005.

(94) (a) Clark, W. M.; Badham, N. F.; Dai, Q.; Eldridge, A. M.; Matsuhashi, H. *A preparation of derivatives of benzofuran-2-carboxylic acid amide, useful as cysteine protease inhibitors*, WO2005069981A2, 2005; (b) Wang, H.; Matsuhashi, H.; Doan, B. D.; Goodman, S. N.; Ouyang, X.; Clark Jr, W. M. *Tetrahedron* **2009**, *65*, 6291; (c) Cummings, M. D.; Marquis, R. W., Jr.; Ru, Y.; Thompson, S. K.; Veber, D. F.; Yamashita, D. S. *Preparation of C1-6 alkyl-4-aminoazepan-3-one derivatives as protease inhibitors*, WO2001070232A1, 2001.

(95) Fürstner, A.; Langemann, K. *J. Am. Chem. Soc.* **1997**, *119*, 9130.

(96) Wang, H. In *Transition Metal-Catalyzed Couplings in Process Chemistry*; Wiley-VCH Verlag GmbH & Co. KGaA, 2003.

(97) Melis, K.; De Vos, D.; Jacobs, P.; Verpoort, F. *J. Mol. Catal. A: Chem.* **2001**, *169*, 47.

(98) Bek, D.; Balcar, H.; Žilková, N. z. d.; Zukal, A. t.; Horáček, M.; Čejka, J. i. *ACS Catalysis* **2011**, *1*, 709.

(99) Allen, D. P.; Van Wingerden, M. M.; Grubbs, R. H. *Org. Lett.* **2009**, *11*, 1261.

(100) Park, K. H.; Kim, S.; Chung, Y. K. *Bull. Korean Chem. Soc.* **2008**, *29*, 2057.

(101) Nieczypor, P.; Buchowicz, W.; Meester, W. J. N.; Rutjes, F. P. J. T.; Mol, J. C. *Tetrahedron Lett.* **2001**, *42*, 7103.

(102) (a) Krause, J. O.; Nuyken, O.; Wurst, K.; Buchmeiser, M. R. *Chem. Eur. J.* **2004**, *10*, 777; (b) Halbach, T. S.; Mix, S.; Fischer, D.; Maechling, S.; Krause, J. O.; Sievers, C.; Blechert, S.; Nuyken, O.; Buchmeiser, M. R. *J. Org. Chem.* **2005**, *70*, 4687.

(103) (a) Gawin, R.; Makal, A.; Woźniak, K.; Mauduit, M.; Grela, K. *Angew. Chem. Int. Ed.* **2007**, *46*, 7206; (b) Bek, D.; Gawin, R.; Grela, K.; Balcar, H. *Catal. Commun.* **2012**, *21*, 42.

(104) Marciniec, B.; Rogalski, S.; Potrzebowski, M. J.; Pietraszuk, C. *ChemCatChem* **2011**, *3*, 904.

(105) (a) Borja, G.; Pleixats, R.; Alibes, R.; Cattoen, X.; Man, M. W. C. *Molecules* **2010**, *15*, 5756; (b) Lim, J.; Lee, S. S.; Riduan, S. N.; Ying, J. Y. *Adv. Synth. Catal.* **2007**, *349*, 1066; (c) Lim, J.; Lee, S. S.; Ying, J. Y. *Chem. Commun.* **2008**, 4312; (d) Elias, X.; Pleixats, R.; Wong Chi Man, M. *Tetrahedron* **2008**, *64*, 6770.

(106) Fischer, D.; Blechert, S. *Adv. Synth. Catal.* **2005**, *347*, 1329.

(107) (a) Jee, J.-E.; Cheong, J. L.; Lim, J.; Chen, C.; Hong, S. H.; Lee, S. S. *J. Org. Chem.* **2013**, *78*, 3048; (b) Lim, J.; Seong Lee, S.; Ying, J. Y. *Chem. Commun.* **2010**, *46*, 806.

(108) Vorfalt, T.; Wannowius, K. J.; Thiel, V.; Plenio, H. *Chem. Eur. J.* **2010**, *16*, 12312.

(109) Cheong, J. L.; Wong, D.; Lee, S.-G.; Lim, J.; Lee, S. S. *Chem. Commun.* **2015**, *51*, 1042.

(110) Conrad, J. C.; Parnas, H. H.; Snelgrove, J. L.; Fogg, D. E. *J. Am. Chem. Soc.* **2005**, *127*, 11882.

(111) Van Berlo, B.; Houthoofd, K.; Sels, B. F.; Jacobs, P. A. *Adv. Synth. Catal.* **2008**, *350*, 1949.

(112) Balcar, H.; Shinde, T.; Žilkova, N.; Basti, Z. *Beilstein J. Org. Chem.* **2011**, *7*, 22.

(113) Pastva, J.; Skowerski, K.; Czarnocki, S. J.; Žilková, N.; Čejka, J.; Bastl, Z.; Balcar, H. *ACS Catalysis* **2014**, *4*, 3227.

(114) (a) Staub, H.; Guillet-Nicolas, R.; Even, N.; Kayser, L.; Kleitz, F.; Fontaine, F.-G. *Chem. Eur. J.* **2011**, *17*, 4254; (b) Cabrera, J.; Padilla, R.; Bru, M.; Lindner, R.; Kageyama, T.; Wilckens, K.; Balof, S. L.; Schanz, H.-J.; Dehn, R.; Teles, J. H.; Deuerlein, S.; Müller,

K.; Rominger, F.; Limbach, M. *Chem. Eur. J.* **2012**, *18*, 14717; (c) Solodenko, W.; Doppiu, A.; Frankfurter, R.; Vogt, C.; Kirschning, A. *Aust. J. Chem.* **2013**, *66*, 183.
(115) (a) Schachner, J. r. A.; Cabrera, J.; Padilla, R.; Fischer, C.; van der Schaaf, P. A.; Pretot, R.; Rominger, F.; Limbach, M. *ACS Catalysis* **2011**, 872; (b) Cabrera, J.; Padilla, R.; Dehn, R.; Deuerlein, S.; Gułajski, Ł.; Chomiszczak, E.; Teles, J. H.; Limbach, M.; Grela, K. *Adv. Synth. Catal.* **2012**, *354*, 1043.
(116) Bru, M.; Dehn, R.; Teles, J. H.; Deuerlein, S.; Danz, M.; Müller, I. B.; Limbach, M. *Chem. Eur. J.* **2013**, *19*, 11661.
(117) Nguyen, S. B. T.; Grubbs, R. H. *J. Organomet. Chem.* **1995**, *497*, 195.
(118) Ahmed, M.; Barrett, A. G. M.; Braddock, D. C.; Cramp, S. M.; Procopiou, P. A. *Tetrahedron Lett.* **1999**, *40*, 8657.
(119) (a) Jafarpour, L.; Nolan, S. P. *Org. Lett.* **2000**, *2*, 4075; (b) Jafarpour, L.; Heck, M.-P.; Baylon, C.; Lee, H. M.; Mioskowski, C.; Nolan, S. P. *Organometallics* **2002**, *21*, 671.
(120) (a) Connon, S. J.; Blechert, S. *Bioorg. Med. Chem. Lett.* **2002**, *12*, 1873; (b) Connon, S. J.; Dunne, A. M.; Blechert, S. *Angew. Chem. Int. Ed.* **2002**, *41*, 3835; (c) Randl, S.; Buschmann, N.; Connon, S. J.; Blechert, S. *Synlett* **2001**, *2001*, 1547.
(121) (a) Hoveyda, A. H.; Gillingham, D. G.; Van Veldhuizen, J. J.; Kataoka, O.; Garber, S. B.; Kingsbury, J. S.; Harrity, J. P. A. *Organic & Biomolecular Chemistry* **2004**, *2*, 8; (b) Kingsbury, J. S.; Garber, S. B.; Giftos, J. M.; Gray, B. L.; Okamoto, M. M.; Farrer, R. A.; Fourkas, J. T.; Hoveyda, A. H. *Angew. Chem. Int. Ed.* **2001**, *40*, 4251.
(122) Dowden, J.; Savovic, J. *Chem. Commun.* **2001**, 37.
(123) Grela, K.; Tryznowski, M.; Bieniek, M. *Tetrahedron Lett.* **2002**, *43*, 9055.
(124) Keraani, A.; Fischmeister, C.; Renouard, T.; Le Floch, M.; Baudry, A.; Bruneau, C.; Rabiller-Baudry, M. *J. Mol. Catal. A: Chem.* **2012**, *357*, 73.
(125) (a) Wang, D.; Astruc, D. *Molecules* **2014**, *19*, 4635(b) Gleeson, O.; Tekoriute, R.; Gun'ko, Y. K.; Connon, S. J. *Chem. Eur. J.* **2009**, *15*, 5669; (c) Jun, C.-H.; Park, Y. J.; Yeon, Y.-R.; Choi, J.-r.; Lee, W.-r.; Ko, S.-j.; Cheon, J. *Chem. Commun.* **2006**, 1619(d) Luo, S.; Zheng, X.; Cheng, J.-P. *Chem. Commun.* **2008**, 5719; (e) Kawamura, M.; Sato, K. *Chem. Commun.* **2006**, 4718; (f) Phan, N. T. S.; Gill, C. S.; Nguyen, J. V.; Zhang, Z. J.; Jones, C. W. *Angew. Chem. Int. Ed.* **2006**, *45*, 2209; (g) Lee, D.; Lee, J.; Lee, H.; Jin, S.; Hyeon, T.; Kim, B. M. *Adv. Synth. Catal.* **2006**, *348*, 41; (h) Zheng, Y.; Stevens, P. D.; Gao, Y. *J. Org. Chem.* **2005**, *71*, 537; (i) Lu, A.-H.; Schmidt, W.; Matoussevitch, N.; Bönnemann, H.; Spliethoff, B.; Tesche, B.; Bill, E.; Kiefer, W.; Schüth, F. *Angew. Chem. Int. Ed.* **2004**, *43*, 4303; (j) Hu, A.; Yee, G. T.; Lin, W. *J. Am. Chem. Soc.* **2005**, *127*, 12486; (k) Claesson, M. E.; Mehendale, N. C.; Klein Gebbink, R. J. M.; van Koten, G.; Philipse, A. P. *J. Magn. Magn. Mater.* **2007**, *311*, 41; (l) Wang, D.; Astruc, D. *Chem. Rev.* **2014**, *114*, 6949.
(126) Yinghuai, Z.; Kuijin, L.; Huimin, N.; Chuanzhao, L.; Stubbs, L. P.; Siong, C. F.; Muihua, T.; Peng, S. C. *Adv. Synth. Catal.* **2009**, *351*, 2650.
(127) Che, C.; Li, W.; Lin, S.; Chen, J.; Zheng, J.; Wu, J.-C.; Zheng, Q.; Zhang, G.; Yang, Z.; Jiang, B. *Chem. Commun.* **2009**, 5990.
(128) (a) Chen, S.-W.; Zhang, Z.-C.; Ma, M.; Zhong, C.-M.; Lee, S.-g. *Org. Lett.* **2014**, *16*, 4969; (b) Chen, S.-W.; Zhang, Z.-C.; Zhai, N.-N.; Zhong, C.-M.; Lee, S.-g. *Tetrahedron* **2015**, *71*, 648.
(129) Tomasek, J.; Schatz, J. *Green Chem.* **2013**, *15*, 2317.
(130) Mohr, B.; Lynn, D. M.; Grubbs, R. H. *Organometallics* **1996**, *15*, 4317.
(131) (a) Gläser, R. In *Handbook of Green Chemistry*; Wiley-VCH Verlag GmbH & Co. KGaA, 2010; (b) DeSimone, J. M. *Science* **2002**, *297*, 799.
(132) (a) Wasserscheid, P.; Keim, W. *Angew. Chem. Int. Ed.* **2000**, *39*, 3772; (b) Dupont, J.; de Souza, R. F.; Suarez, P. A. Z. *Chem. Rev.* **2002**, *102*, 3667; (c) Smiglak, M.; Reichert, W. M.; Holbrey, J. D.; Wilkes, J. S.; Sun, L.; Thrasher, J. S.; Kirichenko, K.; Singh, S.; Katritzky, A. R.; Rogers, R. D. *Chem. Commun.* **2006**, 2554.
(133) Csihony, S.; Fischmeister, C.; Bruneau, C.; Horvath, I. T.; Dixneuf, P. H. *New J. Chem.* **2002**, *26*, 1667.

(134) (a) Audic, N.; Clavier, H.; Mauduit, M.; Guillemin, J.-C. *J. Am. Chem. Soc.* **2003**, *125*, 9248; (b) Clavier, H.; Audic, N.; Mauduit, M.; Guillemin, J.-C. *Chem. Commun.* **2004**, 2282; (c) Clavier, H.; Audic, N.; Guillemin, J.-C.; Mauduit, M. *J. Organomet. Chem.* **2005**, *690*, 3585; (d) Yao, Q.; Zhang, Y. *Angew. Chem. Int. Ed.* **2003**, *42*, 3395; (e) Yao, Q.; Sheets, M. *J. Organomet. Chem.* **2005**, *690*, 3577.

(135) Consorti, C. S.; Aydos, G. L. P.; Ebeling, G.; Dupont, J. *Org. Lett.* **2007**, *10*, 237.

(136) (a) Gułajski, Ł.; Michrowska, A.; Bujok, R.; Grela, K. *J. Mol. Catal. A: Chem.* **2006**, *254*, 118; (b) Gułajski, Ł.; Grela, K. In *Green Metathesis Chemistry*; Dragutan, V., Demonceau, A., Dragutan, I., Finkelshtein, E. S., Eds.; Springer Netherlands, 2010; (c) Gułajski, Ł.; Mauduit, M.; Grela, K. *Pure Appl. Chem.* **2009**, *81*, 2001.

(137) Rix, D.; Clavier, H.; Coutard, Y.; Gułajski, Ł.; Grela, K.; Mauduit, M. *J. Organomet. Chem.* **2006**, *691*, 5397.

(138) Michrowska, A.; Mennecke, K.; Kunz, U.; Kirschning, A.; Grela, K. *J. Am. Chem. Soc.* **2006**, *128*, 13261.

(139) (a) Clousier, N.; Filippi, A.; Borré, E.; Guibal, E.; Crévisy, C.; Caijo, F.; Mauduit, M.; Dez, I.; Gaumont, A.-C. *ChemSusChem* **2014**, *7*, 1040; (b) Ceylan, S.; Kirschning, A. In *Recoverable and Recyclable Catalysts*; John Wiley & Sons, Ltd, 2009; (c) Kirschning, A. *Beilstein J. Org. Chem.* **2009**, *5*, 15; (d) Autenrieth, B.; Frey, W.; Buchmeiser, M. R. *Chem. Eur. J.* **2012**, *18*, 14069; (e) Nasrallah, H.; Pagnoux, A.; Didier, D.; Magnier, C.; Toupet, L.; Guillot, R.; Crévisy, C.; Mauduit, M.; Schulz, E. *Eur. J. Org. Chem.* **2014**, *2014*, 7781; (f) Autenrieth, B.; Willig, F.; Pursley, D.; Naumann, S.; Buchmeiser, M. R. *ChemCatChem* **2013**, *5*, 3033.

(140) Borré, E.; Rouen, M.; Laurent, I.; Magrez, M.; Caijo, F.; Crévisy, C.; Solodenko, W.; Toupet, L.; Frankfurter, R.; Vogt, C.; Kirschning, A.; Mauduit, M. *Chem. Eur. J.* **2012**, *18*, 16369.

(141) Duque, R.; Ochsner, E.; Clavier, H.; Caijo, F.; Nolan, S. P.; Mauduit, M.; Cole-Hamilton, D. J. *Green Chem.* **2011**, *13*, 1187.

(142) (a) Balof, S. L.; P'Pool, S. J.; Berger, N. J.; Valente, E. J.; Shiller, A. M.; Schanz, H.-J. *Dalton T.* **2008**, 5791(b) Balof, S. L.; Yu, B.; Lowe, A. B.; Ling, Y.; Zhang, Y.; Schanz, H.-J. *Eur. J. Inorg. Chem.* **2009**, *2009*, 1717.

(143) (a) Skowerski, K.; Wierzbicka, C.; Szczepaniak, G.; Gulajski, L.; Bieniek, M.; Grela, K. *Green Chem.* **2012**, *14*, 3264; (b) Skowerski, K.; Kasprzycki, P.; Bieniek, M.; Olszewski, T. K. *Tetrahedron* **2013**, *69*, 7408.

(144) (a) Kosnik, W.; Grela, K. *Dalton T.* **2013**, *42*, 7463; (b) Kluciar, M.; Grela, K.; Mauduit, M. *Dalton T.* **2013**, *42*, 7354; (c) Olszewski, T. K.; Bieniek, M.; Skowerski, K.; Grela, K. *Synlett* **2013**, *24*, 903.

(145) (a) Studer, A.; Hadida, S.; Ferritto, R.; Kim, S.-Y.; Jeger, P.; Wipf, P.; Curran, D. P. *Science* **1997**, *275*, 823; (b) Horváth, I. T.; Rábai, J. *Science* **1994**, *266*, 72.

(146) (a) Horváth, I. T. *Acc. Chem. Res.* **1998**, *31*, 641; (b) Curran, D. P. *Angew. Chem. Int. Ed.* **1998**, *37*, 1174; (c) de Wolf, E.; van Koten, G.; Deelman, B.-J. *Chem. Soc. Rev.* **1999**, *28*, 37; (d) Fish, R. H. *Chem. Eur. J.* **1999**, *5*, 1677; (e) Dobbs, A. P.; Kimberley, M. R. *J. Fluorine Chem.* **2002**, *118*, 3(f) Hope, E. G.; Stuart, A. M. *J. Fluorine Chem.* **1999**, *100*, 75; (g) Samojlowicz, C.; Kajetanowicz, A.; Grela, K., in *Olefin Metathesis: Theory and Practice, First Edition*, John Wiley & Sons, Inc., 2014; p 537.

(147) Matsugi, M.; Curran, D. P. *J. Org. Chem.* **2005**, *70*, 1636.

(148) (a) da Costa, R. C.; Gladysz, J. A. *Chem. Commun.* **2006**, 2619; (b) da Costa, R. C.; Gladysz, J. A. *Adv. Synth. Catal.* **2007**, *349*, 243.

(149) Matsugi, M.; Kobayashi, Y.; Suzumura, N.; Tsuchiya, Y.; Shioiri, T. *J. Org. Chem.* **2010**, *75*, 7905.

(150) Kvíčala, J.; Schindler, M.; Kelbichová, V.; Babuněk, M.; Rybáčková, M.; Kvíčalová, M.; Cvačka, J.; Březinová, A. *J. Fluorine Chem.* **2013**, *153*, 12.

(151) (a) Bergbreiter, D. E.; Tian, J.; Hongfa, C. *Chem. Rev.* **2009**, *109*, 530; (b) Bergbreiter, D. E. *Chem. Rev.* **2002**, *102*, 3345; (c) Bergbreiter, D. E. *ACS Macro Letters* **2014**, *3*, 260.

(152) (a) Torborg, C.; Samojlowicz, C.; Grela, K. In *Science of Synthesise, Water in Organic Synthesis, Aqueous Media: Reaction of C-C Multiple Bonds*, 2012; (b) Grela, K.; Gulajski, L.; Skowerski, K., *Alkene Metathesis* in water in *Metal-Catalyzed Reaction in Water*, Wiley-VCH, 2013, Chap. 8, p 291; (c) Gułajski, Ł.; Sledz, P.; Lupa, A.; Grela, K. *Green Chem.* **2008**, *10*, 271; (d) Burtscher, D.; Grela, K. *Angew. Chem. Int. Ed.* **2009**, *48*, 442; (e) Schaper, L.-A.; Hock, S. J.; Herrmann, W. A.; Kühn, F. E. *Angew. Chem. Int. Ed.* **2013**, *52*, 270.
(153) Hong, S. H.; Grubbs, R. H. *Org. Lett.* **2007**, *9*, 1955.
(154) (a) Yao, Q. *Angew. Chem. Int. Ed.* **2000**, *39*, 3896(b) Yao, Q.; Rodriguez Motta, A. *Tetrahedron Lett.* **2004**, *45*, 2447.
(155) (a) Bergbreiter, D. E.; Liu, Y.-S.; Osburn, P. L. *J. Am. Chem. Soc.* **1998**, *120*, 4250; (b) Bergbreiter, D. E.; Osburn, P. L.; Smith, T.; Li, C.; Frels, J. D. *J. Am. Chem. Soc.* **2003**, *125*, 6254.
(156) (a) Bergbreiter, D. E.; Li, C.; Besinaiz, J. O.; Li, J.; Sung, S. D. *Phase selective functional polymer supports for catalysis*, US20040082463A1, 2004; (b) Bergbreiter, D. E.; Bazzi, H. S.; Hongfa, C. *Nonpolar Phase-Soluble Methathesis Catalysts* A1 US20080286745 20081001 ed., 2009.
(157) Hongfa, C.; Tian, J.; Bazzi, H. S.; Bergbreiter, D. E. *Org. Lett.* **2007**, *9*, 3259.
(158) Hongfa, C.; Su, H.-L.; Bazzi, H. S.; Bergbreiter, D. E. *Org. Lett.* **2009**, *11*, 665.
(159) Al-Hashimi, M.; Hongfa, C.; George, B.; Bazzi, H. S.; Bergbreiter, D. E. *J. Polym. Sci., Part A: Polym. Chem.* **2012**, *50*, 3954.
(160) Bergbreiter, D. E.; Osburn, P. L.; Wilson, A.; Sink, E. M. *J. Am. Chem. Soc.* **2000**, *122*, 9058.
(161) Hobbs, C.; Yang, Y.-C.; Ling, J.; Nicola, S.; Su, H.-L.; Bazzi, H. S.; Bergbreiter, D. E. *Org. Lett.* **2011**, *13*, 3904.
(162) Wang, L. K. *Membrane and desalination technologies*; Humana Press: New York, 2011.
(163) (a) Thamaraiselvan, C.; Noel, M. *Crit. Rev. Environ. Sci. Technol.* **2014**, *45*, 1007; (b) Fane, A. G.; Wang, R.; Jia, Y. *Handb. Environ. Eng.* **2011**, *13*, 1; (c) Vandezande, P.; Gevers, L. E. M.; Vankelecom, I. F. J. *Chem. Soc. Rev.* **2008**, *37*, 365; (d) Peeva, L. G.; Sairam, M.; Livingston, A. G., *Nanofiltration operations in nonaqueous systems* in *Comprehensive Membrane Science and Engineering*, Elsevier Ltd., 2010; p 91; (e) Volkov, A. V.; Korneeva, G. A.; Tereshchenko, G. F. *Russ. Chem. Rev.* **2008**, *77*, 983; (f) Afonso, C. A. M.; Crespo, J. G. *Green separation processes : fundamentals and applications*; Wiley: Weinheim; Chichester, 2005; (g) Rundquist, E. M.; Pink, C. J.; Livingston, A. G. *Green Chem.* **2012**, *14*, 2197; (h) Van der Bruggen, B. *Ind. Eng. Chem. Res.* **2013**, *52*, 10335.
(164) Marchetti, P.; Jimenez Solomon, M. F.; Szekely, G.; Livingston, A. G. *Chem. Rev.* **2014**, *114*, 10735.
(165) Fane, A. G.; Schaefer, A.; Waite, T. D. *Nanofiltration Principles and Applications*; Elsevier: Amsterdam, 2004.
(166) (a) Buonomenna, M. G.; Bae, J. *Sep. Purif. Rev.* **2014**, *44*, 157; (b) Cheng, X. Q.; Zhang, Y. L.; Wang, Z. X.; Guo, Z. H.; Bai, Y. P.; Shao, L. *Adv. Polym. Tech.* **2014**, *33*, 21455; (c) Jimenez Solomon, M. F.; Bhole, Y.; Livingston, A. G. *J. Membrane Sci.* **2012**, *423–424*, 371.
(167) Evonik MET Ltd., London, U. K.; http://duramem.evonik.com/product/duramem-puramem/en/Pages/default.aspx.
(168) See Toh, Y. H.; Loh, X. X.; Li, K.; Bismarck, A.; Livingston, A. G. *J. Membrane Sci.* **2007**, *291*, 120.
(169) Schrock, R. R. *J. Am. Chem. Soc.* **1990**, *112*, 3875.
(170) Kozmin, S. A.; Iwama, T.; Huang, Y.; Rawal, V. H. *J. Am. Chem. Soc.* **2002**, *124*, 4628.
(171) White, L. S. *J. Membrane Sci.* **2002**, *205*, 191.
(172) Garber, S. B.; Kingsbury, J. S.; Gray, B. L.; Hoveyda, A. H. *J. Am. Chem. Soc.* **2000**, *122*, 8168.
(173) Pregler, B. *Wine Business Monthly* **2010**, *15*.

(174) (a) Stewart, I. C.; Douglas, C. J.; Grubbs, R. H. *Org. Lett.* **2008**, *10*, 441; (b) Tsang, W. C. P. *J. Am. Chem. Soc.* **2003**, *125*, 2652.
(175) Singh, R.; Schrock, R. R.; Muller, P.; Hoveyda, A. H. *J. Am. Chem. Soc.* **2007**, *129*, 12654.
(176) (a) Dijkstra, H. P.; van Klink, G. P. M.; van Koten, G. *Acc. Chem. Res.* **2002**, *35*, 798; (b) Wiese, K.-D.; Baumgarten, G.; Kuppinger, F.-F.; Moeller, O.; Ortmann, D.; Borgmann, C.; Bueschken, W. *Method for separation of organic transition metal complex catalysts from a crude reaction product in metal-catalyzed hydroformylation reaction*, DE102005046250A1, 2007; (c) De Smet, K.; Aerts, S.; Ceulemans, E.; Vankelecom, I. F. J.; Jacobs, P. A. *Chem. Commun.* **2001**, 597; (d) Scarpello, J. T.; Nair, D.; Freitas dos Santos, L. M.; White, L. S.; Livingston, A. G. *J. Membrane Sci.* **2002**, *203*, 71; (e) Müller, C.; Nijkamp, M. G.; Vogt, D. *Eur. J. Inorg. Chem.* **2005**, *2005*, 4011; (f) Wong, H.-T.; See-Toh, Y. H.; Ferreira, F. C.; Crook, R.; Livingston, A. G. *Chem. Commun.* **2006**, 2063; (g) de Pater, J. J. M.; Deelman, B.-J.; Elsevier, C. J.; van Koten, G. *Adv. Synth. Catal.* **2006**, *348*, 1447; (h) Chavan, S. A.; Maes, W.; Gevers, L. E. M.; Wahlen, J.; Vankelecom, I. F. J.; Jacobs, P. A.; Dehaen, W.; De Vos, D. E. *Chem. Eur. J.* **2005**, *11*, 6754.
(177) Aerts, S.; Weyten, H.; Buekenhoudt, A.; Gevers, L. E. M.; Vankelecom, I. F. J.; Jacobs, P. A. *Chem. Commun.* **2004**, 710.
(178) (a) Nair, D.; Scarpello, J. T.; White, L. S.; Freitas dos Santos, L. M.; Vankelecom, I. F. J.; Livingston, A. G. *Tetrahedron Lett.* **2001**, *42*, 8219; (b) Datta, A.; Ebert, K.; Plenio, H. *Organometallics* **2003**, *22*, 4685; (c) Nair, D.; Scarpello, J. T.; Vankelecom, I. F. J.; Freitas Dos Santos, L. M.; White, L. S.; Kloetzing, R. J.; Welton, T.; Livingston, A. G. *Green Chem.* **2002**, *4*, 319; (d) Pink, C. J.; Wong, H.-t.; Ferreira, F. C.; Livingston, A. G. *Org. Proc. Res. Dev.* **2008**, *12*, 589; (e) Peeva, L.; da Silva Burgal, J.; Vartak, S.; Livingston, A. G. *J. Catal.* **2013**, *306*, 190.
(179) Nair, D.; Wong, H.-T.; Han, S.; Vankelecom, I. F. J.; White, L. S.; Livingston, A. G.; Boam, A. T. *Org. Proc. Res. Dev.* **2009**, *13*, 863.
(180) Branco, L. C.; Ferreira, F. C.; Santos, J. L.; Crespo, J. G.; Afonso, C. A. M. *Adv. Synth. Catal.* **2008**, *350*, 2086.
(181) (a) Janssen, M.; Muller, C.; Vogt, D. *Dalton T.* **2010**, *39*, 8403; (b) Janssen, M.; Muller, C.; Vogt, D. *Green Chem.* **2011**, *13*, 2247; (c) Rosen, B. M.; Wilson, C. J.; Wilson, D. A.; Peterca, M.; Imam, M. R.; Percec, V. *Chem. Rev.* **2009**, *109*, 6275.
(182) Keraani, A.; Renouard, T.; Fischmeister, C.; Bruneau, C.; Rabiller-Baudry, M. *ChemSusChem* **2008**, *1*, 927.
(183) Schoeps, D.; Sashuk, V.; Ebert, K.; Plenio, H. *Organometallics* **2009**, *28*, 3922.
(184) Wijkens, P.; Jastrzebski, J. T. B. H.; van der Schaaf, P. A.; Kolly, R.; Hafner, A.; van Koten, G. *Org. Lett.* **2000**, *2*, 1621.
(185) van der Gryp, P.; Barnard, A.; Cronje, J.-P.; de Vlieger, D.; Marx, S.; Vosloo, H. C. M. *J. Membrane Sci.* **2010**, *353*, 70.
(186) Schoeps, D.; Buhr, K.; Dijkstra, M.; Ebert, K.; Plenio, H. *Chem. Eur. J.* **2009**, *15*, 2960.
(187) Nasser, G.; Renouard, T.; Shahane, S.; Fischmeister, C.; Bruneau, C.; Rabiller-Baudry, M. *ChemPlusChem* **2013**, *78*, 728.
(188) (a) Gaikwad, A. V.; Boffa, V.; ten Elshof, J. E.; Rothenberg, G. *Angew. Chem. Int. Ed.* **2008**, *47*, 5407; (b) Gaab, M.; Bellemin-Laponnaz, S.; Gade, L. H. *Chem. Eur. J.* **2009**, *15*, 5450.
(189) Pijnenburg, N. J. M.; Tomás-Mendivil, E.; Mayland, K. E.; Kleijn, H.; Lutz, M.; Spek, A. L.; van Koten, G.; Klein Gebbink, R. J. M. *Inorg. Chim. Acta* **2014**, *409, Part A*, 163.
(190) (a) Buonomenna, M. G.; Choi, S. H.; Drioli, E. *Asia-Pac. J. Chem. Eng.* **2010**, *5*, 26; (b) Vankelecom, I. F. J. *Chem. Rev.* **2002**, *102*, 3779.
(191) (a) Li, H.; Bhadury, P. S.; Song, B.; Yang, S. *RSC Advances* **2012**, *2*, 12525; (b) Mehnert, C. P. *Chem. Eur. J.* **2005**, *11*, 50; (c) Olivier-Bourbigou, H.; Magna, L.; Morvan, D. *Appl. Catal. A: Gen.* **2010**, *373*, 1.

(192) Keraani, A.; Rabiller-Baudry, M.; Fischmeister, C.; Bruneau, C. *Catal. Today* **2010**, *156*, 268.
(193) O'Neal, E. J.; Jensen, K. F. *ChemCatChem* **2014**, *6*, 3004.
(194) (a) Ulman, M.; Grubbs, R. H. *J. Org. Chem.* **1999**, *64*, 7202; (b) Scholz, J.; Loekman, S.; Szesni, N.; Hieringer, W.; Görling, A.; Haumann, M.; Wasserscheid, P. *Adv. Synth. Catal.* **2011**, *353*, 2701.
(195) Ormerod, D.; Bongers, B.; Porto-Carrero, W.; Giegas, S.; Vijt, G.; Lefevre, N.; Lauwers, D.; Brusten, W.; Buekenhoudt, A. *RSC Advances* **2013**, *3*, 21501.
(196) Darvishmanesh, S.; Degrève, J.; Van der Bruggen, B. *ChemPhysChem* **2010**, *11*, 404.
(197) Hong, S. H.; Sanders, D. P.; Lee, C. W.; Grubbs, R. H. *J. Am. Chem. Soc.* **2005**, *127*, 17160.
(198) Czaban, J.; Schertzer, B. M.; Grela, K. *Adv. Synth. Catal.* **2013**, *355*, 1997.
(199) Hartmann-Thompson, C. *Applications of Polyhedral Oligomeric Silsesquioxanes*; Springer Netherlands, 2011.
(200) Liu, J.; Chen, J.; Zhao, J.; Zhao, Y.; Li, L.; Zhang, H. *Synthesis* **2003**, *2003*, 2661.
(201) HybridCatalysis; http://www.hybridcatalysis.com/#capabilities.
(202) Gerritsen, G., Technische Universiteit Eindhoven, 2011.
(203) (a) Barbasiewicz, M.; Michalak, M.; Grela, K. *Chem. Eur. J.* **2012**, *18*, 14237; (b) Tzur, E.; Szadkowska, A.; Ben-Asuly , A.; Makal, A.; Goldberg, I.; Woźniak, K.; Grela , K.; Lemcoff, N. G. *Chem. Eur. J.* **2010**, *16*, 8726.
(204) Vehlow, K.; Maechling, S.; Blechert, S. *Organometallics* **2006**, *25*, 25.
(205) Conrad, J. C.; Yap, G. P. A.; Fogg, D. E. *Organometallics* **2003**, *22*, 1986.
(206) Weskamp, T.; Schattenmann, W. C.; Spiegler, M.; Herrmann, W. A. *Angew. Chem. Int. Ed.* **1998**, *37*, 2490.
(207) Meyer, E. A.; Castellano, R. K.; Diederich, F. *Angew. Chem. Int. Ed.* **2003**, *42*, 1210.
(208) (a) Gawin, R.; Grela, K. *Eur. J. Inorg. Chem.* **2012**, *2012*, 1477; (b) Gawin, R.; Czarnecka, P.; Grela, K. *Tetrahedron* **2010**, *66*, 1051.
(209) Wappel, J.; Urbina-Blanco, C. A.; Abbas, M.; Albering, J. H.; Saf, R.; Nolan, S. P.; Slugovc, C. *Beilstein J. Org. Chem.* **2010**, *6*, 1091.
(210) Kawashima, M.; Sato, T.; Fujisawa, T. *Tetrahedron* **1989**, *45*, 403.
(211) Liu, G.; Wang, J. *Angew. Chem. Int. Ed.* **2010**, *49*, 4425.
(212) Frisch, A. C.; Shaikh, N.; Zapf, A.; Beller, M. *Angew. Chem. Int. Ed.* **2002**, *41*, 4056.
(213) Nakamura, M.; Matsuo, K.; Ito, S.; Nakamura, E. *J. Am. Chem. Soc.* **2004**, *126*, 3686.
(214) Cahiez, G.; Habiak, V.; Duplais, C.; Moyeux, A. *Angew. Chem. Int. Ed.* **2007**, *46*, 4364.
(215) (a) Cahiez, G.; Chaboche, C.; Duplais, C.; Giulliani, A.; Moyeux, A. *Adv. Synth. Catal.* **2008**, *350*, 1484; (b) Nasielski, J.; Hadei, N.; Achonduh, G.; Kantchev, E. A. B.; O'Brien, C. J.; Lough, A.; Organ, M. G. *Chem. Eur. J.* **2010**, *16*, 10844.
(216) Cahiez, G.; Gager, O.; Buendia, J. *Synlett* **2010**, *2010*, 299.
(217) Cahiez, G. r.; Chaboche, C.; Duplais, C.; Moyeux, A. *Org. Lett.* **2008**, *11*, 277.
(218) (a) Bieniek, M., doctoral dissertation, 2008; (b) Bieniek, M.; Bujok, R.; Cabaj, M.; Lugan, N.; Lavigne, G.; Arlt, D.; Grela, K. *J. Am. Chem. Soc.* **2006**, *128*, 13652.
(219) Bieniek, M.; Samojłowicz, C.; Sashuk, V.; Bujok, R.; Śledź, P.; Lugan, N. l.; Lavigne, G.; Arlt, D.; Grela, K. *Organometallics* **2011**, *30*, 4144.
(220) Grela, K.; Michrowska, A.; Bieniek, M. *The Chemical Record* **2006**, *6*, 144.
(221) Dastgir, S.; Coleman, K. S.; Green, M. L. H. *Dalton T.* **2011**, *40*, 661.
(222) Gawin, R. doctoral dissertation, 2012.
(223) Bujok, R.; Bieniek, M.; Masnyk, M.; Michrowska, A.; Sarosiek, A.; Stępowska, H.; Arlt, D.; Grela, K. *J. Org. Chem.* **2004**, *69*, 6894.